



affiliate Columbia University College of Physicians and Surgeons  
member New York-Presbyterian Healthcare System  
A Planetree Hospital

August 13, 2015

Lisa Davis, MBA, BSN, RN  
Deputy Commissioner  
State of Connecticut  
Department of Public Health  
Office of Health Care Access Division  
410 Capital Avenue  
MS#13HCA  
P.O. Box 340308  
Hartford, CT 06134



Re: Certificate of Need Application to Acquire and Operate a  
SPECT/CT Camera System at The Stamford Hospital in Stamford, CT

Dear Deputy Commissioner Davis:

Enclosed is the original Certificate of Need Application for the acquisition and operation of a SPECT/CT Camera System at The Stamford Hospital in Stamford, CT. Also, enclosed are four copies of the application and a CD of the scanned application and documents in MS format.

Please do not hesitate to contact me at 203-276-7510 or our outside counsel, Stephen Cowherd, at 203-259-7900 if you have any questions regarding this application.

I look forward to working with you during the review process.

Sincerely,

A handwritten signature in black ink, appearing to read 'David L. Smith', written over a light blue horizontal line.

David L. Smith  
Senior Vice President, Strategy  
Chief Strategy and Network Development Officer

cc: Stephen M. Cowherd, Esq. (w/ encl.)

## Application Checklist

## Instructions:

1. Please check each box below, as appropriate; and
2. The completed checklist **must** be submitted as the first page of the CON application.

- ☐ Attached is the CON application filing fee in the form of a certified, cashier or business check made out to the "Treasurer State of Connecticut" in the amount of \$500.

## For OHCA Use Only:

Docket No.: 15-32020-CON Check No.: 389296  
 OHCA Verified by: GR Date: 8.17.15

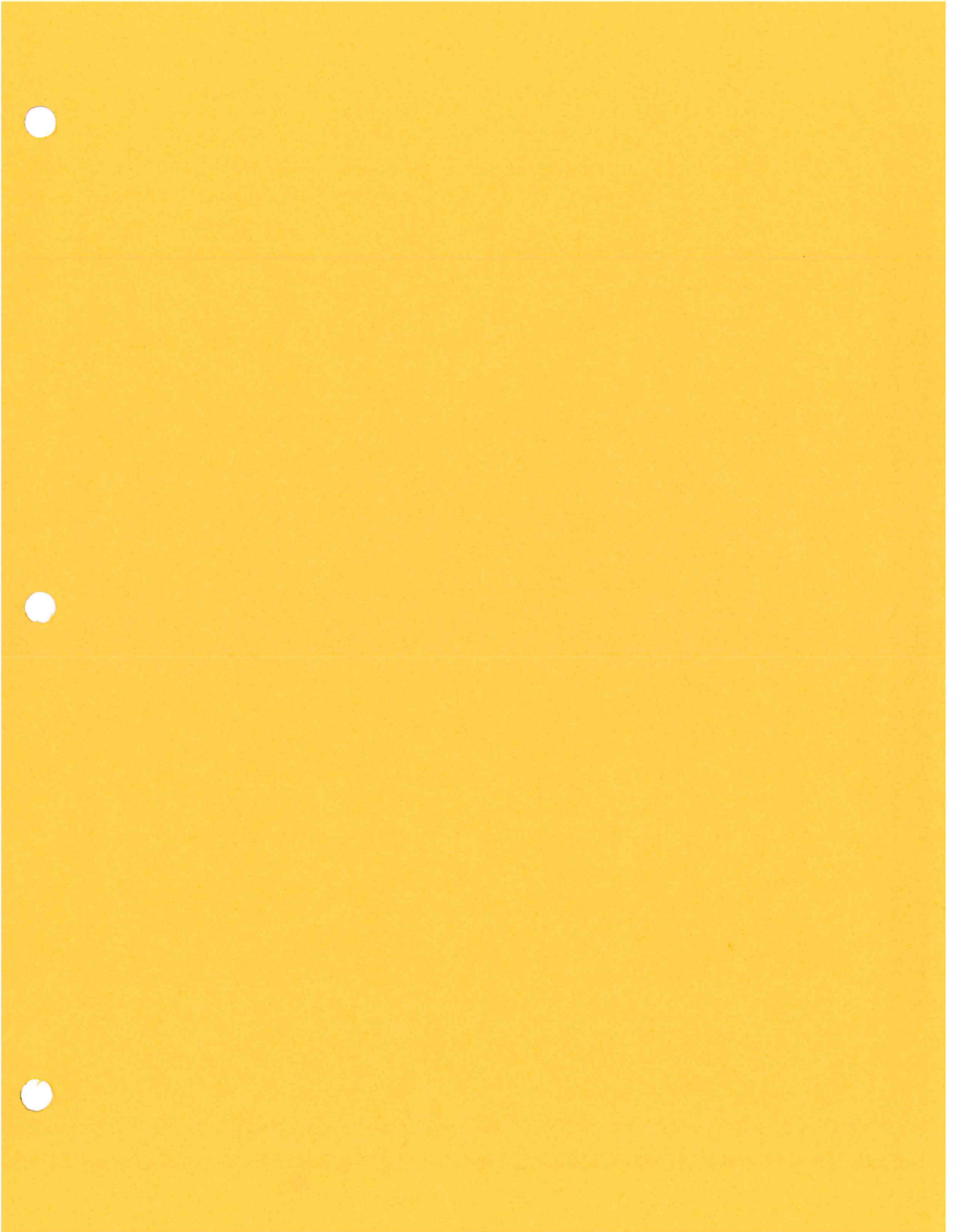
- ☐ Attached is evidence demonstrating that public notice has been published in a suitable newspaper that relates to the location of the proposal, 3 days in a row, at least 20 days prior to the submission of the CON application to OHCA. *(OHCA requests that the Applicant fax a courtesy copy to OHCA (860) 418-7053, at the time of the publication)*
- ☐ Attached is a paginated hard copy of the CON application including a completed affidavit, signed and notarized by the appropriate individuals.
- ☐ Attached are completed Financial Attachments I and II.
- ☐ Submission includes one (1) original and four (4) hard copies with each set placed in 3-ring binders.

**Note:** A CON application may be filed with OHCA electronically through email, if the total number of pages submitted is 50 pages or less. In this case, the CON Application must be emailed to [ohca@ct.gov](mailto:ohca@ct.gov).

**Important:** For CON applications (less than 50 pages) filed electronically through email, the signed affidavit and the check in the amount of \$500 must be delivered to OHCA in hardcopy.

- ☐ The following have been submitted on a CD
1. A scanned copy of each submission in its entirety, including all attachments in Adobe (.pdf) format.
  2. An electronic copy of the documents in MS Word and MS Excel as appropriate.





0003

VENDOR NAME: TREASURER STATE OF CONN

VENDOR NUMBER: 02302

DATE  
07/07/15CHECK NO.  
389296

DATE	INVOICE / CREDIT MEMO	DESCRIPTION	INVOICE AMOUNT	DISCOUNT	NET PAID
07/06/15	CON 2015	FEE	500.00	0.00	500.00
					*****\$500.00

THE FACE OF THIS DOCUMENT HAS A MULTI-COLORED BACKGROUND ON WHITE PAPER

Stamford Hospital  
30 Shelburne Rd.  
P.O. Box 9317  
Stamford, Connecticut 06904-9317

Wells Fargo Bank, N.A.  
Hartford, CT

51-110  
211

CHECK NO.  
389296

DATE 07/07/15

PAY FIVE HUNDRED 00/100

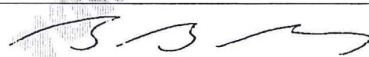
CHECK AMOUNT

\*\*\*\*\*\$500.00

TO THE ORDER OF

TREASURER STATE OF CONN  
OFFICE OF HEALTH CARE ACCESS  
410 CAPITOL AVE MS#13HCA  
P O BOX 340308

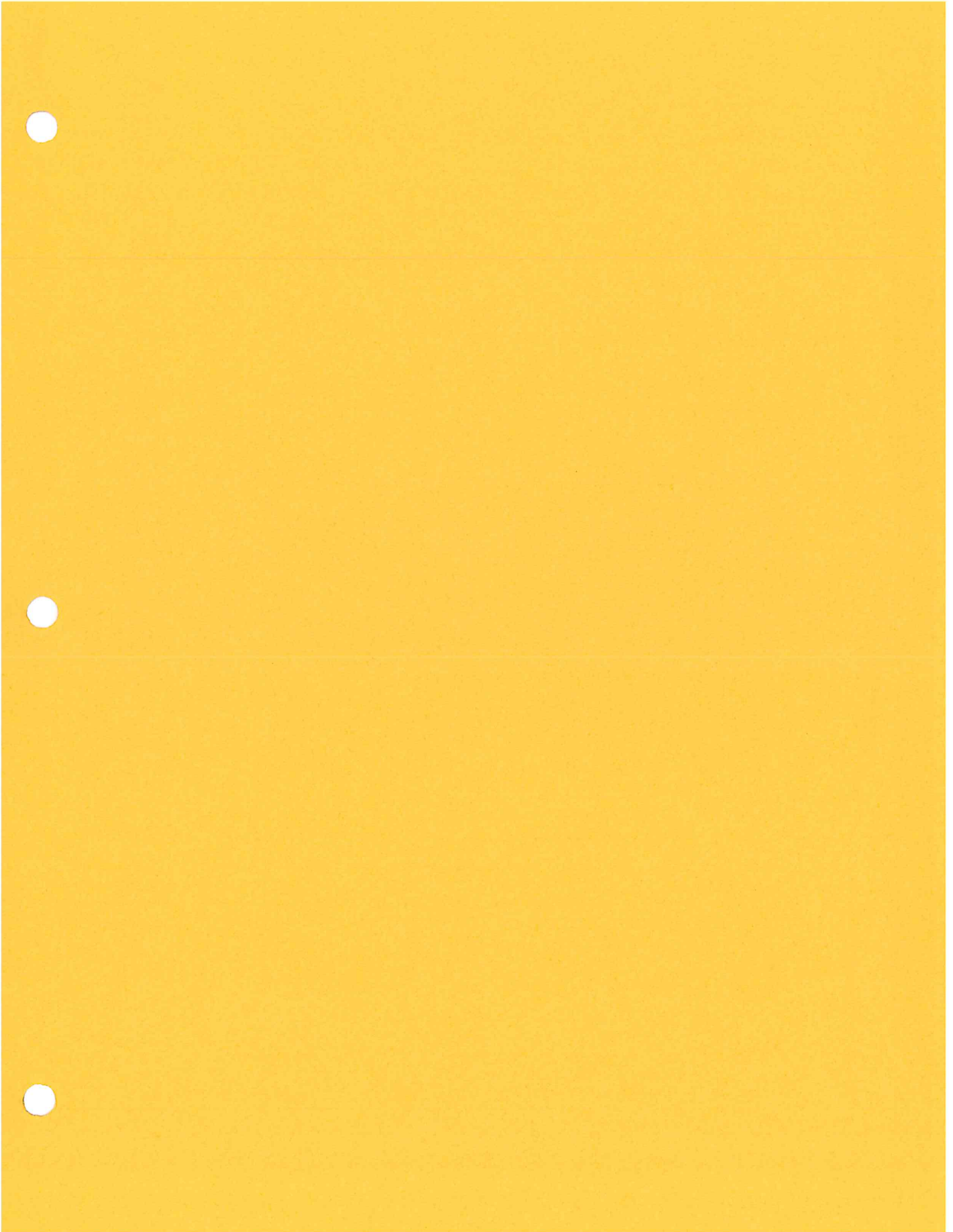
\*\*\* VOID AFTER 90 DAYS \*\*\*



HARTFORD, CT 06134

SECURITY FEATURES INCLUDED. DETAILS ON BACK.

Authorized Signature

















# The ADVOCATE

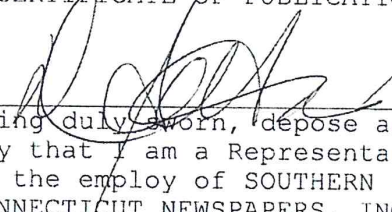
TOUCHPOINT INTEG. COMM.  
16 THORNDALE CIRCLE  
DARIEN CT 06820

THE ADVOCATE  
9 Riverbend Drive South  
Building 9A  
P.O. Box 4910  
Stamford, CT 06907-0910  
Telephone: 203-330-6208  
Fax: 203-384-1158  
Legal.notices@scni.com

## PUBLIC NOTICE

The Stamford Hospital is filing an application for a Certificate of Need under section 19a-638(a)(9) of the Connecticut General Statutes for the acquisition and operation of a SPECT/CT camera system to be located on the main hospital campus located at 30 Shelburne Road, Stamford, CT. The estimated capital expenditure for the project is \$765,000.

## THE ADVOCATE CERTIFICATE OF PUBLICATION

I,   
Being duly sworn, depose and say that I am a Representative in the employ of SOUTHERN CONNECTICUT NEWSPAPERS, INC., Publisher of *The Advocate* and *Greenwich Time*, that a LEGAL NOTICE as stated below was published in THE ADVOCATE.

Subscribed and sworn to before me on this 22nd Day of June, A.D. 2015.

  
Pamela Caluori/Notary Public

My commission expires on  
January 2018

PO Number

Publication

Stamford Advocate

Ad Number

0002088411-01

Ad Caption

PUBLIC NOTICE The Stamford

Publication Schedule

6/19/2015, 6/20/2015, 6/21/2015



## AFFIDAVIT

Applicant: The Stamford Hospital

Project Title: Acquisition and Operation of a SPECT/CT Camera System at The Stamford Hospital, 30 Shelburne Road, Stamford, CT.

I, Brian G. Grissler, President  
(Individual's Name) (Position Title – CEO or CFO)

of The Stamford Hospital being duly sworn, depose and state that  
(Hospital or Facility Name)

The Stamford Hospital's information submitted in this Certificate of  
(Hospital or Facility Name)

Need Application is accurate and correct to the best of my knowledge.

[Signature]  
Signature

7/24/15  
Date

Subscribed and sworn to before me on July 24, 2015

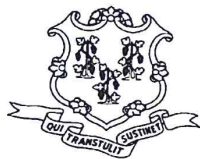
[Signature]

Notary Public/Commissioner of Superior Court

My commission expires: 7-31-20







**State of Connecticut**  
**Office of Health Care Access**  
**Certificate of Need Application**

**Instructions:** Please complete all sections of the Certificate of Need ("CON") application. If any section or question is not relevant to your project, a response of "Not Applicable" may be deemed an acceptable answer. If there is more than one applicant, identify the name and all contact information for each applicant. OHCA will assign a Docket Number to the CON application once the application is received by OHCA.

**Docket Number:**

**Applicant:** The Stamford Hospital

**Contact Person:** David L. Smith

**Contact Person's Title:** Senior Vice President, Strategy  
 Chief Strategy and Network Development Officer

**Contact Person's Address:** 30 Shelburne Road  
 Stamford, CT 06907

**Contact Person's Phone Number:** 203-276-7510

**Contact Person's Fax Number:** 203-276-5529

**Contact Person's Email Address:** DSmith@stamhealth.org

**Project Town:** Stamford

**Project Name:** Acquisition and Operation of a SPECT/CT Camera System at  
 The Stamford Hospital

**Statute Reference:** C.G.S. Section 19a-638 (a) (10)

**Estimated Total Capital Expenditure:** \$764,308

## 1. Project Description: Acquisition of Equipment

### a. Please provide a narrative detailing the proposal.

The Stamford Hospital (the “Hospital”) proposes to acquire and operate a new SPECT/CT camera that will replace and relocate one of the Hospital’s five existing nuclear cameras. Specifically, the Hospital proposes to replace its GE Ventri nuclear camera operated at its Mill River Cardiology Imaging Center, located at 80 Mill River Street, Stamford, with a new GE Optima NM/CT 640 SPECT / CT Camera System to be located in the Hospital’s new Heart and Vascular Institute (“HVI”) Center of Excellence – scheduled to open at the end of September 2016 on the Hospital’s existing campus at 30 Shelburne Road, Stamford.

The existing GE Ventri camera has reached the end of its useful life. It has been in operation since 2006 and has been leased by the Hospital since November 2011. As the Hospital’s employed cardiology group – The Heart Physicians – moves onto the Hospital’s main campus, the Hospital believes that this is the correct time to replace the existing nuclear camera with the upgraded technology offered by SPECT / CT. The new GE Optima SPECT / CT Camera System possesses a number of important upgrades from the current nuclear camera, allowing for better image quality and more rapid image acquisition.

### Background of the Heart and Vascular Institute Center of Excellence

On February 9, 2010, Stamford Hospital received approval from OHCA to proceed with its Master Facility Plan (“MFP”) under OHCA Docket Number: 08-312840-CON. Part of the MFP included construction of a new “Specialty Building” which would, among other services, include the new HVI – including four interventional labs (two cardiac catheterization labs, one VIR lab, and one dedicated electrophysiology lab).

As proposed in the CON application for the MFP, the fit-out of the space will integrate the interventional cardiac services provided in the laboratories with a wide array of diagnostic services to provide cardiac patients with more comprehensive and convenient access. Among the interventional services that the HVI will provide in a “one-stop” environment of care are elective and emergency angioplasty procedures, pacemaker/defibrillator implantation, electrophysiology, as well as vascular and peripheral stenting.

Non-invasive diagnostic studies that will be offered in the same space will include ECG, stress testing, echocardiograms (stress echo, TEE), holter and ambulatory blood pressure monitoring, tilt table studies, pacemaker and AICD evaluation and follow up. Adjacency of these services to new and updated catheterization, VIR and EPS labs will help speed diagnosis and treatment, and facilitate the development of clinical pathways. The co-location of these services will also foster collaboration between interventional cardiologists and their non-interventional colleagues who will be overseeing other aspects of the patient’s treatment.



### **Current and Proposed Equipment Operated at Hospital and Mill River**

The Hospital currently possesses and operates five nuclear cameras, including the unit this CON application seeks to replace, which is currently located at the Mill River facility. Two nuclear cameras (a GE Infinia and GE Infinia Hawkeye) are operated in the Hospital's existing radiology suite. Two additional nuclear cameras are operated at the Hospital's Tully Center, which offers outpatient services, located at 32 Strawberry Hill Court in Stamford.

The Hospital's existing radiology suite will not be relocated and will be substantially isolated from the HVI once the new Specialty Building is open. The Hospital is proposing to replace the GE Ventri nuclear camera that it currently operates at the Mill River Cardiology Imaging Center with a GE Optima SPECT / CT Camera System to be located within the HVI of the new Specialty Building. The unit had previously been leased by the Hospital's employed cardiology group – "The Heart Physicians" – beginning in 2006. The Hospital took responsibility for the lease when The Heart Physicians joined Stamford Health's employed physician network – Stamford Health Integrated Practices (SHIP) in 2011.

The Mill River Cardiology Imaging Center is currently located adjacent to the offices of Stamford Health's employed cardiology group - The Heart Physicians. However, it is planned that The Heart Physicians will be relocated to a new Medical Office Building (Integrated Care Pavilion) to be constructed on the Hospital's main campus- adjacent to the new Specialty Building- and projected to open in late Fall 2016.

Thus, as the Hospital prepares to relocate its cardiology group it is also proposing the relocation and upgrade of the nuclear imaging technology, which is now at the end of its useful life, to now offer dedicated cardiac SPECT/ CT services in the new HVI.

#### **b. Provide letters that have been received in support of the proposal.**

Please see Exhibit A for letters received in support of the proposal.

#### **c. Provide the Manufacturer, Model, Number of slices/tesla strength of the proposed scanner (as appropriate to each piece of equipment).**

The proposed GE Camera is a GE Optima NM/CT 640 with an integrated low-dose, 4 slice CT sub-system designed for attenuation correction. Please see Exhibit B for a copy of the GE Healthcare quotation for the Hospital's purchase of the new SPECT /CT system.

**d. List each of the Applicant's sites and the imaging modalities and other services currently offered by location.**

Modalities	Stamford Hospital	Tully Health Center	Darien Imaging Center	Chelsea Piers	Mill River (Office of The Heart Physicians)*	Tully Urgent Care
Diagnostic Radiology	X	X	X	X		X
CT Scan	X	X	X			
MRI	X	X	X			
PET		X (mobile)				
Ultrasound	X	X	X			
Mammography	X	X	X			
Nuclear Medicine	X	X			X	
Interventional Radiology	X					
Bone Density		X	X			
Lab	X	X				X
Inpatient	X					
Outpatient	X	X	X	X	X	
Emergency / Urgent Care	X	X				X
Cardiac Stress Testing	X	X			X	

\* To be relocated to the Hospital's new HVI upon opening of the new Specialty Building.

**2. Clear Public Need**

**a. Explain why there is a clear public need for the proposed equipment. Provide evidence that demonstrates this need.**

As noted in Response 1A above, the Hospital's existing GE Ventri camera has reached the end of its useful life. As the Hospital's employed cardiology group – The Heart Physicians – moves onto the Hospital's main campus, the Hospital believes that this is the correct time to replace the existing nuclear camera with the upgraded technology offered by a combined SPECT / CT system, rather than incur the costs of disassembling, moving and reassembling an obsolete piece of equipment.

In its 2013 Community Health Needs Assessment, the Hospital identified cardiovascular diseases to be among the leading causes of hospitalization and death in the



Hospital's service area. This is consistent with state and national trends – with over one-third of adults in the nation managing one or more cardiovascular diseases. In addition to being the first and third leading causes of death nationwide, heart disease and stroke result in serious illness and disability, decreased quality of life, and hundreds of billions of dollars in economic loss every year.<sup>1</sup>

The combination of SPECT and CT systems provides nuclear medicine physicians with a valuable tool in diagnosis and treatment planning through the combination of anatomic and functional images into a single registered dataset acquired in a single imaging session. These combined datasets provide increased levels of confidence not only in locating abnormal radiopharmaceutical distributions but also in differentiating between abnormal and normal uptake in body regions of complex anatomy. In addition, the combination of SPECT and CT provides the capability for accurate attenuation correction of measured radiopharmaceutical distributions.

### **Higher quality imaging**

The proposed GE Optima SPECT / CT Camera system will allow the Hospital to provide its patients higher quality myocardial perfusion studies in a comprehensive diagnostic and interventional Heart and Vascular Institute Center of Excellence. The CT component of the proposed GE Optima Camera delivers attenuation correction for the myocardial perfusion imaging studies which improves the diagnostic accuracy of the studies. Nuclear cardiology imaging has certain inherent limitations due to the variation and the density of tissues within the body. For example, when imaging the heart, overlying breast or adipose tissue can create shadows and attenuation artifacts which inhibit the ability to interpret the studies in diagnostic heart disease.<sup>2</sup> To mitigate the attenuation artifacts, the CT component of the proposed GE Optima camera will remove these artifacts. This will result in a higher quality myocardial perfusion imaging study which decreases false positive results and eliminates unnecessary follow up testing.<sup>3</sup> While one of the cameras in the Hospital's Radiology suite does have CT attenuation correction, its location is geographically isolated from the new HVI. Relocation is not possible as the camera is used for numerous other studies beyond cardiac (e.g. bone scans, renal scans, HIDA (gallbladder) scans, brain specs, white blood cell scans, bleeding scans, Meckel Diverticular scans and thyroids scans). Further, the volume of myocardial perfusion imaging studies currently performed at the Mill River location cannot be accommodated by the Hospital's one existing GE Infinia Hawkeye SPECT / CT camera.

---

<sup>1</sup> *Healthy People 2020 Topics and Objectives: Heart Disease and Stroke.*  
<http://healthypeople.gov/2020/topicsobjectives2020/overview.aspx?topicid=21>

<sup>2</sup> Seo Y., Mari C., Hasegawa B. H. *Technological development and advances in single-photon emission computed tomography/computed tomography.* Seminars in Nuclear Medicine. 2008;38(3):177–198. doi: 10.1053/j.semnuclmed.2008.01.001

<sup>3</sup> *Id.* See also, Pazhenkottil AP, Ghadri JR, Nkoulou RN, Wolfrum M, Buechel RR, Küest SM, Husmann L, Herzog BA, Gaemperli O, Kaufmann PA. *Improved outcome prediction by SPECT myocardial perfusion imaging after CT attenuation correction.* J Nucl Med. 2011;52:196–200.

### **Larger Field of View**

The proposed GE Optima Camera will also allow for a larger field of view to accommodate the Hospital's larger sized patients.<sup>4</sup> With the increasing rates of obesity seen in the Hospital's patient population – the Hospital has found it difficult to obtain accurate images for these patients on smaller footprint cameras. The existing GE Ventri camera that will be replaced has a small footprint, while the proposed GE Optima Camera offers a large field of view that can accommodate obese and non-ambulatory patients. In addition, the table of the large field of view cameras can accommodate heavier and more debilitated patients who require adaptive and other medical equipment.

### **Lower Radiation and More Efficient Image Capture**

Currently, patients undergoing myocardial perfusion testing without attenuation correction are required to be scanned twice. The patient is initially scanned supine; then repositioned in a prone state and scanned a second time. Although the patient is not re-injected, the prone position can be very uncomfortable and unstable for large breasted or barrel chested patients. If a patient is unstable then there could be inaccuracies in the attenuation correction or the scan may have to be repeated a third time.

While the radiation dose from the CT portion of the scan does need to be taken into account when considering overall radiation exposure, it is important to note that the Hospital adheres to "Image Wisely" guidelines of the American College of Radiology and the Radiological Society of North America's Joint Task Force on Adult Radiation Protection. These guidelines have resulted in processing techniques that lower the CT portion of additional radiation to negligible levels.

Accurate diagnosis– including the use of nuclear stress test – is a critical first step in the effective treatment of heart disease. In order to meet the demand for accurate diagnoses – the Hospital proposes to upgrade the existing GE Ventri Camera (which has reached the end of its useful life) with the more clinically advanced GE Optima camera. The proposed GE Optima camera will provide superior image quality with shorter image acquisition times and thus, less radiation exposure to patients. Furthermore, the addition of CT attenuation will allow the Hospital to more effectively provide myocardial perfusion imaging studies for larger and more physically debilitated patients.

#### **b. Provide the utilization of existing health care facilities and health care services in the Applicant's service area.**

The Hospital has no information on whether other providers in its service area have the same capability.

---

<sup>4</sup> Fiechter M, Gebhard C, Fuchs TA, et al. *Cadmium-zinc-telluride myocardial perfusion imaging in obese patients*. J Nucl Med. 2012;53:1401–1406.



- c. Complete Table 1 for each piece of equipment of the type proposed currently operated by the Applicant at each of the Applicant's sites.

**Table 1: Existing Equipment Operated by the Applicant**

Provider Name Street Address Town, Zip Code	Description of Service *	Hours/Days of Operation **	Utilization *** FY14
Stamford Hospital 30 Shelburne Road Stamford, CT 06902	Unit 1: GE Infinia  Unit 2: GE Infinia Hawkeye – CT 2 Slice	Monday – Friday 7 AM – 4 PM  Emergency Call 7 days	1,308  <i>Data is not tracked by machine; breakdown between 2 units unavailable.</i>
Tully Health Center 32 Strawberry Hill Court Stamford, CT 06902	Unit 1: Philips Forte  Unit 2: Philips Axis	Monday – Friday 7 AM – 4 PM	1,220  <i>Data is not tracked by machine; breakdown between 2 units unavailable.</i>
Mill River Cardiology Imaging Center 80 Mill River Street, Suite 1400 Stamford, CT 06902	Unit 1: GE Ventri	Monday – Friday 7 AM – 3:30 PM	704

\* Include equipment strength (e.g. slices, tesla strength), whether the unit is open or closed (for MRI)

\*\* Days of the week unit is operational, and start and end time for each day; and

\*\*\* Number of scans/exams performed on each unit for the most recent 12-month period (identify period).

- d. Provide the following regarding the proposal's location:

- i. The rationale for locating the proposed equipment at the proposed site;

As noted in Response 1a above – with the construction of the Hospital's new Specialty Building, and the creation of the HVI, the Hospital will create a "one-stop" environment that integrates interventional cardiac services with a wide array of diagnostic services to provide cardiac patients with more comprehensive and convenient access than is presently the case. Adjacency of diagnostic services to new and updated catheterization, VIR and EPS labs will help speed diagnosis and treatment, and facilitate the development of clinical pathways. The co-location of these services will also foster collaboration between interventional cardiologists and their non-interventional colleagues who will be overseeing other aspects of the patient's treatment.

The two (2) nuclear cameras currently operated in the Hospital's existing radiology suite (a GE Infinia and GE Infinia Hawkeye) will not be relocated within the new facility and will be substantially isolated from the HVI once the new facility is open. Furthermore, these cameras cannot be dedicated for use by the HVI as they are also used

to complete bone scans, renal scans, HIDA (gallbladder) scans, brain specs, white blood cell scans, bleeding scans, Meckel Diverticular scans and thyroid scans.

Thus, the Hospital is proposing to replace, upgrade and relocate the GE Ventri nuclear camera that it currently operates at the Mill River Cardiology Imaging Center to the HVI- thereby enabling the delivery of dedicated cardiac SPECT/ CT services within the HVI.

The distance between the Mill River and Shelburne Road sites is approximately 0.5 miles and therefore requires a negligible difference in travel time for patients. Also, as noted above, the Mill River Cardiology Imaging Center is currently located adjacent to the offices of The Heart Physicians. However, it is planned that The Heart Physicians will be relocated to a new Medical Office Building (Integrated Care Pavilion) to be constructed on the Hospital Campus- adjacent to the new Specialty Building- and projected to open in late Fall 2016.

**ii. The population to be served, including specific evidence such as incidence, prevalence, or other demographic data that demonstrates need;**

The population to be served by the proposed GE Optima SPECT / CT system is the same population currently being served by the existing GE Ventri nuclear camera. The population includes residents from the towns that make up the Hospital's Primary and Secondary Service areas as listed below, as well as patients referred from beyond these towns.

*Primary Service Area:* Stamford, Darien

*Secondary Service Area:* Norwalk, Greenwich, New Canaan, Westport, Wilton, Weston

As noted in Response 2a above – Stamford Hospital's 2013 Community Health Needs Assessment identified cardiovascular diseases to be among the leading causes of hospitalization and death in the Hospital's service area. Accurate diagnosis– including the use of nuclear stress testing – is a critical first step in the effective treatment of heart disease.

In the past three fiscal years, an average of 1,030 patients have undergone stress testing with myocardial perfusion imaging utilizing the three existing nuclear cameras at the main campus of Stamford Hospital and the Mill River Cardiology Imaging Center.

**iii. How and where the proposed patient population is currently being served;**

The patient population is currently being served at the Mill River Cardiology Imaging Center located at 80 Mill River Street in Stamford Connecticut, as well as in the Nuclear Imaging Department of Stamford Hospital located at 30 Shelburne Road in

Stamford Connecticut. The patient population will be the same with the proposed GE Optima SPECT / CT system.

**iv. All existing providers (name, address) of the proposed service in the towns listed above and in nearby towns;**

The Hospital is of the understanding that there are no other providers of SPECT imaging with CT attenuation in the towns listed above.

**v. The effect of the proposal on existing providers; and**

The Hospital does not expect there to be any significant impact on existing providers because the proposed GE Optima Camera is simply replacing and relocating one of the Hospital's existing SPECT cameras and is expected to serve the same population being served now with the GE Ventri camera at Mill River.

**vi. If the proposal involves a new site of service, identify the service area towns and the basis for their selection.**

Not Applicable

**e. Explain why the proposal will not result in an unnecessary duplication of existing or approved health care services.**

The proposed GE Optima Camera will replace the GE Ventri Camera currently operated at the Mill River Cardiology Imaging Center, and relocate it to the HVI in the new Specialty Building. The proposed GE Optima Camera will perform the same myocardial perfusion imaging studies as the old GE Ventri that it is replacing and the old GE Ventri will be dismantled and returned to the manufacturer. As a result, the number of nuclear cameras operated by the Hospital will remain the same.

The existing GE Infinia Hawkeye SPECT / CT Camera operated at the Hospital does not have the capacity to accommodate the volume currently performed at the Mill River Cardiology Imaging Center. Furthermore, the two nuclear cameras in service at the Hospital are operated in the Nuclear Medicine Department – a department that will not be relocated with the opening of the new Specialty Building. This results in a significant geographic distance between the Nuclear Medicine Department (located in a portion of the old Stamford Hospital facility) and the new HVI (located in the newest portion currently under construction) thereby creating inefficiencies in patient flow, and a barrier to the “one stop” destination for diagnosis and treatment that has been planned for the HVI.

### **3. Actual and Projected Volume**

**a. Complete the following tables for the past three fiscal years (“FY”), current fiscal year (“CFY”), and first three projected FYs of the proposal, for each of**



the Applicant's existing and proposed pieces of equipment (of the type proposed, at the proposed location only). In Table 2a, report the units of service by piece of equipment, and in Table 2b, report the units of service by type of exam (e.g. if specializing in orthopedic, neurosurgery, or if there are scans that can be performed on the proposed scanner that the Applicant is unable to perform on its existing scanners).

**Table 2a: Historical, Current, and Projected Volume, by Equipment Unit**

	Actual Volume (Last 3 Completed FYs)			CFY Volume*	Projected Volume (First 3 Full Operational FYs)**		
	FY2012	FY2013	FY2014	FY 2015 - YTD MAY Ann.	FY17	FY18	FY19
Stamford Hospital - GE Infinia	745	717	644	654	645	645	645
Stamford Hospital - GE Infinia Hawkeye - CT 2 Slice	745	717	644	654	645	645	645
Stamford Hospital - Proposed GE Optima (HVI Suite)	n/a	n/a	n/a	n/a	722	722	722
Mill River - GE Ventri	643	626	685	704	n/a	n/a	n/a
<b>Total</b>	<b>2,132</b>	<b>2,060</b>	<b>1,973</b>	<b>2,012</b>	<b>2,012</b>	<b>2,012</b>	<b>2,012</b>

\* For periods greater than 6 months, report annualized volume, identifying the number of actual months covered and the method of annualizing. For periods less than six months, report actual volume and identify the period covered.

\*\* If the first year of the proposal is only a partial year, provide the first partial year and then the first three full FYs. Add columns as necessary.

\*\*\* Identify each scanner separately and add lines as necessary. Also break out inpatient/outpatient/ED volumes if applicable.

\*\*\*\* Fill in years. In a footnote, identify the period covered by the Applicant's FY (e.g. July 1-June 30, calendar year, etc.).



**Table 2b: Historical, Current, and Projected Volume, by Type of Scan/Exam**

	Actual Volume (Last 3 Completed FYs)			CFY Volume*	Projected Volume (First 3 Full Operational FYs)**		
	FY2012	FY2013	FY2014	FY 2015 - YTD MAY Ann.	FY17	FY18	FY19
Stamford Hospital - Myocardial SPECT - Multiple Study	418	374	329	272	946	946	946
Stamford Hospital - Myocardial SPECT Single Study	5	7	5	0	27	27	27
Stamford Hospital - Other Non-Cardiac Study	1,066	1,053	954	1,037	1,039	1,039	1,039
Mill River- Myocardial SPECT - Multiple Study	600	606	666	674	n/a	n/a	n/a
Mill River - Myocardial SPECT Single Study	43	19	16	27	n/a	n/a	n/a
Mill River - Other Non- Cardiac Study	0	1	3	3	n/a	n/a	n/a
<b>Total</b>	<b>2,132</b>	<b>2,060</b>	<b>1,973</b>	<b>2,012</b>	<b>2,012</b>	<b>2,012</b>	<b>2,012</b>

\* For periods greater than 6 months, report annualized volume, identifying the number of actual months covered and the method of annualizing. For periods less than six months, report actual volume and identify the period covered.

\*\* If the first year of the proposal is only a partial year, provide the first partial year and then the first three full FYs. Add columns as necessary.

\*\*\* Identify each type of scan/exam (e.g. orthopedic, neurosurgery or if there are scans/exams that can be performed on the proposed piece of equipment that the Applicant is unable to perform on its existing equipment) and add lines as necessary.

\*\*\*\* Fill in years. In a footnote, identify the period covered by the Applicant's FY (e.g. July 1-June 30, calendar year, etc.).

- b. Provide a breakdown, by town, of the volumes provided in Table 2a for the most recently completed full FY.**

<b>FY14</b>	<b>Stamford Hospital</b>	<b>Mill River</b>	<b>Total</b>
Stamford	890	495	1385
Darien	49	31	80
Norwalk	89	44	133
Greenwich	60	33	93
Wilton	8	3	11
Weston	5	0	5
Westport	12	6	18
New Canaan	32	20	52
Other	143	53	196
<b>TOTAL</b>	<b>1288</b>	<b>685</b>	<b>1973</b>

- c. Describe existing referral patterns in the area to be served by the proposal.**

Patients are referred to the Stamford Hospital Nuclear Medicine Department and the Mill River Cardiology Imaging Center from various internal medicine and cardiology practices within the Hospital's primary and secondary service areas.

- d. Explain how the existing referral patterns will be affected by the proposal.**

The Hospital does not expect any change in referral patterns as a result of this proposal.

- e. Explain any increases and/or decreases in volume seen in the tables above.**

Volume declines from FY2012 – FY2014 as shown in Table 2(a) are believed to be driven by a number of factors – including:

- the shift of a portion of cardiac nuclear stress test volume to stress echo exams which can be performed by cardiologists in their offices.
- Severe shortages of the radioisotope technetium-99 (Tc99) between 2008-2010 resulted in increased radiopharmaceutical prices; this led not only to changes in practice patterns by physicians, but also increased scrutiny by managed care companies before authorizing an exam – particularly for cardiac perfusion studies.
- the shift of a portion of oncology related nuclear scans to instead be performed on a PET/CT unit

It is noted that FY15 YTD volume is projected to be up from FY14 levels and the Hospital is projecting volume to remain essentially flat going forward (FY17-FY19).

**f. Provide a detailed explanation of all assumptions used in the derivation/ calculation of the projected volume by scanner and scan type.**

Volumes are based on historical and current fiscal year volume. Given the replacement nature of this proposal, no incremental volumes have been projected. It is expected that the approximately 705 outpatient cardiac perfusion studies that are currently performed at Mill River will be shifted to the proposed GE Optima unit in the HVI, along with approximately 25 outpatient cardiac perfusion studies that are currently performed at the Hospital. The Hospital currently performs approximately 250 cardiac perfusion studies on inpatients and observation patients annually; these studies will continue to be performed on the SPECT/CT system located in the existing Nuclear Medicine suite.

**g. Provide a copy of any articles, studies, or reports that support the need to acquire the proposed scanner, along with a brief explanation regarding the relevance of the selected articles.**

- 1) “Improved outcome prediction by SPECT Myocardial Perfusion Imaging After CT Attenuation Correction” discusses the benefits of Attenuation Correction in Myocardial Perfusion Imaging studies- including improved image quality and diagnostic accuracy – as well as incremental prognostic value allowing for improved risk stratification of patients.
- 2) “A review on the clinical uses of SPECT/CT” discusses the capabilities of SPECT/CT for improving specificity in the imaging of various diseases and laying out the advantages of better attenuation correction – particularly in precisely defining the diagnostic and prognostic profile of cardiovascular patients.
- 3) “Clinical validation of SPECT attenuation correction using x-ray computed tomography-derived attenuation maps: Multicenter clinical trial with angiographic correlation” discusses the impact that CT-based attenuation correction of SPECT images has on consistently improving overall diagnostic performance of readers with different interpretive attitudes and experience.
- 4) Cadmium-Zinc-Myocardial Perfusion Imaging in Obese Patients” discusses the benefits of using SPECT / CT imaging on obese patients.
- 5) “Technological Development and Advances in SPECT/CT” provides an overview of the benefits of SPECT/CT with a specific section dedicated to the benefits of such technology in cardiac imaging.
- 6) “Healthy People 2020 Topics and Objectives: Heart Disease and Stroke.” describes heart disease and stroke as being the first and third leading causes of death nationwide and that the two conditions also result in serious illness and



disability, decreased quality of life, and hundreds of billions of dollars in economic loss every year.

Please see Exhibit C for copies of such articles.

#### 4. Quality Measures

**a. Submit a list of all key professional, administrative, clinical, and direct service personnel related to the proposal. Attach a copy of their Curriculum Vitae.**

- Sarah Bull – Chief Physicist
- Harvey Leon Hecht, MD, D.A.B.R., F.A.C.R., D.A.B.N.M. – Radiologist
- Eilish C. Hourihan MS, RN, NEA-BC – Service Line Director, Heart and Vascular Institute
- David H. Hsi, MD – Chief, Cardiology
- Michael H. King, MD – Interim Chair, Department of Radiology
- Marci D. Paulk, RT(R), CRA, MHA
- Kathleen A. Silard, RN, BSN, MS, FACHE – Executive Vice President / Chief Operating Officer
- Beth Ann Vara – Executive Director of Radiology
- Jane Vigilante, RT,R,N - Chief Nuclear Medicine Technologist

Please see Exhibit D for copies of each individual's curriculum vitae.

**b. Explain how the proposal contributes to the quality of health care delivery in the region.**

The existing GE Ventri camera at the Mill River location has reached the end of its useful life. By replacing the existing nuclear camera with the upgraded technology offered by SPECT / CT, the Hospital will possess more accurate images and thereby more accurately diagnose its patients. See Response 2a for the expected benefits of the new GE Optima NM/CT 640 SPECT / CT Camera System.

#### 5. Organizational and Financial Information

**a. Identify the Applicant's ownership type(s) (e.g. Corporation, PC, LLC, etc.).**

Connecticut non-stock corporation

**b. Does the Applicant have non-profit status?**

☒ Yes (Provide documentation) ☐ No

Please see Exhibit E for documentation.

- c. Provide a copy of the State of Connecticut, Department of Public Health license(s) currently held by the Applicant and indicate any additional licensure categories being sought in relation to the proposal.

Please see Exhibit F for a copy of the Hospital's license.

d. Financial Statements

- i. **If the Applicant is a Connecticut hospital:** Pursuant to Section 19a-644, C.G.S., each hospital licensed by the Department of Public Health is required to file with OHCA copies of the hospital's audited financial statements. If the hospital has filed its most recently completed fiscal year audited financial statements, the hospital may reference that filing for this proposal.
- ii. **If the Applicant is not a Connecticut hospital (other health care facilities):** Audited financial statements for the most recently completed fiscal year. If audited financial statements do not exist, in lieu of audited financial statements, provide other financial documentation (e.g. unaudited balance sheet, statement of operations, tax return, or other set of books.)

Stamford Hospital's most recent audited financial statements (FY 2013) are on file with OHCA.

- e. Submit a final version of all capital expenditures/costs as follows:

**Table 3: Proposed Capital Expenditures/Costs**

Medical Equipment Purchase	\$539,308
Imaging Equipment Purchase	
Non-Medical Equipment Purchase	
Land/Building Purchase *	
Construction/Renovation **	\$225,000
Other Non-Construction (Specify)	
<b>Total Capital Expenditure (TCE)</b>	\$764,308
Medical Equipment Lease (Fair Market Value) ***	\$
Imaging Equipment Lease (Fair Market Value) ***	
Non-Medical Equipment Lease (Fair Market Value) ***	
Fair Market Value of Space ***	
<b>Total Capital Cost (TCC)</b>	\$764,308
<b>Total Project Cost (TCE + TCC)</b>	\$764,308
Capitalized Financing Costs (Informational Purpose Only)	
Total Capital Expenditure with Cap. Fin. Costs	\$764,308

\* If the proposal involves a land/building purchase, attach a real estate property appraisal including the amount; the useful life of the building; and a schedule of depreciation.

\*\* If the proposal involves construction/renovations, attach a description of the proposed building work, including the gross square feet; existing and proposed floor plans; commencement date for the construction/renovation; completion date of the construction/renovation; and commencement of operations date.

\*\*\* If the proposal involves a capital or operating equipment lease and/or purchase, attach a vendor quote or invoice; schedule of depreciation; useful life of the equipment; and anticipated residual value at the end of the lease or loan term.

The construction relating to this proposal includes the build-out of a new 357 square foot Gamma room with an adjacent and supporting Hot Lab room of 95 square feet. Construction within the space includes walls and wall covering, doors and frames, flooring, HVAC, electrical, medical gases, and acoustical ceiling system. The work is concurrent with the construction of the Specialty Building in which this function is housed, so the construction also includes the structural steel and concrete work to create this space within the building. The electrical and HVAC infrastructure systems will be part of the new electrical and mechanical systems installed for the entire new building. Please see Exhibit G for a copy of the building plans.

Note: the cost of construction for the nuclear camera room, adjacent hot lab and purchase of the equipment are all included within the previously approved Master Facility Plan budget of \$450 million.

- f. List all funding or financing sources for the proposal and the dollar amount of each. Provide applicable details such as interest rate; term; monthly payment; pledges and funds received to date; letter of interest or approval from a lending institution.**

The capital costs for the proposed project are included in the funding from the originally approved \$450 million capital budget related to the Hospital's Master Facility Plan (MFP). The MFP is being funded through a combination of debt (\$250 million in revenue bonds), philanthropy (projected at \$150 million), and cash from operations (\$50 million).

- g. Demonstrate how this proposal will affect the financial strength of the state's health care system.**

The replacement and relocation of the GE Ventri system with the proposed GE Optima System will allow for improved efficiency and precision of cardiac nuclear imaging at the Hospital. The new SPECT /CT system will allow for better imaging, which will reduce the need for additional and unnecessary testing to assess false positives and negatives that may result from attenuation artifacts. In addition, modern SPECT /CT machines can reduce scan time and allow for more efficient use of the equipment. As one clinical journal notes "the inclusion of a highly efficient SPECT system can decrease the scan time of the SPECT study, and in doing so also increases the utilization of CT and patient throughput compared to conventional SPECT/CT systems."<sup>5</sup> Overall, the proposal

<sup>5</sup> Seo Y., Mari C., Hasegawa B. H. *Technological development and advances in single-photon emission computed tomography/computed tomography*. Seminars in Nuclear Medicine. 2008;38(3):177–198. doi: 10.1053/j.semnuclmed.2008.01.001



will result in safer and more accurate nuclear cardiology services in a one-stop Heart and Vascular Center of Excellence.

## 6. Patient Population Mix: Current and Projected

- a. Provide the current and projected patient population mix (based on the number of patients, not based on revenue) with the CON proposal for the proposed program.

**Table 4: Patient Population Mix**

	FY 15 YTD May	FY 17	FY 18	FY 19
Medicare*	54%	54%	54%	54%
Medicaid*	12%	12%	12%	12%
CHAMPUS & TriCare	0%	0%	0%	0%
<b>Total Government</b>	66%	66%	66%	66%
Commercial Insurers*	33%	33%	33%	33%
Uninsured	1%	1%	1%	1%
Workers Compensation	0%	0%	0%	0%
<b>Total Non-Government</b>	34%	34%	34%	34%
<b>Total Payer Mix</b>	100%	100%	100%	100%

\* Includes managed care activity.

\*\* New programs may leave the “current” column blank.

\*\*\* Fill in years. Ensure the period covered by this table corresponds to the period covered in the projections provided.

- b. Provide the basis for/assumptions used to project the patient population mix.

The payer mix represented in Table 4 is based on the patient population currently being served by the Hospital’s nuclear imaging service; the Hospital does not project material changes in the patient population mix in future years.

## 7. Financial Attachments I & II

- a. Provide a summary of revenue, expense, and volume statistics, without the CON project, incremental to the CON project, and with the CON project. Complete Financial Attachment I. (Note that the actual results for the fiscal year reported in the first column must agree with the Applicant’s audited financial statements.) The projections must include the first three full fiscal years of the project.

Please see attached Exhibit H.

- b. Provide a three year projection of incremental revenue, expense, and volume statistics attributable to the proposal by payer. Complete Financial

**Attachment II. The projections must include the first three full fiscal years of the project.**

Please see attached Exhibit I.

- c. Provide the assumptions utilized in developing both Financial Attachments I and II (e.g., full-time equivalents, volume statistics, other expenses, revenue and expense % increases, project commencement of operation date, etc.).**

This proposal is for equipment replacement and relocation; as such – no incremental volumes have been projected. Please see Tables 2a and 2b for volume projections related to this project.

The only incremental expenses that have been projected are the depreciation expense associated with the cost of the proposed GE Optima camera and the construction of the space, as well as the cost of a new service contract beginning in year 2 of operation.

- d. Provide documentation or the basis to support the proposed rates for each of the FYs as reported in Financial Attachment II. Provide a copy of the rate schedule for the proposed service(s).**

Please see the Hospital's chargemaster as filed with OHCA.

- e. Provide the minimum number of units required to show an incremental gain from operations for each fiscal year.**

This proposal is for equipment replacement and relocation; as such – no incremental volumes have been projected. Please see Tables 2a and 2b for volume projections related to this project.

- f. Explain any projected incremental losses from operations contained in the financial projections that result from the implementation and operation of the CON proposal.**

The incremental losses are due to the incremental depreciation and service contract expenses described in 6(c) above.

- g. Describe how this proposal is cost effective.**

The replacement of outdated nuclear imaging equipment with more efficient and effective equipment will result in higher quality imaging studies and a reduction in the number of false positive or negative tests that would require additional follow up and testing.

# EXHIBIT A





July 30, 2015

State of Connecticut  
Department of Public Health  
Office of Health Care Access Division  
410 Capital Avenue  
Hartford, CT 06134

RE: Certificate of Need Application to Acquire and Operate a SPECT/CT Camera System at The Stamford Hospital in Stamford, CT.

To whom it may concern:

I am writing in support of Stamford Hospital's CON application to replace and relocate one of its current nuclear cameras with a new, updated SPECT / CT camera system. Stamford Hospital is proposing to replace and relocate its existing GE Ventri nuclear camera currently operated at 80 Mill River Street with an upgraded unit – the GE Optima NM/CT 640 SPECT / CT Camera System to be operated in the new Heart and Vascular Institute (HVI) Center of Excellence currently under construction on the Stamford Hospital campus at 30 Shelburne Road in Stamford.

The proposed GE Optima Camera will allow the Hospital to provide its patients with higher quality myocardial perfusion studies in the new comprehensive diagnostic and interventional HVI Center of Excellence. The upgraded technology combines SPECT and CT technology which provides nuclear medicine physicians with a valuable tool in diagnosis and treatment planning through the combination of anatomic and functional images into a single registered dataset acquired in a single imaging session. These combined datasets provide increased levels of confidence not only in locating abnormal radiopharmaceutical distributions but also in differentiating between abnormal and normal uptake in body regions of complex anatomy.

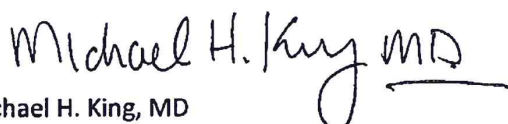
In addition, the combination of SPECT and CT provides the capability for accurate attenuation correction of measured radiopharmaceutical distributions. By removing artifacts often caused by more dense tissues surrounding the heart (e.g. breast or adipose tissues), the CT component of the proposed GE Optima Camera will allow for higher quality, more efficient myocardial

perfusion imaging studies – decreasing false positive results and eliminating the need for unnecessary follow up testing.

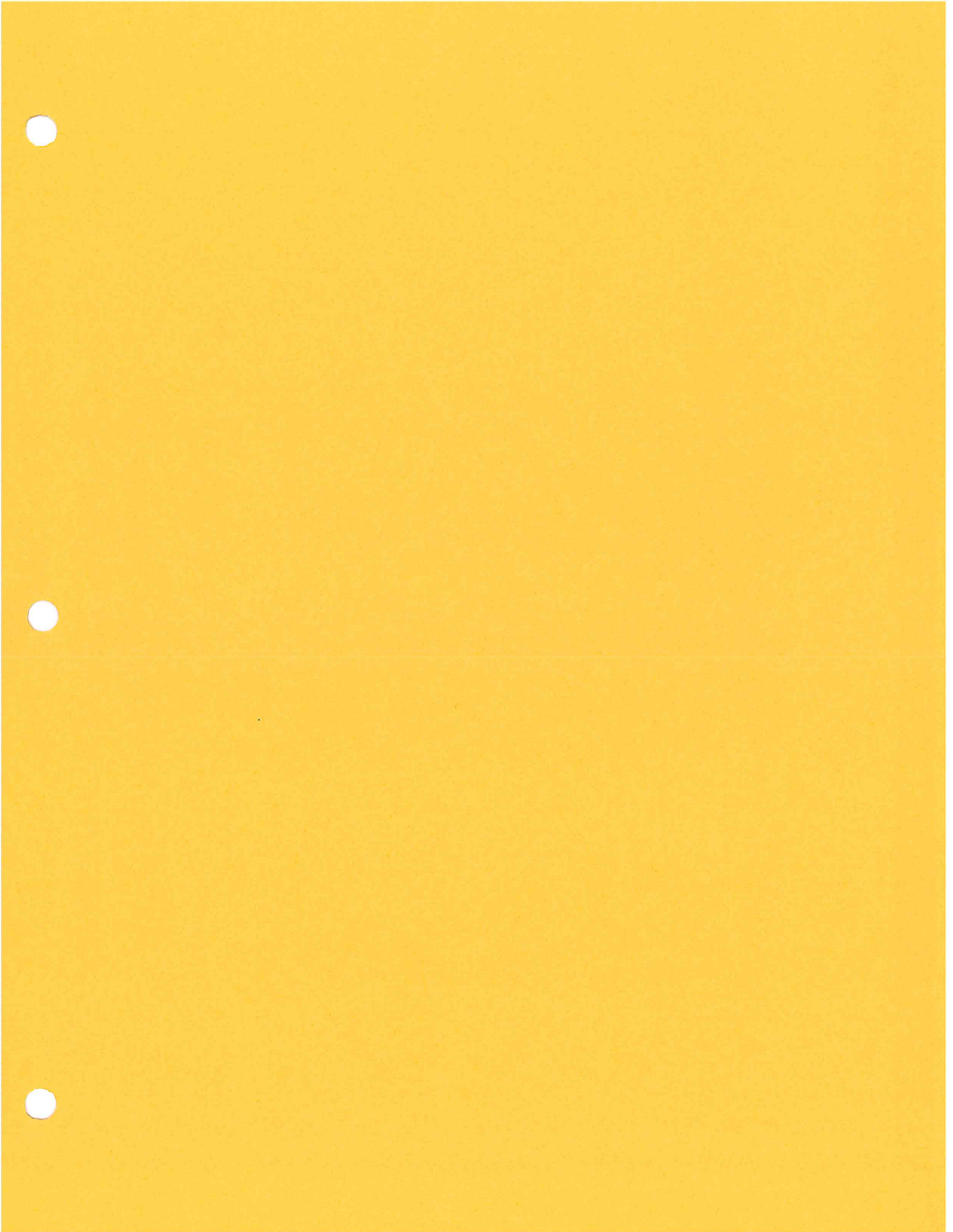
Thus, as the hospital prepares to open its new HVI Center of Excellence, and relocate the nuclear camera currently operated at 80 Mill River Street, I fully support the proposed replacement and upgrade to the GE Optima SPECT / CT camera system.

If you have any questions regarding this request, I would be happy to speak further.

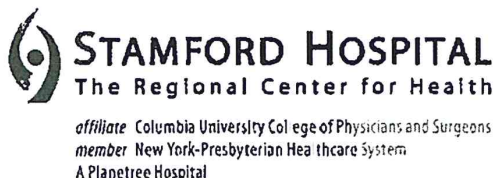
Respectfully submitted,

A handwritten signature in black ink that reads "Michael H. King MD". The signature is written in a cursive style with a horizontal line extending from the end of the "g" in "King".

Michael H. King, MD  
Interim Chair, Department of Radiology







July 30, 2015

State of Connecticut  
Department of Public Health  
Office of Health Care Access Division  
410 Capital Avenue  
Hartford, CT 06134

RE: Certificate of Need Application to Acquire and Operate a SPECT/CT Camera System at The Stamford Hospital in Stamford, CT.

To whom it may concern:

I am writing in support of Stamford Hospital's CON application to replace and relocate one of its current nuclear cameras with a new, updated SPECT / CT camera system. Stamford Hospital is proposing to replace and relocate its existing GE Ventri nuclear camera currently operated at 80 Mill River Street with an upgraded unit – the GE Optima NM/CT 640 SPECT / CT Camera System – to be operated in the new Heart and Vascular Institute (HVI) Center of Excellence currently under construction on the Stamford Hospital campus at 30 Shelburne Road in Stamford.

As part of Stamford Hospital's previously approved Facility Master Plan, a new Specialty Building is scheduled to open in September 2016 which will, among other services, include the new HVI Center of Excellence. This center has been designed to integrate interventional cardiac services provided in four interventional labs, with a wide array of diagnostic services to provide cardiac patients with more comprehensive and convenient access in a "one stop" environment of care. A key component of the diagnostic services to be provided in the HVI Center of Excellence is myocardial perfusion imaging utilizing the proposed GE Optima camera. With the upgrade in technology, and the addition of CT attenuation correction, the GE Optima Camera will provide superior image quality with shorter acquisition times and less radiation exposure to patients and staff than the existing GE Ventri Camera that it will replace.

Due to the variation and the density of tissues within the body, nuclear cardiology imaging has certain inherent limitations as overlying breast or adipose tissues can create shadows and attenuation artifacts which inhibit the ability to accurately interpret myocardial perfusion studies and diagnose heart disease. Utilizing the CT component of the proposed GE Optima Camera, attenuation correction will remove these artifacts and ultimately improve the diagnostic accuracy of the studies performed at Stamford Hospital – decreasing false positive

results and eliminating unnecessary follow up testing. Given the prevalence of cardiovascular diseases in Stamford Hospital's service area, It is imperative that patients have access to efficient and accurate diagnostic services and I therefore fully support the Hospital's CON application to acquire and operate a SPECT / CT Camera system in the new HVI Center of Excellence.

If you have any questions regarding this request, I would be happy to speak further.

Respectfully submitted,



David H. Hsi, MD  
Chief of Cardiology

# **EXHIBIT B**





GE Healthcare

Date: 06-10-2015  
 Quote #: PR6-C40697  
 Version #: 13

Stamford Hospital  
 30 Shelburne Rd  
 Stamford CT 06902-3628

Attn: Timothy N Tinari  
 FMP Capital Procurement Manager  
 Materials Management  
 30 Shelburne Rd Stamford  
 CT 06902-3628

Customer Number :  
 Quotation Expiration Date: 06-26-2015

This Agreement (as defined below) is by and between the Customer and the GE Healthcare business ("GE Healthcare"), each as identified herein. "Agreement" is defined as this Quotation and the terms and conditions set forth in either (i) the Governing Agreement identified below or (ii) if no Governing Agreement is identified, the following documents:

- 1) This Quotation that identifies the Product offerings purchased or licensed by Customer;
- 2) The following documents, as applicable, if attached to this Quotation: (i) GE Healthcare Warrantylies; (ii) GE Healthcare Additional Terms and Conditions; (iii) GE Healthcare Product Terms and Conditions; and (iv) GE Healthcare General Terms and Conditions.

In the event of conflict among the foregoing items, the order of precedence is as listed above.

This Quotation is subject to withdrawal by GE Healthcare at any time before acceptance. Customer accepts by signing and returning this Quotation or by otherwise providing evidence of acceptance satisfactory to GE Healthcare. Upon acceptance, this Quotation and the related terms and conditions listed above (or the Governing Agreement, if any) shall constitute the complete and final agreement of the parties relating to the Products identified in this Quotation.

No agreement or understanding, oral or written, in any way purporting to modify this Agreement, whether contained in Customer's purchase order or shipping release forms, or elsewhere, shall be binding unless hereafter agreed to in writing by authorized representatives of both parties.

By signing below, each party certifies that it has not made any handwritten modifications.

Governing Agreement:	Stamford Hospital MPA #12450
Terms of Delivery:	FOB Destination
Billing Terms:	80% delivery / 20% Installation
Payment Terms:	60 DAYS NET
Total Quote Net Selling Price:	\$539,308.00

#### INDICATE FORM OF PAYMENT:

If "GE HFS Loan" or "GE HFS Lease" is NOT selected at the time of signature, then you may NOT elect to seek financing with GE Healthcare Financial Services (GE HFS) to fund this arrangement after shipment.

☐ Cash/Third Party Loan  
☐ GE HFS Lease  
☐ GE HFS Loan  
☐ Third Party Lease (please identify financing company) \_\_\_\_\_

By signing below, each party certifies that it has not made any handwritten modifications. Manual changes or mark-ups on this Agreement (except signatures in the signature blocks and an indication in the form of payment section below) will be void.

Each party has caused this agreement to be executed by its duly authorized representative as of the date set forth below.

#### CUSTOMER

\_\_\_\_\_  
 Authorized Customer Signature Date

\_\_\_\_\_  
 Print Name Print Title

\_\_\_\_\_  
 Purchase Order Number (if applicable)

GE HEALTHCARE  
 Lawrence Abreu

06-10-2015

\_\_\_\_\_  
 Signature Date

Product Sales Specialist, Nuclear

Email: lawrence.abreu@ge.com  
 Office: +1 781 413 4426  
 Mobile: 781-413-4426  
 Fax: 508-401-6574

1/12



Date: 06-10-2015  
 Quote #: PR6-C40697  
 Version #: 13

**Total Quote Selling Price**  
 Trade-In and Other Credits

**\$539,308.00**  
 \$0.00

**Total Quote Net Selling Price**

-----  
**\$539,308.00**

**To Accept this Quotation**

Please sign and return this Quotation together with your Purchase Order To:  
**Lawrence Abreu**  
 Office: +1 781 413 4426  
 Mobile: 781-413-4426  
 Email: lawrence.abreu@ge.com  
 Fax: 508-401-6574

**Payment Instructions**

Please **Remit** Payment for invoices associated with this quotation to:  
**GE Healthcare**  
**P.O. Box 96483**  
**Chicago, IL 60693**

**To Accept This Quotation**

- Please sign the quote and any included attachments (where requested).
- If requested, please indicate, your form of payment.
- If you include the purchase order, please make sure it references the following information
  - The correct Quote number and version number above
  - The correct Remit To information as indicated in "Payment Instructions" above
  - The correct SHIP TO site name and address
  - The correct BILL TO site name and address
  - The correct Total Quote Net Selling Price as indicated above



GE Healthcare

Date: 06-10-2015  
 Quote #: PR6-C40697  
 Version #: 13

Item No.	Qty	Catalog No.	Description
	1		<b>Optima NM/CT 640</b>
1	1	S0640NA	<p>Optima NM/CT 640 Excel Nuclear Imaging Integrated with an Xeleris 3.1 Workstation</p> <p>The Optima NM/CT 640 Excel is a premium, all purpose, high performance, hybrid SPECT/CT imaging system. It combines an integrated nuclear imaging sub-system featuring a dual-detector free-geometry slim gantry, advanced all-digital Elite NXT detectors with 3/8" detectors, cantilevered patient table and powerful acquisition station, with a dedicated low-dose high resolution CT imaging sub-system designed for attenuation correction of SPECT and anatomic localization of radiotracer uptake in the body.</p> <p>The two Elite NXT detectors are designed for all-purpose nuclear imaging with excellent image quality originating from two highly stable, slim, large rectangular field-of-view digital detectors, featuring five corrections performed on each detected event in real time, even at high count rates. The key features include:</p> <ul style="list-style-type: none"> <li>o 3/8" (9.5 mm) NaI crystal thickness</li> <li>o 59 high quantum efficiency circular PMTs, each coupled with one analog to digital converter (ADC)</li> <li>o Extra Large Rectangular UFOV with no cut-off corners: 21.25" x 15.75" (54 x 40 cm)</li> <li>o Shielded energy range: 40 - 620 keV</li> <li>o Contoured detector housing for optimal cardiac and brain SPECT imaging</li> </ul> <p>The Optima NM/CT 640 Excel features an integrated low-dose, 4 slice CT sub-system designed for attenuation correction and localization with the following key features:</p> <ul style="list-style-type: none"> <li>o GE CT tube (GE MX135CT)</li> <li>o GE Gedi 42 AC Generator</li> <li>o Clinical operational tube current of 10-30 mA and maximum generator power of 4.2 kW</li> <li>o 120 kVp or 140 kVp</li> <li>o 2.0 MHU tube anode heat storage capacity</li> <li>o Scan times of 1 or 2 seconds per rotation</li> <li>o 2.5mm slice thickness on each of the 4 slices</li> <li>o Ceramic detector made of Gadolinium OxySulfide (Gd<sub>2</sub>O<sub>2</sub>S)</li> <li>o Pitch factors of 0.75:1, 1.25:1 and 1.75:1</li> </ul> <p>Optima NM/CT 640 Excel features a wide 70 cm bore and slim gantry with</p>

3/12





Date: 06-10-2015  
 Quote #: PR6-C40697  
 Version #: 13

Item No.	Qty	Catalog No.	Description
			<p>free-geometry, enabling cardiac SPECT (90 degrees), general SPECT (180 degrees), whole body and planar imaging in various geometries to facilitate imaging a wide patient population.</p> <p>The gantry design includes several features designs for maximum clinical versatility and enhanced operational flexibility:</p> <ul style="list-style-type: none"> <li>o Externally mounted detectors for ease of positioning in all major clinical studies, including those for stretcher, standing and seated patients</li> <li>o Simultaneous rapid gantry orientation transitions between procedures</li> <li>o Upright and horizontal detector orientations</li> <li>o Real-time, infrared-based Automatic Body Contouring (ABC) for enhanced scanning efficiency and resolution</li> <li>o User-definable, pre-programmed, home positions for the gantry orientation and patient table set up</li> <li>o Gantry display unit with real-time status display and an intuitive, icon-based 20-function handset-accessible from either side of the gantry</li> <li>o Fast, semi-automatic dual collimator exchange</li> </ul> <p>The Optima NM/CT 640 Excel utilizes an ergonomic, dual-axis patient table, with a cantilevered telescoping design to be used for planar, whole body and SPECT applications. The low-attenuation carbon fiber table top supports a maximum patient weight of 227 kg (500 lb.) and has a maximum scan range of 200 cm (79"). A minimum table height of 59 cm (23.2") facilitates patient loading and unloading from a wheelchair or stretcher.</p> <p>Other key patient table features include:</p> <ul style="list-style-type: none"> <li>o Automated positioning via protocol selection           <ul style="list-style-type: none"> <li>• Easy swivel of table away from gantry to enable collimator changes and facilitate imaging of patients who are seated or on hospital bed/stretcher</li> </ul> </li> <li>o Included patient bed mattress with straps</li> <li>o Manual emergency patient egress</li> <li>o Optional table accessories including a head holder, table extender, arm support, leg support and additional table pads/straps</li> </ul> <p>The Optima NM/CT 640 Excel hybrid SPECT/CT acquisition station is based on a Linux operating system with an Xeleris look-and-feel graphical user interface. The acquisition station performs exam scheduling, protocol editing, NM and CT scan</p>



GE Healthcare

Date: 06-10-2015  
 Quote #: PR6-C40697  
 Version #: 13

Item No.	Qty	Catalog No.	Description
			<p>acquisition, QC acquisition, CT reconstruction along with routing analysis, and networking.</p> <p>Acquisition Station Hardware Features:</p> <ul style="list-style-type: none"> <li>o High performance Intel based HP Z400 computer</li> <li>o Intel Processor - 2.5Ghz</li> <li>o 4 GB RAM (2 x 2 GB)</li> <li>o 160 GB hard drive</li> <li>o Flat panel display (LCD) operating at 1280 x 1024 in true color</li> </ul> <p>Operation is via an interactive, GE common Graphical user interface with the following software features:</p> <ul style="list-style-type: none"> <li>o Simultaneous acquisition and energy spectrum histogram (PHA) display with up to 64 independent windows per detector for multi-isotope/ multi-peak scanning versatility</li> <li>o Acquisition termination by preset time, preset count or manual stop and the ability to resume paused acquisitions for whole body, SPECT, and gated SPECT</li> <li>o Pre-defined or user-configurable protocols for rapid recall and setup</li> <li>o Universal imaging system connectivity via DICOM 3.0 (per DICOM conformance statement) and Interfile 3.3 TCP/IP based protocols</li> <li>o HIS/RIS integrated workflow including DICOM Modality Work List</li> <li>o Ability to connect to broadband/high speed network. This virtual private network (VPN) connection to GE is a single point of access using 3DES encryption for faster data transfer with increased system uptime and productivity.</li> <li>o Data acquisitions may be performed using single or multiple isotopes in any of the following imaging modes: Static, Dynamic, Multi-Gated, Whole Body Scanning, SPECT and Gated SPECT</li> </ul> <p>Xeleris 3.1 Workstation</p> <p>Included in the integrated system is the Xeleris 3.1 functional imaging workstation for Nuclear Medicine, PET, NM/CT and PET/CT processing, analysis, and review system. Designed with productivity in mind, it can accelerate workflow and provides a powerful clinical diagnostic tool to the medical imaging community. Combining streamlined workflow with a comprehensive clinical library and extensive networking capabilities on a functional imaging workstation, Xeleris 3.1 is at the nucleus of productivity in the clinical imaging department. Utilizing the GE Healthcare-wide</p>



Date: 06-10-2015  
 Quote #: PR6-C40697  
 Version #: 13

Item No.	Qty	Catalog No.	Description
			<p>graphical user interface, Xeleris 3.1 is the processing and review platform of the Discovery*, Optima* and Brivo* NM and NM/CT series, Infinia* Hawkeye* 4, Ventri, Discovery PET/CT 600 series, and all other molecular imaging cameras in GE Healthcare's current offering. Xeleris 3.1 provides the automated processing and connectivity necessary in today's demanding environment.</p> <p>Included is X2 AAO Motion DC</p> <p>MDC - Motion Detection and Correction</p> <p>Automated cardiac and general purpose SPECT motion correction integrated into Xeleris applications.</p> <p>Detect and correct automatically for motion in the X and/or Y-axis, with dual head, image masking and gradient mode selectable options for improved accuracy. QA tools include: Cine of original and corrected projection data with reference lines; Side by side original and corrected Sinograms and Selective Linograms; Graphs of X-Shifts and Y-Shifts (in pixels) and Integrated into Myovation Cardiac Suite and other general purpose SPECT reconstruction packages.</p> <ul style="list-style-type: none"> <li>o 23" widescreen flat panel display</li> <li>o Keyboard and mouse</li> </ul>
2	1	H2506TB	<p>Discovery NM LEHR Collimators with Cart</p> <p>D670 Low Energy High Resolution Collimators Includes: o Two LEHR Collimators o Collimators Mounted on a Dedicated Collimator Cart</p>
3	1	H3100PE	An L-shaped metal plate attachable to the wall with an opening for a syringe in order to acquire point source-based flood acquisition at a few meters distance from vertically positioned detector for QA purposes.
4	1	H3100PF	Quality Control Flood Source Holder Kit A large plate mounted at a small distance above the NM detector on which the flood source is positioned in order to perform acquisition of flood studies for QA/QC purposes.
5	1	H3602SL	Center of rotation source holder for Quality assurance , easily attached to Infinia or Ventri table.
6	1	H3100PL	<p>bar phantom for spatial resolution and linearity tests of gamma cameras. The phantom consists of four quadrants with different bar specification:</p> <p>For each of the quadrant, bar spacing is 2.5mm, 3.2mm, 3.5mm &amp; 4.0mm.</p>
7	1	H3100YY	A set of cables designed to support the connection of the system to a 480V UPS for

6/12





Date: 06-10-2015  
 Quote #: PR6-C40697  
 Version #: 13

Item No.	Qty	Catalog No.	Description
			O640 power regulation purposes.
8	1	B77292CA	Service cabinet for system accessories storage
9	1	H3901RH	Cedars Sinai Cardiac Packages (option) A comprehensive set of nuclear cardiology protocols for advanced cardiac analysis, including: o Cedars Sinai Quantitative Perfusion SPECT? (option) o Automatic 3-Dimensional software approach to quantitative Perfusion SPECT. o Cedars Sinai Quantitative Gated SPECT? (option) o An application calculating the ejection fraction of the left ventricle and a 3D surface display is generated. o Cedars Sinai Companion (option) o Optional module for QGS and QPS applications features - 17 segment scores and templates in QPS - Diastolic filling parameters in QGS - Eccentricity ratio in QGS
10	1	H3901NZ	Cedars Sinai Automatic Report Generator An Optional Package Available for the QGS/QPS Applications for Generating Reports
11	1	S8006RZ	Xeleris 3 Plug-in for Evolution Family - JHU RR 1st Resolution recovery license for first workstations or Evolution products
12	1	S8006SC	Xeleris 3 Evolution for Cardiac Software License for a single Xeleris 3 Workstation with one Camera License  This item contains two software licenses that are also available separately.  o Evolution for Cardiac provides EfC provides Evolution Resolution Recovery Reconstruction on SPECT Myocardial Perfusion Imaging (MPI) scans. The EfC application may be utilized to provide equivalent image quality on half-dose or half-time MPI scans. This license H3901ME processes Infinia, Infinia Hawkeye 4, Ventri and Discovery 670 family of camera data. This license can only function with pre-requisite JHU-RR (S8006RZ / S8006S)and (H3602NJ) EFC SPECT CAMERA LICENSE  o Enables Camera capability to provide data for Evolution for Cardiac (EfC). EfC provides Evolution Resolution Recovery reconstruction on SPECT Myocardial Perfusion Imaging (MPI) scans. The EfC application may be utilized to provide equivalent image quality on half-dose or half-time MPI scans. this license H3602NJ is for the Infinia, Infinia Hawkeye 4, Discovery 670 and Ventri family of cameras. This license can only function with pre-requisite JHU-RR (H3901KS/H3901KT) and EFC FOR XELERIS3 (H3901ME)
13	1	W0310NM	8 Days Onsite plus 10 Hours TVA  Eight days onsite delivered in 3 visits, one 4 day, and two 2 day plus 10 hours TVA training for NM Camera System and Workstation.



GE Healthcare

Date: 06-10-2015  
 Quote #: PR6-C40697  
 Version #: 13

Item No.	Qty	Catalog No.	Description
			Onsite training is delivered Monday through Friday between 8AM and 5PM. T&L expenses are included. This training program must be scheduled and completed within 36 months after the date of product delivery.
14	1	E4502JJ	<p>6 KVA UPS for Nuclear Medicine</p> <p>FEATURES/BENEFITS</p> <ul style="list-style-type: none"> <li>• The use of uninterruptible power enables the system imaging to be completed after the loss of supply power, and allows for saving of valuable data and orderly system shutdown</li> <li>• The Online Double Conversion UPS eliminates all power anomalies such as noise, transients, overvoltage and undervoltage, which could damage the imaging system's sensitive computer components</li> <li>• Improves imaging system reliability, reduces service costs, and increases system uptime</li> <li>• Cell Saver Technology provides conditioned power even during severe brownout conditions without depleting battery resources</li> <li>• System monitoring via: LanSafe III / FailSafe III software, (2) RS-232 Ports</li> <li>• PowerPass Module further enhances reliability through Maintenance Bypass Switch which performs maintenance or upgrade your UPS without powering down your critical systems</li> </ul> <p>SPECIFICATIONS</p> <ul style="list-style-type: none"> <li>• Dimensions (H x W x D): 33.6" x 9.9" x 15.8"</li> <li>• Weight: 218 lbs.</li> <li>• Input Voltage: 200 - 240 VAC</li> <li>• Output Voltage: 120/240, 120/208 VAC</li> <li>• Frequency: 45-65 Hz</li> </ul> <p>COMPATIBILITY</p> <ul style="list-style-type: none"> <li>• Maxxus NM</li> </ul> <p>NOTES:</p> <ul style="list-style-type: none"> <li>• Customer is responsible for rigging and arranging for installation with a certified electrician</li> <li>• ITEM IS NON-RETURNABLE AND NON-REFUNDABLE</li> </ul>
15	1	E8500NB	<p>Patient Arm Support for NM, PET/CT, MR</p> <p>Padded Arm Rest combines total arm support and passive restraint, increasing patient</p>

8/12



GE Healthcare

Date: 06-10-2015  
 Quote #: PR6-C40697  
 Version #: 13

Item No.	Qty	Catalog No.	Description
			comfort during extended procedures. Designed to accommodate virtually all patients. Compatible with most Nuclear Imaging systems and can also be used in MRI, CT and PET applications. Constructed with a comfortable, full support polyfoam with a seamless coated finish. Warranty Code: H
16	1	E8500NC	<p>Patient Leg Rest for Nuclear, PET/CT, MRI</p> <p>Contoured Leg Rest prevents low back stress and pain that occurs during supine imaging and treatment, measures 7 in. H x 17 in. D x 13 in. W. Designed to accommodate virtually all patients. Compatible with most Nuclear Imaging systems and can also be used in MRI, CT and PET applications. Constructed with a comfortable, full support polyfoam with a seamless coated finish. Warranty Code: H</p>
17	1	E8007DC	Ivy 7600 Cardiac Trigger Monitor Kit - No Recorder, Americas Labeling. For GEHC Nuclear Med.
18	1	R12022AC	Standard Level 2 service package delivered for the warranty period
	1		<b>Xeleris 3.1</b>
19	3	S8000AF	<p>Xeleris 1 Software and Hardware upgrade to Xeleris 3.1</p> <p>Xeleris* 3.1 functional imaging workstation is a Nuclear Medicine, PET, NM/CT, and PET/CT processing, analysis, and review system. Designed with productivity in mind, it can accelerate workflow and provides a powerful clinical diagnostic tool to the medical imaging community. Combining streamlined workflow with a comprehensive clinical library and extensive networking capabilities on a functional imaging workstation, Xeleris 3.1 is at the nucleus of productivity in the clinical imaging department. Utilizing the GE Healthcare-wide graphical user interface, Xeleris 3.1 is the processing and review platform of the Discovery*, Optima* and Brivo* NM and NM/CT series, Infinia* Hawkeye* 4, Ventri, Discovery PET/CT 600 series, and all other molecular imaging cameras in GE Healthcare's current offering. Xeleris 3.1 provides the automated processing and connectivity necessary in today's demanding environment.</p> <p>NOTE: The Xeleris Workstation that is to be upgraded with this purchase becomes the property of GE Healthcare. Upon installation of the new Xeleris Workstation, the current Xeleris Unit must be De-Installed and returned to GE Healthcare.</p>
20	1	H3900MA	Concurrent Use Client for Xeleris Suite Server
21	1	H3901KK	Xeleris 3 Server License Enables XFL functionality on the Xeleris 3 Workstation.
22	1	H3901KL	XFL Remote Office Extends Xeleris Floating License over Wide Area Network (WAN).

9/12





GE Healthcare

Date: 06-10-2015  
Quote #: PR6-C40697  
Version #: 13

Item No.	Qty	Catalog No.	Description
23	1	H3901RN	Requires XFL Server and Client. 1st XFL Client for Cedars Suite

**Quote Summary:****Total Quote Net Selling Price** **\$539,308.00**

(Quoted prices do not reflect state and local taxes if applicable. Total Net Selling Price  
Includes Trade In allowance, if applicable. )



Date: 06-10-2015  
 Quote #: PR6-C40697  
 Version #: 13

## Options

(These items are not included in the total quotation amount)

Item No.	Qty	Catalog No.	Description	Ext Sell Price	
24	1	H2506TC	Discovery NM MEGP Collimators with Cart D670 Medium Energy General Purpose Collimators Includes: o Two MEGP Collimators o Collimators Mounted on a Dedicated Collimator Cart	\$13,200.00	X_____
25	1	H3100YR	A DVD player which functions with the boom mounted gantry display unit in order to provide video display during the scan for patient entertainment purposes.	\$2,750.00	X_____
26	1	H3100YJ	An intercom positioned at the Optima NM/CT 640 scan room enabling vocal communication between the operator and the patient while the operator is positioned at the system operator console.	\$1,925.00	X_____
27	1	H3901CB	Xeleris 3.1 View configuration shares the same basic functionality of the Xeleris 3.1 platform with no reconstruction features.	\$27,720.00	X_____
28	1	H3901RJ	Quote Description Text Cedars Sinai Cardiac Packages (option) A comprehensive set of nuclear cardiology protocols for advanced cardiac analysis, including: o Cedars Sinai Quantitative Perfusion SPECT? (option) o Automatic 3-Dimensional software approach to quantitative Perfusion SPECT. o Cedars Sinai Quantitative Gated SPECT? (option) o An application calculating the ejection fraction of the left ventricle and a 3D surface display is generated. o Cedars Sinai Companion (option) o Optional module for QGS and QPS applications features - 17 segment scores and templates in QPS - Diastolic filling parameters in QGS - Eccentricity ratio in QGS	\$10,285.00	X_____
29	1	H3901MG	AdreView Planar 1st or 2nd license AdreView Planar provides semi-automated of Heart to Mediastinum	\$5,500.00	X_____

11/12



GE Healthcare

Date: 06-10-2015  
 Quote #: PR6-C40697  
 Version #: 13

Item No.	Qty	Catalog No.	Description	Ext Sell Price	
			(H/M) ratio on Planar Images		
30	1	H3900MB	Additional Concurrent Use Client for Xeleris Suite Server (2nd)	\$16,500.00	X_____
31	1	H3901RP	2nd and 3rd XFL Client for Cedars Suite	\$6,035.70	X_____
32	1	W3001HC	TiP HQ Class NM Workstation - Full Service	\$5,000.00	X_____
			3.5 day TiP NM Workstation course held in the Milwaukee area. Includes travel and modest living expenses.		
			This course will prepare the technologists and Physicians for performing the daily workstation operations.		
			This training program must be scheduled and completed within 12 months after the date of product delivery.		
33	1	W0002NM	2 Days NM TiP Onsite Training	\$4,400.00	X_____
			Two Day NM Onsite Training provided from 8AM to 5PM, Monday through Friday. Includes T&L expenses. Days provided consecutively.		
			This training program must be scheduled and completed within 12 months after the date of product delivery.		
34	1	W0004NM	4 Days NM TiP Onsite Training	\$8,500.00	X_____
			Four Days NM Onsite Training provided from 8AM to 5PM, Monday through Friday. Includes T&L expenses. Days provided consecutively.		
			This training program must be scheduled and completed within 12 months after the date of product delivery.		

(Quoted prices do not reflect state and local taxes if applicable. Total Net Selling Price Includes Trade In allowance, if applicable. )



**EXHIBIT C**

## Improved Outcome Prediction by SPECT Myocardial Perfusion Imaging After CT Attenuation Correction

Aju P. Pazhenkottil\*, Jelena-Rima Ghadri\*, Rene N. Nkoulou, Mathias Wolfrum, Ronny R. Buechel, Silke M. Küest, Lars Husmann, Bernhard A. Herzog, Oliver Gaemperli, and Philipp A. Kaufmann

*Cardiac Imaging, University Hospital Zurich, Zurich, Switzerland*

The aim of this study was to determine the impact of attenuation correction with CT (CT-AC) on the prognostic value of SPECT myocardial perfusion imaging (SPECT MPI). **Methods:** The summed stress score (SSS; 20-segment model) was obtained from filtered backprojection (FBP) and iterative reconstruction with CT-AC in 876 consecutive patients undergoing a 1-d stress-rest  $^{99m}\text{Tc}$ -tetrofosmin SPECT MPI study for the evaluation of known or suspected coronary artery disease. Survival free of major adverse cardiac events (MACEs; cardiac death or nonfatal myocardial infarction) and survival free of any adverse cardiac events (including cardiac hospitalization, unstable angina, and late coronary revascularization) were analyzed by Kaplan–Meier analysis. **Results:** At a mean follow-up of  $2.3 \pm 0.6$  y, a total of 184 adverse events occurred in 145 patients, including 35 MACEs (16 cardiac deaths [rate, 1.8%] and 19 nonfatal myocardial infarctions [rate, 2.2%]). With FBP, an SSS of 0–3 best distinguished patients with a low MACE rate (0.6%), followed by an SSS of 4–8 (4.3%), with increased MACE rate, and an SSS of 9–13 (3.8%), which was comparable. By contrast, with CT-AC the discrimination of low from intermediate MACE rate was best observed between an SSS of 0 (0%) and an SSS of 1–3 (3.7%), with a plateau at an SSS of 4–8 (3.2%). **Conclusion:** CT-AC for SPECT MPI allows improved risk stratification. The prognostically relevant SSS cutoff is shifted toward lower values.

**Key Words:** CT-attenuation correction; single-photon emission computed tomography; myocardial perfusion imaging; major adverse cardiac events; outcome

**J Nucl Med 2011; 52:196–200**

DOI: 10.2967/jnumed.110.080580

**S**PECT myocardial perfusion imaging (SPECT MPI) is a widely used and well-established method for the evaluation of known or suspected coronary artery disease (CAD). Several studies have shown the strong prognostic value of SPECT MPI (1–3). Nevertheless, attenuation artifacts have remained an important issue. Common sources of artifacts

in MPI studies are soft-tissue attenuation and prominent subdiaphragmatic gastrointestinal activity. To overcome these problems and to better discriminate perfusion defects from artifacts, several methods have been proposed such as integrating findings from gated SPECT (4,5), scanning patients in the prone position (6), and using an external source of irradiation, either a line source (7) or CT (8,9). Attenuation correction (AC) by CT (CT-AC) has been shown to improve image quality and diagnostic accuracy (8–12). CT-AC proved superior to prone MPI acquisition (13) and has several advantages over external radionuclide sources for AC, such as higher photon flux and hence no influence by cross-talk from the SPECT radionuclide, no decay of transmission source, and shorter scan times (14,15). The American Society of Nuclear Cardiology and the Society of Nuclear Medicine have jointly recommended the use of AC in addition to electrocardiography (ECG) gating for SPECT MPI studies (16). The use of CT-AC is likely to increase soon because of the widespread availability of multislice CT scanners. This is particularly true with the integration of the multislice scanners into hybrid SPECT/CT scanners because the low-dose multislice CT images for AC can also be used for coronary calcium scoring (8,17). Although the use of AC in SPECT MPI is emerging and there is evidence of superiority in diagnostic confidence and accuracy of AC over noncorrected SPECT MPI (9,10,12), prognostic SPECT MPI studies using CT-AC are lacking. Thus, the aim of this study was to evaluate the impact of CT-AC on the prognostic value of SPECT MPI.

### MATERIALS AND METHODS

#### Study Population

Consecutive patients who underwent a 1-d adenosine stress-rest  $^{99m}\text{Tc}$ -tetrofosmin SPECT MPI study between May 2005 and June 2008 at the Cardiac Imaging Service of the University Hospital Zurich (Switzerland) for the evaluation of known or suspected CAD, with follow-up information available in our clinical database, were identified ( $n = 930$ ). Additional information was gathered from the registry of government authorities in the case of death. Of these, 54 patients were revascularized in the first 30 d after nuclear testing and therefore excluded from further analysis, because during this period any revascularization could potentially be directly triggered by the MPI test result, which would introduce a confounder between diagnostic and prognostic values. Thus, the

Received Jun. 28, 2010; revision accepted Nov. 18, 2010.

For correspondence or reprints contact: Philipp A. Kaufmann, Cardiac Imaging, University Hospital Zurich, Ramistrasse 100, CH-8091 Zurich, Switzerland.

E-mail: pak@usz.ch

\*Contributed equally to this work.

COPYRIGHT © 2011 by the Society of Nuclear Medicine, Inc.



prognostic data presented here are based on a subset of 876 patients.

### SPECT MPI Image Acquisition and Reconstruction

In all patients, a weight-adjusted dose of 300–400 MBq of  $^{99m}\text{Tc}$ -tetrofosmin was injected 3 min into the adenosine infusion (0.14 mg/kg/min). After a delay of 45–60 min, the ECG-gated stress images were acquired. Then, a 3-fold-higher dose of  $^{99m}\text{Tc}$ -tetrofosmin was administered, followed by a delay of 45–60 min before acquisition of the ECG-gated rest data. The SPECT MPI acquisition was performed on a dual-head camera (Infinia [until 2006] and Venti [from 2006 to 2008]; GE Healthcare) with a low-energy, high-resolution collimator; a 20% symmetric window at 140 keV; a  $64 \times 64$  matrix; and an elliptic orbit with step-and-shoot acquisition at  $3^\circ$  intervals over a  $180^\circ$  arc ( $45^\circ$  right anterior oblique to  $45^\circ$  left posterior oblique) with 30 steps (60 views). Scan time was set to 25 s per frame for stress and rest, resulting in a total acquisition time of 14 min 52 s (including interstep rotation time) for each scan, as recommended by the American Society of Nuclear Cardiology (18). Gating included 16 frames per R-R cycle.

For AC, all patients underwent low-dose CT performed using either a Hawkeye system (Infinia; GE Healthcare [until 2006]; 140 kV, 3.0 mA, with a single slice being imaged in about 14 s) or a Light Speed VCT scanner (GE Healthcare [since 2006]; 120 kV and 200–250 mA, depending on the patient's size) during breath-hold as previously reported (8). After reconstruction and transfer to a Xeleris workstation (GE Healthcare), AC maps were generated as previously reported in detail (8,17). SPECT images were reconstructed into short and vertical and horizontal long axes using standard reconstruction—that is, filtered backprojection (FBP)—and iterative reconstruction with CT-AC (Fig. 1). The data were thereafter quantitatively analyzed on the commercially available QPS/QGS software (Cedars-Sinai Medical Center) (19).

### Data Analysis

A 20-segment model was used to determine percentage uptake of the radionuclide (18). The following scale was used to stratify percentage uptake in each segment (20): more than 70%, normal (score, 0); 50%–69%, mildly reduced (score, 1); 30%–49%, moderately reduced (score, 2); 10%–29%, severely reduced (score, 3); and less than 10% absent (score, 4). A summed stress score (SSS) was obtained by adding the scores of the 20 segments. For FBP, previously established cutoff values were used (1): SSS less than 4 was considered normal, 4–8 mildly abnormal, 9–13 moderately abnormal, and more than 13 severely abnormal. By contrast, no cutoff values have been established for CT-AC.

### Follow-up

The following major adverse cardiac events (MACEs) were defined as endpoints: cardiac death and nonfatal myocardial infarction. For the analysis of any adverse cardiac events, hospitalizations for any cardiac reason, including unstable angina and coronary revascularization, were combined with MACEs.

### Statistical Analysis

SPSS software (version 15.0; SPSS Inc.) was used for statistical testing. Quantitative variables were expressed as mean  $\pm$  SD and categorical variables as frequencies, mean, or percentages. A Wilcoxon signed rank test was used to compare mean values of SSSs. Patient groups were compared using 1-way ANOVA for continuous variables and an  $\chi^2$  test for categorical variables. Differ-

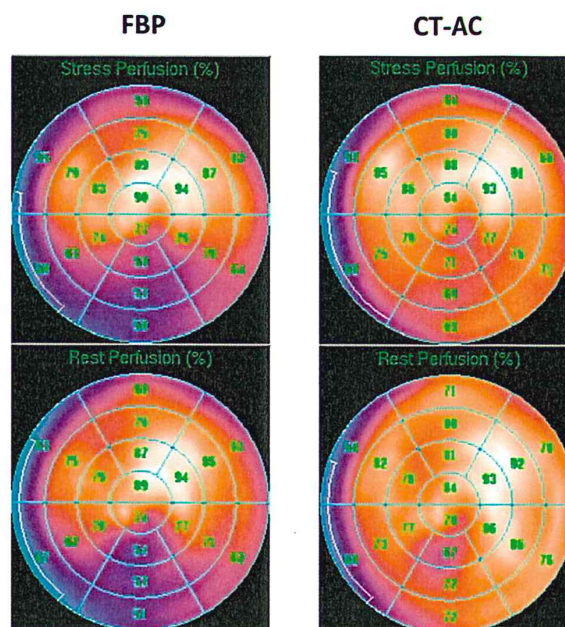


**FIGURE 1.** MPI polar map showing inferior attenuation artifact with FBP, which is resolved by applying CT-AC.

ences in survival over time were analyzed by the Kaplan–Meier method. The log-rank test was used to compare the survival curves. *P* values of less than 0.05 were considered statistically significant.

### RESULTS

The baseline characteristics of the final population (*n* = 876) are presented in Table 1.

#### SSS in CT-AC and Noncorrected SPECT MPI

Mean ( $\pm$ SD) FBP SSS in all patients was  $7.9 \pm 5.9$ , and mean CT-AC SSS was  $5.9 \pm 5.5$  (decrease of 25.3%,  $P < 0.001$ ). Of the 876 patients, 862 patients had an FBP SSS greater than 0 and 833 patients a CT-AC SSS greater than 0. An FBP SSS greater than 3 was present in 712 patients, and a CT-AC SSS greater than 3 was found in 533 patients.

#### Outcome

During a mean follow-up of  $2.3 \pm 0.6$  y, a total of 184 adverse events occurred in 145 patients, including 35 MACEs, with 16 cardiac deaths (rate, 1.8%) and 19 nonfatal myocardial infarctions (rate, 2.2%). Notably, the MACE rate was significantly higher in patients with known CAD than in patients with suspected (but no known) CAD (7.3% vs. 1.5%,  $P < 0.001$ ).

Figure 2 shows the MACE rates according to the SSS values (0, 1–3, 4–8, 9–13, and  $>13$ ). With FBP, there was a marked increase in MACE rate from an SSS of 1–3 (0.7%; *n* = 150) to an SSS of 4–8 (4.3%; *n* = 413), with no further increase at an SSS of 9–13 (3.8%; *n* = 199). An SSS greater than 13 was identified as a cutoff indicating the high-risk group (MACE rate, 9.0%; *n* = 100). By contrast,



**TABLE 1**  
Baseline Characteristics of Study Population (*n* = 876)

Characteristic	<i>n</i>
Male sex	558 (63.7)
Age (y)	65 ± 11
Body mass index (kg/m <sup>2</sup> )	27.1 ± 4.9
Known CAD	343 (39.2)
Cardiovascular risk factors	
Hypertension	529 (60.4)
Dyslipidemia	360 (41.1)
Diabetes	165 (18.8)
Smoking	366 (41.8)
Positive family history	259 (29.6)

Data are mean ± SD or number, with percentages in parentheses.

with CT-AC the sharpest increase from low to intermediate MACE rate was observed at a lower SSS, namely between an SSS of 0 (0%; *n* = 43) and 1–3 (3.7%; *n* = 300), with a plateau at 4–8 (3.2%; *n* = 347). A further increase was seen at a CT-AC SSS of 9–13 (6.7%; *n* = 119) and greater than 13 (7.5%; *n* = 67). This increase yielded optimal cutoff values for a CT-AC SSS of 0, 1–8, and greater than 8 to describe low, intermediate, and high risk for MACEs (0%, 3.4%, and 7.0%, respectively; *P* < 0.01) and for all adverse events (2.3%, 18.2%, and 34.9%, respectively; *P* < 0.001). Figure 3 illustrates the survival free of MACEs (A) and free of any event (B) for the low-, intermediate-, and high-risk groups (i.e., CT-AC SSS 0, 1–8, and >8). Direct comparison of CT-AC and FBP of an SSS of 1–3 by a  $\chi^2$  test reached a *P* value of 0.05 for MACEs and a *P* value less than 0.01 for any cardiac events.

## DISCUSSION

Our study is the first, to our knowledge, to assess the prognostic value of CT-AC for SPECT MPI. The present results demonstrate that CT-AC is helpful for risk stratification of SPECT MPI, adding incremental prognostic value.

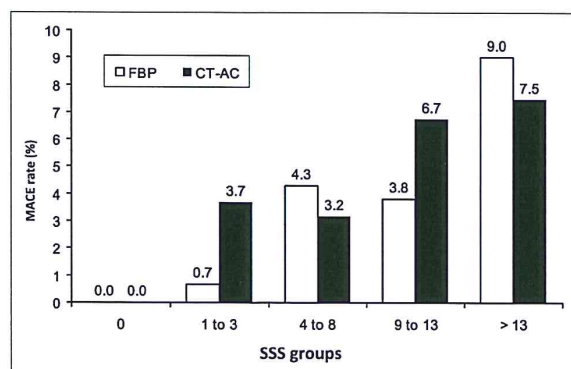


**FIGURE 2.** Rates of MACEs (cardiac death or myocardial infarction) are given for different ranges of SSS. With attenuation correction, prognostically relevant SSS cutoff is shifted toward lower values.

The relevant SSS cutoff value for predicting prognosis is shifted toward lower values when using CT-AC.

SPECT MPI is a well-established method for the evaluation of known or suspected CAD, and several studies have shown the strong prognostic value of SPECT MPI (1–3). Soft-tissue attenuation and subdiaphragmatic gastrointestinal activity play a major role in SPECT MPI because they can affect the diagnostic accuracy, mainly by decreasing specificity, and as a consequence reduce cost-effectiveness (21,22) or even lead to nondiagnostic studies (22). AC has provided higher left ventricular count homogeneity in healthy patients (9,12,23), facilitating interpretation of MPI studies and resulting in improved diagnostic accuracy (23,24). Therefore, several strategies for AC have been evaluated, among which CT-AC has proved most successful (9,25). Despite the fact that AC is increasingly used for SPECT MPI scans, there is a lack of data on the impact of CT-AC on the prognostic value of SPECT MPI. So far, only 2 studies have shown the prognostic value of AC in SPECT MPI (26,27). Both studies used an external gadolinium (<sup>153</sup>Gd) line source for AC. Baghdasarian et al. demonstrated that AC provides powerful risk stratification when added to clinical variables in SPECT MPI in patients in whom ECG gating was not feasible because of arrhythmia (26). Our study extends this observation to x-ray-based AC and to an unselected patient population. CT-AC has the advantage of being more convenient in clinical practice than radioisotope transmission sources because they need replacement at regular intervals to maintain high-quality transmission maps, and cross-talk of <sup>99m</sup>Tc into the <sup>153</sup>Gd window has been shown to cause artifacts in patients with intense gastrointestinal uptake (9). Our results suggest a more homogeneous count distribution after CT-AC as the cutoff for SSS values indicating a high risk of events are shifted toward lower levels—clearly a result of a reduced number of false-positive scan results with CT-AC. The discrimination between true and false defects has been one of the major challenges in nuclear cardiology. Our results show that attenuation correction, especially with CT, successfully reduces the number of false-positive results. Although with standard FBP reconstruction patients with an SSS of 0–3 were considered at low risk, our results show that a CT-AC SSS of 1 or more already is associated with intermediate MACE risk. Moreover, the SSS cutoff value identifying high-risk patients is lower with than without CT-AC (CT-AC SSS > 8 vs. SSS > 13), implying that more attention has to be paid to smaller defects. Considering smaller defects more closely is necessary, in particular, because a CT-AC SSS of 0 is associated with no risk (0% MACE event rate) whereas the event rate in the traditionally “healthy” FBP SSS group of 0–3 was 0.6%, showing an improved risk stratification with CT-AC. The fact that smaller defects in AC images are associated with higher risk should also be considered in further patient management.

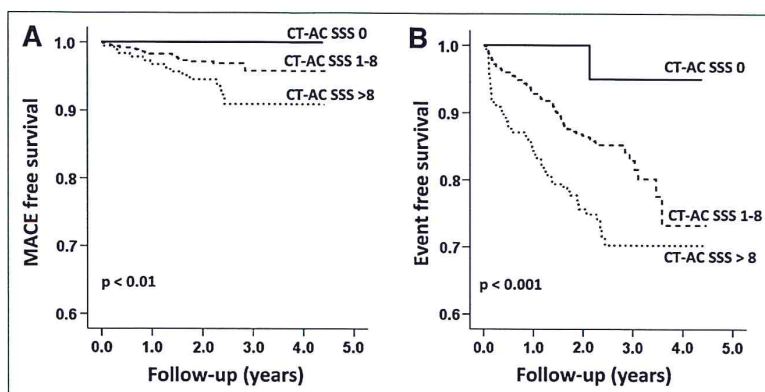


FIGURE 3. Kaplan-Meier survival curves for MACE-free and event-free survival.

The low event rate in patients with a CT-AC SSS of 0 was maintained over at least 4 y, perhaps suggesting a warranty period of more than 4 y for this low-risk population. By contrast, many events were observed in the intermediate-risk group (CT-AC SSS, 1–8) after 2.8 y, leading to a merging with the high-risk group (CT-AC SSS, >8) after 3.5 y (Fig. 3B). This merge may be interpreted as a process of atherosclerosis precipitating after 2.8 y, causing a shift toward the high-risk population.

We acknowledge the following limitations to our study. First, our data are based on a single-center study with a limited population. Further studies in larger populations may be helpful to study the prognostic value of CT-AC in different subgroups to assess the impact of sex and obesity. Second, because we included patients with follow-up information available in medical charts, the possibility cannot be excluded that the event rate for those patients lost to follow-up (17%) may have been different. On the other hand, because those patients with the largest findings at SPECT MPI were not deferred from treatment in our observational study, their risk of MACEs may be underestimated. Finally, the use of x-ray-based AC maps is associated with an additional radiation exposure.

## CONCLUSION

The present study documented that CT-AC for SPECT MPI adds incremental prognostic value allowing improved risk stratification. Patients with a CT-AC SSS of 0 have an excellent prognosis, with a warranty period of at least 4 y. The prognostically relevant SSS cutoff is shifted toward lower values, which needs to be considered in patient management.

## ACKNOWLEDGMENTS

We are grateful to Ennio Mueller, Edlira Loga, Mirjam De Bloeme, and Désirée Beutel for their excellent technical support. The study was supported by a grant from the Swiss National Science Foundation and from the Zurich Center for Integrative Human Physiology (ZIHP).

## REFERENCES

- Hachamovitch R, Berman DS, Shaw LJ, et al. Incremental prognostic value of myocardial perfusion single photon emission computed tomography for the prediction of cardiac death: differential stratification for risk of cardiac death and myocardial infarction. *Circulation*. 1998;97:535–543.
- Gimelli A, Rossi G, Landi P, et al. Stress/rest myocardial perfusion abnormalities by gated SPECT: Still the best predictor of cardiac events in stable ischemic heart disease. *J Nucl Med*. 2009;50:546–553.
- Galassi AR, Azzarelli S, Tomaselli A, et al. Incremental prognostic value of technetium-99m-tetrofosmin exercise myocardial perfusion imaging for predicting outcomes in patients with suspected or known coronary artery disease. *Am J Cardiol*. 2001;88:101–106.
- Fleischmann S, Koepfli P, Namdar M, Wyss CA, Jenni R, Kaufmann PA. Gated <sup>99m</sup>Tc-tetrofosmin SPECT for discriminating infarct from artifact in fixed myocardial perfusion defects. *J Nucl Med*. 2004;45:754–759.
- DePuey EG, Rozanski A. Using gated technetium-99m-sestamibi SPECT to characterize fixed myocardial defects as infarct or artifact. *J Nucl Med*. 1995;36:952–955.
- Segall GM, Davis MJ. Prone versus supine thallium myocardial SPECT: a method to decrease artifactual inferior wall defects. *J Nucl Med*. 1989;30:548–555.
- Tan P, Bailey DL, Meikle SR, Eberl S, Fulton RR, Hutton BF. A scanning line source for simultaneous emission and transmission measurements in SPECT. *J Nucl Med*. 1993;34:1752–1760.
- Schepis T, Gaemperli O, Koepfli P, et al. Use of coronary calcium score scans from stand-alone multislice computed tomography for attenuation correction of myocardial perfusion SPECT. *Eur J Nucl Med Mol Imaging*. 2007;34:11–19.
- Masood Y, Liu YH, Depuey G, et al. Clinical validation of SPECT attenuation correction using x-ray computed tomography-derived attenuation maps: multicenter clinical trial with angiographic correlation. *J Nucl Cardiol*. 2005;12:676–686.
- Duvernoy CS, Ficaro EP, Karabajakian MZ, Rose PA, Corbett JR. Improved detection of left main coronary artery disease with attenuation-corrected SPECT. *J Nucl Cardiol*. 2000;7:639–648.
- Hoeftlinghaus T, Husmann L, Valenta I, et al. Role of attenuation correction to discriminate defects caused by left bundle branch block versus coronary stenosis in single photon emission computed tomography myocardial perfusion imaging. *Clin Nucl Med*. 2008;33:748–751.
- Ficaro EP, Fessler JA, Shreve PD, Kritzman JN, Rose PA, Corbett JR. Simultaneous transmission/emission myocardial perfusion tomography: diagnostic accuracy of attenuation-corrected <sup>99m</sup>Tc-sestamibi single-photon emission computed tomography. *Circulation*. 1996;93:463–473.
- Malkenecker D, Brenner R, Martin WH, et al. CT-based attenuation correction versus prone imaging to decrease equivocal interpretations of rest/stress Tc-99m tetrofosmin SPECT MPI. *J Nucl Cardiol*. 2007;14:314–323.
- Koepfli P, Hany TF, Wyss CA, et al. CT attenuation correction for myocardial perfusion quantification using a PET/CT hybrid scanner. *J Nucl Med*. 2004;45:537–542.
- O'Connor MK, Kemp BJ. Single-photon emission computed tomography/computed tomography: basic instrumentation and innovations. *Semin Nucl Med*. 2006;36:258–266.
- Heller GV, Links J, Bateman TM, et al. American Society of Nuclear Cardiology and Society of Nuclear Medicine joint position statement: attenuation



- correction of myocardial perfusion SPECT scintigraphy. *J Nucl Cardiol.* 2004; 11:229–230.
17. Burkhard N, Herzog BA, Husmann L, et al. Coronary calcium score scans for attenuation correction of quantitative PET/CT  $^{13}\text{N}$ -ammonia myocardial perfusion imaging. *Eur J Nucl Med Mol Imaging.* 2010;37:517–521.
  18. Hansen CL, Goldstein RA, Akinboboye OO, et al. Myocardial perfusion and function: single photon emission computed tomography. *J Nucl Cardiol.* 2007; 14:e39–e60.
  19. Berman DS, Kang X, Van Train KF, et al. Comparative prognostic value of automatic quantitative analysis versus semiquantitative visual analysis of exercise myocardial perfusion single-photon emission computed tomography. *J Am Coll Cardiol.* 1998;32:1987–1995.
  20. Hesse B, Tagil K, Cuocolo A, et al. EANM/ESC procedural guidelines for myocardial perfusion imaging in nuclear cardiology. *Eur J Nucl Med Mol Imaging.* 2005;32:855–897.
  21. Fleischmann KE, Hunink MG, Kuntz KM, Douglas PS. Exercise echocardiography or exercise SPECT imaging? A meta-analysis of diagnostic test performance. *JAMA.* 1998;280:913–920.
  22. Kuntz KM, Fleischmann KE, Hunink MG, Douglas PS. Cost-effectiveness of diagnostic strategies for patients with chest pain. *Ann Intern Med.* 1999;130:709–718.
  23. Grossman GB, Garcia EV, Bateman TM, et al. Quantitative Tc-99m sestamibi attenuation-corrected SPECT: development and multicenter trial validation of myocardial perfusion stress gender-independent normal database in an obese population. *J Nucl Cardiol.* 2004;11:263–272.
  24. Heller GV, Bateman TM, Johnson LL, et al. Clinical value of attenuation correction in stress-only Tc-99m sestamibi SPECT imaging. *J Nucl Cardiol.* 2004;11:273–281.
  25. Fricke E, Fricke H, Weise R, et al. Attenuation correction of myocardial SPECT perfusion images with low-dose CT: evaluation of the method by comparison with perfusion PET. *J Nucl Med.* 2005;46:736–744.
  26. Baghdasarian SB, Noble GL, Ahlberg AW, Katten D, Heller GV. Risk stratification with attenuation corrected stress Tc-99m sestamibi SPECT myocardial perfusion imaging in the absence of ECG-gating due to arrhythmias. *J Nucl Cardiol.* 2009;16:533–539.
  27. Gibson PB, Demus D, Noto R, Hudson W, Johnson LL. Low event rate for stress-only perfusion imaging in patients evaluated for chest pain. *J Am Coll Cardiol.* 2002;39:999–1004.





The Journal of  
NUCLEAR MEDICINE

## Improved Outcome Prediction by SPECT Myocardial Perfusion Imaging After CT Attenuation Correction

Aju P. Pazhenkottil, Jelena-Rima Ghadri, Rene N. Nkoulou, Mathias Wolfrum, Ronny R. Buechel, Silke M. Küest, Lars Husmann, Bernhard A. Herzog, Oliver Gaemperli and Philipp A. Kaufmann

*J Nucl Med.* 2011;52:196-200.  
Doi: 10.2967/jnumed.110.080580

---

This article and updated information are available at:  
<http://jnm.snmjournals.org/content/52/2/196>

---

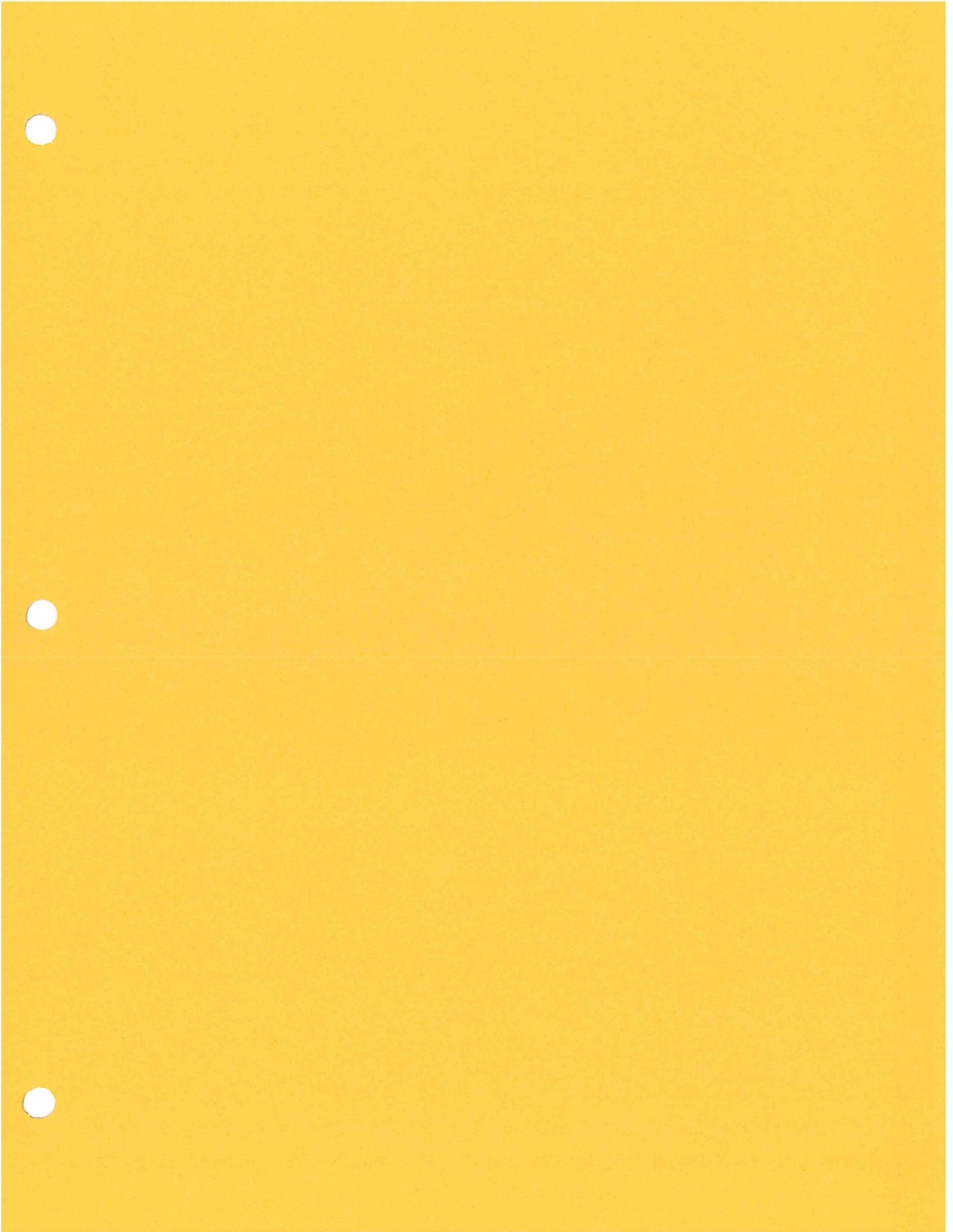
Information about reproducing figures, tables, or other portions of this article can be found online at:  
<http://jnm.snmjournals.org/site/misc/permission.xhtml>

Information about subscriptions to JNM can be found at:  
<http://jnm.snmjournals.org/site/subscriptions/online.xhtml>

*The Journal of Nuclear Medicine* is published monthly.  
SNMMI | Society of Nuclear Medicine and Molecular Imaging  
1850 Samuel Morse Drive, Reston, VA 20190.  
(Print ISSN: 0161-5505, Online ISSN: 2159-662X)

© Copyright 2011 SNMMI; all rights reserved.

The logo for the Society of Nuclear Medicine and Molecular Imaging (SNMMI) consists of the letters 'SNMMI' in a stylized, bold, sans-serif font, with the 'S' and 'M' being larger and more prominent. To the right of the logo, the text 'SOCIETY OF NUCLEAR MEDICINE AND MOLECULAR IMAGING' is written in a smaller, all-caps, sans-serif font.  
SOCIETY OF  
NUCLEAR MEDICINE  
AND MOLECULAR IMAGING



## A review on the clinical uses of SPECT/CT

Giuliano Mariani · Laura Bruselli · Torsten Kuwert ·  
 Edmund E. Kim · Albert Flotats · Ora Israel ·  
 Maurizio Dondi · Naoyuki Watanabe

Received: 26 June 2009 / Accepted: 11 January 2010 / Published online: 25 February 2010  
 © Springer-Verlag 2010

**Abstract** In the era when positron emission tomography (PET) seems to constitute the most advanced application of nuclear medicine imaging, still the conventional procedure of single photon emission computed tomography (SPECT) is far from being obsolete, especially if combined with computed tomography (CT). In fact, this dual modality

imaging technique (SPECT/CT) lends itself to a wide variety of useful diagnostic applications whose clinical impact is in most instances already well established, while the evidence is growing for newer applications. The increasing availability of new hybrid SPECT/CT devices with advanced technology offers the opportunity to shorten acquisition time and to provide accurate attenuation correction and fusion imaging. In this review we analyse and discuss the capabilities of SPECT/CT for improving sensitivity and specificity in the imaging of both oncological and non-oncological diseases. The main advantages of SPECT/CT are represented by better attenuation correction, increased specificity, and accurate depiction of the localization of disease and of possible involvement of adjacent tissues. Endocrine and neuroendocrine tumours are accurately localized and characterized by SPECT/CT, as also are solitary pulmonary nodules and lung cancers, brain tumours, lymphoma, prostate cancer, malignant and benign bone lesions, and infection. Furthermore, hybrid SPECT/CT imaging is especially suited to support the increasing applications of minimally invasive surgery, as well as to precisely define the diagnostic and prognostic profile of cardiovascular patients. Finally, the applications of SPECT/CT to other clinical disorders or malignant tumours is currently under extensive investigation, with encouraging results in terms of diagnostic accuracy.

G. Mariani (✉) · L. Bruselli  
 Regional Center of Nuclear Medicine,  
 University of Pisa Medical School,  
 Via Roma 67,  
 56126 Pisa, Italy  
 e-mail: g.mariani@med.unipi.it

T. Kuwert  
 Clinic of Nuclear Medicine, Friedrich-Alexander-University,  
 Erlangen-Nuremberg, Germany

E. E. Kim  
 Nuclear Medicine Service, MD Anderson Cancer Center,  
 Houston, TX, USA

A. Flotats  
 Hospital de Sant Pau, Nuclear Medicine Department,  
 Universitat Autònoma de Barcelona,  
 Barcelona, Spain

O. Israel  
 Department of Nuclear Medicine, Rambam Health Care Campus,  
 Haifa, Israel

M. Dondi · N. Watanabe  
 Nuclear Medicine Section, Division of Human Health,  
 International Atomic Energy Agency,  
 Vienna, Austria

*Present Address:*

N. Watanabe  
 Department of Radiological Technology,  
 Gunma Prefectural College of Health Sciences,  
 Gunma, Japan

**Keywords** SPECT/CT · Hybrid imaging ·  
 Attenuation correction · Diagnostic specificity ·  
 Localization and extent of disease ·  
 Malignant and benign disorders

The increasing clinical demand for more specific diagnostic systems and improved algorithms aimed at optimizing patients'



management has contributed to the recent development of hybrid imaging devices capable of coregistering anatomical and functional data. The diffusion into clinical practice of multimodality imaging performed with PET/CT and SPECT/CT enhances both sensitivity and specificity of the non-invasive diagnostic approach to patients with various disorders.

Hybrid imaging can also improve the staging, prognostic and treatment monitoring potential of the functional and metabolic information provided by nuclear medicine tests. Radionuclide imaging has per se the capability of identifying disease at early stages, since it visualizes molecular targets that may change before structural tissue changes occur. Addition of the CT component not only improves correction for photon attenuation, but also allows for easier correlation of areas with physiological variants or abnormal tracer accumulation to anatomical landmarks [1, 2].

### General architecture and acquisition protocols

Four basic SPECT/CT systems are currently commercially available. In the most recent version manufactured by GE Healthcare (Infinia™ Hawkeye® 4) a dual-detector gamma camera and a low-dose four-slice CT are mounted on the same rotation platform. The CT operates at 140 mV–2.5 mA, with a 4 min scanning time to acquire a 40-cm axial field of view, and the 20 mm (4×5 mm) axial coverage per CT slice best matches SPECT resolution. The very low X-ray radiation requires minimal room shielding in addition to what is commonly employed for nuclear medicine, and the overall external dimensions of the equipment are similar to those of a conventional gamma camera.

The Philips' Precedence™ system combines a Skylight gamma camera (two detectors suspended to moving arms) with a Brilliance™ CT, a high-power 6- or 16-slice CT component (which operates at 80 mA for the purpose of attenuation correction and image coregistration), with a minimum axial 0.65-mm slice thickness and whole-body scanning time shorter than 60 s. Recently, Philips has commercialized a new SPECT/CT system, the BrightView XCT, which integrates SPECT with flat-detector CT technology, high-resolution localization (0.33 mm isotropic voxels) and high-quality attenuation correction with the potential for fewer artefacts and shorter examination times. Paradoxically, although the flat-detector technology utilized in this system has higher resolution than even the latest diagnostic CT, it cannot be employed for routine CT examinations because, due to a relatively slow acquisition process, dynamic contrast-enhanced diagnostic examinations are not possible.

Siemens Medical Solutions features the Symbia™ TruePoint SPECT/CT, which combines a variable angle dual-detector SPECT with the Emotion™ CT scanner in four different configurations named Symbia T, Symbia T2,

Symbia T6 and Symbia T16, respectively. Symbia T only performs attenuation correction, while diagnostic quality images are obtained with the multidetector CT components. Axial slice thickness can be as thin as 0.63 mm with the Symbia T6 or T16 model. Both the Philips and the Siemens systems require some additional room shielding with respect to a conventional gamma camera.

All four devices imply SPECT acquisition times that do not differ from SPECT stand-alone procedures.

In addition to performing attenuation correction based on individual patient-based tissue density data, the SPECT/CT workstations allow image reconstruction, three plane (transaxial, coronal, sagittal) and 3-D display, including maximum-intensity projection and surface volume rendering. SPECT, CT and fused images are shown on the same screen, and an interconnected pointer is available to exactly co-localize the morphological and functional areas of interest identified in either one of the two study components.

The effective dose deriving from the CT component of a SPECT/CT examination ranges from 0.3–0.9 mSv when exploring the chest to 1–1.5 mSv when exploring the abdomen and pelvis, while a full diagnostic CT of the chest delivers 2.3–3 mSv and 2.1–3.1 mSv for the abdomen [3] (information supplied by the manufacturers).

The cost of SPECT/CT systems is considerably higher than that of a conventional gamma camera, especially for devices including a full diagnostic capability CT. This has limited so far their diffusion into several countries with limited financial resources.

As a technological perspective, new SPECT devices have recently been developed using CdTe/CdZnTe semiconductors instead of the classic NaI(Tl) scintillation crystals [4]. Such newer systems are smaller and have higher sensitivity and intrinsic resolution than conventional cameras. Assuming that this technology will soon reach full maturity, it can be speculated that its application for clinical SPECT/CT devices will render such systems smaller, more compact and also more clinically efficient.

### Endocrine and neuroendocrine diseases

#### Differentiated thyroid carcinoma

In patients with differentiated thyroid carcinoma,  $^{131}\text{I}$ -iodide is widely used for therapy, but also for diagnosis and localization of disease.  $^{131}\text{I}$ -iodide whole-body scintigraphy is commonly performed 2–3 days after administration of  $^{123}\text{I}$ –/ $^{131}\text{I}$ -iodide for a diagnostic scan, and 5–10 days after administration of  $^{131}\text{I}$ -iodide for ablation of the postsurgical residue or for therapy of metastatic disease.

Due to the unfavourable physical properties of  $^{131}\text{I}$  for imaging with gamma cameras, planar whole-body and spot



scans are generally characterized by rather poor anatomical definition. Owing to these intrinsic limitations of scintigraphy with  $^{131}\text{I}$ , SPECT is not routinely used as a stand-alone imaging technique [5]. Identification and correct topographic localization of iodine-avid metastases may be hampered by their small size, especially when located in areas whose anatomy has been altered by prior surgery, or in close vicinity to sites of physiological radioiodine accumulation (Fig. 1). In particular, cervical lymph node metastases or other metastatic sites may go undetected on the post-ablation whole-body scan because of the much higher radioiodine uptake in the thyroid residue (Fig. 1). On the other hand, false-positive radioiodine-avid findings on whole-body scintigraphy may be due to tracer accumulation in the thymus

(physiological), in cancers of non-thyroid origin, in organs excreting radioiodine with structural abnormalities (Fig. 2) or in contaminated skin areas.

Recent reports have demonstrated that SPECT/CT improves the diagnostic accuracy of the  $^{131}\text{I}$  scan in differentiated thyroid cancer, by better distinguishing cervical lymph node metastases from residual thyroid tissue, lung from mediastinal metastases or bone from soft tissue metastases [5–10]. This has resulted in an overall increment in diagnostic accuracy, ranging between 21 and 73.9% on both post-treatment and diagnostic follow-up scans. In particular, SPECT/CT led to modification of therapeutic management in a fraction as high as 35–47% and avoided unnecessary treatment in about 20% of the patients; stratification of risk was modified

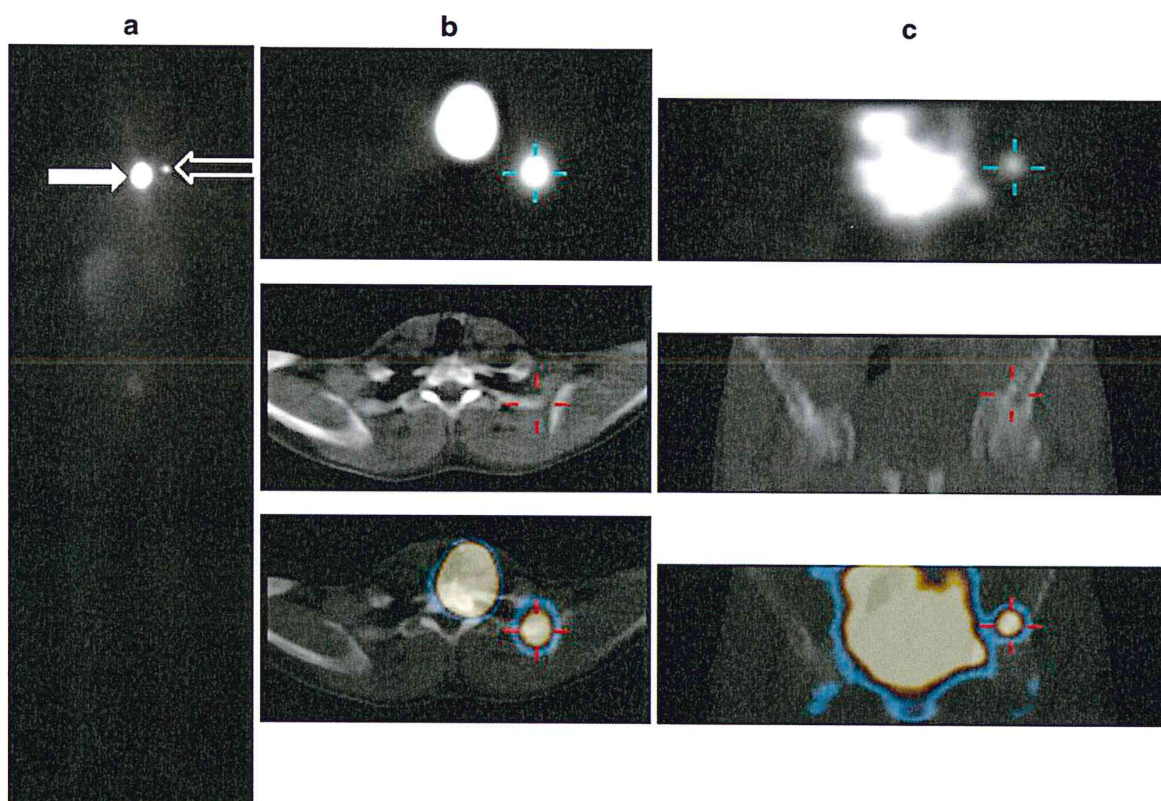


**Fig. 1** **a** Post-ablation whole-body scan in a 33-year-old man who had been submitted to thyroidectomy and left cervical lymphadenectomy because of papillary thyroid cancer of the left lobe (follicular variant) with pre-surgical diagnosis of lymph node metastasis; serum thyroglobulin was 94 ng/ml at the time of administering  $^{131}\text{I}$ -iodide (under stimulation with human recombinant thyroid-stimulating hormone). Besides intense uptake in the thyroid remnant (white closed arrow), there was an area of focal uptake in the left cervical region (interpreted as a lymph node metastasis in the whole-body scan, white open arrow), while important bladder activity hampered

correct interpretation of the pelvic region. **b** Representative transverse SPECT/CT section of the cervical region (SPECT component at the top, CT component in the middle, SPECT/CT fusion at the bottom): the focal area of uptake was actually bone metastasis located in the posterior arc of a left rib (target lesion indicated by pointing cross sign). **c** Representative coronal SPECT/CT section of the pelvic region (SPECT component at the top, CT component in the middle, SPECT/CT fusion at the bottom): the distinct focal area of uptake lateral to radioactivity accumulation in the bladder represented metastasis in the left iliac bone (target lesion indicated by pointing cross sign)



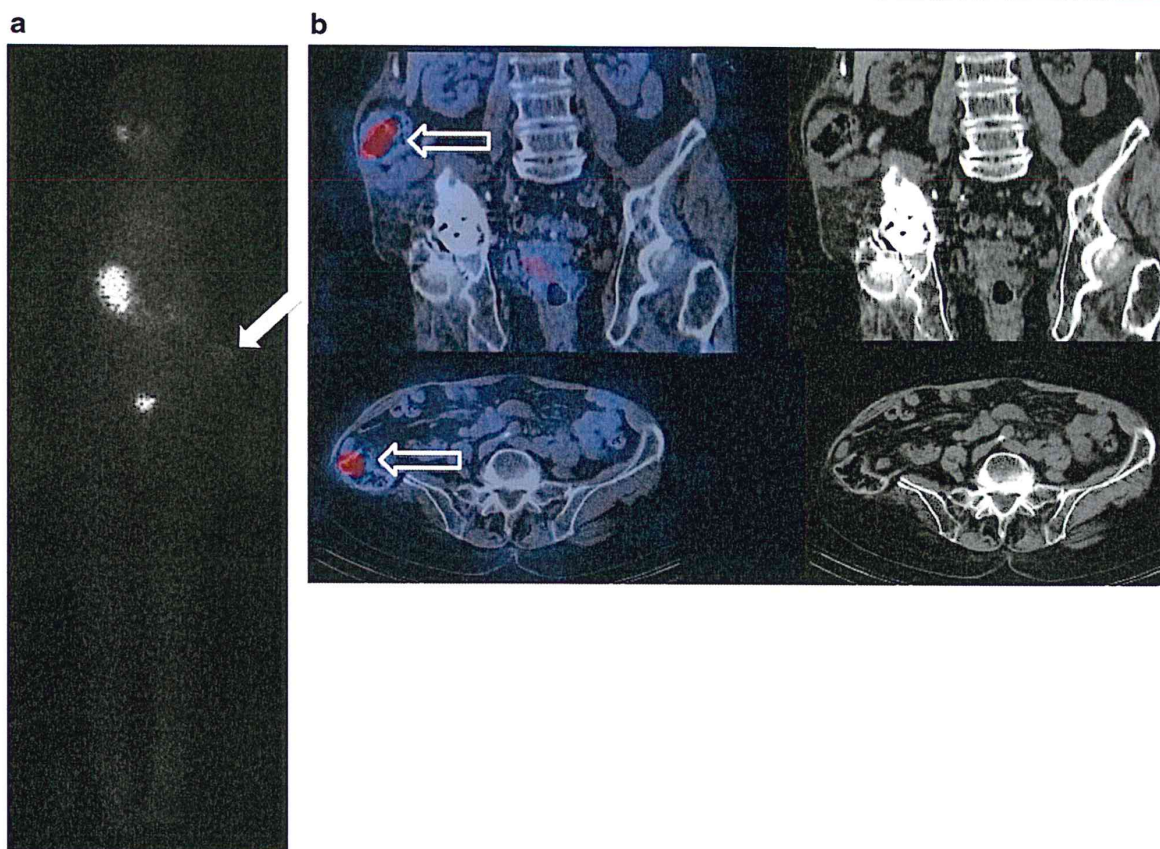


**Fig. 2** **a** Planar  $^{131}\text{I}$ -iodide whole-body scan in a patient with differentiated follicular thyroid carcinoma after pelvic surgery for a radioiodine-positive metastasis (posterior view). An indeterminate focus of radioiodine uptake is visualized, projecting to the region of the right pelvis (white closed arrow). **b** CT (right column) and

SPECT/CT fusion images (middle column) of this patient disclose a benign tracer accumulation in the colon (white open arrow); parts of the iliac bone are missing due to prior surgery. Note physiological asymmetric uptake in salivary glands, as well as radioactivity accumulation in the stomach and urinary bladder

by the SPECT/CT findings in 25% of the patients [7, 8, 10].

Thus, SPECT/CT allows precise localization of equivocal lesions and their characterization as malignant or benign, with an ensuing relevant impact on patient management, by suggesting the need for the most appropriate further therapeutic approach. It is in this scenario of particular interest that  $^{131}\text{I}$  SPECT/CT allows for the first time a reliable diagnosis of lymph node involvement as early as at the time of radioablation of the thyroid remnant [5, 8, 9], thus opening a new avenue to more accurate staging of patients with differentiated thyroid carcinoma.

Moreover, the possibility of combining true attenuation-corrected information on tissue distribution of radioactivity within the body with anatomical definition of tumour lesions allows better estimates for treatment planning to be derived in terms of both target size and radioiodine avidity [11].

#### Medullary thyroid carcinoma

Medullary thyroid carcinoma (MTC) constitutes 3–10% of all thyroid tumours and frequently presents with cervical and mediastinal lymph node metastases at diagnosis. However, even when locoregional lymph nodes already harbour metastases, surgical resection can be curative.

The role of conventional nuclear medicine in the diagnosis and staging of MTC has traditionally been based on scintigraphic imaging following the administration of tumour-seeking radiopharmaceuticals such as  $^{99\text{m}}\text{Tc}$ -(V)-dimercaptosuccinate (DMSA), radioiodinated metaiodobenzylguanidine (MIBG),  $^{99\text{m}}\text{Tc}$ -sestamibi or radiolabelled anti-carcinoembryonic antigen (CEA) monoclonal antibodies (MoAb) [12–15]. In particular, the sensitivity of immunoscintigraphy with radiolabelled anti-CEA MoAb is higher than that of other radionuclide imaging modalities, even including [ $^{18}\text{F}$ ]FDG PET (86 versus 50%, or less)



[13]. Although promising results have been reported in pilot studies with radiolabelled cholecystokin-B/gastrin receptor-targeting peptides [16, 17], the perspective that these agents will become routinely available is at present poor.

Somatostatin receptor scintigraphy with  $^{111}\text{In}$ -diethylenetriaminepentaacetic acid (DTPA)-pentetreotide (Octreoscan<sup>®</sup>) does not exhibit satisfactory diagnostic performance, mainly because of wide heterogeneity of MTC in receptor expression (even in different areas of the same tumour lesion), and because of important dedifferentiation. Nevertheless, coregistration of SPECT with CT may allow accurate definition of tumour foci in pre-surgical staging and planning, either by excluding the invasion of surrounding tissues or by sparing unnecessary surgery in locally advanced disease. For example, by defining an area of abnormal uptake detected by SPECT in the upper right chest wall as involvement of the upper mediastinum and right clavicle, SPECT/CT changed the treatment strategy from surgery to radiotherapy [18].

Finally, in a retrospective study involving 14 subjects with recurrent or metastatic MTC aimed at evaluating the sensitivity of Octreoscan<sup>®</sup> versus  $^{99\text{m}}\text{Tc}$ -(V)-DMSA scintigraphy (the latter radiopharmaceutical being no longer available in most countries),  $^{111}\text{In}$ -octreotide performed better in identifying tumour lesions (78.5 versus 57.1%) [19].

#### Gastro-enteropancreatic tumours (GEP)

Carcinoid and islet cell tumours require accurate detection and localization of all sites of disease for adequately planning surgery or other forms of treatment. Functioning GEP tumours are characterized by the appearance of clinical symptoms and signs in their early stages, when the lesions are small. Precise identification and localization of small tumour foci is difficult even with high-definition

imaging modalities such as CT or ultrasound (US), with a reported low and widely variable sensitivity ranging between 13 and 85% [20, 21].

While the newly developed PET radiopharmaceutical  $^{68}\text{Ga}$ -DOTA-D-Phe<sup>1</sup>-Tyr<sup>3</sup>-octreotide (DOTATOC) is undergoing extensive clinical validation, the single photon emitting  $^{111}\text{In}$ -DTPA-pentetreotide (Octreoscan<sup>®</sup>) is at present the only approved radiopharmaceutical for assessing somatostatin receptor-positive GEP tumours, SPECT being routinely added to planar imaging. Although Octreoscan<sup>®</sup> scintigraphy is suboptimal because of the unfavourable physical characteristics of the  $^{111}\text{In}$  gamma emission which may lead to false-negative results, it has nevertheless an overall 82–95% sensitivity for neuroendocrine tumours. Nevertheless, the specificity of Octreoscan<sup>®</sup> planar imaging is only around 50%, mostly because of the interference in image interpretation by areas with high physiological activity such as the pituitary gland, thyroid, liver, spleen, kidney, bowel and occasionally gall bladder (Fig. 3) [22]. It may be difficult to distinguish between physiological gall bladder uptake and a somatostatin receptor-expressing mass in the head of the pancreas, in the small bowel or in the right adrenal gland. False-positive findings may be also caused by non-specific tracer uptake in benign processes, such as inflammation, recent surgery, colostomy, accessory spleen, renal parapelvic cyst, Graves' disease, breast disease and sarcoidosis (Fig. 4).

In cases with a completely negative planar and SPECT somatostatin receptor scintigraphy, it is usually not justified to perform SPECT/CT. On the other hand, in cases with abnormal tracer accumulation SPECT/CT improves the diagnostic accuracy by enabling to distinguish physiological tracer accumulation or activity due to benign lesions from tumour uptake; thus, in the majority of patients it also avoids the need for delayed acquisitions. Octreoscan<sup>®</sup> SPECT/CT has shown 86% specificity and 85% positive

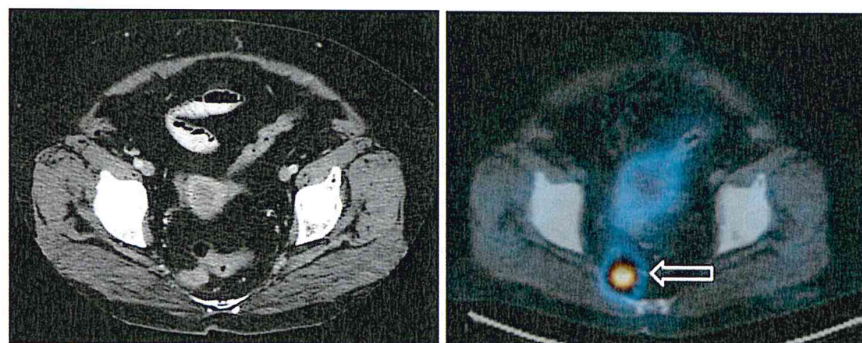


**Fig. 3** SPECT/CT with  $^{111}\text{In}$ -pentetreotide (Octreoscan<sup>®</sup>) performed in a 55-year-old man to localize the site of recurrence after prior surgery of an ileal carcinoid tumour; after several months of biochemical remission, serum levels of chromogranin A started to

rise again. The SPECT/CT fusion image (*right panel*) shows the retroperitoneal location of a lymph node metastasis with high expression of somatostatin receptors (*white open arrow*), for which surgery is now being contemplated



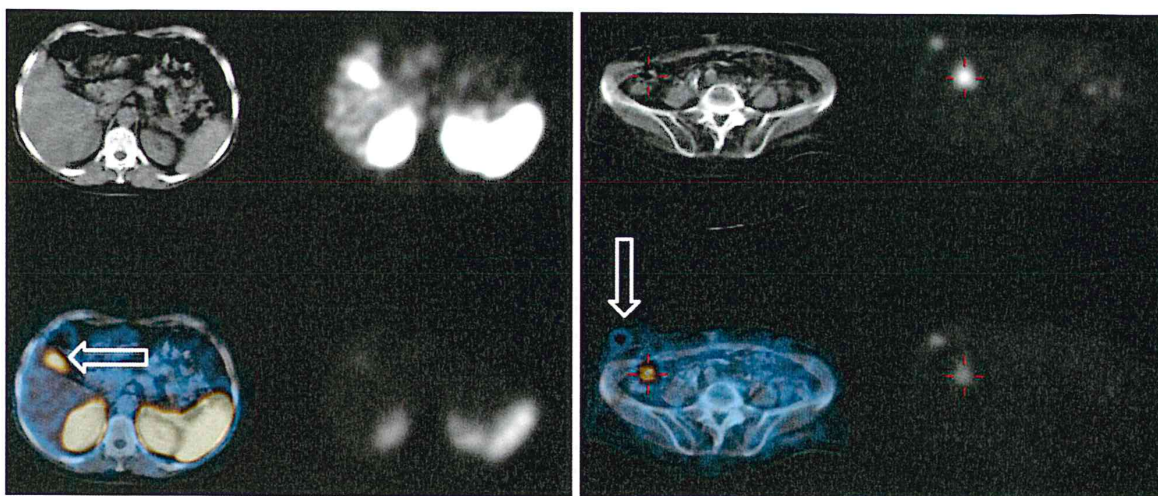


**Fig. 4** Examples of SPECT/CT avoiding interpretation as false-positive findings sites of Octreoscan® accumulation not related to tumour recurrence after surgery for GEP tumours. The two different transverse section levels in the same patient demonstrate physiological

accumulation in the gall bladder (*left panel, open arrow*) and physiological accumulation in the caecum (*right panel, indicated by centring signs*) combined with skin contamination in the right pelvic region (*indicated by open arrow in right panel*)

predictive value (PPV); it also changed patient management in 3–14% of the cases, mainly by sparing unnecessary surgery [18]. In particular, hybrid imaging helps in more accurately defining the organ involved and the overall extent of disease, including possible invasion of adjacent tissues (through analysis of the CT component of the study). SPECT/CT can therefore be crucial for choosing the most appropriate treatment for each individual patient—surgery or chemoembolization if the tumour is confined to a single organ without invasion of surrounding tissues, systemic therapy if the disease is extensive or disseminated. A recent study from the Pisa group, based on histopathology or clinical and imaging follow-up as the standard of reference, showed a 95% accuracy of Octreoscan® SPECT/CT for identifying and localizing neuroendocrine tumours, significantly higher than 46% for SPECT alone, especially for lesions located in the abdominal area [23].

In patients with post-surgery advanced stages of disease, Octreoscan® scintigraphy is also employed for planning treatment with somatostatin analogues labelled with adequate beta-emitting radionuclides [24].  $^{90}\text{Y}$  and  $^{177}\text{Lu}$  are the radionuclides most commonly employed in ongoing clinical trials. Since  $^{90}\text{Y}$  does not emit gamma photons suitable for imaging, pre-therapy radiodosimetric estimates can therefore be derived through scintigraphy with Octreoscan® as a surrogate radiopharmaceutical before therapy with the  $^{90}\text{Y}$ -labelled somatostatin analogues [25]. Quantitation of Octreoscan® uptake in the tumour lesions is optimized by SPECT/CT, which allows for tissue attenuation correction based on true transmission density data in the individual patient to be treated, rather than on standardized phantom-derived density

data [18, 26, 27]. SPECT/CT imaging may also play an increasing role in dosimetry estimations after treatment with  $^{177}\text{Lu}$ -DOTA<sup>0</sup>-Tyr<sup>3</sup>-octreotate [28].

#### Neuroendocrine tumours originating from chromaffin cells

Early diagnosis, accurate staging and a correct follow-up strategy are crucial for proper management of patients with chromaffin cell tumours, such as pheochromocytoma and paraganglioma [29]. Surgery is the first-line therapy for resectable masses, while advanced or recurrent disease may benefit from radiometabolic therapy with high doses of  $^{131}\text{I}$ -MIBG, either alone or in sequential combination with other treatment modalities [30]. In a study reporting on over 15 years of follow-up,  $^{131}\text{I}$ -MIBG therapy resulted in disease stabilization in up to 82% of patients, with an overall 71% survival (85% at 5 years) [30]. In order to reach optimal tumour response to this therapeutic approach, selection of patients should be based on high tracer uptake in the tumour on pre-treatment  $^{123}\text{I}$ - or  $^{131}\text{I}$ -MIBG scintigraphy [22].

In addition to morphological imaging with MR and/or CT, whose main purpose is accurate definition of the local extent and invasion of the primary tumour, scintigraphy with  $^{123}\text{I}$ - or  $^{131}\text{I}$ -MIBG offers the advantage of whole-body assessment for estimating the total tumour burden, with accuracy ranging from 86 to 100% [31–33] (Fig. 5), and for monitoring treatment response [22].

Morphological distortion caused by surgery and/or radiotherapy, such as fibrous scarring or altered anatomical relationships with adjacent organs, can result in abnormalities that may be misinterpreted on CT imaging [34]. On the



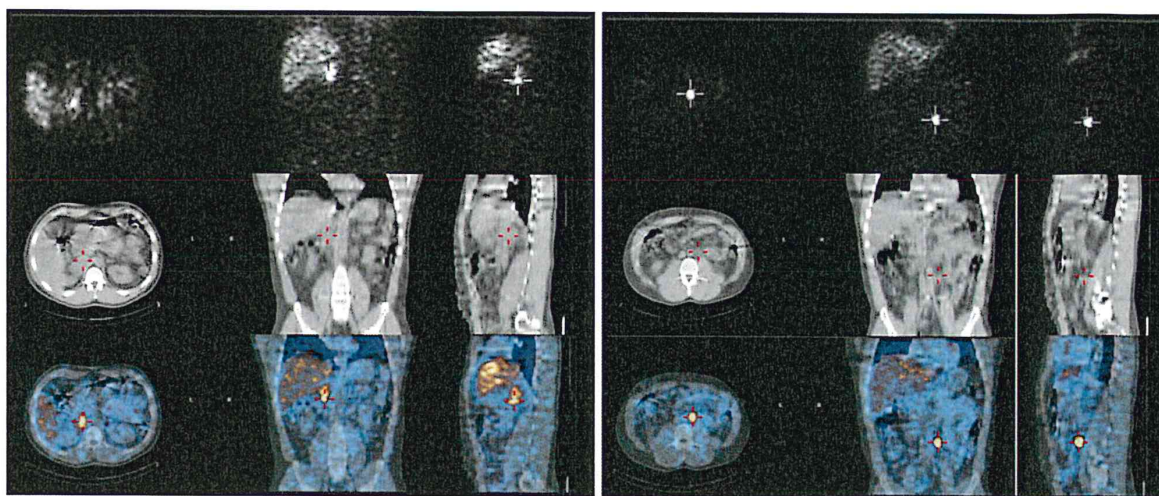


**Fig. 5** SPECT/CT with [ $^{123}\text{I}$ ]MIBG in a 27-year-old male patient with long-standing arterial hypertension associated with increased urinary catecholamine excretion; diagnostic CT had shown an undefined mass in the right adrenal gland, without any distinctive pattern. The scan was performed to better localize the lesion (or lesions) responsible for the hypertensive syndrome. In each panel, SPECT sections are shown in the *upper*, CT in the *middle* and fused SPECT/CT in the *lower* row, while transaxial sections are shown in the *left*, coronal in the *middle* and sagittal sections in the *right* column. Besides confirming high

[ $^{123}\text{I}$ ]MIBG uptake in the right adrenal mass (indicated by *centring signs* in *left panel*), SPECT/CT also localized an additional area of focal tracer uptake in the left retroperitoneal space, lateral to the aorta and below the left kidney (indicated by *pointing cross sign* in *right panel*). These findings guided the surgeon to remove both lesions that proved to be a primary pheochromocytoma (right adrenal mass) and, respectively, a metastatic lymph node (left lesion). The patient is now in biochemical and symptomatic remission since over 2 years

other hand, planar MIBG scintigraphy may fail in distinguishing uptake in tumour lesions from areas of physiological accumulation. Such diagnostic dilemmas are not always solved by SPECT alone.

SPECT/CT is of value in the case of non-diagnostic planar or SPECT images with an uncertain anatomical localization of MIBG, especially for tumours adjacent to organs with high physiological activity such as the liver and myocardium [35, 36]. In fact, such a hybrid imaging technique improves the diagnostic specificity of the MIBG scan by correctly identifying physiological gastrointestinal (GI), hepatic or renal accumulation [37], by correctly localizing recurrent disease or metastases, as well as by differentiating malignant foci from benign variants, for example retroperitoneal recurrence versus adrenal hyperplasia after contralateral adrenalectomy [38]. Moreover, SPECT/CT enables identification of pathological sites difficult to detect with diagnostic CT alone and ascertains disease remission when a residual mass is visualized on the diagnostic CT [34]. Finally, in patients referred for radiometabolic therapy with [ $^{131}\text{I}$ ]MIBG, a CT-based measurement of the target volume of interest is useful to quantify the effective radiation dose [36].

#### Adrenocortical disorders

Adrenocorticotrophic hormone (ACTH)-independent Cushing's disease, Conn's syndrome and hyperandrogenism are

the main indications for radionuclide imaging of adrenocortical disorders in patients with biochemically proven disorder and/or with incidentaloma. Despite the excellent sensitivity of morphological imaging, functional scintigraphy frequently represents the procedure that can identify and localize adrenocortical dysfunction, a crucial factor for planning surgery.

Adrenocortical scintigraphy with [ $^{131}\text{I}$ ]labelled 6- $\beta$ -iodomethyl-19-norcholesterol provides important information about the function of the adrenal glands and thus guides further patient management. When adrenal venous sampling is not available, adrenal scintigraphy or spiral CT are the methods of choice for diagnosing an aldosterone-producing adenoma [39]. Scintigraphy with [ $^{131}\text{I}$ ]norcholesterol can distinguish between Cushing's syndrome due to adenoma from hyperfunctioning carcinoma or bilateral nodular hyperplasia, a differential diagnosis that cannot be achieved by biochemical evaluation and anatomical imaging alone. In primary hyperaldosteronism, suppression of tracer uptake in the fasciculate cortex with dexamethasone is necessary to evaluate the outer *glomerulosa* cortex. Bilateral hyperplasia and unilateral adenoma can be distinguished based on the scintigraphic pattern and the timing of gland visualization.

PET/CT and SPECT/CT have redefined the role of functional imaging in clinical practice, as the intrinsic integration of functional with morphological information



allows one to distinguish benign from malignant masses and to identify small adrenal lesions [40, 41]. Instead of becoming obsolete, SPECT combined with CT or MR is taking a more crucial role than either separate imaging component [41], SPECT/CT representing the really advanced current technology. In a recent study including 27 patients with primary aldosteronism with inconclusive CT and adrenal venous sampling,  $^{131}\text{I}$ -norcholesterol SPECT/CT performed much better than planar imaging in terms of both diagnostic accuracy ( $p=0.0390$ ) and prognostic predicting ability ( $p=0.0141$ ) for differentiating hyperfunctioning adenomas from idiopathic adrenal hyperplasia and for identifying those patients for whom medical therapy is preferable to surgical treatment [42].

### Hyperparathyroidism

The main clinical indication for parathyroid imaging is localization of adenoma(s) sustaining hyperparathyroidism, either primary (usually caused by a solitary adenoma) or secondary (usually due to chronic renal failure and frequently associated with multigland disease). The primary goal of parathyroid scintigraphy is to enable a minimally invasive resection through exact preoperative localization of the abnormal parathyroid(s). US and scintigraphy with  $^{99\text{m}}\text{Tc}$ -sestamibi play a well-established role in preoperative identification of the lesion [43, 44]. In fact, functional parathyroid imaging is important to correctly identify the hyperfunctioning tissue, and the intraoperative use of a hand-held gamma-counting probe represents a useful adjunct to  $^{99\text{m}}\text{Tc}$ -sestamibi imaging for radioguided parathyroidectomy [43]. Parathyroid scintigraphy with  $^{99\text{m}}\text{Tc}$ -sestamibi can be performed according to various imaging protocols (such as the single-tracer dual-phase protocol) or by subtraction imaging following the injection of a thyroid-imaging-only tracer [43].

Although SPECT offers some definite advantages over planar scintigraphy [45], the additional localizing value of SPECT/CT is especially useful as a guide to surgery. In particular, SPECT/CT is highly appreciated for correctly localizing ectopic glands (Fig. 6) by providing topographic correlation with adjacent anatomical structures, as well as in patients in whom prior neck surgery guided by planar imaging had failed to identify the adenoma [46].

A recent investigation has comparatively evaluated the parathyroid adenoma-localizing performance of single- and dual-phase  $^{99\text{m}}\text{Tc}$ -sestamibi planar imaging, SPECT and SPECT/CT. The highest localizing value was observed with dual-phase scintigraphy with added SPECT/CT. In particular, early SPECT/CT combined with any delayed imaging protocol was significantly superior to the other methods [47]. In another study, SPECT/CT correctly localized 100% of the scintigraphy-positive lesions versus 61% for SPECT

alone. Hybrid imaging had a significant surgical impact in 39% of the cases and changed the surgical approach in patients with retrotracheal parathyroid adenomas [48]. In an additional report, SPECT/CT had an 89% diagnostic accuracy for single adenomas and predicted the intra-operative location of a lesion within 19 mm with 95% confidence. Nevertheless, accurate detection of multigland disease was still difficult [49].

### Other cancers

#### Malignant bone disease

Skeletal metastases are most frequently detected by means of bone scintigraphy with  $^{99\text{m}}\text{Tc}$ -labelled phosphonates, e.g.  $^{99\text{m}}\text{Tc}$ -methylene diphosphonate ( $^{99\text{m}}\text{Tc}$ -MDP). This imaging procedure affords visualization of the entire skeleton with an extremely high sensitivity (close to 100%), at least for breast and prostate cancer [50]. However, its rather low specificity often requires further investigation with e.g. X-ray-based imaging, CT or MR.

Besides accurate definition of the lesion boundaries for primitive bone tumours (Fig. 7), SPECT/CT offers the unique opportunity to correlate the scintigraphic findings with anatomical images for better classification of indeterminate, non-diagnostic bone lesions detected at  $^{99\text{m}}\text{Tc}$ -MDP scintigraphy in patients with extra-skeletal cancers (Fig. 8). In a study of 47 patients with 104 equivocal lesions on bone scintigraphy, with histological confirmation or long-term follow-up as the reference gold standard, SPECT/CT allowed correct diagnosis in 85% of the cases, especially by characterizing the true nature of focal areas of increased uptake in the spine, rib cage, skull and pelvis [51]. Besides the improved diagnostic accuracy obtained by correlating functional with morphological images, SPECT/CT also provides better diagnostic confidence than side-by-side viewing of separate sets of images [52].

The term "SPECT-guided CT" refers to the adaptation of the CT field of view to foci of increased bone metabolism. Using this method in 52 undetermined lesions in 44 patients, 92% of abnormal uptake foci visualized by SPECT were correctly classified, with distinct usefulness especially for lesions in the spine column, ribs and pelvis [53]. These results have been validated in another study whereby certainty in classifying focal lesions of the axial skeleton reached 100% by employing such a methodological approach, with significant advantages over both planar imaging and SPECT alone ( $p=0.004$ ) [54].

An innovative method to calculate radiation dosimetry to bone marrow and bone lesions for palliative therapy with the bone-seeking agent  $^{153}\text{Sm}$ -ethylene diamine tetramethylene phosphonate (EDTMP) in patients with hormone-



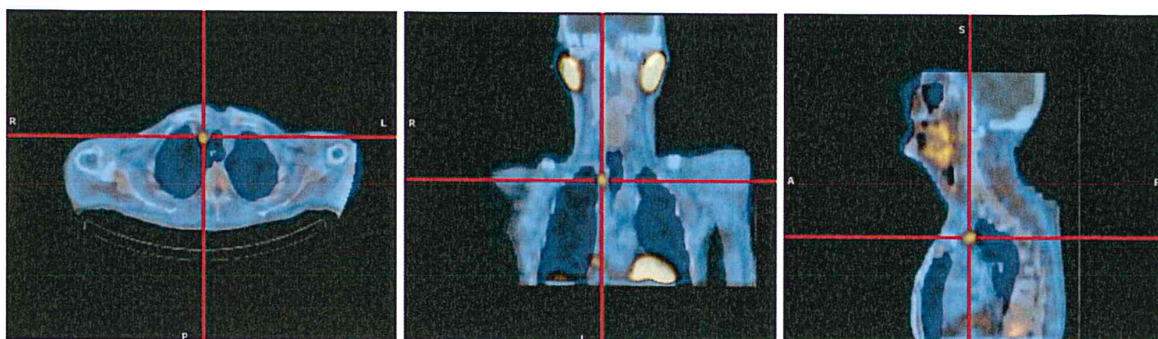


**Fig. 6** Parathyroid scintigraphy with  $^{99m}\text{Tc}$ -sestamibi in a 70-year-old man with recurrent primary hyperparathyroidism. The patient had been submitted about 1 year earlier to surgery for removing a parathyroid adenoma (located scintigraphically at the right lower thyroid lobe) and to thyroidectomy because of concomitant multinodular goiter; after initial remission, hyperparathyroidism recurred within about 6 months, and the patient was referred for further

characterization. Fused SPECT/CT images (transverse section on the left, coronal section in the middle, sagittal section on the right) clearly show the ectopic location of a parathyroid adenoma in the upper mediastinum, right paratracheal region (indicated by pointing cross sign). Such topographic localization was crucial for guiding second surgery, which proved completely successful

refractory metastatic prostate cancer employs SPECT/CT emission/transmission data to correct for the true tissue attenuation and scatter in the individual patient. The system is phantom-calibrated for tissue density, and voxel-by-voxel analysis is performed after reconstruction of an S-value matrix based on the individual attenuation map. This method has demonstrated that conventional techniques based on planar imaging overestimate the radiation dose to bone marrow, while SPECT/CT can potentially optimize measurement of the effective dose to bone marrow as well as to the bone lesions, the latter parameter not being assessable with conventional techniques [55].

#### Solitary pulmonary nodules and lung cancer

Reliable differential diagnosis is crucial in patients with a solitary pulmonary nodule (SPN), because bronchogenic carcinoma has been recognized as one of the leading underlying conditions. The 5-year survival rate of lung cancer is  $\geq 80\%$  when diagnosed at an early resectable stage, but is  $< 5\%$  when diagnosed with disseminated disease. The ideal imaging procedure should therefore be conclusive in distinguishing patients who need surgical resection of a malignant nodule from those for whom surgery is not indicated.

A meta-analysis of the clinical usefulness of imaging procedures for diagnostic classification of SPNs has shown virtually identical performances of CT, MR,  $^{18}\text{F}$ FDG PET and SPECT with  $^{99m}\text{Tc}$ -depreotide (a ligand for the somatostatin receptor subtypes 2, 3 and 5, with high affinity in particular for subtype 2) [56, 57]. When PET is not available,  $^{99m}\text{Tc}$ -depreotide SPECT represents a valid diagnostic alternative, with 84% sensitivity and 88% specificity [56].

SPECT/CT with tumour-seeking agents or radiolabelled antibodies has been employed in the evaluation of patients

with lung cancer and SPNs. SPECT/CT with  $^{99m}\text{Tc}$ -sestamibi correctly classified 10 of 11 malignant nodules and 11 of 12 benign nodules, with a resulting 91% sensitivity and 92% specificity [58].

SPECT with  $^{99m}\text{Tc}$ -sestamibi or  $^{99m}\text{Tc}$ -tetrofosmin plays an important role in the biological characterization of enlarged mediastinal lymph nodes on CT, reducing the need for surgical resection if they do not exhibit increased metabolic activity. However, the limited spatial resolution of SPECT hampers defining the exact number and location of involved lymph nodes. With SPECT/CT the extent of disease can be defined more accurately, while also enhancing the specificity of functional imaging [59]. In the follow-up of patients with lung cancer SPECT/CT has also been reported to improve detection of tumour recurrence and to play an important role for monitoring the efficacy of therapy [60].

#### Breast cancer

The incidence of breast carcinoma, the first cause of cancer-related death among women, has been increasing in recent decades, especially in the younger age group. Since mortality might be reduced by early diagnosis, mammography has been largely developed as screening in women over 50 years of age. On the contrary, in premenopausal patients the diagnosis of breast cancer can be problematic, because of the dense and hyperproliferative glandular tissue, which reduces the sensitivity of mammography.

While the value of planar scintimammography with  $^{99m}\text{Tc}$ -sestamibi in characterizing breast lesions  $> 10$  mm as also in patients with microcalcifications is well known [61, 62], the added diagnostic value of SPECT/CT has recently been investigated in 53 patients with mammographically suspicious lesions, using histopathology as the diagnostic



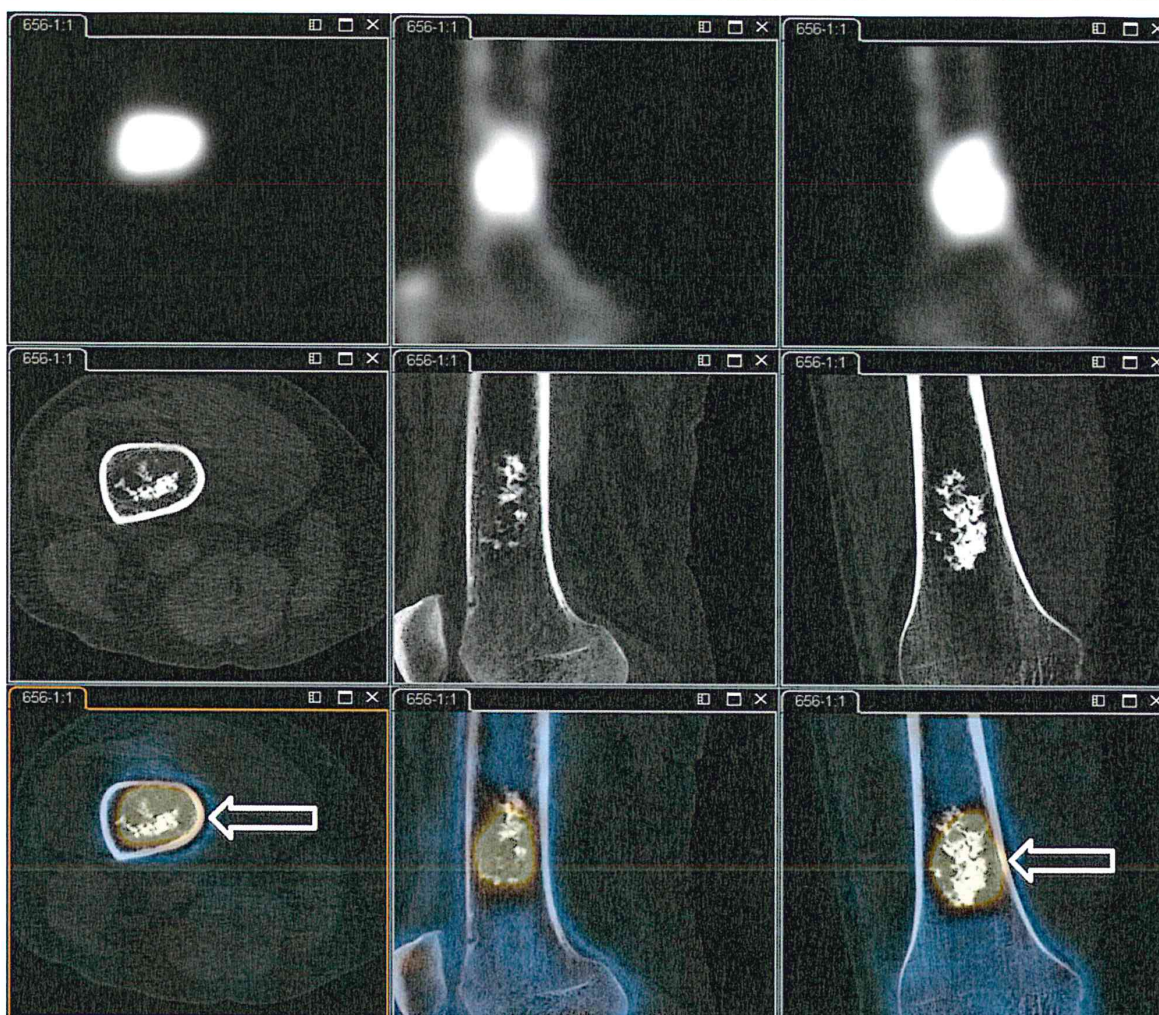


**Fig. 7** SPECT/CT of the distal femur performed to assess the extent and boundaries of an enchondroma, a cartilage tumour that grows in the bone marrow and can sometimes become malignant. *Top row* shows the SPECT sections, *middle row* shows the CT sections and *bottom row* shows the fused sections; transverse, coronal and sagittal planes are arranged in the *left, middle* and *right columns*, respectively. The excellent detail of the CT images (provided in this case by the

flat-panel detector of the CT component) enables identification of the exact boundaries of the tumour and of the osteoblastic reaction in surrounding bone, which involves only a limited section of the cortical bone (as indicated by the *white open arrows*). (Images kindly supplied by Prof. Thomas Krause, Nuclear Medicine Service, Inselspital, Universitätsspital Bern, Bern, Switzerland)

standard. The overall sensitivity of planar imaging was 73% (42.9% for lesions  $\leq 10$  mm, 91.3% for those  $> 10$  mm), while the sensitivity of SPECT/CT was 89.2% (71.4% for lesions  $\leq 10$  mm, 100% for those  $> 10$  mm), with equal specificity (93.8%) [63].

Thus, SPECT/CT may overcome the limitation of planar imaging represented by tumour size and therefore revive the role of radionuclide imaging in the diagnostic work-up of breast cancer, in which mammography and US play today a major role before proceeding to core biopsy.

#### Lymphoscintigraphy for radioguided sentinel node biopsy

Due to its high prognostic value, sentinel lymph node biopsy (SLNB) has already been included in the most recent version of the TNM staging system for patients with various types of cancer [64]. SLNB is currently employed on a routine basis for staging the lymph node status in patients with clinically N0, T1a-b breast cancer, as well as in patients with malignant cutaneous melanoma with Breslow thickness between 1.5 and 4 mm [65, 66]. The



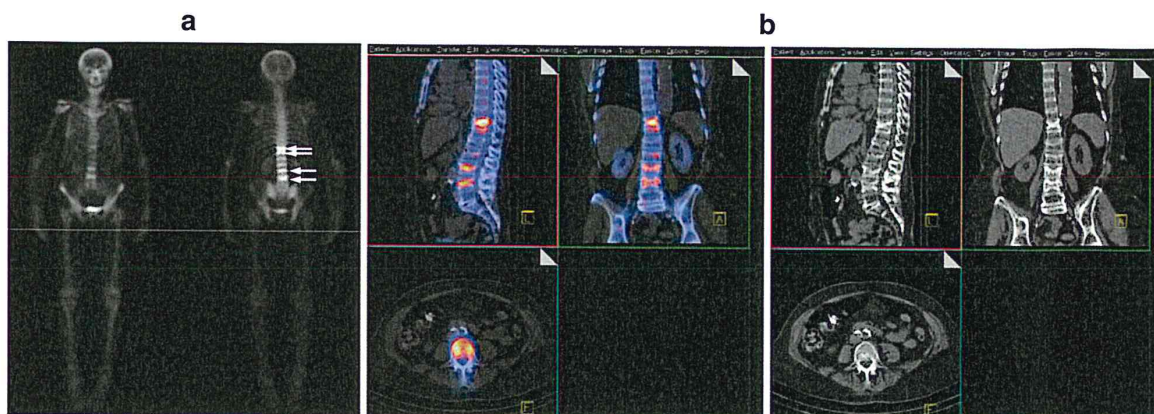


**Fig. 8** **a** Four foci of  $^{99m}\text{Tc}$ -MDP accumulation in the spine (indicated by white arrows) are observed on the planar whole-body scan of this woman referred for staging breast cancer (left: anterior

view; right: posterior view). **b** SPECT/CT fusion (left panel) and CT images (right panel) identify vertebral compression fractures as the benign cause of enhanced tracer uptake

accurate preoperative anatomical localization of SLN is crucial when minimally invasive surgery is planned. During surgery, identification of the SLN and verification of its complete removal is guided by counting rates measured with a hand-held intraoperative gamma probe.

In the region of the head and neck, SPECT/CT correlates the site of  $^{99m}\text{Tc}$ -colloid uptake in the SLN to important anatomical landmarks, thus better guiding the surgeon to perform SLNB; the advantage of fusion imaging is

especially helpful when the SNL is located in close proximity to the injection site (Fig. 9). Similar considerations hold true for the chest, where there are three levels of axillary lymph nodes depending on their location relative to the *pectoralis minor* muscle. For the pelvis identification of the exact location of the SLN is also crucial, since resection of the external iliac lymph nodes requires a different surgical strategy as compared to e.g. resection of the inguinal lymph nodes [67].

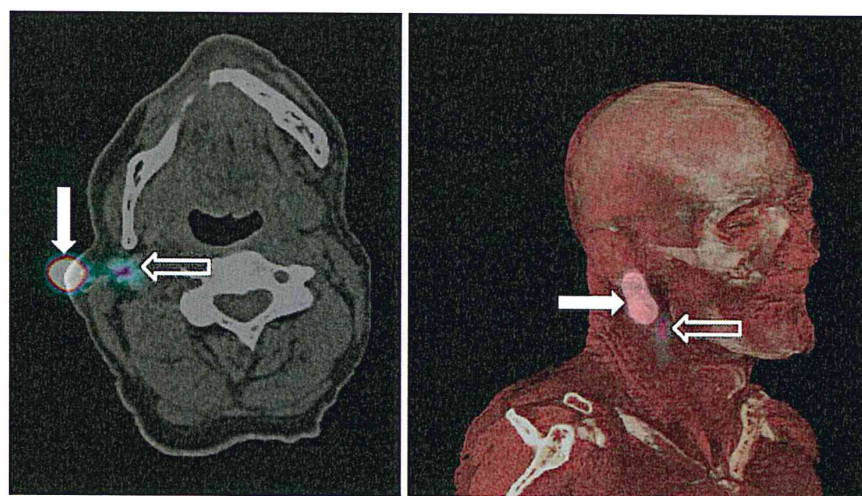


**Fig. 9** Lymphoscintigraphy with  $^{99m}\text{Tc}$ -sulfur colloid for SLNB in a patient recently submitted to removal of a cutaneous melanoma in the right subauricular region. Fusion SPECT/CT imaging (transverse section on the left panel) demonstrates deep location of a sentinel lymph node (indicated by the white open arrow) whose cutaneous projection is masked by radioactivity in the injection sites (white closed arrow). 3-D surface volume rendering (right panel) provides

spatial anatomical coordinates that are especially helpful for planning the most adequate surgical approach (injections sites and sentinel lymph node indicated by white closed and white open arrows, respectively). (Images kindly supplied by Prof. Homer A. Macapinlac, Department of Nuclear Medicine, University of Texas, MD Anderson Cancer Center, Houston, TX, USA)



SPECT/CT accurately characterizes the number, size, depth and regional location of SLNs in patients with invasive breast cancer less than 3 cm in diameter. Low-dose CT added to SPECT can distinguish SLNs from second echelon nodes, thus reducing the workload for the pathologist and associated costs related to the need of examining multiple nodes [68, 69]. Furthermore, SPECT/CT improved SLN detection in obese patients with breast cancer and correctly localized sentinel nodes in 75% of patients when the use of blue dye failed [70].

Image fusion with SPECT/CT enabled precise localization of the SLN also in the cervical region, allowing a radioguided surgical approach in 90% of cases with clinically N0 oral squamous cell carcinoma [71].

Furthermore, SPECT/CT has been employed to identify SLNs in patients with clinical stage Ia non-small cell lung carcinoma, where it performed better than intraoperative gamma probe counting for localizing hilar SLNs, whereas intraoperative gamma probe counting was more useful for identifying mediastinal SLNs. The combined use of SPECT/CT imaging and intraoperative gamma probe counting optimizes SLN localization before and during surgery in the hilum and mediastinum [72].

Finally, hybrid SPECT/CT represents an excellent procedure to identify pelvic tumour-draining lymph nodes in patients with malignant melanoma of the groin or thigh (Fig. 10) [73–75].

#### Lymphoma

[ $^{18}\text{F}$ ]FDG PET/CT is rapidly becoming the diagnostic gold standard for initial staging of lymphoma, as also the imaging procedure of choice for monitoring the efficacy

of therapy and for follow-up [76]. Nevertheless, when access to PET imaging is limited, scintigraphy with  $^{67}\text{Ga}$ -citrate retains advantages over CT in patients with lymphoma, especially for assessing complete response or relapse after treatment and for distinguishing viable lymphoma tissue from residual fibrotic or necrotic mass [77].  $^{67}\text{Ga}$ -citrate scintigraphy is also useful to predict outcome and long-term prognosis early during or after completion of current therapy protocols in both Hodgkin's disease (HD) and non-Hodgkin's lymphoma (NHL) [78].

Since biodistribution of  $^{67}\text{Ga}$ -citrate is characterized by areas of physiological accumulation in the liver, bone, bone marrow, spleen, kidney and colon and by non-specific tracer uptake in benign processes (such as recent surgery, infection, inflammation, thymus, benign parathyroid adenopathy and lactating breast),  $^{67}\text{Ga}$  scans are difficult to interpret. SPECT/CT has the potential of correctly identifying sites of lymphoma and differentiating them from non-specific, benign or equivocal tracer uptake both in the chest and abdomen. In particular, hybrid imaging has been shown to differentiate involvement of the skeleton from that of adjacent lymph nodes, to localize areas of abnormal uptake in the lower chest versus physiological uptake in the hepatic dome and to correctly classify abnormal uptake in processes other than lymphoma, such as sialoadenitis in submandibular glands, rib fractures and bone marrow activation after recent radiotherapy. It has been reported that SPECT/CT changed the diagnostic information in 20–25% of the scans compared to  $^{67}\text{Ga}$ -citrate SPECT or to CT alone, thus influencing the treatment strategy, for instance by better defining the target volume for external beam radiation therapy [79, 80].

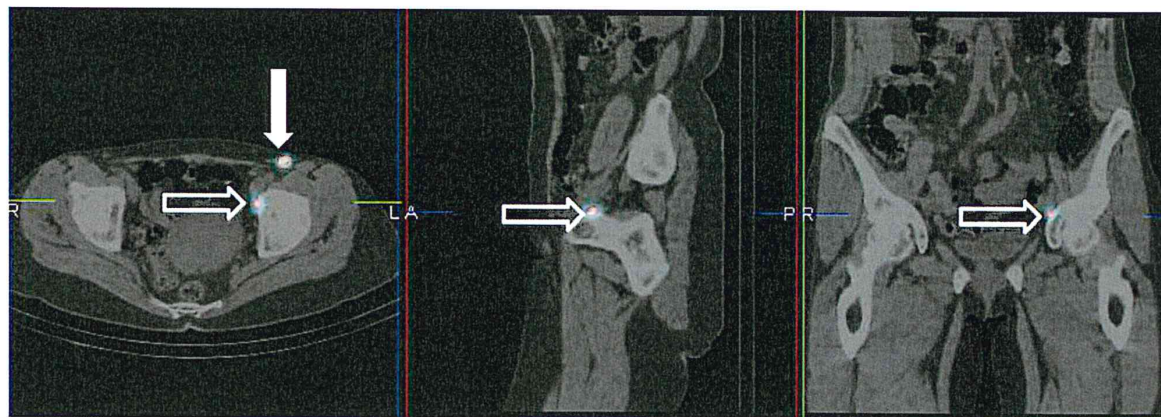


**Fig. 10** Lymphoscintigraphy with  $^{99\text{m}}\text{Tc}$ -sulfur colloid for SLNB in a patient recently submitted to removal of a cutaneous melanoma in the anterior left thigh. Fusion SPECT/CT imaging (transverse section on the left panel) demonstrates that, in addition to a superficial sentinel lymph node (indicated by white closed arrow), there is a deeply located sentinel node within the pelvis (indicated by white open

arrows). Sagittal (centre panel) and coronal sections (right panel) centred on the deep sentinel lymph node are also shown. (Images kindly supplied by Prof. Homer A. Macapinlac, Department of Nuclear Medicine, University of Texas, MD Anderson Cancer Center, Houston, TX, USA)



The use of radioimmunotherapy with anti-CD20 MoAb ( $^{131}\text{I}$ -tositumomab in the USA,  $^{90}\text{Y}$ -ibritumomab tiuxetan in Europe) is growing in patients with relapsed NHL previously submitted to chemotherapy and frequently to radiotherapy as well, in whom myelosuppression is the dose-limiting toxicity. In this scenario, SPECT/CT has enabled bone marrow tracer concentration to be quantified for better dosimetric estimates resulting from radioimmunotherapy with  $^{131}\text{I}$ -rituximab [81].

#### Cerebral masses

Contrast-enhanced CT and T1-weighted MRI enable accurate detection of brain tumour and margins, which is important for adequately planning surgery and external beam radiation therapy. However, following surgery and/or radiotherapy anatomical imaging frequently fails in differentiating residual tumour infiltration versus surrounding oedema, as well as recurrent tumour versus radiation necrosis and gliosis [82]. Furthermore, CT and MRI cannot accurately distinguish primary brain lymphoma from cerebral toxoplasmosis in patients with acquired immunodeficiency syndrome (AIDS) [83].

Since PET with [ $^{18}\text{F}$ ]FDG has a limited use for this clinical indication, different PET tracers have been developed such as  $^{11}\text{C}$ -choline,  $^{18}\text{F}$ -FDOPA,  $^{11}\text{C}$ -methionine,  $^{18}\text{F}$ -fluoroethyl-L-tyrosine and  $^{18}\text{F}$ -fluorocholine [84–87]. Nevertheless, in areas with limited access to PET, SPECT/CT has the potential of solving some of the above-mentioned clinical dilemmas using various radiopharmaceuticals, such as  $^{201}\text{Tl}$ -chloride (Fig. 11),  $^{99\text{m}}\text{Tc}$ -tetrafosmin,  $^{99\text{m}}\text{Tc}$ -sestamibi, and L-3- $^{123}\text{I}$ - $\alpha$ -methyltyrosine. In this scenario, several studies have demonstrated the usefulness of SPECT/CT for accurate preoperative detection and localization, for radiotherapy planning and for treatment monitoring. SPECT/CT achieves precise anatomical localization of viable tumour lesions versus adjacent sites with physiological tracer uptake, such as the ventricles, choroid plexus and venous sinuses [88, 89], with a proven clinical impact on management in 43% of patients [88]. Furthermore, SPECT/CT imaging with  $^{201}\text{Tl}$ -chloride has been integrated into surgical planning as a useful guide for directing biopsy to the target with the highest uptake within the brain mass, thus reducing possible tissue sampling errors when relying on morphological imaging alone [90].

The potential role of SPECT/CT in planning intra-tumoural therapy with  $^{90}\text{Y}$ -labelled substance P in glioma has been investigated, with a technique that uses individual voxel-by-voxel dosimetry on pre- and post-therapeutic SPECT coregistered with a contrast-enhanced CT scan [91]. It is therefore conceivable that hybrid SPECT/CT can be employed for accurate assessment of radiation dosimetry to the biological target volume in patients referred for  $^{90}\text{Y}$ -peptide local therapy of brain tumours.

#### Liver tumours

Both primary and metastatic hepatic tumours (hepatocarcinoma and metastatic diseases) are often associated with abnormal intra- and extra-hepatic arterial shunting to the lung or the GI tract. Local treatments based on liver vascular embolization must exclude or at least quantify this event in order to prevent as much as possible damage to the lungs or the GI tract.

Radioembolization with  $^{90}\text{Y}$ -microspheres is a novel local therapy for unresectable liver tumours, also defined as selective internal radiation therapy (SIRT). Pre-SIRT hepatic arteriography and  $^{99\text{m}}\text{Tc}$ -macroaggregated albumin (MAA) scintigraphy are generally performed to simulate the intra-hepatic distribution of  $^{90}\text{Y}$ -microsphere; radionuclide imaging is especially useful for this purpose because of the similarity in size between  $^{99\text{m}}\text{Tc}$ -MAA and  $^{90}\text{Y}$ -microspheres. Pre-treatment evaluation of hepatic perfusion with  $^{99\text{m}}\text{Tc}$ -MAA SPECT/CT is an essential prerequisite in planning SIRT [92, 93] and it has been stated that SPECT/CT liver perfusion imaging often results in modification of SIRT dosing, reposition of the infusion catheter or treatment cancellation [92]. In the most recent study involving 58 patients with hepatocellular carcinoma, sensitivity (100%), specificity (94%) and accuracy (96%) of fused SPECT/CT surpassed by far those of planar imaging and SPECT alone [93].

SPECT/CT plays a relevant role also in the assessment of atypical haemangiomas, which sometimes mimic hepatocellular carcinoma on double-phase CT hepatic angiography. Furthermore, haemangiomas can be located adjacent to the inferior vena cava, the heart or hepatic vessels, with ensuing difficult imaging interpretation.  $^{99\text{m}}\text{Tc}$ -labelled red blood cell (RBC) SPECT/CT performed in 12 patients with 24 liver lesions had a significant added value in 4 patients (33%), precisely identifying hot spot foci sited near vascular structures; thus, fused imaging was crucial for confirming or excluding liver haemangiomas in areas difficult to explore [94].

#### Prostate cancer

In cases of suspected local recurrence from prostate carcinoma, digital rectal exam and/or transrectal US-guided biopsy frequently fail to identify patients amenable to salvage treatment. MRI, PET with [ $^{11}\text{C}$ ]- or  $^{18}\text{F}$ -choline or [ $^{11}\text{C}$ ]-acetate and immunoscintigraphy with a MoAb against a prostate specific membrane glycoprotein ( $^{111}\text{In}$ -capromab pendetide, or ProstaScint<sup>®</sup>, an agent which is commercially available in the USA) have better capabilities for assessing recurrent prostate cancer [95] (Fig. 12).

ProstaScint<sup>®</sup> has been shown to outperform cross-sectional imaging with CT or MR for detecting lymph node involvement in patients at high risk of extra-prostatic



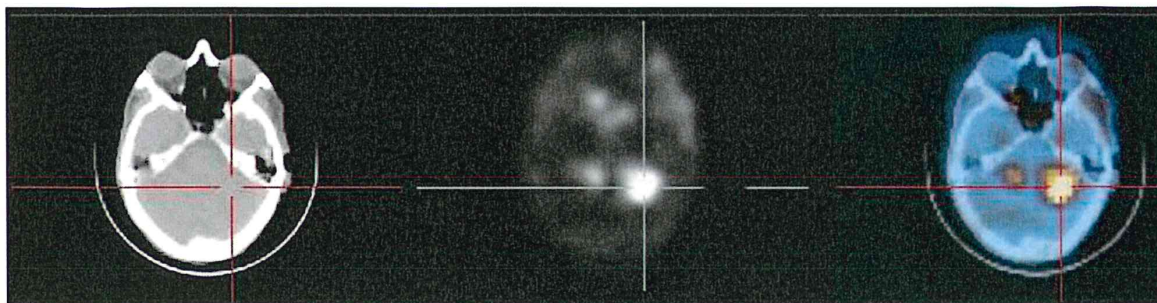


**Fig. 11** Human immunodeficiency virus (HIV)-infected patient with cerebral lymphoma. Transaxial slices of brain CT (*left panel*),  $^{201}\text{Tl}$ -chloride SPECT (*centre panel*) and SPECT/CT fused images (*right panel*); the *centring signs* indicate the target lesion (lymphoma).

(Reproduced from IAEA-TECDOC-1597: Clinical applications of SPECT/CT: new hybrid nuclear medicine imaging systems. Vienna: IAEA, 2008)

disease [96]. Furthermore, ProstaScint<sup>®</sup> predicts poor prognosis in patients referred for staging who have foci of abnormal uptake in the central abdominal area, when biopsy for histological confirmation is difficult and invasive [97].

Pre-treatment ProstaScint<sup>®</sup> SPECT/CT independently predicted an increased risk of biochemical failure in patients referred to primary radiotherapy for localized adenocarcinoma of the prostate [98]. Furthermore, in a dose escalation study in patients with T1c-T3b Nx M0 prostate adenocarcinoma, SPECT/CT was reported to accurately identify biological target volumes planned for brachytherapy (transrectal seed implant). In particular, pre-treatment SPECT/CT permitted dose intensification to occult targets to be achieved without increasing rectal morbidity [99]. ProstaScint<sup>®</sup> imaging can be also employed to better define the prostate *fossa* clinical target volume in patients scheduled for external beam radiation therapy after prostatectomy, by integrating radioimmunoscintigraphic and CT images [100]. While simultaneous dual-radionuclide imaging (i.e. ProstaScint<sup>®</sup> combined with autologous  $^{99\text{m}}\text{Tc}$ -radiolabelled RBCs for blood pool imaging) has proven useful [101], ProstaScint<sup>®</sup> SPECT/CT can be performed without the need for  $^{99\text{m}}\text{Tc}$ -labelled RBCs, so that imaging can be performed employing the full 20%  $^{111}\text{In}$  energy window (with resulting increased efficiency) [102].

### Other non-oncological disorders

#### Benign bone diseases

Although MRI represents today the standard of reference for benign orthopaedic disease, bone scintigraphy is still frequently used, since it offers a high sensitivity for osseous lesions and an overall view of the whole skeleton at acceptable costs. Its major drawback (besides its inability to

visualize the soft tissue structures of the joints) is, however, low specificity.

SPECT/CT appears to overcome most of the diagnostic limitations of bone scintigraphy, by enabling precise anatomical localization of bone turnover abnormalities [103]. Post-acquisition SPECT and CT fusion has been used in the past to assess areas of focal abnormal tracer uptake in a case diagnosed as stress fractures in bilateral pedicles of the spine, in which early detection led subsequently to appropriate treatment [104]. In 2009, Dore and co-workers assessed the value of this technology in diagnosing osteonecrosis of the jaw associated with i.v. bisphosphonate therapy [105] and demonstrated that SPECT/CT allowed discrimination of the osteonecrotic core from nearby hyperactivity due to viable bone. In their patients, MRI was not able to visualize bone destruction, but proved helpful to detect soft tissue involvement.

In one study that has systematically analysed the clinical benefit of SPECT/CT in benign orthopaedic conditions, 89 consecutive non-oncological patients with inconclusive  $^{99\text{m}}\text{Tc}$ -MDP bone scans, for which further correlation with morphological imaging was required, were investigated [106]. In 59% of the subjects multislice low-dose CT added to SPECT was critical for correctly diagnosing the lesions. In another 30% of the patients, SPECT/CT optimized the subsequent imaging algorithm of patients. SPECT/CT represented therefore a clinically relevant component of the diagnostic process in patients with non-oncological orthopaedic conditions referred for bone scintigraphy [106, 107].

#### Infection and inflammation

Infection remains a major cause of morbidity and mortality, and precise localization of infectious foci can be problematic. CT and MR provide high-quality morphological imaging, but are often non-diagnostic because structural changes underlying the infectious process are non-specific,



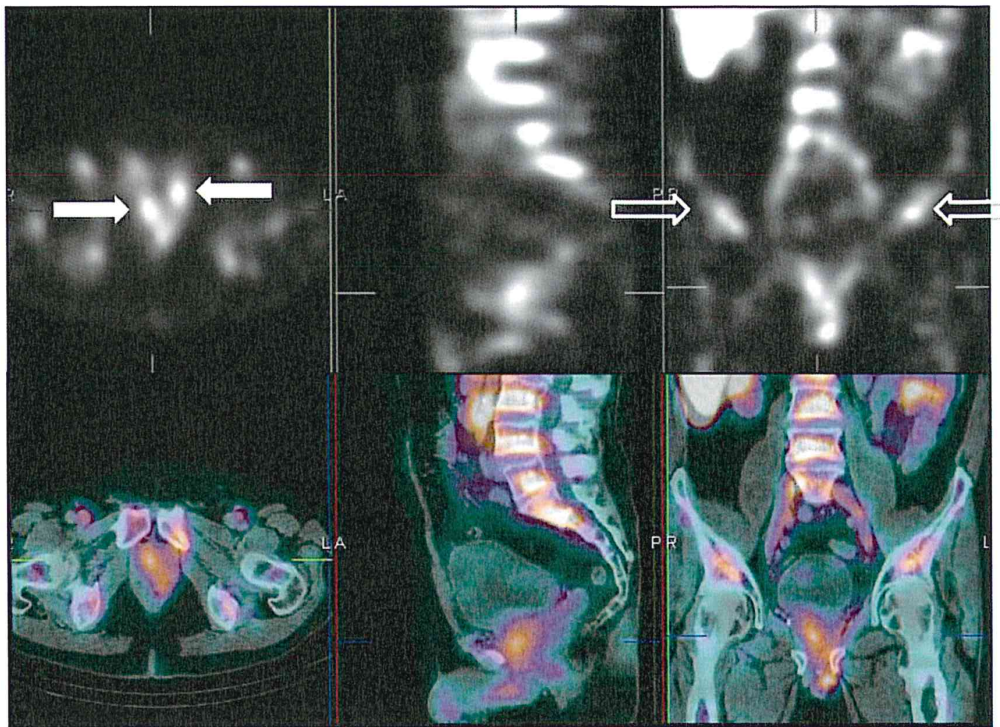


**Fig. 12** ProstaScint® SPECT/CT in a 55-year-old man who had intensity-modulated radiation therapy 1 year earlier with favourable biochemical response lasting 6 months, but then rising prostate-specific antigen (PSA) levels. While MRI and US studies were non-diagnostic due to prior treatments, the ProstaScint® scan (transaxial, sagittal and coronal SPECT in *upper panel*) shows two areas with mild non-specific increased activity in the pelvis (indicated by *white closed arrows* in the

transaxial section); high non-specific uptake in the bone marrow (iliac bones indicated by *white open arrows* in the coronal section) and liver is also to be noted. Exact location of such focal uptakes in the right and left peripheral zones of prostate is only possible in the fused SPECT/CT images (*lower panel*), which also helped to guide biopsy that confirmed recurrent prostate adenocarcinoma

or become detectable only in the subacute or late stages of the disease.

Radionuclide imaging plays a significant role in the evaluation of patients suspected of harbouring infection, especially because of its potential for detecting physiological processes and metabolic alterations that often precede morphological changes, by several days or even weeks. While  $^{67}\text{Ga}$ -citrate may be still indicated for a few well-defined clinical applications, i.e. osteomyelitis (especially of the spine) [108], scintigraphy with  $^{111}\text{In}$ -oxine- or  $^{99\text{m}}\text{Tc}$ -hexamethyl propyleneamine oxime (HMPAO)-labelled autologous leukocytes (WBC) is at present the radionuclide imaging technique of choice for infection [109] (Figs. 13 and 14). In vivo leukocyte labelling with monoclonal antigranulocyte antibodies (Leukoscan®) is a potential alternative to autologous leukocyte radiolabelling [110, 111], as is also scintigraphy with radiolabelled antibiotics [112] or natural antimicrobial peptides, such as  $^{99\text{m}}\text{Tc}$ -fluconazole,  $^{99\text{m}}\text{Tc}$ -ubiquitin and  $^{99\text{m}}\text{Tc}$ -lactoferrin [113], and finally [ $^{18}\text{F}$ ]FDG PET.

WBC and  $^{67}\text{Ga}$ -citrate scintigraphy are characterized by poor spatial resolution and low specificity due to the lack or paucity of morphological information. This limitation is of major clinical concern when assessing involvement by an infectious process of soft tissue adjacent to bone, or vascular grafts. The contribution of SPECT/CT with WBC or  $^{67}\text{Ga}$ -citrate scintigraphy has been evaluated in a variety of clinical indications, demonstrating a definite added value in distinguishing physiological uptake of labelled WBCs from infectious processes and defining the precise anatomical location of infection in up to 85% of cases [114–117]. In particular, substantial benefits were observed in scans of the thoracic or abdominal regions, when it is often problematic to identify and discriminate sites of WBC accumulation near major vessels or bowel loops. The capability of excluding infection foci by characterizing physiological abdominal tracer activity as such may avoid the inconvenience and cost of delayed  $^{67}\text{Ga}$ -citrate scintigraphy. Hybrid imaging can distinguish blood-pool activity from infectious foci, with significant advantages for



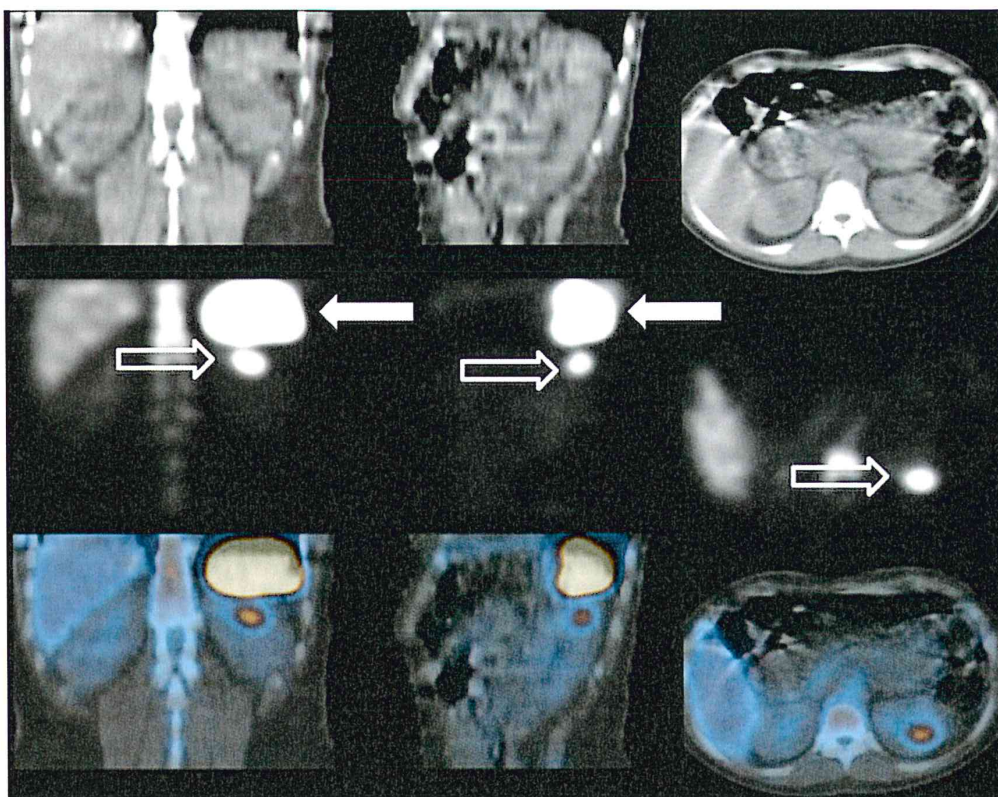


**Fig. 13** Examples of SPECT/CT imaging correctly localizing sites of infection, as visualized after i.v. infusion of autologous  $^{99m}\text{Tc}$ -HMPAO-labelled white blood cells. Focal accumulation of labelled leukocytes in a small area (indicated by *white open arrow* in the three SPECT sections, *top row*) located below the physiological high uptake in the spleen (*white closed arrows*) in a patient with antibiotic-

resistant fever of unknown origin; the SPECT/CT fusion images (*bottom row*) clearly show the intra-renal location of an abscess (the kidney is not a site of physiological radioactivity excretion/accumulation when performing scintigraphy with autologous  $^{99m}\text{Tc}$ -HMPAO leukocytes)

assessment of suspected vascular graft infection as well as in patients with fever of unknown origin. WBC SPECT/CT was found to be more accurate than  $^{67}\text{Ga}$  SPECT/CT, probably because of its higher specificity and target to background ratio [114].

In patients with osteomyelitis, WBC SPECT/CT can also detect areas of tracer accumulation in surrounding soft tissues, thus defining the precise extent of infection with ensuing relevant clinical impact on patient management. In this regard,  $^{99m}\text{Tc}$ -HMPAO WBC SPECT/CT allowed the correct diagnosis of bone and soft tissue involvement in 15 patients with suspected osteomyelitis and 13 cases with suspected infection of orthopaedic implants. In particular, this modality had major advantages for diagnosing relapsed osteomyelitis in patients with post-traumatic structural bone alterations [118].

Following the introduction of new infection-imaging radiopharmaceuticals (such as labelled antigranulocyte

MoAb, labelled ciprofloxacin and biotin), SPECT/CT has demonstrated definite advantages over single-modality imaging [119, 120].  $^{111}\text{In}$ -Biotin SPECT/CT has been reported to have a high diagnostic value by allowing precise anatomical assignment to spinal infectious foci and by distinguishing vertebral from paravertebral soft tissue involvement [120].

In a similar fashion, imaging with  $^{99m}\text{Tc}$ -labelled antigranulocyte antibody ( $^{99m}\text{Tc}$ -AGA) has been reported to have high sensitivity and specificity, but fails in exact anatomical definition of the infected sites. A recent report in patients with suspected chronic post-traumatic osteomyelitis has demonstrated that, while planar and SPECT/CT studies with  $^{99m}\text{Tc}$ -AGA have an equal sensitivity (100%), the specificity of SPECT/CT was definitely better (89 versus 78%).  $^{99m}\text{Tc}$ -AGA SPECT/CT was therefore of clinical relevance in selecting patients for surgery [119].



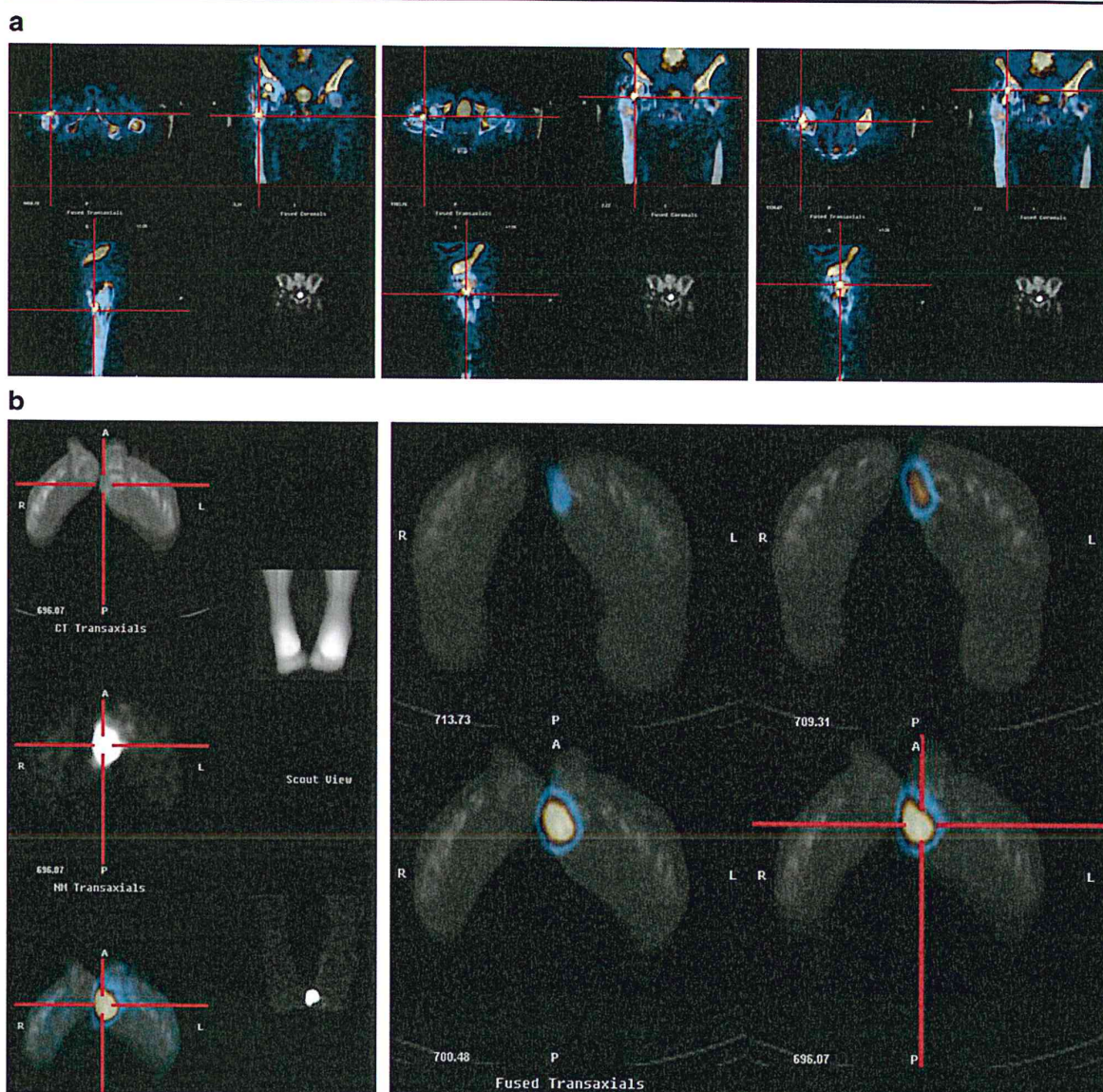


**Fig. 14 a**  $^{99m}\text{Tc}$ -HMPAO leukocyte SPECT/CT in a 78-year-old man submitted to implant of right hip prosthesis about 18 months earlier; he complained of pain and instability while walking (but no fever). Multiple areas of focal accumulation of labelled leukocytes in different sites (indicated by *pointing cross signs* in the three panels depicting the fused SPECT/CT corresponding to three different target points); SPECT/CT demonstrates accumulation of labelled leukocytes involving different anatomical structures, respectively, the cortical bone anterior to the prosthesis in the subtrochanteric region (true osteomyelitis, *panel patient*), an area around the prosthetic neck (soft tissues, *centre panel*) and an area between the cup and the head of the prosthetic implant (intra-articular infection, *right panel*). **b**  $^{99m}\text{Tc}$ -

HMPAO leukocyte SPECT/CT in a 53-year-old diabetic man with long-lasting infection (resistant to antibiotic therapy) at the medial aspect of his left foot; in addition to the scout CT view and the MIP image of distal lower limbs, the *left panel* shows the CT (*top*), the SPECT (*centre*) and the fused SPECT/CT transaxial (*bottom*) sections at a single level, while the *right panel* shows a series of adjacent transaxial fused SPECT/CT sections in and around the area of the left foot with abnormal  $^{99m}\text{Tc}$ -HMPAO leukocyte accumulation (indicated by the *pointing cross sign*). The images demonstrate that the source of infection in the superficial soft tissues is actually deeply seated, involving also the distal portion of the first metatarsal bone (osteomyelitis)



### Gastrointestinal bleeding and Meckel's diverticulum

GI bleeding is usually classified as upper (originating above the first jejunal loop) or lower (originating below such loop). Upper GI bleeding is mostly due to oesophageal varices, oesophagitis, gastritis, gastric and duodenal ulcers, Mallory-Weiss tear or tumours, whereas common causes of lower GI bleeding are angiodysplasia, diverticula, inflammation, tumours and, in paediatric patients, ectopic gastric mucosa in Meckel's diverticulum.

While endoscopy and angiography can directly localize the bleeding sites and sometimes allow local therapy to be performed in the same session, scintigraphy with  $^{99m}\text{Tc}$ -labelled RBCs is more sensitive and can also detect intermittent bleeding. Early positivity of GI bleeding can be crucial for identifying patients with active bleeding, who should be referred to immediate surgical treatment. On the other hand, a negative 24-h  $^{99m}\text{Tc}$ -labelled RBC planar scintigraphy usually predicts favourable patient outcome [121].

While  $^{99m}\text{Tc}$ -labelled RBC SPECT has already shown definite advantages over planar imaging alone, some authors have assessed the additional value of SPECT/CT to localize the precise site of bleeding [122, 123] (Fig. 15). In a group of 27 patients in whom dynamic and planar imaging detected only 50% of the bleeding sites, hybrid SPECT/CT provided exact anatomical localization in most patients, changing the conclusions of planar scintigraphy in 37% of them. Since SPECT/CT was acquired 60–90 min after the administration of  $^{99m}\text{Tc}$ -labelled RBC, there was concern that this timing might affect identification of the bleeding site because of the peristaltic and antiperistaltic bowel movements; nevertheless, in only 1 of 19 patients did hybrid imaging misrecognize the site of bleeding [124]. SPECT/CT coregistration in the same session and with the patient still has been emphasized to be important in order to avoid as much as possible artefacts of internal organs or respiratory movements [124].

The presence of ectopic gastric mucosa in Meckel's diverticulum (a vestige of the omphalomesenteric duct localized on the ileum about 50–80 cm from the ileocaecal valve) can cause bleeding because of acid secretion (in 50% of diverticula);  $^{99m}\text{Tc}$ -pertechnetate scintigraphy, which should be performed when there is no active bleeding, is a well-established imaging procedure to ascertain the presence of gastric mucosa in Meckel's diverticulum. Hybrid SPECT/CT imaging significantly helps in discriminating Meckel's diverticulum from potential artefacts and in correctly identifying as Meckel's diverticulum an abdominal paramedian area of  $^{99m}\text{Tc}$ -pertechnetate uptake shown by the dynamic scan [125].

In conclusion, patients with GI bleeding are often referred to surgery, except if they have a transient

haemodynamic instability or may benefit from medical treatment. CT added to SPECT provides helpful information to differentiate these two conditions; furthermore, SPECT/CT also improves detection and anatomical location of the site of radioactivity accumulation, both in cases of GI bleeding and in cases of ectopic gastric mucosa in Meckel's diverticulum.

### Pulmonary embolism

The clinical suspicion of pulmonary embolism (PE) arises in cases of unexplained dyspnoea, tachypnoea and/or chest pain. Pulmonary CT angiography (PCTA) is capable of directly visualizing thromboembolic filling defects, pleural effusion, vascular remodelling and oligoemia, besides allowing the differential diagnosis of pneumonia, aortic dissection, tumour or pneumothorax [126]. Nevertheless, because of its high diagnostic sensitivity, lung ventilation/perfusion scintigraphy (V/Q) or perfusion scintigraphy alone [127] are commonly performed as valid alternatives to PCTA in centres without multislice spiral CT and in cases of contraindications to intravenous administration of contrast [128].

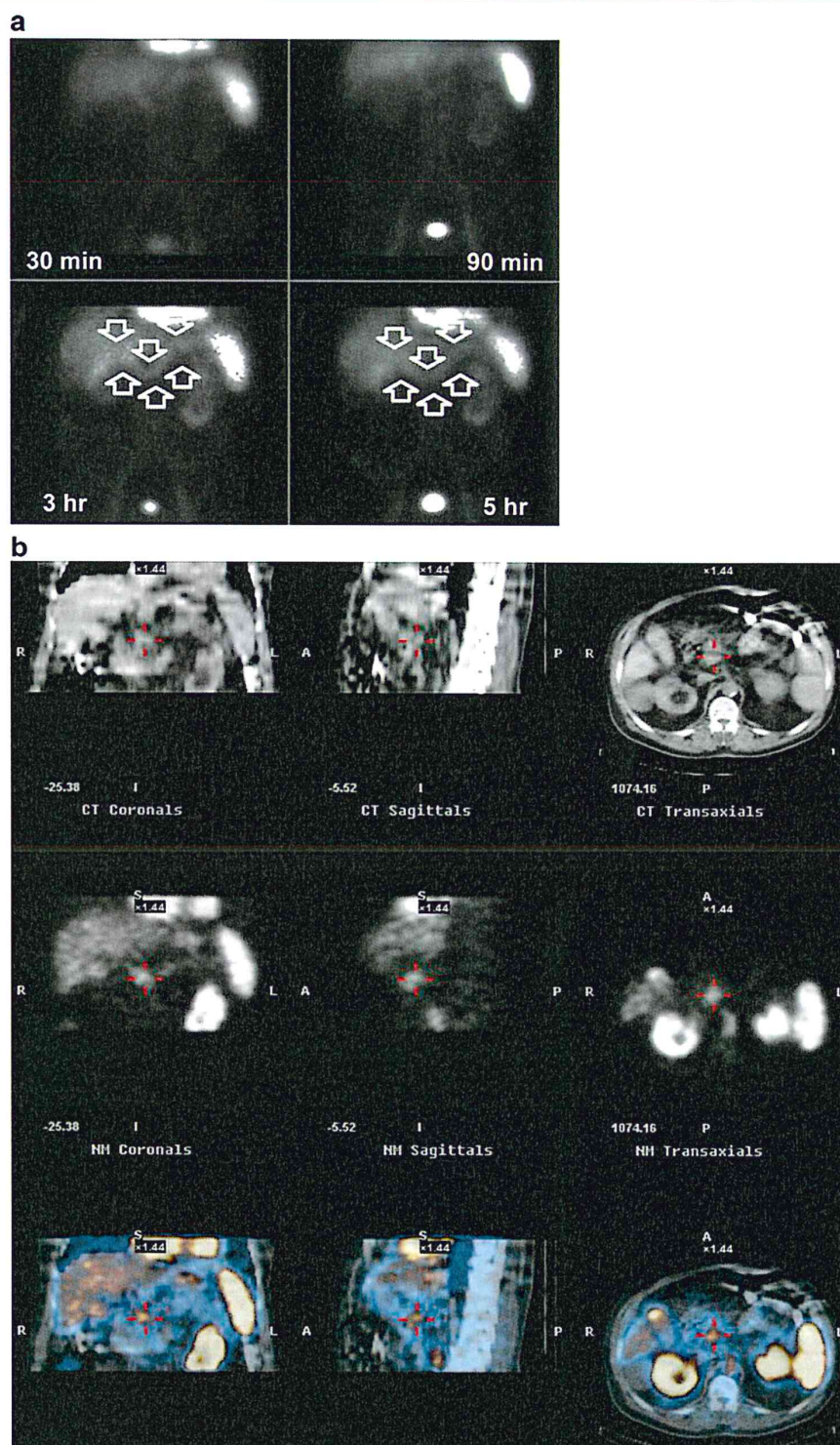
With the introduction of SPECT, the V/Q scan has undergone a transition from two-dimensional planar to three-dimensional volumetric imaging, reported to demonstrate improved sensitivity, specificity and inter-observer agreement [129]. In fact, tomographic images resolve equivocal interpretation due to partial volume and shine-through effect, and their higher spatial resolution enables detection of abnormalities, particularly at the subsegmental level and at the base of the lungs where segments are tightly packed. It has been suggested that SPECT should be used for diagnosis of postoperative PE [130].

SPECT/CT may provide a significant contribution to the differential diagnosis between acute PE-induced and inflammatory disease-induced lesions (Fig. 16). In particular, 75% of acute PE-induced consolidation opacities have been preferentially located at the peripheral lung interface between severely decreased and adjacent relatively preserved perfusion areas within wedge-shaped perfusion defects, whereas 45% of inflammatory disease-induced opacities have been described at the proximal portion of defects [131]. Nevertheless, SPECT/CT acquisition of the chest constitutes a challenge due to respiratory movements, which can cause image artefacts and thus decrease diagnostic accuracy.

A recent study evaluated the feasibility of deep-inspiratory breath-hold (DIBrH) perfusion SPECT in patients with chronic obstructive pulmonary disease (COPD), PE and interstitial lung disease (ILD). DIBrH SPECT/CT images showed excellent matching of anatomical landmarks and corresponding defects in the lungs. Furthermore, it enabled correlation of wedge-shaped perfusion defects with specific



**Fig. 15** GI bleeding scintigraphy with  $^{99m}\text{Tc}$ -labelled erythrocytes. **a** Sequential planar images, showing accumulation of radioactivity at the later imaging times (3 and 5 h) in the upper abdomen, with a pattern suggesting accumulation in the transverse colon (indicated by *white open arrows*). **b** SPECT/CT images in the three section planes (CT component at the *top*, SPECT component in the *middle*, fusion SPECT/CT at the *bottom*) show that radioactivity accumulation (indicated by *pointing cross sign*) is located in a posterior rather than in an anterior abdominal area (as it would be in the case of bleeding in the transverse colon), thus suggesting that bleeding has occurred in a jejunal loop, possibly immediately distal to the duodenum





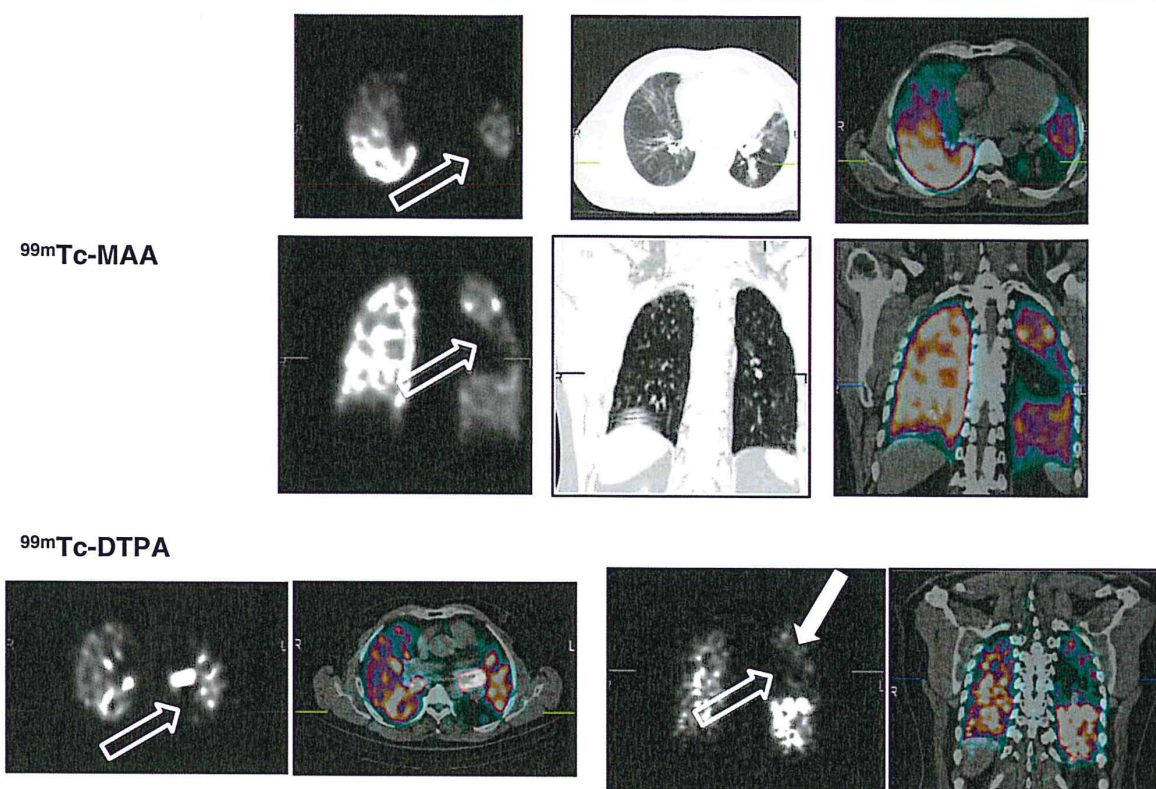


**Fig. 16** SPECT/CT of lung ventilation and perfusion in a 51-year-old man who had chest pain and inhomogeneous parenchymal opacity in left mid lung.  $^{99m}\text{Tc}$ -MAA perfusion scintigraphy (*upper panel*) shows a perfusion defect in the superior segment of the left lower lobe (indicated by *white open arrows* in the transaxial and coronal SPECT sections).  $^{99m}\text{Tc}$ -DTPA-aerosol scintigraphy (*lower panel*) shows a matching ventilation defect in the same lung zone (indicated

by *white open arrows* in the transaxial and coronal SPECT sections); according to conventional criteria, this V/Q pattern indicates low probability for pulmonary embolism. In addition, there was also decreased ventilation in a portion of the upper left lobe (*white closed arrow* in the coronal SPECT section), corresponding to a mass detected on the CT component of the examination. Surgery showed a squamous cell carcinoma obstructing the upper left lobe bronchus

pulmonary arterial branches in acute PE and heterogeneous defects with airway or parenchymal abnormalities in COPD and ILD. DIBrH CT was helpful in clarifying the cause of perfusion defects detected by SPECT and the relationship between perfusion distribution and abnormal lung CT attenuation [132].

#### Coronary artery disease (CAD)

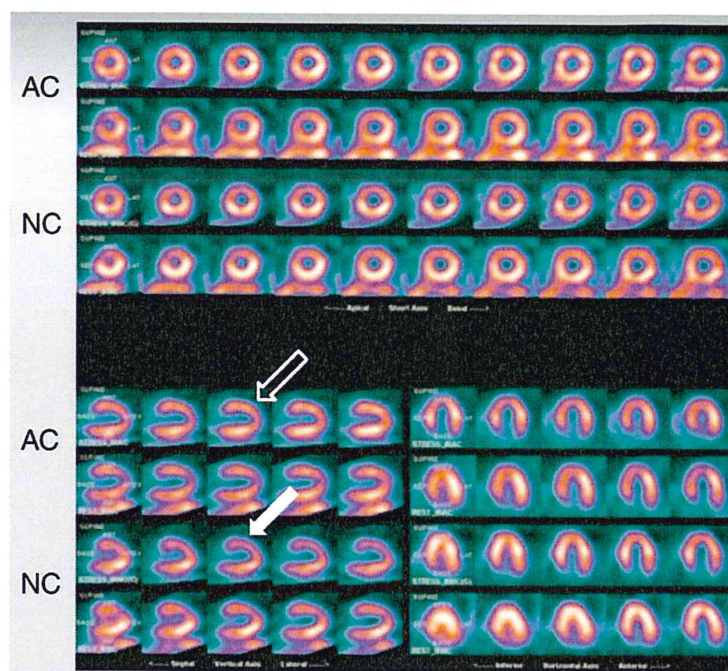
Myocardial perfusion imaging (MPI) with single photon emitting agents is of great value for evaluating the physiological significance of coronary artery lesions [133]. Nevertheless, image artefacts related to either patient movement, subdiaphragmatic activity and/or breast attenuation frequently affect stress/rest SPECT MPI. Furthermore, in cases of three-vessel disease MPI often underestimates the degree or even misses the presence of CAD. While earlier techniques generating patient-specific attenuation maps for attenuation

correction using external radionuclide sources have consistently yielded disappointing results [134], CT-based attenuation correction SPECT exhibits high resolution, high count rate and low noise attenuation maps, thus improving the diagnostic capability of MPI (Fig. 17) [135].

CT coronary angiography (CTCA) performed with 16-detector and over multislice spiral CT is characterized by high spatial and temporal resolution; combination of this procedure with SPECT MPI has consistently resulted in considerable improvements of the diagnostic performance over the use of either imaging alone [136–138]. In fact, SPECT/CTCA can improve specificity and PPV by providing physiological information on myocardial perfusion and function correlated to detailed anatomical information regarding the coronary vasculature, thus allowing a precise non-invasive identification of culprit coronary lesions and correlating their location with functional significance.



**Fig. 17** Cardiac SPECT/low-dose CT using a single isotope ( $^{99m}\text{Tc}$ -sestamibi) same-day stress/rest acquisition protocol in a 45-year-old obese woman (body mass index: 31) with shortness of breath 6 months after percutaneous angioplasty with insertion of a stent in the mid-left anterior descending coronary artery. Non-attenuation-corrected images (NC, lower rows stress, rest) indicate the presence of a fixed perfusion defect in the anterior wall, more prominent in the short and vertical long axis images (white closed arrow). CT attenuation-corrected images (AC, upper rows stress, rest) demonstrate resolution of the area of decreased myocardial perfusion (white open arrow). Abnormalities in the non-attenuation-corrected images were therefore interpreted as caused by attenuation artefact from the overlying bulky breast, and the study was reported as negative for ischaemia



Compared to the combined criteria from invasive coronary angiography and SPECT as a reference standard, SPECT/CTCA showed 96% sensitivity, 95% specificity, 77% PPV and 99% negative predictive value for defining haemodynamically significant lesions, whereas CTCA as a stand-alone procedure had shown performance indices of 84, 74, 61 and 90%, respectively, for identifying stenotic lesions in the coronary arteries [139].

In another study, SPECT/CTCA provided additional information regarding the functional consequences of lesions in 22% of coronary stenoses of 12 patients, especially in patients with involvement of small vessels and of diagonal branches [140].

The addition of CTCA to MPI SPECT may avoid false-negative scintigraphic findings in advanced three-vessel disease, showing a balanced impairment of blood flow in all cardiac segments. On the other hand, MPI permits one to correctly interpret the functional consequences of stenoses in patients with dense coronary plaques at CTCA [141].

In summary, combined functional data of normal or impaired perfusion with the presence or absence of coronary stenosis may enable a better stratification of patients with suspected ischaemic heart disease, with specific diagnostic algorithms having yet to be developed.

## Splenosis

Ectopic splenic tissue (or splenosis) can be due to proliferation resulting from seeding of splenic cells occurring during splenectomy or splenic rupture, or to accessory spleens (congenital duplications of splenic tissue in heterotopic sites, more frequent in patients with haematological disorders). Splenic implants are generally multiple and can be localized anywhere in the peritoneal cavity, or even in the chest.

Nuclear medicine agents employed to detect areas of splenosis are  $^{99m}\text{Tc}$ -labelled heat-denatured RBC and  $^{99m}\text{Tc}$ -sulfur colloid, the former more sensitive than the latter [142]. Although the clinical impact of combined SPECT/CT has been explored in few studies, interesting observations have nevertheless emerged. In particular, in splenectomized patients with relapsing anaemia or thrombocytopaenia, SPECT/CT correctly identified all equivocal lesions on CT or MRI, and also detected unsuspected additional sites of splenosis. The best diagnostic performance was observed for intra-hepatic, intra-pulmonary or pleural splenic implants, thus demonstrating the capability of hybrid SPECT/CT imaging to precisely localize heterotopic splenic tissue [143].



In a further report, SPECT/CT localized splenic remnants that planar imaging had failed to detect in a splenectomized patient; the use of an intraoperative gamma probe (directed by preoperative imaging) subsequently helped to eradicate the small splenic remnants located lateral to the descending colon [144].

#### Neurodegenerative disorders

Differential diagnosis and early detection of neurodegenerative disorders have relevant prognostic implications for planning and optimizing the therapeutic strategy, including the implementation of new approaches such as neuroprotection and neuroreparation. While MRI is very useful in most atypical parkinsonian disorders, in some cases CT may demonstrate atrophic changes when they are typically distributed [145].

Although data regarding the added value of cerebral SPECT/CT in neurodegenerative disorders are still rather limited, the diagnostic value of brain SPECT investigations increases in the presence of additional CT data. In fact, CT attenuation correction for measuring regional cerebral blood flow (rCBF) using  $^{123}\text{I}$ -iodoamphetamine prevented possible overestimation of regional CBF in low-flow regions and underestimation in high-flow areas [146]. Furthermore, a fully automated registration with CT enabled fast and accurate non-uniform attenuation correction in brain receptor SPECT, and coregistration has been suggested for group comparisons of SPECT receptor data [147].

A recent study investigated the additional diagnostic value of the low-dose CT component of  $^{99\text{m}}\text{Tc}$ -HMPAO SPECT/CT performed for assessing CBF in a population of 240 subjects. Interestingly, 25% of the low-dose CT studies showed abnormalities such as infarcts, cerebral atrophy, dilated ventricles, basal ganglia calcifications, post-surgical changes, or even chronic subdural haematoma, meningioma, and posterior fossa cyst. It has been therefore recommended that the CT component of cerebral perfusion SPECT/CT examinations should be routinely reported separately [108].

Finally, the possibility to perform high-quality diagnostic CT examinations simultaneously with brain SPECT may offer the incremental value of detecting vascular abnormalities, i.e. cerebral ischaemia, stroke or carotid stenosis, and represents a very attractive opportunity for further clinical investigations.

#### Concluding remarks

Combining SPECT with CT in a single device has further enhanced the unquestionable role of nuclear medicine imaging in the identification and characterization of many different disorders. Advantages deriving from the use of

such hybrid equipments are dual: (1) improved correction for attenuation in single photon emission tomography and (2) improved accuracy in identifying the anatomical site and extent of disease. These effects translate mostly into increased specificity (an especially worthy feature considering that relatively low specificity is a traditional drawback of radionuclide imaging), therefore into increased overall accuracy of diagnostic nuclear medicine procedures.

Relevant improvements in diagnostic performance of nuclear medicine imaging afforded by SPECT/CT explain the growing worldwide diffusion of such hybrid equipments, whose applications span now over a wide spectrum of conventional single photon investigations including primarily endocrine and neuroendocrine diseases, infection/inflammation, benign and malignant bone diseases, radioguided surgery, GI and pulmonary circulation emergencies, and coronary artery disease, but also extending to other applications such as, for example, liver tumours, splenosis and neurodegenerative disorders.

These recent technological and scientific developments add considerable matter to the ongoing, lively debate about the potential of conventional, single photon imaging (planar and SPECT) to survive the challenges arising from PET imaging, considering that PET is superior to single photon imaging for investigating the regional distribution of agents and considering the growing spectrum of PET radiopharmaceuticals [148]. On the other hand, it has been emphasized that in many practical uses single photon emitting agents are not replaceable by PET radiopharmaceuticals because of a variety of reasons, ranging from logistical considerations (e.g. physical half-life, formal approval by regulatory authorities and commercial availability) to patient-related considerations (e.g. radiation burden, selectivity of biological targeting, possibility to perform dynamic and dual-radionuclide imaging); important socio-economic considerations (with special reference to the vast majority of the world population living in developing countries) must also be taken into account [149, 150]. In particular, cost-related issues take on a special role today, considering the current worldwide financial and economic crisis with inevitable reduction in health resources, thus affecting the perspectives of nuclear medicine centres to acquire new devices, as well as the motivations of manufacturers to develop, produce and distribute new SPECT or PET imaging agents. In this scenario, the recent increase of single photon imaging procedures also in countries with consolidated clinical use of PET for more than a decade [151, 152] and the relative stabilization of conventional nuclear medicine imaging in Europe, despite the development of new diagnostic techniques including PET [153], should be considered in the perspectives outlined above.

Thus, while many innovative PET applications will probably enter the clinical arena and will therefore compete



with SPECT within a relatively short period, on the other hand newer and more accurate single photon radionuclide imaging procedures also keep growing. Far from suggesting that SPECT is becoming obsolete to be replaced by PET, this trend indicates that the future of nuclear medicine is represented by hybrid imaging in general.

## References

- Seo Y, Mari C, Hasegawa BH. Technological development and advances in single-photon emission computed tomography/computed tomography. *Semin Nucl Med* 2008;38:177–98.
- Buck AK, Nekolla S, Ziegler S, Beer A, Krause BJ, Herrmann K, et al. SPECT/CT. *J Nucl Med* 2008;49:1305–19 [Erratum in: *J Nucl Med* 2008;49:1407].
- Sawyer LJ, Starritt HC, Hiscock SC, Evans MJ. Effective doses to patients from CT acquisitions on the GE Infinia Hawkeye: a comparison of calculation methods. *Nucl Med Commun* 2008;29:144–9.
- Madsen MT. Recent advances in SPECT imaging. *J Nucl Med* 2007;48:661–73.
- Tharp K, Israel O, Hausmann J, Bettman L, Martin WH, Daitzchman M, et al. Impact of  $^{131}\text{I}$ -SPECT/CT images obtained with an integrated system in the follow-up of patients with thyroid carcinoma. *Eur J Nucl Med Mol Imaging* 2004;31:1435–42.
- Wong KK, Zarzhevsky N, Cahill JM, Frey KA, Avram AM. Incremental value of diagnostic  $^{131}\text{I}$  SPECT/CT fusion imaging in the evaluation of differentiated thyroid carcinoma. *AJR Am J Roentgenol* 2008;191:1785–94.
- Chen L, Luo Q, Shen Y, Yu Y, Yuan Z, Lu H, et al. Incremental value of  $^{131}\text{I}$  SPECT/CT in the management of patients with differentiated thyroid carcinoma. *J Nucl Med* 2008;49:1952–7.
- Schmidt D, Szikszai A, Linke R, Bautz W, Kuwert T. Impact of  $^{131}\text{I}$  SPECT/spiral CT on nodal staging of differentiated thyroid carcinoma at the first radioablation. *J Nucl Med* 2009;50:18–23.
- Spanu A, Solinas ME, Chessa F, Sanna D, Nuvoli S, Madeddu G.  $^{131}\text{I}$  SPECT/CT in the follow-up of differentiated thyroid carcinoma: incremental value versus planar imaging. *J Nucl Med* 2009;50:184–90.
- Wang H, Fu HL, Li JN, Zou RJ, Gu ZH, Wu JC. The role of single-photon emission computed tomography/computed tomography for precise localization of metastases in patients with differentiated thyroid cancer. *Clin Imaging* 2009;33:49–54.
- Patel CN, Famid U, Chowdhury FU, Scarsbrook AF. Clinical utility of hybrid SPECT-CT in endocrine neoplasia. *AJR Am J Roentgenol* 2008;190:815–24.
- Learoyd DL, Roach PJ, Briggs GM, Delbridge LW, Wilmshurst EG, Robinson BG. Technetium-99m-sestamibi scanning in recurrent medullary thyroid carcinoma. *J Nucl Med* 1997;38:227–30.
- Behr TM, Gratz S, Markus PM, Dunn RM, Hüfner M, Schauer A, et al. Anti-carcinoembryonic antigen antibodies versus somatostatin analogs in the detection of metastatic medullary thyroid carcinoma: are carcinoembryonic antigen and somatostatin receptor expression prognostic factors? *Cancer* 1997;80:2436–57.
- Rufini V, Castaldi P, Treglia G, Perotti G, Gross MD, Al-Nahhas A, et al. Nuclear medicine procedures in the diagnosis and therapy of medullary thyroid carcinoma. *Biomed Pharmacother* 2008;62:139–46.
- Castellani MR, Seregini E, Maccauro M, Chiesa C, Aliberti G, Orunesu E, et al. MIBG for diagnosis and therapy of medullary thyroid carcinoma: is there still a role? *Q J Nucl Med Mol Imaging* 2008;52:430–40.
- Behr TM, Béhé MP. Cholecystokinin-B/gastrin receptor-targeting peptides for staging and therapy of medullary thyroid cancer and other cholecystokinin-B receptor-expressing malignancies. *Semin Nucl Med* 2002;32:97–109.
- Gothardt M, Béhé MP, Beuter D, Battmann A, Bauhofer A, Schurrat T, et al. Improved tumour detection by gastrin receptor scintigraphy in patients with metastasised medullary thyroid carcinoma. *Eur J Nucl Med Mol Imaging* 2006;33:1273–9.
- Krausz Y, Keidar Z, Kogan I, Even-Sapir E, Bar-Shalom R, Engel A, et al. SPECT/CT hybrid imaging with  $^{111}\text{In}$ -pentetretotide in assessment of neuroendocrine tumors. *Clin Endocrinol (Oxf)* 2003;59:565–73.
- Arslan N, Ilgan S, Yuksel D, Serdengeci M, Bulakbasi N, Ugur O, et al. Comparison of In-111 octreotide and Tc-99m (V) DMSA scintigraphy in the detection of medullary thyroid tumor foci in patients with elevated levels of tumor markers after surgery. *Clin Nucl Med* 2001;26:683–8.
- Lamberts SW, Chayvialle JA, Krenning EP. The visualization of gastroenteropancreatic endocrine tumors. *Metabolism* 1992;41:111–5.
- Kaltsas GA, Besser GM, Grossman AB. The diagnosis and medical management of advanced neuroendocrine tumors. *Endocr Rev* 2004;25:458–511.
- Rufini V, Calcagni ML, Baum RP. Imaging of neuroendocrine tumors. *Semin Nucl Med* 2006;36:228–47.
- Perri M, Erba P, Volterrani D, Lazzeri E, Boni G, Grosso M, et al. Octreo-SPECT/CT imaging for accurate detection and localization of suspected neuroendocrine tumors. *Q J Nucl Med Mol Imaging* 2008;52:323–33.
- Bodei L, Ferone D, Grana CM, Cremonesi M, Signore A, Dierckx RA, et al. Peptide receptor therapies in neuroendocrine tumors. *J Endocrinol Invest* 2009;32:360–9.
- Cremonesi M, Ferrari M, Bodei L, Tosi G, Paganelli G. Dosimetry in peptide radionuclide receptor therapy: a review. *J Nucl Med* 2006;47:1467–75.
- Forrer F, Mueller-Brand J, Maecke H. Pre-therapeutic dosimetry with radiolabelled somatostatin analogues in patients with advanced neuroendocrine tumours. *Eur J Nucl Med Mol Imaging* 2005;32:511–2.
- Barone R, Walrand S, Konijnenberg M, Valkema R, Kvols LK, Krenning EP, et al. Therapy using labelled somatostatin analogues: comparison of the absorbed doses with  $^{111}\text{In}$ -DTPA-D-Phe<sup>1</sup>-octreotide and yttrium-labelled DOTA-D-Phe<sup>1</sup>-Tyr<sup>3</sup>-octreotide. *Nucl Med Commun* 2008;29:283–90.
- Chowdhury FU, Scarsbrook AF. The role of hybrid SPECT-CT in oncology: current and emerging clinical applications. *Clin Radiol* 2008;63:241–51.
- Amar L, Servais A, Gimenez-Roqueplo AP, Zinzindohoue F, Chatellier G, Plouin PF. Year of diagnosis, features at presentation, and risk of recurrence in patients with pheochromocytoma or secreting paraganglioma. *J Clin Endocrinol Metab* 2005;90:2110–6.
- Mukherjee JJ, Kaltsas GA, Islam N, Plowman PN, Foley R, Hikmat J, et al. Treatment of metastatic carcinoid tumours, pheochromocytoma, paraganglioma and medullary carcinoma of the thyroid with  $^{131}\text{I}$ -meta-iodobenzylguanidine ( $^{131}\text{I}$ -MIBG). *Clin Endocrinol (Oxf)* 2001;55:47–60.
- Maurea S, Cuocolo A, Reynolds JC, Neumann RD, Salvatore M. Diagnostic imaging in patients with paragangliomas. Computed tomography, magnetic resonance and MIBG scintigraphy comparison. *Q J Nucl Med* 1996;40:365–71.
- Bhatia KS, Ismail MM, Sahdev A, Rockall AG, Hogarth K, Canizales A, et al.  $^{123}\text{I}$ -metaiodobenzylguanidine (MIBG) scintigraphy for the detection of adrenal and extra-adrenal pheochromocytomas: CT and MRI correlation. *Clin Endocrinol (Oxf)* 2008;69:181–8.



33. Gao YC, Lu HK, Luo QY, Chen LB, Ding Y, Zhu RS. Comparison of free plasma metanephrines enzyme immunoassay with  $^{131}\text{I}$ -MIBG scan in diagnosis of pheochromocytoma. *Clin Exp Med* 2008;8:87–91.
34. Rozovsky K, Koplewitz BZ, Krausz Y, Revel-Vilk S, Weintraub M, Chisin R, et al. Added value of SPECT/CT for correlation of MIBG scintigraphy and diagnostic CT in neuroblastoma and pheochromocytoma. *AJR Am J Roentgenol* 2008;190:1085–90.
35. Schillaci O. Hybrid SPECT/CT: a new era for SPECT imaging? *Eur J Nucl Med Mol Imaging* 2005;32:521–4.
36. Krausz Y, Israel O. Single-photon emission computed tomography/computed tomography in endocrinology. *Semin Nucl Med* 2006;36:267–74.
37. Ozer S, Dobrozemsky G, Kienast O, Beheshti M, Becherer A, Niederle B, et al. Value of combined XCT/SPECT technology for avoiding false positive planar  $^{123}\text{I}$ -MIBG scintigraphy. *Nuklearmedizin* 2004;43:164–70.
38. Keidar Z, Israel O, Krausz Y. SPECT/CT in tumor imaging: technical aspects and clinical applications. *Semin Nucl Med* 2003;33:205–18.
39. Rayner B. Primary aldosteronism and aldosterone-associated hypertension. *J Clin Pathol* 2008;61:825–31.
40. Avram AM, Fig LM, Gross MD. Adrenal gland scintigraphy. *Semin Nucl Med* 2006;36:212–27.
41. Gross MD, Avram A, Fig LM, Rubello D. Contemporary adrenal scintigraphy. *Eur J Nucl Med Mol Imaging* 2007;34:547–57.
42. Yen RF, Wu VC, Liu KL, Cheng MF, Wu YW, Chueh SC, et al.  $^{131}\text{I}$ -6beta-iodomethyl-19-norcholesterol SPECT/CT for primary aldosteronism patients with inconclusive adrenal venous sampling and CT results. *J Nucl Med* 2009;50:1631–7.
43. Mariani G, Gulec SA, Rubello D, Boni G, Puccini M, Pelizzo MR, et al. Preoperative localization and radioguided parathyroid surgery. *J Nucl Med* 2003;44:1443–58.
44. Rubello D, Gross MD, Mariani G, AL-Nahhas A. Scintigraphic techniques in primary hyperparathyroidism: from pre-operative localisation to intra-operative imaging. *Eur J Nucl Med Mol Imaging* 2007;34:926–33.
45. Lorberboy M, Minski I, Macadziob S, Nikolov G, Schachter P. Incremental diagnostic value of preoperative  $^{99\text{m}}\text{Tc}$ -MIBI SPECT in patients with a parathyroid adenoma. *J Nucl Med* 2003;44:904–8.
46. Papathanassiou D, Flament JB, Pochart JM, Patey M, Marty H, Liehn JC, et al. SPECT/CT in localization of parathyroid adenoma or hyperplasia in patients with previous neck surgery. *Clin Nucl Med* 2008;33:394–7.
47. Lavery WC, Goetze S, Friedman KP, Leal JP, Zhang Z, Garret-Mayer E, et al. Comparison of SPECT/CT, SPECT, and planar imaging with single- and dual-phase ( $^{99\text{m}}\text{Tc}$ -sestamibi parathyroid scintigraphy. *J Nucl Med* 2007;48:1084–9.
48. Serra A, Bolasco P, Satta L, Nicolosi A, Uccheddu A, Piga M. Role of SPECT/CT in the preoperative assessment of hyperparathyroid patients. *Radiol Med* 2006;111:999–1008.
49. Harris L, Yoo J, Driedger A, Fung K, Franklin J, Gray D, et al. Accuracy of technetium- $^{99\text{m}}$  SPECT-CT hybrid images in predicting the precise intraoperative anatomical location of parathyroid adenomas. *Head Neck* 2008;30:509–17.
50. Even-Sapir E. Imaging of malignant bone involvement by morphologic, scintigraphic, and hybrid modalities. *J Nucl Med* 2005;47:1356–67.
51. Horger M, Eschmann SM, Pfannenbergl C, Vonthein R, Besenfelder H, Claussen CD, et al. Evaluation of combined transmission and emission tomography for classification of skeletal lesions. *AJR Am J Roentgenol* 2004;183:655–61.
52. Utsunomiya D, Shiraiishi S, Imuta M, Tomiguchi S, Kawanaka K, Morishita S, et al. Added value of SPECT/CT fusion in assessing suspected bone metastasis: comparison with scintigraphy alone and nonfused scintigraphy and CT. *Radiology* 2006;238:264–71.
53. Römer W, Nömayr A, Uder M, Bautz W, Kuwert T. SPECT-guided CT for evaluating foci of increased bone metabolism classified as indeterminate on SPECT in cancer patients. *J Nucl Med* 2006;47:1102–6.
54. Strobel K, Burger C, Seifert B, Husarik DB, Soyka JD, Hany TF. Characterization of focal bone lesions in the axial skeleton: performance of planar bone scintigraphy compared with SPECT and SPECT fused with CT. *AJR Am J Roentgenol* 2007;188:W467–74.
55. Genovesi D, Di Martino F, Loi A, Lazzeri M, Boni G, Mariani G. Use of SPECT/CT for optimizing dosimetry estimates in patients with metastatic bone disease treated with  $^{153}\text{Sm}$ -EDTMP. *Q J Nucl Med Mol Imaging* 2007;51:380.
56. Ferran N, Ricart Y, Lopez M, Martinez-Ballarín I, Roca M, Gámez C, et al. Characterization of radiologically indeterminate lung lesions:  $^{99\text{m}}\text{Tc}$ -depreotide SPECT versus  $^{18}\text{F}$ -FDG PET. *Nucl Med Commun* 2006;27:507–14.
57. Cronin P, Dwamena BA, Kelly AM, Carlos RC. Solitary pulmonary nodules: meta-analytic comparison of cross-sectional imaging modalities for diagnosis of malignancy. *Radiology* 2008;246:772–82.
58. Sergiacomi G, Schillaci O, Leporace M, Laviani F, Cariani M, Manni C, et al. Integrated multislice CT and  $^{99\text{m}}\text{Tc}$ -sestamibi SPECT-CT evaluation of solitary pulmonary nodules. *Radiol Med* 2006;111:213–24.
59. Israel O, Krausz Y. SPECT/CT in tumor imaging. In: von Shultness GK, editor. *Clinical molecular anatomic imaging*. Philadelphia: Lippincott Williams & Wilkins; 2003. p. 447–62.
60. Schillaci O. Single-photon emission computed tomography/computed tomography in lung cancer and malignant lymphoma. *Semin Nucl Med* 2006;36:275–85.
61. Palmedo H, Biersack HJ, Lastoria S, Maublant J, Prats E, Stegner HE, et al. Scintimammography with technetium- $^{99\text{m}}$  methoxyisobutylisonitrile: results of a prospective European multicentre trial. *Eur J Nucl Med* 1998;25:375–85.
62. Grosso M, Chiacchio S, Bianchi F, Traino C, Marini C, Cilotti A, et al. Comparison between  $^{99\text{m}}\text{Tc}$ -sestamibi scintimammography and X-ray mammography in the characterization of clusters of microcalcifications: a prospective long-term study. *Anticancer Res* 2009;29:4251–7.
63. Schillaci O, Danieli R, Filippi L, Romano P, Cossu E, Manni C, et al. Scintimammography with a hybrid SPECT/CT imaging system. *Anticancer Res* 2007;27:557–62.
64. Mariani G, Giuliano AE, Strauss HW, editors. *Radioguided surgery: a comprehensive team approach*. New York: Springer; 2008.
65. Mariani G, Moresco L, Viale G, Villa G, Bagnasco M, Canavese G, et al. Radioguided sentinel lymph node biopsy in breast cancer surgery. *J Nucl Med* 2001;42:1198–215.
66. Mariani G, Gipponi M, Moresco L, Villa G, Bartolomei M, Mazzarol G, et al. Radioguided sentinel lymph node biopsy in malignant cutaneous melanoma. *J Nucl Med* 2002;43:811–27.
67. van der Ploeg IM, Valdés Olmos RA, Kroon BB, Wouters MW, van den Brekel MW, Vogel WV, et al. The yield of SPECT/CT for anatomical lymphatic mapping in patients with melanoma. *Ann Surg Oncol* 2009;16:1537–42.
68. Gallowitsch HJ, Kraschl P, Igger I, Hussein T, Kresnik E, Mikosch P, et al. Sentinel node SPECT-CT in breast cancer. Can we expect any additional and clinically relevant information? *Nuklearmedizin* 2007;46:252–6.
69. van der Ploeg IM, Nieweg OE, Kroon BB, Rutgers EJ, Baas-Vrancken Peeters MJ, Vogel WV, et al. The yield of SPECT/CT for anatomical lymphatic mapping in patients with breast cancer. *Eur J Nucl Med Mol Imaging* 2009;36:903–9.



70. Lerman H, Lievshitz G, Zak O, Metser U, Schneebaum S, Even-Sapir E. Improved sentinel node identification by SPECT/CT in overweight patients with breast cancer. *J Nucl Med* 2007;48:201–6.
71. Lopez R, Payoux P, Gantet P, Esquerré JP, Boutault F, Paoli JR. Multimodal image registration for localization of sentinel nodes in head and neck squamous cell carcinoma. *J Oral Maxillofac Surg* 2004;62:1497–504.
72. Nomori H, Ikeda K, Mori T, Shiraishi S, Kobayashi H, Iwatani K, et al. Sentinel node identification in clinical stage Ia non-small cell lung cancer by a combined single photon emission computed tomography/computed tomography system. *J Thorac Cardiovasc Surg* 2007;134:182–7.
73. Kretschmer L, Altenvoerde G, Meller J, Zutt M, Funke M, Neumann C, et al. Dynamic lymphoscintigraphy and image fusion of SPECT and pelvic CT-scans allow mapping of aberrant pelvic sentinel lymph nodes in malignant melanoma. *Eur J Cancer* 2003;39:175–83.
74. Leijte JA, van der Ploeg IM, Valdés Olmos RA, Nieweg OE, Horenblas S. Visualization of tumor blockage and rerouting of lymphatic drainage in penile cancer patients by use of SPECT/CT. *J Nucl Med* 2009;50:364–7.
75. van der Ploeg IM, Kroon BB, Valdés Olmos RA, Nieweg OE. Evaluation of lymphatic drainage patterns to the groin and implications for the extent of groin dissection in melanoma patients. *Ann Surg Oncol* 2009;16:2994–9.
76. Schaefer NG, Hany TF, Taverna C, Seifert B, Stumpe KDM, von Schulthess GK, et al. Non-Hodgkin lymphoma and Hodgkin disease: coregistered FDG PET and CT at staging and restaging—do we need contrast-enhanced CT? *Radiology* 2004;232:823–9.
77. Front D, Israel O, Epelbaum R, Ben Haim S, Sapir EE, Jerushalmi J, et al. Ga-67 SPECT before and after treatment of lymphoma. *Radiology* 1990;175:515–9.
78. Front D, Bar-Shalom R, Mor M, Haim N, Epelbaum R, Frenkel A, et al. Hodgkin disease: prediction of outcome with  $^{67}\text{Ga}$  scintigraphy after one cycle of chemotherapy. *Radiology* 1999;210:487–91.
79. Chajari M, Lacroix J, Peny AM, Chesnay E, Batalla A, Henry-Amar M, et al. Gallium-67 scintigraphy in lymphoma: is there a benefit of image fusion with computed tomography? *Eur J Nucl Med Mol Imaging* 2002;29:380–7.
80. Palumbo B, Sivoletta S, Palumbo I, Liberati AM, Palumbo R.  $^{67}\text{Ga}$ -SPECT/CT with a hybrid system in the clinical management of lymphoma. *Eur J Nucl Med Mol Imaging* 2005;32:1011–7.
81. Boucek JA, Turner JH. Validation of prospective whole-body bone marrow dosimetry by SPECT/CT multimodality imaging in  $^{131}\text{I}$ -anti-CD20 rituximab radioimmunotherapy of non-Hodgkin's lymphoma. *Eur J Nucl Med Mol Imaging* 2005;32:458–69.
82. Brandes AA, Tosoni A, Spagnolli F, Frezza G, Leonardi M, Calucci F, et al. Disease progression or pseudoprogression after concomitant radiochemotherapy treatment: pitfalls in neuro-oncology. *Neuro Oncol* 2008;10:361–7.
83. Chinn RJ, Wilkinson ID, Hall-Craggs MA, Paley MN, Miller RF, Kendall BE, et al. Toxoplasmosis and primary central nervous system lymphoma in HIV infection: diagnosis with MR spectroscopy. *Radiology* 1995;197:649–54.
84. Spaeth N, Wyss MT, Weber B, Scheidegger S, Lutz A, Verwey J, et al. Uptake of  $^{18}\text{F}$ -fluorocholine,  $^{18}\text{F}$ -fluoroethyl-L-tyrosine, and  $^{18}\text{F}$ -FDG in acute cerebral radiation injury in the rat: implications for separation of radiation necrosis from tumor recurrence. *J Nucl Med* 2004;45:1931–8.
85. Astner S, Grosu A, Weber W, Wester H, Schwaiger M, Molls M. O-(2-[ $^{18}\text{F}$ ]fluoroethyl)-L-tyrosine compared to L-(methyl- $^{11}\text{C}$ ) methionine in positron emission tomography for tumor volume delineation of gliomas and metastases. *Int J Radiat Oncol Biol Phys* 2005;63:S65.
86. Chen W, Silverman DHS, Delaloye S, Czernin J, Kamdar N, Pope W, et al.  $^{18}\text{F}$ -FDOPA PET imaging of brain tumors: comparison study with  $^{18}\text{F}$ -FDG PET and evaluation of diagnostic accuracy. *J Nucl Med* 2006;47:904–11.
87. Huang Z, Zuo C, Guan Y, Zhang Z, Liu P, Xue F, et al. Misdiagnoses of  $^{11}\text{C}$ -choline combined with  $^{18}\text{F}$ -FDG PET imaging in brain tumours. *Nucl Med Commun* 2008;29:354–8.
88. Filippi L, Schillaci O, Santoni R, Manni C, Danieli R, Simonetti G. Usefulness of SPECT/CT with a hybrid camera for the functional anatomical mapping of primary brain tumors by [ $^{99\text{m}}$ Tc] tetrofosmin. *Cancer Biother Radiopharm* 2006;21:41–8.
89. Schillaci O, Filippi L, Manni C, Santoni R. Single-photon emission computed tomography/computed tomography in brain tumors. *Semin Nucl Med* 2007;37:34–47.
90. Hemm S, Vayssiere N, Zanca M, Ravel P, Coubes P. Thallium SPECT-based stereotactic targeting for brain tumor biopsies. A technical note. *Stereotact Funct Neurosurg* 2004;82:70–6.
91. Kneifel S, Bernhardt P, Uusijärvi H, Good S, Plasswilm L, Buitrago-Téllez C, et al. Individual voxelwise dosimetry of targeted  $^{90}\text{Y}$ -labelled substance P radiotherapy for malignant gliomas. *Eur J Nucl Med Mol Imaging* 2007;34:1388–95.
92. Machac J, Heiba S, Zhang Z, Weintraub J, Nowakowski F, Stangl A, et al. Value of planar and SPECT/CT Tc-99m MAA liver perfusion imaging in planning of yttrium-90 Sir Sphere therapy of tumors of the liver. *J Nucl Med* 2008;49(Suppl 1):144P.
93. Hamami ME, Poeppel TD, Müller S, Heusner T, Bockisch A, Hilgard P, et al. SPECT/CT with  $^{99\text{m}}$ Tc-MAA in radioembolization with  $^{90}\text{Y}$  microspheres in patients with hepatocellular cancer. *J Nucl Med* 2009;50:688–92.
94. Schillaci O, Danieli R, Manni C, Capocchetti F, Simonetti G. Technetium-99m-labelled red blood cell imaging in the diagnosis of hepatic haemangiomas: the role of SPECT/CT with a hybrid camera. *Eur J Nucl Med Mol Imaging* 2004;31:1011–5.
95. Pucar D, Sella T, Schöder H. The role of imaging in the detection of prostate cancer local recurrence after radiation therapy and surgery. *Curr Opin Urol* 2008;18:87–97.
96. Manyak MJ, Hinkle GH, Olsen JO, Chiaccherini RP, Partin AW, Piantadosi S, et al. Immunoscintigraphy with indium-111-capromab pendetide: evaluation before definitive therapy in patients with prostate cancer. *Urology* 1999;54:1058–63.
97. Haseman MK, Rosenthal SA, Kipper SL, Trout JR, Manyak MJ. Central abdominal uptake of indium-111 capromab pendetide (ProstaScint) predicts for poor prognosis in patients with prostate cancer. *Urology* 2007;70:303–8.
98. Ellis RJ, Zhou EH, Fu P, Kaminsky DA, Sodee DB, Faulhaber PF, et al. Single photon emission computerized tomography with capromab pendetide plus computerized tomography image set co-registration independently predicts biochemical failure. *J Urol* 2008;179:1768–73.
99. Ellis RJ, Zhou H, Kaminsky DA, Fu P, Kim EY, Sodee DB, et al. Rectal morbidity after permanent prostate brachytherapy with dose escalation to biologic target volumes identified by SPECT/CT fusion. *Brachytherapy* 2007;6:149–56.
100. Jani AB, Spelbring D, Hamilton R, Blend MJ, Pelizzari C, Brendler C, et al. Impact of radioimmunoscintigraphy on definition of clinical target volume for radiotherapy after prostatectomy. *J Nucl Med* 2004;45:238–46.
101. Kelly NL, Holder LE, Khan SH. Dual-isotope protocol for indium-111 capromab pendetide monoclonal antibody imaging. *J Nucl Med Technol* 1998;26:174–7.
102. Wong TZ, Turkington TG, Polascik TJ, Coleman RE. ProstaScint (capromab pendetide) imaging using hybrid gamma camera-CT technology. *AJR Am J Roentgenol* 2005;184:676–80.
103. Römer W, Olk A, Hennig FF, Bautz W, Kuwert T. Assessment of aseptic loosening of the acetabular component in a total hip



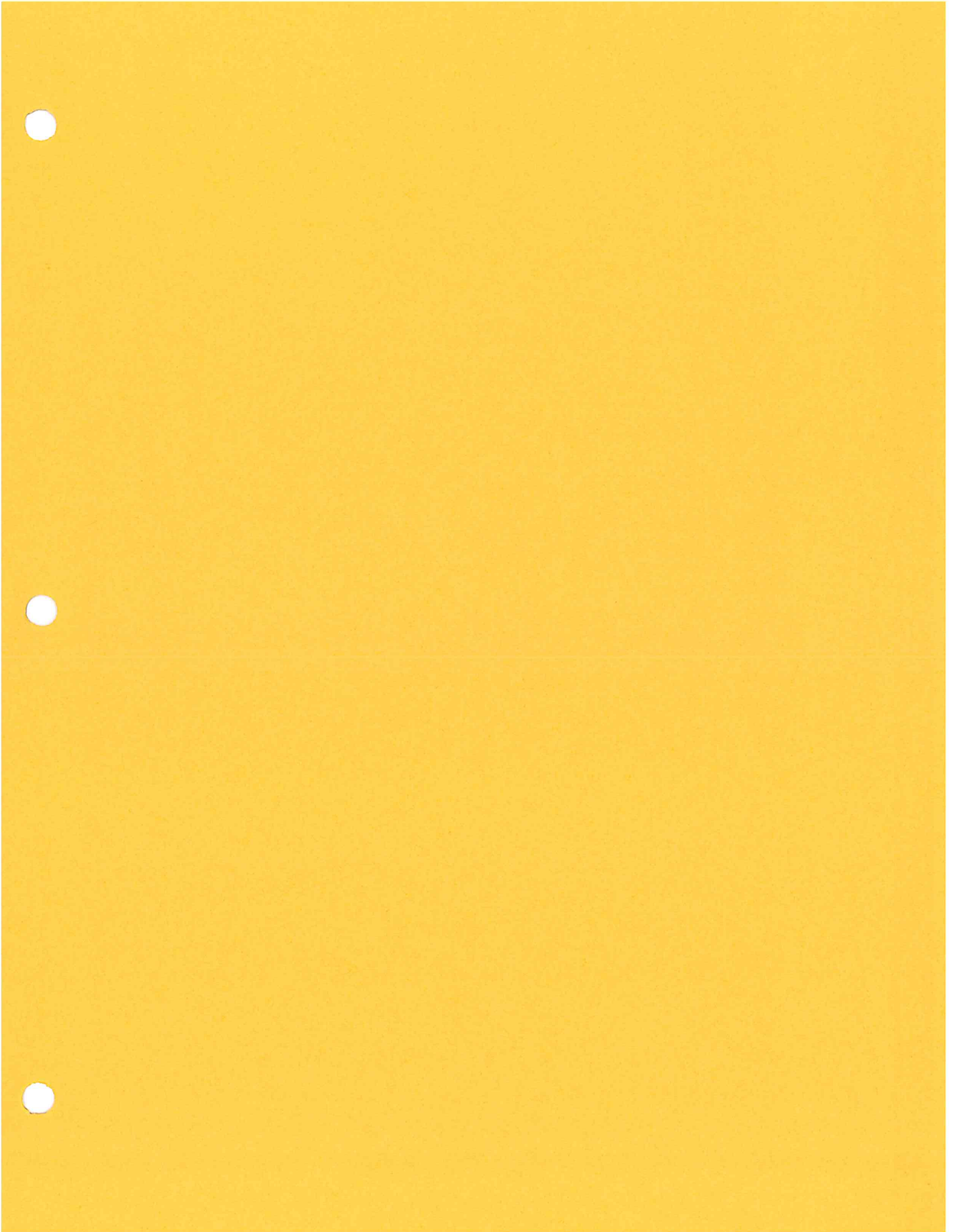
- replacement with  $^{99m}\text{Tc}$ -DPD-SPECT/spiral-CT hybrid imaging. *Nuklearmedizin* 2005;44:N58–60.
104. Traugher PD, Havlina JM Jr. Bilateral pedicle stress fractures: SPECT and CT features. *J Comput Assist Tomogr* 1991;15:338–40.
  105. Dore F, Filippi L, Biasotto M, Chiandussi S, Cavalli F, Di Lenarda R. Bone scintigraphy and SPECT/CT of bisphosphonate-induced osteonecrosis of the jaw. *J Nucl Med* 2009;50:30–5.
  106. Even-Sapir E, Flusser G, Lerman H, Lievshitz G, Metser U. SPECT/multislice low-dose CT: a clinically relevant constituent in the imaging algorithm of nononcologic patients referred for bone scintigraphy. *J Nucl Med* 2007;48:319–24.
  107. Scharf S. SPECT/CT imaging in general orthopedic practice. *Semin Nucl Med* 2009;39:293–307.
  108. El-Maghraby TA, Moustafa HM, Pauwels EK. Nuclear medicine methods for evaluation of skeletal infection among other diagnostic modalities. *Q J Nucl Med Mol Imaging* 2006;50:167–92.
  109. Prandini N, Lazzeri E, Rossi B, Erba P, Parisella MG, Signore A. Nuclear medicine imaging of bone infections. *Nucl Med Commun* 2006;27:633–44.
  110. Iyengar KP, Vinjamuri S. Role of  $^{99m}\text{Tc}$  sulesomab in the diagnosis of prosthetic joint infections. *Nucl Med Commun* 2005;26:489–96.
  111. Kaisidis A, Megas P, Apostolopoulos D, Spiridonidis T, Koumoundourou D, Zouboulis P, et al. Diagnosis of septic loosening of hip prosthesis with LeukoScan. SPECT scan with  $^{99m}\text{Tc}$ -labeled monoclonal antibodies. *Orthopade* 2005;34:462–9. German.
  112. Sierra JM, Rodriguez-Puig D, Soriano A, Mensa J, Píera C, Vila J. Accumulation of  $^{99m}\text{Tc}$ -ciprofloxacin in *Staphylococcus aureus* and *Pseudomonas aeruginosa*. *Antimicrob Agents Chemother* 2008;52:2691–2.
  113. Lupetti A, Welling MM, Pauwels EK, Nibbering PH. Detection of fungal infections using radiolabeled antifungal agents. *Curr Drug Targets* 2005;6:945–54.
  114. Bar-Shalom R, Yefremov N, Guralnik L, Keidar Z, Engel A, Nitecki S, et al. SPECT/CT using  $^{67}\text{Ga}$  and  $^{111}\text{In}$ -labeled leukocyte scintigraphy for diagnosis of infection. *J Nucl Med* 2006;47:587–94.
  115. Ingui CJ, Shah NP, Oates ME. Infection scintigraphy: added value of single-photon emission computed tomography/computed tomography fusion compared with traditional analysis. *J Comput Assist Tomogr* 2007;31:375–80.
  116. Grubstein A, Bernstein H, Steinmetz AP. Chest CT and gallium-67 SPECT scintigraphy scan co-registration in a post-heart transplantation patient with unresolved fever. *Isr Med Assoc J* 2007;9:827–8.
  117. Bajaj SK, Seitz JP, Qing F. Diagnosis of acute bacterial prostatitis by Ga-67 scintigraphy and SPECT-CT. *Clin Nucl Med* 2008;33:813–5.
  118. Filippi L, Schillaci O. Usefulness of hybrid SPECT/CT in  $^{99m}\text{Tc}$ -HMPAO-labeled leukocyte scintigraphy for bone and joint infections. *J Nucl Med* 2006;47:1908–13.
  119. Horger M, Eschmann SM, Pfannenberger C, Storek D, Dammann F, Vonthein R, et al. The value of SPET/CT in chronic osteomyelitis. *Eur J Nucl Med Mol Imaging* 2003;30:1665–73.
  120. Lazzeri E, Erba PA, Perri M, Tascini C, Doria R, Dell'Anno B. Role of one-step radiolabeled Biotin SPECT/CT in the diagnosis of spinal infection. *J Nucl Med* 2007;48:280P.
  121. Feingold DL, Caliendo FJ, Chinn BT, Notaro JR, Oliver GC, Salvati EP, et al. Does hemodynamic instability predict positive technetium-labeled red blood cell scintigraphy in patients with acute lower gastrointestinal bleeding? A review of 50 patients. *Dis Colon Rectum* 2005;48:1001–4.
  122. Yama N, Ezoe E, Kimura Y, Mukaiya M, Fujimori K, Kurimoto Y, et al. Localization of intestinal bleeding using a fusion of  $^{99m}\text{Tc}$ -labeled RBC SPECT and X-ray CT. *Clin Nucl Med* 2005;30:488–9.
  123. Kimura Y, Yama N, Isobe M, Nobuoka T, Furuhashi T, Asai Y, et al. A novel method for the detection and the localization of intestinal bleeding using a fusion image of  $^{99m}\text{Tc}$ -labeled RBC SPECT and X-ray CT. *J Abdom Emerg Med* 2006;26:387–9.
  124. Schillaci O, Spanu A, Tagliabue L, Filippi L, Danieli R, Palumbo B, et al. SPECT/CT with a hybrid imaging system in the study of lower gastrointestinal bleeding with technetium-99m red blood cells. *Q J Nucl Med Mol Imaging* 2009;53:281–9.
  125. Papathanassiou D, Liehn JC, Men  roux B, Amans J, Domange-Testard A, Belouadah M, et al. SPECT-CT of Meckel diverticulum. *Clin Nucl Med* 2007;32:218–20.
  126. Schoepf UJ, Goldhaber SZ, Costello P. Spiral computed tomography for acute pulmonary embolism. *Circulation* 2004;109:2160–7.
  127. Miniati M, Marini C, Allescia G, Tonelli L, Formichi B, Prediletto R, et al. Non-invasive diagnosis of pulmonary embolism. *Int J Cardiol* 1998;65:S83–6.
  128. Reid JH, Coche EE, Inoue T, Kim EE, Dondi M, Watanabe N, et al. Is the lung scan alive and well? Facts and controversies in defining the role of lung scintigraphy for the diagnosis of pulmonary thromboembolism in the era of MDCT. *Eur J Nucl Med Mol Imaging* 2009;36:505–21.
  129. Reinartz P, Wildberger JE, Schaefer W, Nowak B, Mahnen AH, Buell U. Tomographic imaging in the diagnosis of pulmonary embolism: a comparison between V/Q lung scintigraphy in SPECT technique and multislice spiral CT. *J Nucl Med* 2004;45:1501–8.
  130. Hata T, Ikeda M, Nakamori S, Suzuki R, Kim T, Yasui M, et al. Single-photon emission computed tomography in the screening for postoperative pulmonary embolism. *Dig Dis Sci* 2006;51:2073–80.
  131. Zaki M, Suga K, Kawakami Y, Yamashita T, Shimizu K, Seto A, et al. Preferential location of acute pulmonary thromboembolism induced consolidative opacities: assessment with respiratory gated perfusion SPECT-CT fusion images. *Nucl Med Commun* 2005;26:465–74.
  132. Suga K, Kawakami Y, Iwanaga H, Tokuda O, Matsunaga N. Automated breath-hold perfusion SPECT/CT fusion images of the lungs. *AJR Am J Roentgenol* 2007;189:455–63.
  133. Gimelli A, Rossi G, Landi P, Marzullo P, Iervasi G, L'abbate A, et al. Stress/rest myocardial perfusion abnormalities by gated SPECT: still the best predictor of cardiac events in stable ischemic heart disease. *J Nucl Med* 2009;50:546–53.
  134. Heller EN, DeMan P, Liu YH, Dione DP, Zubal IG, Wackers FJ, et al. Extracardiac activity complicates quantitative cardiac SPECT imaging using a simultaneous transmission-emission approach. *J Nucl Med* 1997;38:1882–90.
  135. Utsunomiya D, Tomiguchi S, Shiraishi S, Yamada K, Honda T, Kawanaka K, et al. Initial experience with X-ray CT based attenuation correction in myocardial perfusion SPECT imaging using a combined SPECT/CT system. *Ann Nucl Med* 2005;19:485–9.
  136. Hacker M, Jakobs T, Matthiesen F, Vollmar C, Nikolaou K, Becker C, et al. Comparison of spiral multidetector CT angiography and myocardial perfusion imaging in the noninvasive detection of functionally relevant coronary artery lesions: first clinical experiences. *J Nucl Med* 2005;46:1294–300.
  137. Hacker M, Jakobs T, Hack N, Nikolaou K, Becker C, von Ziegler F, et al. Combined use of 64-slice computed tomography and gated myocardial perfusion SPECT for the detection of functionally relevant coronary artery stenoses. First results in a clinical setting concerning patients with stable angina. *Nuklearmedizin* 2007;46:29–35.
  138. Hacker M, Jakobs T, Matthiesen F, Nikolaou K, Becker C, Knez A, et al. Combined functional and morphological imaging consisting of gated perfusion SPECT and 16-detector multislice



- spiral CT angiography in the noninvasive evaluation of coronary artery disease: first experience. *Clin Imaging* 2007;31:313–20.
139. Rispler S, Keidar Z, Ghersin E, Roguin A, Soil A, Dragu R, et al. Integrated single-photon emission computed tomography and computed tomography coronary angiography for the assessment of hemodynamically significant coronary artery lesions. *J Am Coll Cardiol* 2007;49:1059–67.
  140. Gaemperli O, Schepis T, Valenta I, Husmann L, Scheffel H, Duerst V, et al. Cardiac image fusion from stand-alone SPECT and CT: clinical experience. *J Nucl Med* 2007;48:696–703.
  141. Gaemperli O, Schepis T, Kalff V, Namdar M, Valenta I, Stefani L, et al. Validation of a new cardiac image fusion software for three-dimensional integration of myocardial perfusion SPECT and stand-alone 64-slice CT angiography. *Eur J Nucl Med Mol Imaging* 2007;34:1097–106.
  142. Hagan I, Hopkins R, Lyburn I. Superior demonstration of splenosis by heat-denatured Tc-99m red blood cell scintigraphy compared with Tc-99m sulfur colloid scintigraphy. *Clin Nucl Med* 2006;31:463–6.
  143. Horger M, Eschmann SM, Lengerke C, Claussen CD, Pfannenbergl C, Bares R. Improved detection of splenosis in patients with haematological disorders: the role of combined transmission-emission tomography. *Eur J Nucl Med Mol Imaging* 2003;30:316–9.
  144. Alvarez R, Diehl KM, Avram A, Brown R, Piert M. Localization of splenosis using <sup>99m</sup>Tc-damaged red blood cell SPECT/CT and intraoperative gamma probe measurements. *Eur J Nucl Med Mol Imaging* 2007;34:969.
  145. Hayashi M, Deguchi J, Utsunomiya K, Yamada M, Komori T, Takeuchi M, et al. Comparison of methods of attenuation and scatter correction in brain perfusion SPECT. *J Nucl Med Technol* 2005;33:224–9.
  146. Van Laere K, Koole M, D'Asseler Y, Versijpt J, Audenaert K, Dumont F, et al. Automated stereotactic standardization of brain SPECT receptor data using single-photon transmission images. *J Nucl Med* 2001;42:361–75.
  147. Sulkin TV, Cousens C. SPECTCT cerebral perfusion scintigraphy; is the low-dose CT component of diagnostic value? *Clin Radiol* 2008;63:289–98.
  148. Alavi A, Basu S. Planar and SPECT imaging in the era of PET and PET-CT: can it survive the test of time? *Eur J Nucl Med Mol Imaging* 2008;35:1554–9.
  149. Mariani G, Bruselli L, Duatti A. Is PET always an advantage versus planar and SPECT imaging? *Eur J Nucl Med Mol Imaging* 2008;35:1560–5.
  150. Gholamrezanezhad A, Mirpour S, Mariani G. Future of nuclear medicine: SPECT versus PET. *J Nucl Med* 2009;50:16N–8.
  151. You JJ, Alter DA, Iron K, Slaughter PM, Kopp A, Przybysz R, et al. Diagnostic services in Ontario: descriptive analysis and jurisdictional review. Toronto: Institute for Clinical Evaluative Sciences; 2007.
  152. Canadian Institute for Health Information. Medical imaging in Canada, 2007. Ottawa: Canadian Institute for Health Information; 2008.
  153. Medical options. Report: European nuclear medicine patients visits show marginal fall. 2008. Available via: [www.medicaloptions.co.uk/assets/MONucpress2008.doc](http://www.medicaloptions.co.uk/assets/MONucpress2008.doc). Accessed 26 May 2009.

Copyright of European Journal of Nuclear Medicine & Molecular Imaging is the property of Springer Science & Business Media B.V. and its content may not be copied or emailed to multiple sites or posted to a listserv without the copyright holder's express written permission. However, users may print, download, or email articles for individual use.





## Clinical validation of SPECT attenuation correction using x-ray computed tomography–derived attenuation maps: Multicenter clinical trial with angiographic correlation

Yasmin Masood, MD,<sup>a</sup> Yi-Hwa Liu, PhD,<sup>a</sup> Gordon DePuey, MD,<sup>b</sup> Raymond Taillefer, MD,<sup>c</sup> Luis I. Araujo, MD,<sup>d</sup> Steven Allen, MD,<sup>e</sup> Dominique Delbeke, MD,<sup>f</sup> Frank Anstett,<sup>g</sup> Aharon Peretz,<sup>g</sup> Mary-Jo Zito, CNMT, BS,<sup>a</sup> Vera Tsatkin, CNMT, MS,<sup>a</sup> and Frans J. Th. Wackers, MD<sup>a</sup>

**Background.** Nonuniform attenuation artifacts cause suboptimal specificity of stress single photon emission computed tomography (SPECT) myocardial perfusion images. In phantoms, normal subjects, and patients suspected of having coronary artery disease (CAD), we evaluated a new hybrid attenuation correction (AC) system that combines x-ray computed tomography (CT) with conventional stress SPECT imaging.

**Methods and Results.** The effect of CT-based AC was evaluated in phantoms by assessing homogeneity of normal cardiac inserts. AC improved homogeneity of normal cardiac phantoms from  $11\% \pm 2\%$  to  $5\% \pm 1\%$  ( $P < .001$ ). Attenuation-corrected normal patient files were created from 37 normal subjects with a low likelihood ( $<3\%$ ) of CAD. The diagnostic performance of AC for detection of CAD was evaluated in 118 patients who had stress technetium 99m sestamibi or tetrofosmin stress SPECT imaging and coronary angiography. SPECT images with and without AC were interpreted by 4 blinded readers with different interpretative attitudes. Overall, AC improved the diagnostic performance of all readers, particularly the normalcy rate. The degree of improvement depended on interpretative attitude. Readers prone to high sensitivity or with less experience had the greatest gain in the normalcy rate, whereas a reader prone to higher specificity had improvements in sensitivity and specificity but not the normalcy rate. Importantly, improvement of one diagnostic variable was not associated with worsening of other variables.

**Conclusion.** CT-based AC of SPECT images consistently improved overall diagnostic performance of readers with different interpretive attitudes and experience. CT-based AC is well suited for routine use in clinical practice. (J Nucl Cardiol 2005;12:676-86.)

**Key Words:** Single photon emission computed tomography • computed x-ray tomography • attenuation correction • coronary artery disease

From the Cardiovascular Nuclear Imaging Laboratory, Yale University School of Medicine, New Haven, Conn<sup>a</sup>; Department of Nuclear Medicine, St. Lukes-Roosevelt Hospital, New York, NY<sup>b</sup>; Department of Nuclear Medicine, Hôtel Dieu de Montréal, Montréal, Québec, Canada<sup>c</sup>; Department of Nuclear Medicine, University of Pennsylvania, Philadelphia, Pa<sup>d</sup>; Department of Nuclear Medicine, Mercy Medical Center, Springfield, Mass<sup>e</sup>; Department of Nuclear Medicine, Vanderbilt University, Nashville, Tenn<sup>f</sup>; GE Healthcare, Waukesha, Wis.<sup>g</sup>

This study was supported in part by an educational grant from GE Healthcare.

Received for publication April 5, 2005; final revision accepted Aug 2, 2005.

Reprint requests: Frans J. Th. Wackers, MD, Yale University School of Medicine, Cardiovascular Nuclear Imaging Laboratory, 333 Cedar St, Fitkin-3, New Haven, CT 06520; [frans.wackers@yale.edu](mailto:frans.wackers@yale.edu). 1071-3581/\$30.00

Copyright © 2005 by the American Society of Nuclear Cardiology. doi:10.1016/j.nuclcard.2005.08.006

Stress radionuclide myocardial perfusion imaging (MPI) by use of single photon emission computed tomography (SPECT) is widely used for the detection of coronary artery disease (CAD) and patient risk stratification. The clinical usefulness of stress SPECT imaging for detecting CAD is supported by ample evidence in the literature in numerous and varying patient populations.<sup>1,2</sup> However, despite considerable technical advances achieved during the last 10 to 15 years, specificity of conventional SPECT imaging has remained suboptimal because of breast and diaphragmatic attenuation artifacts.<sup>3,4</sup> Hardware and software devices have been developed to correct for nonuniform attenuation artifacts. The most widely used attenuation correction (AC) devices utilize scanning radioisotope line sources for obtaining transmission maps.<sup>5-7</sup> Multiple clinical studies have demonstrated that AC devices improve diagnostic



accuracy, in particular specificity, with preservation of sensitivity.<sup>8-15</sup> A disadvantage of radioisotope line sources is the physical decay of the sources over time and hence degraded quality of AC maps. Recently, a new technology has been introduced that combines single-slice computed x-ray tomography (CT) for acquisition of transmission maps with conventional SPECT emission imaging.<sup>16-21</sup> We evaluated the effect of CT-based AC on the homogeneity of SPECT images of normal phantoms and in normal subjects, as well as in a multicenter study in patients suspected of having CAD. In addition, the comparative diagnostic performance of readers with different interpretive attitudes was evaluated.

## METHODS

### Phantoms

An anthropomorphic torso phantom with cardiac, lung, and spine inserts (ECT/TOR/P and ECT/CAR/I; Data Spectrum, Hillsborough, NC) was used to evaluate the effect of AC on the homogeneity of SPECT images of normal phantoms. The left ventricle (LV) was simulated by a cardiac insert consisting of 2 concentric cylinders. The inner cylinder ("cavity" of LV) was filled with water, and the space between the two cylinders (left ventricular "myocardium") was filled with a uniform technetium-99m solution (2.5  $\mu\text{Ci/mL}$ ). We described this cardiac phantom in greater detail previously.<sup>22,23</sup> The purpose of the lung and spine inserts was to create a phantom with nonuniform attenuation.

### Multicenter Study

The multicenter study involved 4 clinical sites: University of Pennsylvania, Philadelphia, Pa; Mercy Medical Center, Springfield, Mass; Vanderbilt Hospital, Nashville, Tenn; and Yale University, New Haven, Conn. Two groups of subjects were prospectively recruited: patients with suspected or known CAD who had stress SPECT MPI and coronary angiography and normal volunteers with a low likelihood of CAD. The institutional review boards at each clinical center approved the study protocols.

### Patients

We enrolled 157 patients who were referred for stress-rest SPECT MPI for suspected or known CAD and had coronary angiography less than 6 months before and less than 3 months after SPECT imaging, without intervening revascularization procedures or cardiac events, in the study. We excluded 39 patients for technical reasons or protocol violations. In 29 patients this was related to the study: 15 had protocol violations, 9 had missing data, and 5 had other technical deficiencies. In 10 patients the exclusion was related to imaging deficiencies: 6 patients had severe motion, and 4 (2.5%) were excluded because of significant misregistration of emission and

**Table 1.** Demographics of patients who underwent coronary angiography

No. of patients	118
Age (y)	61 $\pm$ 12
Men	79 (69%)
Diabetes mellitus	25 (22%)
Hypertension	29 (25%)
Previous infarction	2 (1.7%)

transmission images. Selected demographic data for the remaining 118 patients are shown in Table 1. Of the patients, 104 (88%) performed symptom-limited treadmill exercise, 13 (11%) had adenosine vasodilator stress testing, and 1 patient (1%) had dobutamine stress testing.

### Normal Volunteers

Forty-four normal volunteers with a low likelihood of CAD were recruited. The likelihood of CAD was assessed by sequential Bayesian analysis on the basis of age, gender, and absence of symptoms.<sup>24,25</sup> In addition, the absence of cardiac risk factors, no history of CAD, normal physical examination, normal rest and exercise electrocardiograms, and body mass index lower than 32  $\text{kg/m}^2$  were required. All normal subjects performed maximal physical treadmill exercise. Ultimately, 7 subjects were excluded: 1 had missing data, 1 had severe motion, 1 (2.2%) had misregistration of emission and transmission imaging data, and 4 had marked breast or inferior attenuation artifacts on noncorrected images. The remaining 37 subjects consisted of 19 men and 18 women with a mean age of 39  $\pm$  11 years.

### Stress Testing and Radiotracer Injection

Stress testing was performed in accordance with published guidelines.<sup>26</sup> Symptom-limited treadmill exercise was performed via the Bruce or modified Bruce protocol. Endpoints for stress testing were defined as in the previously published guidelines.<sup>26</sup> Pharmacologic stress testing was performed with either adenosine or dobutamine intravenous infusion. Adenosine was infused for 6 minutes at a rate of 140  $\mu\text{g} \cdot \text{kg}^{-1} \cdot \text{min}^{-1}$ . Dobutamine was infused in stages of 3 minutes' duration, with increasing doses of 10  $\mu\text{g} \cdot \text{kg}^{-1} \cdot \text{min}^{-1}$  to a maximum of 40  $\mu\text{g} \cdot \text{kg}^{-1} \cdot \text{min}^{-1}$ .

Tc-99m sestamibi or Tc-99m tetrofosmin was injected when an exercise endpoint was achieved, at 3 minutes into adenosine infusion, or at maximal dobutamine infusion dose. Exercise stress was continued for 1 to 2 minutes after radiopharmaceutical injection, and pharmacologic stress was continued for 3 minutes after injection of radiotracer.

### SPECT Image Acquisition

Patients had either a 1-day low-dose (10-15 mCi)/high-dose (25-30 mCi) imaging protocol or a 2-day high-dose (30

mCi) imaging protocol following the timing and dosing recommendations in the American Society of Nuclear Cardiology guidelines.<sup>26</sup> All centers used an identical hybrid SPECT/CT dual-head gamma camera (GE Hawkeye; GE Medical Systems, Waukesha, Wis). Emission data were acquired by use of parallel-hole, low-energy, high-resolution collimators, with the patient in the supine position. The acquisition orbits were circular or body contour orbits over either 180° or 360° arcs, with the use of 30 or 60 stops, respectively. For 30 stops, emission data were acquired for 50 to 70 seconds per stop; for 60 stops, data were acquired for 25 to 35 seconds per stop. The image acquisition matrix was  $64 \times 64$ , and the pixel size was 6.5 mm. Images were acquired on the 140-keV photopeak with a 20% symmetrical window.

Cardiac phantom studies were acquired in triplicate via a similar acquisition protocol with the torso placed in the center of orbit.

### Acquisition CT Attenuation Maps

Immediately after acquisition of SPECT images, CT imaging was performed by use of the GE Hawkeye system.<sup>18</sup> This camera consisted of an x-ray tube and 384 detectors located opposite of each other. The fan beam formed by the x-ray tube on the x-ray detectors allowed for measurement of patient attenuation along discrete paths. At the center of rotation, the beam paths from adjacent x-ray detectors were spaced at 1.2 mm for high-resolution transaxial slice reconstruction. The x-ray rotated continuously around the patient through a 216° arc for a 10-mm slice collimation.

Attenuation maps and attenuation coefficients were constructed from CT numbers by use of Hounsfield value settings for bone and water scaling factors. Formulas were used to calculate the correction factor with CT values of less than 0 for energy dependence similar to water and CT values above 0 for energy dependence of the mixture of bone and water.

### Computer Processing of SPECT Images and Coregistration

Each clinical center sent raw SPECT emission data, corrected for nonuniformity, and CT attenuation coefficient maps to the Radionuclide Core Laboratory at Yale University. All studies were uniformly processed in the core laboratory with a commercially available GE Xeleris nuclear medicine workstation (GE Medical Systems). Noncorrected SPECT emission image data were reconstructed by use of conventional filtered backprojection. For application of AC, SPECT emission image data were processed by use of ordered-subsets expectation maximization reconstruction software with 2 iterations and 10 subsets. Reconstructed stress and rest images were smoothed with a 3-dimensional Butterworth low-pass filter with a critical frequency of 0.46 Nyquist with an order of 5.0 and a critical frequency of 0.32 Nyquist with an order of 5.0, respectively. Subsequently, 1-pixel-thick tomographic slices were generated and displayed as short-axis and vertical and horizontal long-axis slices. SPECT emission images were coregistered and fused with the transmission CT images. Fused

emission and transmission images were visually inspected for correctness of coregistration. Studies with misregistration were excluded from further analysis. AC was applied to emission data by use of predetermined attenuation coefficients as indicated previously. No scatter or depth-dependent resolution correction was applied.

### Normal Database

Lower limit-of-normal radiotracer distribution was defined as the mean minus 2 SDs. Stress SPECT images of individuals with a lower 3% likelihood of CAD were processed and quantified by use of Wackers-Liu Cardiac Quantification (WLCQ) quantitative software (MEDX, Arlington Heights, Ill) (as described later).<sup>22,27,28</sup> Circumferential count distribution profiles, comprising 128 data points, were generated over 36 short-axis slices from apex to base. These slices were interpolated to obtain apical, midventricular, and basal left ventricular short-axis slices. Subsequently, 3 averaged circumferential profiles were generated for apical, midventricular, and basal slices for each normal subject. Finally, mean and SD were determined for each of the 128 points of corresponding averaged circumferential profiles of all normal subjects for derivation of the lower limit of normal. The lower limit of normal for the apex was derived in a similar way from midventricular horizontal long-axis slices. For quantitative analysis of noncorrected SPECT images, existing normal files for Tc-99m sestamibi or Tc-99m tetrofosmin were used. For quantitative analysis of attenuation-corrected SPECT images, new limits of normal were created from normal subjects who had attenuation-corrected stress SPECT Tc-99m sestamibi imaging. Before incorporation in the normal database, exercise data and SPECT and CT images of each normal subject were reviewed. If the exercise response was abnormal, if patient motion had occurred, if SPECT images appeared visually abnormal (eg, as a result of breast or diaphragmatic attenuation), or if coregistration of emission-transmission images was inadequate, images were excluded.

### Quantification SPECT With and Without AC

Reconstructed noncorrected and attenuation-corrected SPECT images were quantified by use of WLCQ software and appropriate normal reference databases. This quantitative software has been described and validated previously.<sup>26,27</sup> In brief, reconstructed short-axis slices are divided automatically into 128 radial sectors. The apex cap, derived from a segment of central horizontal long-axis slices, was divided into 64 sectors. Circumferential count distribution profiles were derived from maximal pixel values in each of the radial sectors. Each circumferential count profile was then normalized to the sector with maximal counts. The normalized circumferential count profile is superimposed on lower limit-of-normal curves as defined previously. The portion of a normalized patient's circumferential profile that is below the lower limit-of-normal curve is abnormal and represents a myocardial perfusion defect. By summation of all areas of the circumferential profiles below the normal curve, and after adjustment for the varying volume



of slices, the total defect size is calculated and expressed as a percentage of the LV. In clinical practice we found it useful to categorize defect sizes as small ( $<5\%$  of LV), moderate ( $\geq 5\%$  to  $<10\%$  of LV), or large ( $\geq 10\%$  of LV).<sup>29</sup>

### Percent Variability

To quantitatively assess the homogeneity of radiotracer distribution in phantoms and normal subjects, as well as the improvement in homogeneity with AC, circumferential count profiles were generated from the apical, midventricular, and basal slices of noncorrected and attenuation-corrected images. Image uniformity was assessed by the percent variability (PV) of the count profiles defined by the following:

$$PV = \frac{SD}{Mean} \times 100, \quad (1)$$

where *SD* and *mean* denote the values of the count profiles for each slice. For all slices, mean percent variability can be calculated as follows:

$$Mean\ PV = \frac{1}{3} \sum_{i=1}^3 \frac{SD(i)}{Mean(i)} \times 100, \quad (2)$$

where *SD(i)* and *mean(i)* denote the values of the count profiles for slice *i* (1, apical; 2, midventricle; and 3, basal).

### Coronary Angiography

Most patients were referred to undergo coronary angiography based on the clinical interpretation of noncorrected images, although in 1 center, later in the course of the study, attenuation-corrected data were considered as well. Invasive contrast coronary angiography was performed according to standard percutaneous techniques. Angiograms were analyzed at each clinical site by experienced angiographers unaware of findings on SPECT imaging. Significant CAD was defined as 50% luminal diameter narrowing or greater by visual inspection in at least one of the three main coronary arteries. The clinical coronary angiography reports of each site were used to determine the presence or absence of CAD.

### Analysis

**Blinded reading.** Processed SPECT images were analyzed in 3 reading sessions involving 4 different readers blinded to the patients' clinical information, body habitus, type of stress, and results of coronary angiography, as well as the number of normal volunteers included. Patient gender was only revealed on request. Images were displayed on a computer screen in the standard format for display of tomographic cardiac images<sup>30</sup> in multichrome color scale, with the option to switch to linear gray scale. The 115 SPECT images of patients who had coronary angiography were mixed with 40 SPECT images of normal subjects. The total set of 155 SPECT studies was displayed in random order. To avoid bias, readers were not made aware of the number of normal and abnormal subjects. Each reader first

performed analysis of 155 noncorrected images and then of 155 attenuation-corrected images. Electrocardiography-gated cine images were not included in this analysis. The readers were aware of the type of image reconstruction (ie, no attenuation correction [NC] or AC).

The first blinded reading session was performed by 2 experienced nuclear cardiologists (readers 1 and 2). The interpretive attitude of these 2 readers may be characterized as being disposed toward sensitivity rather than specificity. They provided a consensus interpretation based on visual analysis. The second reading session was performed by an experienced nuclear cardiologist (reader 3) who used quantitative analysis by use of WLCQ quantitative software with visual overread. The interpretative attitude of this reader can be characterized as being disposed toward specificity rather than sensitivity. The third reading session was performed by a less experienced reader (reader 4) who used the same method as reader 3.

The interpretation of studies was recorded on preprinted reading forms. The interpreters marked first whether the overall SPECT study was normal or abnormal. If the study was considered abnormal, the specific coronary artery territory or territories thought to be involved were recorded. Coronary artery territories were designated according to a published 17-segment myocardial model.<sup>30</sup> For the purpose of constructing receiver operating characteristic (ROC) curves, the interpreters used a scoring scale of 1 to 5, in which 1 is definitely normal, 2 is probably normal, 3 is equivocal, 4 is probably abnormal, and 5 is definitely abnormal. For the calculation of sensitivity, specificity, and predictive values for angiographic CAD, an interpretive score of 4 or greater was defined as abnormal.

**ROC curves.** ROC curves were generated by calculating sensitivity and specificity for angiographic CAD ( $\geq 50\%$  stenosis). As previously described, ROC curves were created by shifting the diagnostic criterion level for positives and negatives over the entire range of scores from 1 to 5.<sup>31</sup> Sensitivity and 1 minus specificity for each diagnostic criterion level were plotted against each other.

### Statistical Analysis

Continuous data were expressed as mean  $\pm$  SD. A paired *t* test was used to compare differences of paired data. For calculation of sensitivity, specificity, and predictive values, abnormal MPI results were defined by scores of 4 or greater. Sensitivity, specificity, and accuracy were defined in the usual way by use of both greater than 50% and greater than 70% cutoff values for significant CAD. The normalcy rate was defined as the proportion of normal subjects with a low likelihood of CAD having normal interpretations. For quantitative interpretation of the ROC curves, the area under the curve was calculated. A larger area indicates improved diagnostic performance.

For the evaluation of the effect of AC on quantified defect size, myocardial perfusion abnormalities were analyzed in two groups: anterior (including anteroapical and lateral defects) and inferior (including inferolateral and inferoseptal defects). On

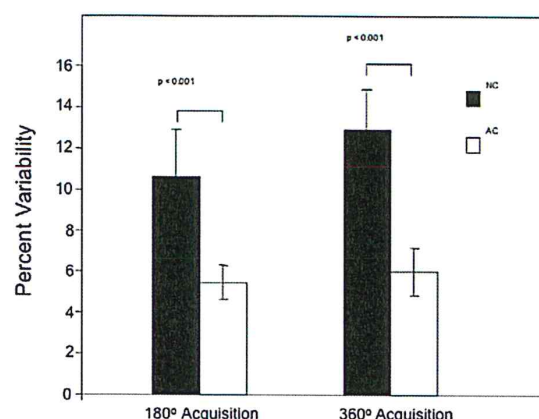


**Figure 1.** Circumferential percent variability, as a measure for image homogeneity, in normal anthropomorphic phantoms. Percent variability improved significantly with the application of SPECT images with AC compared with NC. This improvement was observed regardless of acquisition orbit used.

the basis of previously assessed reproducibility, a significant difference in quantitative SPECT defect size is a change of greater than 5% of the LV.

## RESULTS

### Homogeneity of Cardiac Phantom Images With and Without AC

Figure 1 shows the mean percent variability of circumferential count profiles from short-axis phantom images acquired with NC and AC by use of 180° and 360° orbits. With AC, the percent variability of circumferential count profiles of normal phantoms was significantly reduced, indicating greater image homogeneity ( $11\% \pm 2\%$  vs  $5\% \pm 1\%$  [ $P < .001$ ] for 180° orbit and  $13\% \pm 2\%$  vs  $6\% \pm 1\%$  [ $P < .001$ ] for 360° orbit).

### Patient Lower Limits of Normal With and Without AC

Figure 2 shows examples of midventricular lower limit-of-normal curves for men, women, and men and women combined with and without AC. Table 2 shows the percent variability for apical, midventricular, and basal short-axis slices for men, women, and men and women combined without and with AC. For men, the percent variability was significantly decreased with AC for apical, midventricular, and basal short-axis slices. However, for women, as well as men and women combined, the percent variability was only significantly decreased by AC in the basal slices.

## Patients

Of 118 patients who had coronary angiography, 86 (73%) had significant CAD ( $\geq 50\%$  stenosis). Of the patients, 32 (37%) had single-vessel, 21 (25%) had double-vessel, and 33 (38%) had triple-vessel disease; 32 (27%) had insignificant disease with less than 50% stenosis, 24 of whom had entirely normal coronary angiograms visually. Nine patients had luminal coronary stenoses between 51% and 69%. Thus 77 patients had 70% or greater CAD in one or more vessels.

## SPECT Interpretation

Overall results of SPECT interpretation by various interpreters with and without AC are shown in Figures 3, 4, and 5. For readers 1 and 2, the overall sensitivity, specificity, and accuracy were not greatly affected by AC. However, the normalcy rate improved substantially with AC from 84% to 97%. Reader 3 had improved sensitivity, specificity, and accuracy on attenuation-corrected SPECT images. The normalcy rate of the latter reader was 100% on both noncorrected and attenuation-corrected images. Reader 4 showed slight improvement of sensitivity on attenuation-corrected images but not of specificity and accuracy. However, the normalcy rate of reader 4 improved substantially with AC.

Table 3 compares the diagnostic results by use of either luminal stenosis of 50% or greater or 70% or greater as cutoff values for defining significant CAD. Because of the small number of patients with stenoses of 51% to 69%, differences are relatively small and affected mainly specificity.

## ROC Curve Analysis

For all 4 readers, the area under the ROC curve was larger for attenuation-corrected SPECT images than for noncorrected SPECT images (Figure 6). Reader 3 had the greatest gain using attenuation-corrected SPECT images.

## Detection of CAD in Individual Coronary Arteries

With AC, readers 1 and 2 did not show substantial changes in sensitivity, specificity, or accuracy for detecting CAD in the left anterior descending coronary artery (LAD), left circumflex coronary artery (LCX), or right coronary artery (RCA) compared with interpretation of noncorrected SPECT images (Table 4). In contrast, with the use of AC, reader 3 had improved sensitivity, specificity, and accuracy for detecting disease in the LAD and LCX, as compared with interpretation of noncorrected SPECT images.



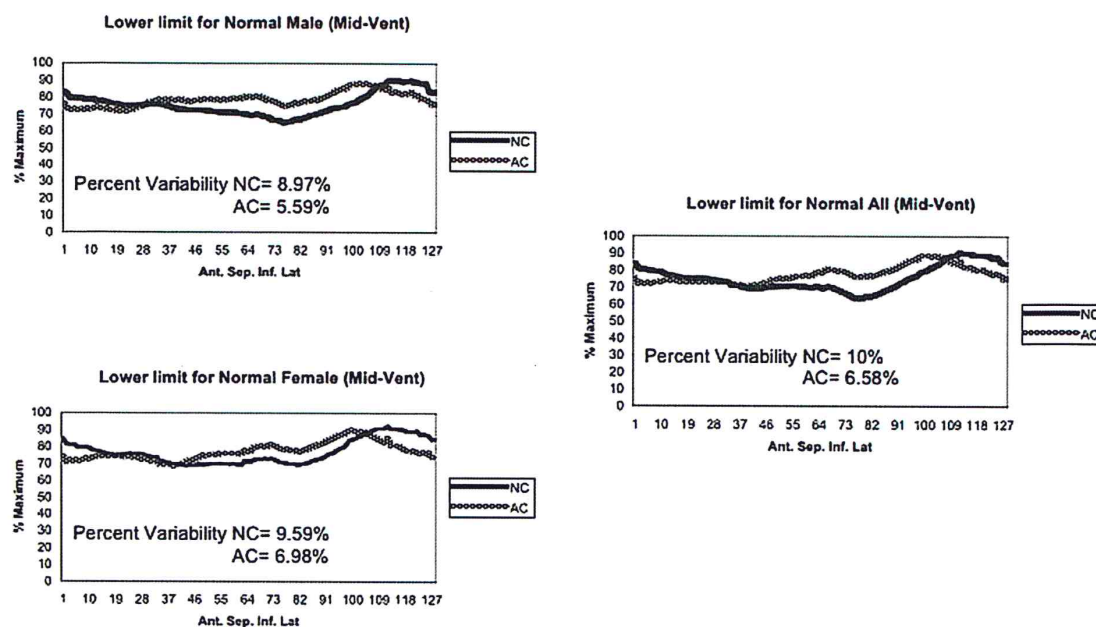


**Figure 2.** Tc-99m sestamibi lower limit-of-normal curves (mean  $\pm$  2 SDs) of midventricular (Mid-Vent) slices for normal men, women, and men and women combined (All). Percent variability as a measure for homogeneity of radiotracer uptake is shown. Ant, Anterior; Sep, septal; Inf, inferior; Lat, lateral.

**Table 2.** Percent variability of regional radiotracer uptake on apical, midventricular, and basal short-axis slices in normal subjects

	Apical	Midventricular	Basal
Men (n = 19)			
NC	7.51 $\pm$ 1.16	8.95 $\pm$ 1.48	10.95 $\pm$ 1.81
AC	5.75 $\pm$ 1.84*	6.00 $\pm$ 1.34*	7.02 $\pm$ 1.95*
Women (n = 18)			
NC	5.52 $\pm$ 1.92	7.79 $\pm$ 1.73	10.79 $\pm$ 2.16
AC	5.65 $\pm$ 1.67	7.28 $\pm$ 1.62	9.14 $\pm$ 2.06*
Men and women combined (n = 37)			
NC	6.54 $\pm$ 1.85	8.38 $\pm$ 1.69	10.87 $\pm$ 1.96
AC	5.70 $\pm$ 1.74*	6.62 $\pm$ 1.60*	8.05 $\pm$ 2.25*

\* $P < .05$  for AC versus NC.

Although reader 3 with AC had improved sensitivity and accuracy for detection of disease in the RCA, specificity did not improve.

With AC, reader 4 had improved sensitivity, specificity, and accuracy for detecting disease of the LAD compared with interpretation of noncorrected SPECT images but not for the detection of disease in the LCX and RCA.

#### Quantification of Defect Size on Noncorrected and Attenuation-Corrected SPECT

Overall, mean quantified stress defect size was significantly larger on attenuation-corrected SPECT images than on noncorrected SPECT images in patients with angiographic CAD, regardless of the anatomic location of defects (Table 5). However, the effect was

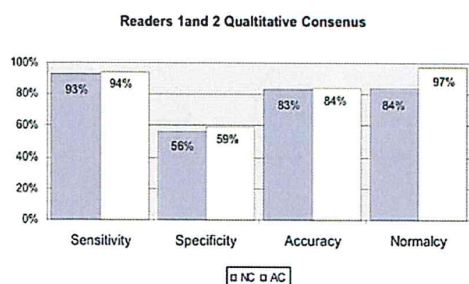


**Figure 3.** Sensitivity, specificity, accuracy for detecting significant CAD ( $\geq 50\%$  stenosis), and normalcy rate of readers 1 and 2, who performed consensus visual interpretation.

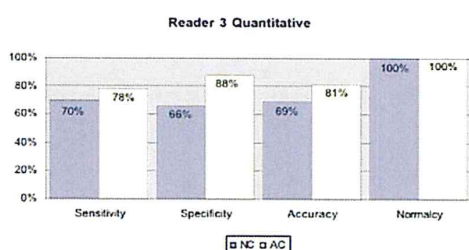


**Figure 4.** Sensitivity, specificity, accuracy for detecting significant CAD ( $\geq 50\%$  stenosis), and normalcy rate of reader 3, who performed quantitative analysis with visual overread.

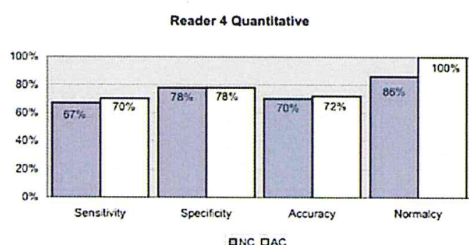


**Figure 5.** Sensitivity, specificity, accuracy for detecting significant CAD ( $\geq 50\%$  stenosis), and normalcy rate of reader 4, who performed quantitative analysis with visual overread.

more marked in patients with anterior wall defects than in those with inferior defects. Significant quantitative differences ( $>5\%$  of LV) of stress defect sizes occurred in 22 individual patients (25%) when comparing AC and NC. Of 25 patients with anterior wall defects, defects were significantly larger with AC in 11 patients (44%). No significant change occurred in 13 patients (52%) with anterior defects, and in only 1 patient (4%), the defect was significantly smaller with AC. Of 43 patients with inferior wall defects, there were no differences in quantified defect sizes in 33 (77%). However, in 6 patients (14%) inferior defects were larger with AC, but in 4 (9%)

**Table 3.** Sensitivity, specificity, and accuracy of various readers for detection of significant angiographic CAD, (defined as either  $\geq 50\%$  or  $\geq 70\%$  stenosis)

	50% Stenosis		70% Stenosis	
	NC	AC	NC	AC
<b>Readers 1 and 2</b> (visual interpretation)				
Sensitivity	93%	94%	92%	93%
Specificity	56%	59%	44%	46%
Accuracy	83%	84%	75%	77%
<b>Reader 3</b> (quantitative interpretation)				
Sensitivity	70%	78%	72%	81%
Specificity	66%	88%	61%	78%
Accuracy	69%	81%	68%	80%
<b>Reader 4</b> (quantitative interpretation)				
Sensitivity	67%	70%	72%	69%
Specificity	78%	78%	76%	66%
Accuracy	70%	72%	73%	68%

they were smaller. In 2 of the latter patients, moderate-sized defects on noncorrected images became falsely normal on attenuation-corrected images.

In patients without significant angiographic CAD, the mean quantified stress defect size was  $1\% \pm 2\%$  of the LV on noncorrected SPECT images and  $1\% \pm 2\%$  of the LV on attenuation-corrected SPECT images ( $P =$  not significant). However, 1 patient with quantitatively normal SPECT images with NC showed a small (5% of LV) false anterior defect with AC.

All SPECT images in 37 normal subjects were quantitatively normal (0% defect) on both noncorrected and attenuation-corrected SPECT images.

## DISCUSSION

This study shows that CT-based AC improves the homogeneity of SPECT images of normal cardiac phantoms and of normal subjects. Moreover, AC consistently improved the diagnostic yield of SPECT imaging for detecting significant angiographic CAD ( $\geq 50\%$  stenosis), as well as the normalcy rate. Our study also indicates that the degree of diagnostic gain by AC may vary among readers. This depends on a reader's interpretive attitude (ie, reading style) and experience. The



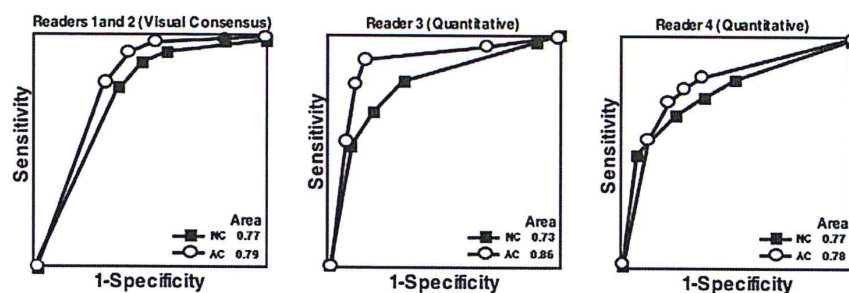


**Figure 6.** ROC curves for readers 1 and 2, reader 3, and reader 4. For each reader, the area under the curve was larger with AC than with NC, with the greatest gain by AC for reader 3.

**Table 4.** Sensitivity, specificity, and accuracy of various readers for detection of significant angiographic CAD ( $\geq 50\%$  stenosis) in individual coronary arteries

	LAD		LCX		RCA	
	NC	AC	NC	AC	NC	AC
Readers 1 and 2 (visual interpretation)						
Sensitivity	92%	93%	96%	96%	97%	98%
Specificity	35%	37%	32%	32%	41%	43%
Accuracy	65%	67%	57%	57%	70%	72%
Reader 3 (quantitative interpretation)						
Sensitivity	70%	84%	74%	85%	75%	85%
Specificity	52%	67%	49%	57%	69%	69%
Accuracy	62%	76%	59%	68%	72%	77%
Reader 4 (quantitative interpretation)						
Sensitivity	69%	75%	52%	54%	77%	75%
Specificity	61%	65%	70%	69%	70%	65%
Accuracy	65%	70%	61%	61%	74%	70%

**Table 5.** Effect of CT-based AC on SPECT defect size in all patients with angiographic CAD ( $\geq 50\%$  stenosis) and in patients with anterior and inferior defects

	Noncorrected SPECT defect size	Attenuation corrected SPECT defect size	P value
All patients with CAD (n = 86)	8% $\pm$ 9% of LV	10% $\pm$ 10% of LV	<.0001
Anterior defects (n = 25)	12% $\pm$ 10% of LV	17% $\pm$ 11% of LV	<.0001
Inferior defects (n = 43)	8% $\pm$ 7% of LV	10% $\pm$ 8% of LV	.04

blinded readers in our study represented the spectrum of interpretive attitudes that may be encountered in clinical practice. Readers 1 and 2 were inclined to read with greater sensitivity, reader 3 was inclined to read with greater specificity, and reader 4 was the least experienced. Readers 1 and 2 each used visual analysis and rendered a consensus reading. Readers 3 and 4 read independently but used the SPECT quantification

method with a normal reference database. Although the impact of AC was different for each reader, each reader had improvements in overall performance. The areas under the ROC curves were greater with AC than without AC; the curves moved up and to the left, indicating improved diagnostic yield. The variable improvement of diagnostic performance was also observed for the detection of disease in individual coronary artery

territories. Importantly, in no instance was improvement of one diagnostic parameter associated with deterioration of another, as was observed in earlier studies.<sup>32-34</sup> The relatively low specificity of all readers may be readily explained by referral bias, as patients with normal noncorrected or attenuation-corrected SPECT images are usually not referred for cardiac catheterization. In general, the beneficial effect of AC was most marked for the normalcy rate, which serves as a surrogate for specificity. Had these normal subjects been included for the construction of ROC curves, which methodologically is inappropriate (because they did not undergo coronary angiography), the improvement with AC would have been more impressive.

We quantitatively evaluated the impact of AC by measuring myocardial perfusion defect sizes with and without AC. In patients with significant CAD, the mean quantitative defect size was significantly larger with AC than with NC. In individual patients, anterior wall defects in particular were often significantly larger with AC whereas inferior defects were mostly unchanged or smaller with AC. The effect of AC on anterior defects is most likely a result of correction of inferior attenuation and the consequent relative increase in the size of an anterior abnormality. Because, in the entire study population, only 1 small, apparently false anterior defect was created in a patient with insignificant CAD, there appears to be no systematic overcorrection of the inferior wall. Overall, 4 false-negative patients with NC became true-positive patients with AC. This explains the modest improvement in sensitivity achieved by some readers. In the patients with insignificant CAD and in normal subjects, the mean quantitative defect size with AC and NC was not different.

This is the first multicenter clinical study evaluating the use of CT-based AC for SPECT imaging. Some strengths of this study are the uniformity of acquisition in multiple centers, the uniformity of processing and quantification in a core laboratory, the uniformity of display for interpreters who were not participants in data acquisition, and the use of data analysis in a core laboratory. Previously published clinical studies all used radioisotope transmission sources (ie, gadolinium 153, germanium 68, or americium 241). A disadvantage of these isotope transmission sources is their physical decay and need for replacement at regular time intervals to maintain high-quality transmission maps. Because there is no need to replace the CT transmission source, the CT-based system is clearly more convenient in clinical practice. Another benefit of the CT-based AC method is the absence of cross-talk of Tc-99m into the Gd-153 window, which may cause artifacts in patients with intense gastrointestinal uptake. Previous studies comparing AC with NC have shown a varying impact of AC on the

diagnostic yield for detecting CAD.<sup>8-15</sup> As in our study, the effect on sensitivity was in general modest, although improved detection of multivessel and left main disease has been noted.<sup>13</sup> A consistent finding in all studies was improvement of specificity, particularly of the normalcy rate, which was also observed in our study.

Although AC improved homogeneity in phantoms and in normal subjects, it did not entirely eliminate the effect of nonuniform tissue attenuation. This is in agreement with observations by O'Connor et al<sup>7</sup> and other authors.<sup>35-37</sup> Nevertheless, because the difference in regional count distribution between genders is less marked with AC, one may consider the use of a genderless normal database for image quantification.<sup>37</sup> We observed that AC improved homogeneity more in men than in women. This may seem surprising but can be explained by the fact that women with marked breast attenuation were not included in the normal database.

### Limitations

An important limitation of this study is the relatively small number of patients involved. Another unavoidable but significant limitation in evaluating the diagnostic performance of AC in our study was the use of conventional contrast coronary angiography as the reference benchmark. The arbitrary cutoff value of 50% or greater for significant stenosis may have affected specificity. When a cutoff value of 70% or greater stenosis was used, only 9 additional patients with stenoses ranging from 51% to 69% were designated as not having significant CAD. The values for sensitivity and specificity changed only slightly with the cutoff value of 70% or greater. Of 32 patients with less than 50% stenosis, only 24 had entirely clean coronary arteries visually. Microvascular disease may have been present in some of the latter patients who were referred for evaluation of chest discomfort; however, some apparently noncritical stenoses also may in fact have been hemodynamically significant. Another limitation was that coronary angiograms were interpreted by the local angiographers and not by an angiographic core laboratory. In contrast, all SPECT images were processed and displayed in a uniform manner, and interpretive criteria were well defined and standardized before the blinded reading.

Nonuniform tissue attenuation is not the only factor responsible for degradation of SPECT images. No scatter correction or depth-dependent blur correction was used in our study.<sup>38-40</sup> Therefore in this study we evaluated the isolated impact of AC on SPECT images. The additional value of scatter correction will have to be evaluated in future studies.

AC devices that use scanning radioactive line sources acquire transmission and emission data simulta-



neously with perfect coregistration, whereas in this study CT-based transmission data were acquired after emission acquisition was completed. Patient motion may occur during the extended imaging time. Nevertheless, overall, only 5 patients (3%) were excluded because of misregistration. A more recent software package (Hawkeye Attenuation Correction Quality Control, GE Healthcare, Waukesha, Wis), which was not available at the time of this trial, allows for correction of misregistration of emission and transmission images.

Although all studies were acquired with electrocardiographic gating, regional wall motion analysis was not incorporated in the analysis. Therefore only the effect of AC on summed static SPECT images was evaluated.

Finally, blinded interpretation of SPECT images may have its own limitations. Although blinding of readers to clinical information enhances the scientific rigor of analysis by avoiding bias based on nonimaging variables, this approach clearly differs from routine clinical reading when all clinical information is available. In our study a patient's gender was only revealed at request and no information on body habitus was given. This may have affected the diagnostic accuracy of interpretation, as the blinded readers may not have taken nonuniform male and female image patterns into consideration.

## Conclusion

CT-based nonuniform AC of Tc-99m sestamibi or tetrofosmin SPECT images resulted in a modest but consistent improvement of diagnostic performance for readers with different interpretative attitudes. The improvement was particularly noticeable for the normalcy rate without a decline in sensitivity. We conclude that CT-based AC of SPECT is well suited for routine use in clinical practice.

## Acknowledgment

*We gratefully acknowledge the dedication and efforts of Jan Davey, MSN, APRN, in recruiting normal volunteers for this study.*

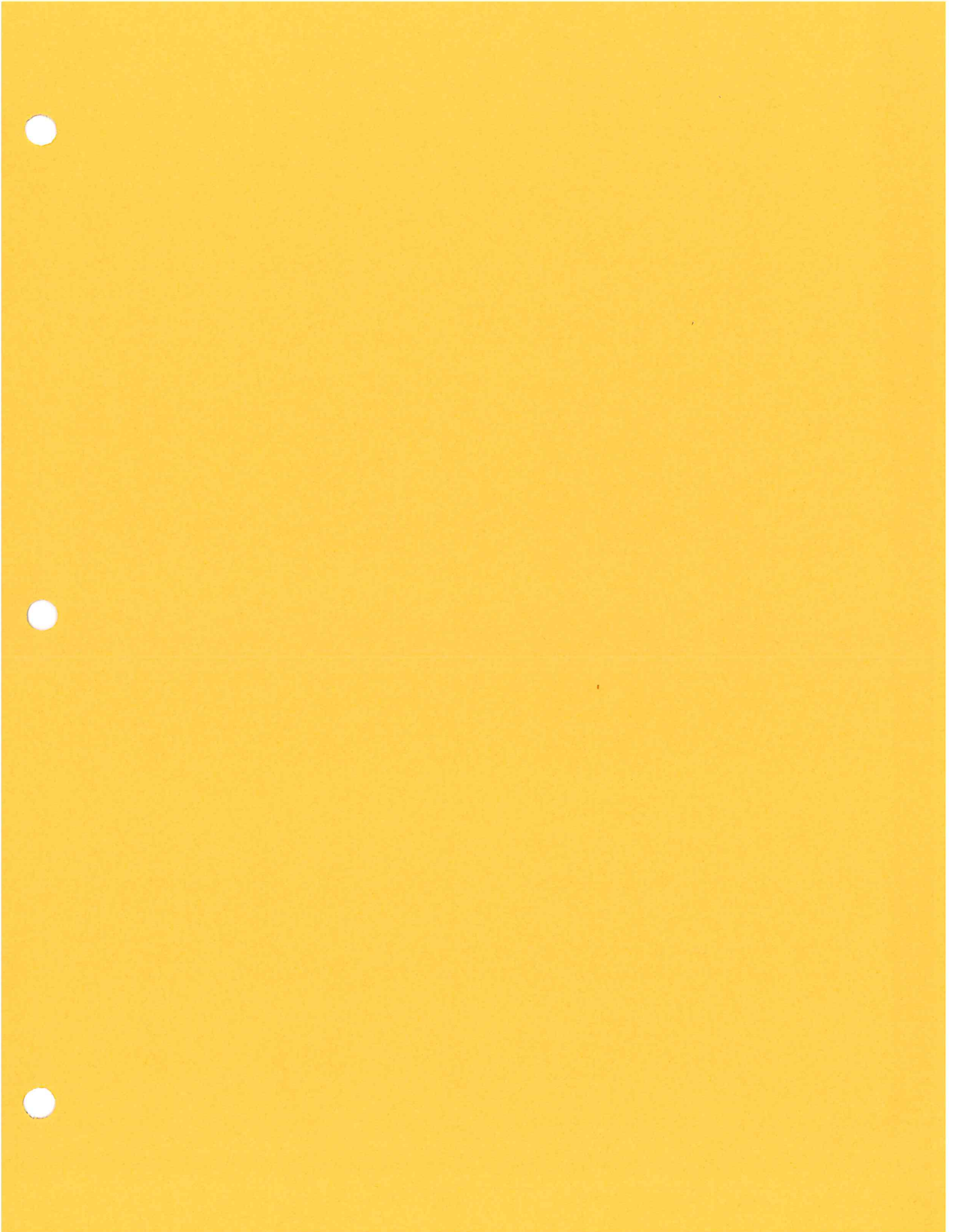
*Drs Wackers and Liu receive royalties from sales of WLCQ quantitative software. At the time of this study, Frank Anstett and Aharon Peretz were employed by GE Healthcare. The other authors have indicated they have no financial conflict of interest. This study was an investigator-initiated study. The sponsor had no role in the analysis and interpretation of data or in the preparation of the manuscript.*

## References

1. Wackers FJTh. Coronary artery disease: exercise stress. Zoghbi GJ, Iskandrian AE. Coronary artery disease: pharmacologic stress. Beller GA. Prognostic applications of myocardial perfusion imaging: exercise stress. Hachamovitch R, Berman DS. Prognostic value of pharmacologic stress: myocardial perfusion scintigraphy and its use in risk stratification. Lidner J, Kramer C, Kaul S. Myocardial perfusion imaging using nonradionuclide techniques. Shaw LJ, Hachamovitch R, Berman DS. Cost effectiveness of myocardial perfusion single-photon-emission computed tomography. Heller GV, Ford-Mukkamala L. Imaging in women. Leppo JA, Dahlberg ST. Imaging for preoperative risk stratification. Rajagopal V, Lauer MS. Nuclear imaging in patients with a history of coronary artery revascularization. Wackers FJTh. Stress myocardial perfusion imaging in patients with diabetes mellitus. In: Zaret BL, Beller GA, editors. Clinical nuclear cardiology: state of the art and future directions. 3rd ed. Mosby; 2005. p. 215-355.
2. Klocke FJ, Baird MG, Lorell BH, Bateman TM, Messer JV, Berman DS, et al. American College of Cardiology; American Heart Association; American Society for Nuclear Cardiology. ACC/AHA/ASNC guidelines for the clinical use of cardiac radionuclide imaging—executive summary: a report of the American College of Cardiology/American Heart Association Task Force on Practice Guidelines (ACC/AHA/ASNC Committee to Revise the 1995 Guidelines for the Clinical Use of Cardiac Radionuclide Imaging). J Am Coll Cardiol 2003;42:1318-33.
3. DePuey G. How to detect and avoid myocardial perfusion SPECT artifacts. J Nucl Med 1994;35:699-702.
4. Desmarais RL, Kaul S, Watson DD, Beller GA. Do false positive thallium-201 scans lead to unnecessary catheterization? Outcome of patients with perfusion defects on quantitative planar thallium-201 scintigraphy. J Am Coll Cardiol 1993;21:1058-63.
5. Tan P, Bailey DL, Meikle SR, Eberl S, Fulton RR, Hutton BF. A scanning line source for simultaneous emission and transmission measurements in SPECT. J Nucl Med 1993;34:1752-60.
6. Bailey DL, Hutton BF, Walker PJ. Improved SPECT using simultaneous emission and transmission tomography. J Nucl Med 1987;28:844-51.
7. O'Connor M, Kemp KB, Anstett F, Christian P, Ficaro EP, Frey E, et al. A multicenter evaluation of commercial attenuation compensation techniques in cardiac SPECT using phantom models. J Nucl Cardiol 2002;9:361-76.
8. Ficaro EP, Fessler JA, Shreve PD, Kritzman JN, Rose PA, Corbett JR. Simultaneous transmission/emission myocardial perfusion tomography: diagnostic accuracy of attenuation-corrected 99mTc-sestamibi single photon emission computed tomography. Circulation 1996;93:463-73.
9. Kluge, R, Sattler B, Seese A, Knapp WH. Attenuation correction by simultaneous emission-transmission myocardial single-photon emission tomography using a technetium-99m-labelled radio-tracer: impact on diagnostic accuracy. Eur J Nucl Med 1997;24:1107-14.
10. Links JM, Becker LC, Rigo P, Taillefer R, Hanelin L, Anstett F, et al. Combined corrections for attenuation, depth-dependent blur, and motion in cardiac SPECT: a multicenter trial. J Nucl Cardiol 2000;7:414-25.
11. Hendel RC, Berman DS, Cullom SJ, Follansbee W, Heller GV, Kiat H, et al. Multicenter clinical trial to evaluate the efficacy of correction for photon attenuation and scatter in SPECT myocardial perfusion imaging. Circulation 1999;99:2742-9.
12. Gallowitsch HJ, Sykora J, Mikosch P, Kresnik E, Unterwieser O, Molnar M, et al. Attenuation-corrected thallium-201 single-photon emission tomography using a gadolinium-153 moving line source: clinical value and the impact of attenuation correction on the extent and severity of perfusion abnormalities. Eur J Nucl Med 1998;25:220-8.

13. Duvernoy CS, Ficaro EP, Karabajakian MZ, Rose PA, Corbet JR. Improved detection of left main coronary artery disease with attenuation-corrected SPECT. *J Nucl Cardiol* 2000;7:639-48.
14. Links JM, DePuey EG, Taillefer R, Becker LC. Attenuation correction and gating synergistically improve the diagnostic accuracy of myocardial perfusion SPECT. *J Nucl Cardiol* 2002;9:183-7.
15. Shotwell M, Singh BM, Fortman C, Bauman BD, Lukes J, Gerson MC. Improved coronary disease detection with quantitative attenuation-corrected TI-201 images. *J Nucl Cardiol* 2002;9:52-61.
16. La Croix KJ, Tsui BMW, Hasegawa BH, Brown JK. Investigation of the use of x-ray CT images for attenuation compensation in SPECT. *IEEE Trans Nucl Med* 1994;41:2793-9.
17. Kalki K, Blankspoor SC, Brown JK, Hasegawa BH, Dae MW, Chin M, et al. Myocardial perfusion imaging with a combined CT and SPECT system. *J Nucl Med* 1997;38:1535-40.
18. Bocher M, Balan A, Krausz Y, Shrem Y, Lonn A, Wilk M, et al. Gamma camera-mounted anatomical x-ray tomography: technology, system characteristics, and first images. *Eur J Nucl Med* 2000;27:619-27.
19. Kashiwagi T, Yutani K, Fukuchi M, Naruse H, Iwasaki T, Yokozuka K, et al. Correction of nonuniform attenuation and image fusion in SPECT imaging by means of separate x-ray CT. *Ann Nucl Med* 2002;16:255-61.
20. Fricke H, Fricke E, Weise R, Kammeier A, Lindner O, Burchert W. A method to remove artifacts in attenuation-corrected myocardial perfusion SPECT Introduced by misalignment between emission scan and CT-derived attenuation maps. *J Nucl Med* 2004;45:1619-25.
21. Tonge CM, Manoharan M, Lawson RS, Shields RA, Prescott MC. Attenuation correction using low resolution computed tomography images. *Nucl Med Commun* 2005;26:231-7.
22. Kirac S, Wackers FJ, Liu YH. Validation of the Yale circumferential quantification method using 201Tl and 99mTc: a phantom study. *J Nucl Med* 2000;41:1436-41.
23. Liu YH, Lam PT, Sinusas AJ, Wackers FJ. Differential effect of 180 degrees and 360 degrees acquisition orbits on the accuracy of SPECT imaging: quantitative evaluation in phantoms. *J Nucl Med* 2002;43:1115-24.
24. Diamond GA, Forrester JS. Analysis of probability as an aid in the clinical diagnosis of coronary-artery disease. *N Engl J Med* 1979;300:1350-8.
25. De Santis F, Perone Pacifico M. Accounting for historical information in designing experiments: the Bayesian approach. *Ann Ist Super Sanita* 2004;40:173-9.
26. American Society of Nuclear Cardiology. Updated imaging guidelines for nuclear cardiology procedures, part 1. *J Nucl Cardiol* 2001;8:G5-G58.
27. Liu YH, Sinusas AJ, DeMan P, Zaret BL, Wackers FJ. Quantification of SPECT myocardial perfusion images: methodology and validation of the Yale-CQ method. *J Nucl Cardiol* 1999;6:190-204.
28. Liu YH, Sinusas AJ, Shi CQ, Shen MY, Dione DP, Heller EN, et al. Quantification of technetium 99m-labeled sestamibi single-photon emission computed tomography based on mean counts improves accuracy for assessment of relative regional myocardial blood flow: experimental validation in a canine model. *J Nucl Cardiol* 1996;3:312-20.
29. Iskandrian AE. Risk assessment of stable patients (panel III). In: Proceedings of the 4th Invitational Wintergreen Conference. Wintergreen, Virginia, USA. July 12-14, 1998. Abstracts. *J Nucl Cardiol* 1999;6:93-155.
30. Cerqueira MD, Weissman NJ, Dilsizian V, Jacobs AK, Kaul S, Laskey WK, et al; American Heart Association Writing Group on Myocardial Segmentation and Registration for Cardiac Imaging. Standardized myocardial segmentation and nomenclature for tomographic imaging of the heart: a statement for healthcare professionals from the Cardiac Imaging Committee of the Council on Clinical Cardiology of the American Heart Association. *J Nucl Cardiol* 2002;9:240-5.
31. Metz CE. Basic principles of ROC analysis. *Semin Nucl Med* 1978;8:283-98.
32. Wackers FJ. Attenuation correction, or the emperor's new clothes? *J Nucl Med* 1999;40:1310-2.
33. Vidal R, Buvat I, Darcourt J, Migneco O, Desvignes P, Baudouy M, et al. Impact of attenuation correction by simultaneous emission/transmission tomography on visual assessment of 201Tl myocardial perfusion images. *J Nucl Med* 1999;40:1301-9.
34. Lee DS, Cheon GJ, Kim KM, Lee MM, Chung JK, Lee MC. Limited incremental diagnostic values of attenuation-noncorrected gating and ungated attenuation correction to rest/stress myocardial perfusion SPECT in patients with an intermediate likelihood of coronary artery disease. *J Nucl Med* 2000;41:852-9.
35. Chouraqui P, Livschitz S, Sharir T, Wainer N, Wilk M, Moalem I, et al. Evaluation of attenuation correction method for thallium-201 myocardial perfusion tomographic imaging of patients with low likelihood of coronary artery disease. *J Nucl Cardiol* 1998;5:369-77.
36. Araujo LI, Jimenez-Hoyuela JM, McClellan JR, Lin E, Viggiano J, Alavi A. Improved uniformity in tomographic myocardial perfusion imaging with attenuation correction and enhanced acquisition and processing. *J Nucl Med* 2000;41:1139-44.
37. Grossman GB, Garcia EV, Bateman TM, Heller GV, Johnson LL, Folks RD, et al. Quantitative Tc-99m sestamibi attenuation-corrected SPECT: development and multicenter trial validation of myocardial perfusion gender-independent normal database in an obese population. *J Nucl Cardiol* 2004;11:263-72.
38. Almqvist H, Arheden H, Arvidsson AH, Pahlm O, Palmer J. Clinical implication of down-scatter in attenuation-corrected myocardial SPECT. *J Nucl Cardiol* 1999;6:406-11.
39. Pretorius PH, Narayanan MV, Dahlberg ST, Leppo JA, King MA. The influence of attenuation and scatter compensation on the apparent distribution of Tc-99m sestamibi in cardiac slices. *J Nucl Cardiol* 2001;8:356-64.
40. Harel F, Genin R, Daou D, Lebtahi R, Delahaye N, Helal BO, et al. Clinical impact of combination of scatter attenuation correction, and depth-dependent resolution recovery for 201-Tl studies. *J Nucl Med* 2001;42:1451-6.





## Cadmium-Zinc-Telluride Myocardial Perfusion Imaging in Obese Patients

Michael Fiechter<sup>\*1,2</sup>, Cathérine Gebhard<sup>\*1</sup>, Tobias A. Fuchs<sup>1</sup>, Jelena R. Ghadri<sup>1</sup>, Julia Stehli<sup>1</sup>, Egle Kazakauskaitė<sup>1</sup>, Bernhard A. Herzog<sup>1</sup>, Aju P. Pazhenkottil<sup>1</sup>, Oliver Gaemperli<sup>1</sup>, and Philipp A. Kaufmann<sup>1,2</sup>

<sup>1</sup>Department of Radiology, Cardiac Imaging, University Hospital Zurich, Zurich, Switzerland; and <sup>2</sup>Zurich Center for Integrative Human Physiology (ZIHP), University of Zurich, Zurich, Switzerland

We have evaluated the impact of increased body mass on the quality of myocardial perfusion imaging using a latest-generation  $\gamma$ -camera with cadmium-zinc-telluride semiconductor detectors in patients with high ( $\geq 40$  kg/m<sup>2</sup>) or very high ( $\geq 45$  kg/m<sup>2</sup>) body mass index (BMI). **Methods:** We enrolled 81 patients, including 18 with no obesity (BMI < 30 kg/m<sup>2</sup>), 17 in World Health Organization obese class I (BMI, 30–34.9 kg/m<sup>2</sup>), 15 in class II (BMI, 35–39.9 kg/m<sup>2</sup>), and 31 in class III (BMI  $\geq 40$  kg/m<sup>2</sup>), including 15 with BMI  $\geq 45$  kg/m<sup>2</sup>. Image quality was scored as poor (1), moderate (2), good (3), or excellent (4). Patients with BMI  $\geq 45$  kg/m<sup>2</sup> and nondiagnostic image quality ( $\leq 2$ ) were rescanned after repositioning to better center the heart in the field of view. Receiver-operating-curve analysis was applied to determine the BMI cutoff required to obtain diagnostic image quality ( $\geq 3$ ). **Results:** Receiver-operating-curve analysis resulted in a cutoff BMI of 39 kg/m<sup>2</sup> ( $P < 0.001$ ) for diagnostic image quality. In patients with BMI  $\geq 40$  kg/m<sup>2</sup>, image quality was nondiagnostic in 81%; after CT-based attenuation correction this decreased to 55%. Repositioning further improved image quality. Rescanning on a conventional SPECT camera resulted in diagnostic image quality in all patients with BMI  $\geq 45$  kg/m<sup>2</sup>. **Conclusion:** Patients with BMI  $\geq 40$  kg/m<sup>2</sup> should be scheduled for myocardial perfusion imaging on a conventional SPECT camera, as it is difficult to obtain diagnostic image quality on a cadmium-zinc-telluride camera.

**Key Words:** BMI; CZT; chest wall circumference; obesity; SPECT

J Nucl Med 2012; 53:1401–1406  
DOI: 10.2967/jnumed.111.102434

Among the many refinements of SPECT myocardial perfusion imaging (MPI) that have occurred over the past decade, most have been related to new reconstruction algorithms (1), early imaging protocols (2,3), and tracer development rather than to fundamental advancements of hardware. Only recently has a new generation of cardiac  $\gamma$ -cameras emerged using the

concept of miniaturized cadmium-zinc-telluride (CZT) semiconductor detectors serially aligned around the patient. The multipinhole design renders rotation of the camera around the patient unnecessary, as it covers the entire heart throughout the scan. This advance has multiplied system sensitivity. The first results (4) from CZT cameras have fuelled high expectations with regard to lower activity (5), shorter scan times (6), and possibly improved image quality (7). In particular, the multipinhole geometry may have the potential to decrease artifacts from extracardiac activity and from abdominal soft-tissue attenuation. This is of particular importance in obese subjects, who represent a growing proportion of patients undergoing evaluation for coronary artery disease and may benefit the most from multipinhole geometry. On the other hand, as a result of this geometry, the heart has to be centered in a much smaller field of view than with conventional cameras, and image acquisition may often be challenging in obese patients even after repositioning of the patient.

The aim of the present study was to systematically assess the feasibility of CZT MPI scanning in patients with high, very high, or excessive body mass index (BMI).

### MATERIALS AND METHODS

#### Study Population

We enrolled 65 obese patients (BMI  $\geq 30$  kg/m<sup>2</sup>) and 18 randomly selected nonobese patients (BMI < 30 kg/m<sup>2</sup>) referred for the assessment of known or suspected coronary artery disease by 1-d stress/rest MPI on a CZT  $\gamma$ -camera (NM/CT 570c; GE Healthcare). Patients were assigned according to the World Health Organization into obese class I (BMI, 30–34.9 kg/m<sup>2</sup>), II (BMI, 35–39.9 kg/m<sup>2</sup>), or III (BMI  $\geq 40$  kg/m<sup>2</sup>). Class III patients were further categorized as “morbid obese” (BMI  $\geq 40$  kg/m<sup>2</sup>) or “super obese” (BMI  $\geq 45$  kg/m<sup>2</sup>) as previously suggested (8). We enrolled a minimum of 15 patients per group. In addition to BMI, the chest wall circumference of supine patients was measured at the level of the mammillae. The need to obtain written informed consent was waived because of the nature of the study, which included solely clinical data collection.

#### Image Acquisition

All patients underwent a 1-d pharmacologic stress/rest SPECT MPI protocol with standard adenosine infusion (0.14 mg/kg/min over 6 min). After  $392 \pm 47$  MBq of <sup>99m</sup>Tc-tetrofosmin had been

Received Dec. 27, 2011; revision accepted Apr. 2, 2012.  
For correspondence or reprints contact: Philipp A. Kaufmann, University Hospital Zurich, Ramistrasse 100, NUK C 42, CH-8091 Zurich, Switzerland.  
E-mail: pak@usz.ch  
Published online Jun. 29, 2012.  
<sup>\*</sup>Contributed equally to this work.  
COPYRIGHT © 2012 by the Society of Nuclear Medicine and Molecular Imaging, Inc.



**TABLE 1**  
Patient Baseline Characteristics

Characteristic (n = 81)	Value
Mean age $\pm$ SD (y)	63 $\pm$ 11
Men (%)	60
BMI $\pm$ SD (kg/m <sup>2</sup> )	
Overall	38 $\pm$ 9
$\leq 29.9$ (n = 18)	25 $\pm$ 2
30–34.9 (n = 17)	33 $\pm$ 1
35–39.9 (n = 15)	37 $\pm$ 1
40–44.9 (n = 16)	42 $\pm$ 2
$\geq 45$ (n = 15)	50 $\pm$ 6
Cardiovascular risk factors (%)	
Hypertension	71
Hypercholesterolemia	61
Diabetes mellitus	27
Smoking	22
Positive family history	29
Clinical history of coronary artery disease (%)	
Coronary artery disease	35
Previous percutaneous coronary intervention	29
Coronary artery bypass grafting	11
Angina symptoms (CCS class $\geq$ 2)	26
Dyspnea (NYHA functional class $\geq$ II)	22
Medication (%)	
Platelet aggregation inhibitors	67
Antithrombotic agents	71
Lipid-lowering agents	63

CCS = Canadian Cardiovascular Society; NYHA = New York Heart Association.

administered, stress MPI images were acquired approximately 60 min later (during 5 min) on the CZT camera. This acquisition was followed by rest MPI using the identical protocol several minutes after administration of a 3 times higher dose of <sup>99m</sup>Tc-tetrofosmin (1,143  $\pm$  133 MBq), as previously validated (9,10). MPI scans were acquired using a multipinhole collimator and 19 stationary detectors simultaneously imaging 19 different views of the heart as previously reported (6). In brief, each detector contains 32  $\times$  32 pixelated (2.46  $\times$  2.46 mm) CZT elements; the system design allows acquisition without detector or collimator motion, and a 10% symmetric energy window at 140 keV was used. An unenhanced low-dose 64-slice CT scan with prospective triggering at 75% of the R-R interval was performed for attenuation correction (AC) of CZT MPI (11,12).

Whenever the heart was out of the camera field of view (19-cm diameter) on supine CZT MPI scanning, the acquisition was immediately repeated on the same camera after repositioning the patient by inclination of the chest by 20°–30° or by shifting the body closer to the CZT detector. All 15 patients with a BMI  $\geq$  45 kg/m<sup>2</sup> were additionally scanned on a conventional dual-head SPECT/CT camera (Infinia; GE Healthcare) at the same session according to our clinical routine for super obese patients. Briefly, emission data were acquired with a parallel-hole, low-energy, high-resolution collimator with a 20% symmetric window centered at 140 keV (3° of rotation per stop, 180° for each head, and 25 s per projection). After MPI, CT for AC was performed using the Infinia system at 140 keV and 3.0 mA (13).

#### MPI Image Reconstruction

CZT images were reconstructed as previously described (6,9) on a dedicated Xeleris workstation (GE Healthcare) applying an iterative reconstruction algorithm with maximum-likelihood expectation maximization. The software Myovation for Alcyon (GE Healthcare) was used for image reconstruction, and a Butterworth postprocessing filter was applied to the reconstructed slices. All MPI scans were reconstructed in standard axes (short axis, vertical long axis, and horizontal long axis), and polar maps of perfusion were generated using a commercially available software package (Cedars QGS/QPS; Cedars-Sinai Medical Center) (14).

#### Image Quality Assessment

MPI scans were visually scored for quality using an adapted 4-grade scoring system (1 = poor, 2 = moderate, 3 = good, and 4 = excellent) (15) by 2 masked experienced nuclear cardiologists based on predefined cardiac image characteristics (homogeneity of myocardial radionuclide uptake, integrity or truncation of left ventricle as previously defined (16), and position of left ventricle in the field of view) or interference from extracardiac radioactivity (no activity, minor activity adjacent to the myocardium but not affecting image interpretation, or excessive blood-pool activity or activity significantly reducing confidence in image interpretation). Discrepancies between the 2 readers were resolved by consensus. If the image quality was at least 3 or better, the MPI was considered diagnostic.

#### Statistical Analysis

Quantitative variables were expressed as mean  $\pm$  SD, and categorical variables as frequencies or percentages. SPSS software, version 19.0 (IBM), was used for all statistical analysis. Receiver-operating-curve analysis was applied to measure the area under the curve (AUC) to determine optimal cutoffs for BMI and

**TABLE 2**  
Image Quality in Patients with BMI < 45 kg/m<sup>2</sup>

BMI (kg/m <sup>2</sup> )	n	Without AC		With AC		P	Normals (%)
		Mean IQ	IQ $\geq$ 3 (n)	Mean IQ	IQ $\geq$ 3 (n)		
<30	18	3.6 $\pm$ 0.5	18	3.6 $\pm$ 0.5	18	NS	50
30–34.9	17	3.4 $\pm$ 0.6	16	3.4 $\pm$ 0.6	16	NS	88
35–39.5	15	2.8 $\pm$ 0.7	10	2.9 $\pm$ 0.5	12	NS	67
40–44.5	16	1.9 $\pm$ 0.8	4	2.4 $\pm$ 0.7	8	NS	75

NS = not significant; IQ = image quality.

**TABLE 3**  
Image Quality in Patients with BMI  $\geq 45$  kg/m<sup>2</sup>

Type of MPI	n	Without AC		With AC		Normals (%)
		Mean IQ	IQ $\geq 3$ (n)	Mean IQ	IQ $\geq 3$ (n)	
CZT						
Standard	15	1.6 $\pm$ 0.7	2	2.1 $\pm$ 0.8	6	87
Repositioning	8	2.8 $\pm$ 1.0*	5	3.1 $\pm$ 0.8*	6	75
SPECT	15	3.4 $\pm$ 0.5*	15	3.6 $\pm$ 0.5*	15	87

\* $P < 0.05$  vs. standard.

IQ = image quality.

chest wall circumference to ensure diagnostic image quality. The Mann–Whitney U test and the Jonckheere Terpstra test were used to check for significant differences in image quality between the different modalities.  $P$  values of less than 0.05 were considered statistically significant.

## RESULTS

After exclusion of 2 patients with a BMI over 60 kg/m<sup>2</sup> from further analysis due to geometric inability to fit into either the CZT or the conventional SPECT camera, this study included 18 nonobese patients (BMI,  $25 \pm 2$  kg/m<sup>2</sup>) and 63 obese patients. The patient baseline characteristics are given in Table 1. Eight patients were rescanned on the CZT camera after repositioning, as the heart was out of the field of view. The upper limit of chest circumference to fit into the gantry of the CZT (and the conventional SPECT) camera in the present study was 141 cm. Chest circumference was closely related to BMI ( $r = 0.87$ ,  $P < 0.001$ ). Image quality from the CZT scanner was significantly higher in men than in women, both with AC ( $3.1 \pm 0.1$  vs.  $2.7 \pm 0.2$ ,  $P < 0.05$ ) and without AC ( $2.9 \pm 0.1$  vs.  $2.4 \pm 0.2$ ). Heart size was comparable in nonobese and obese patients (end-diastolic volume,  $92.3 \pm 42.9$  vs.  $92.4 \pm 50.4$ ,  $P =$  not statistically significant).

Image quality of the different BMI groups is given in Tables 2 and 3. In patients with BMI  $\geq 40$  kg/m<sup>2</sup>, 81% of the CZT scans were nondiagnostic (Fig. 1), mainly because the cardiac position was out of focus, causing truncation artifacts of the left ventricle (Fig. 2). After application of AC, this rate significantly decreased to 55% ( $P < 0.05$ ). In patients with BMI  $\geq 45$  kg/m<sup>2</sup>, the CZT image quality (no AC,  $1.6 \pm 0.7$ ; AC,  $2.1 \pm 0.8$ ) improved significantly (Fig. 3) after patient repositioning within the CZT camera (no AC,  $2.8 \pm 0.7$ ; AC,  $3.1 \pm 0.8$ ;  $P < 0.05$ ). Similarly, image quality from SPECT MPI was substantially and significantly higher (no AC,  $3.4 \pm 0.5$ ; AC,  $3.6 \pm 0.5$ ;  $P < 0.001$ ) than that from CZT MPI, reaching diagnostic image quality in every patient. Overall, 59 (73%) of 81 scans were reported as normal.

Receiver-operating-curve analysis (Fig. 4A) revealed a cutoff BMI of 39 kg/m<sup>2</sup> to obtain diagnostic MPI quality for both non-AC images (AUC, 91%; confidence interval,

0.85–0.97;  $P < 0.001$ ) and AC images (AUC, 84%; confidence interval, 0.75–0.93;  $P < 0.001$ ). Similarly, for chest wall circumference, receiver-operating-curve analysis (Fig. 4B) revealed a cutoff of 123 cm to obtain diagnostic MPI quality for both non-AC images (AUC, 89%; confidence interval, 0.81–0.96;  $P < 0.001$ ) and AC images (AUC, 81%; confidence interval, 0.71–0.91;  $P < 0.001$ ). Differences in image quality between non-AC and AC images were not statistically significant.

## DISCUSSION

Our results suggest that for patients with morbid obesity, MPI on CZT cameras may often yield insufficient image quality; the patient's heart cannot get close enough to the detectors because the body mass is too high for the size of the gantry. As a result, in patients with BMI  $\geq 40$  kg/m<sup>2</sup>, 81% of non-AC scans and 55% of AC scans were non-diagnostic. By contrast, image quality was significantly better from a conventional  $\gamma$ -camera and was diagnostic in all patients.

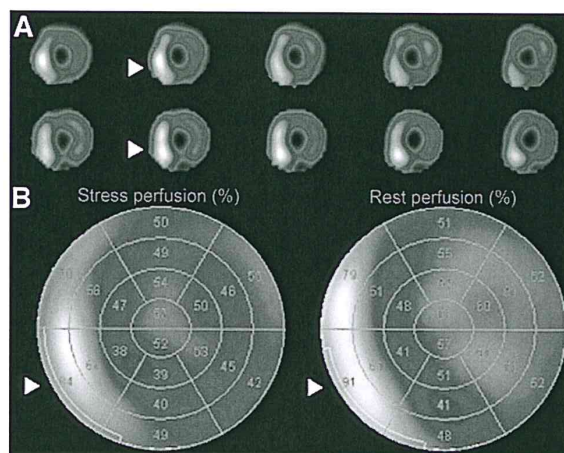
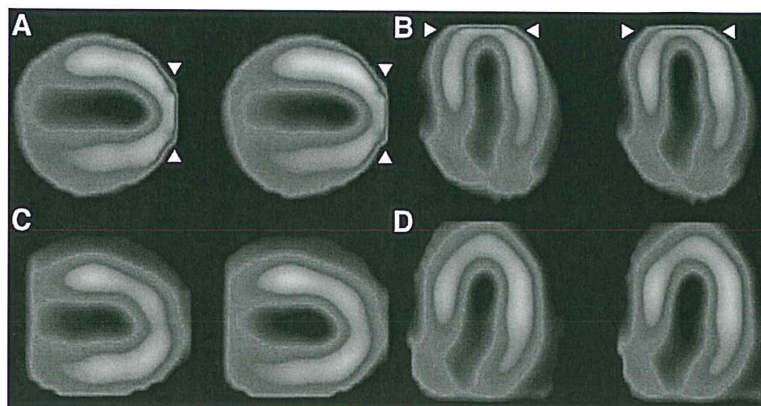


**FIGURE 1.** Obesity artifact in SPECT MPI. Typical artifact (banana shape; arrowheads) observed in CZT scanning of obese patients is shown on short-axis images (A) and corresponding polar maps (B).



**FIGURE 2.** Apical truncation artifact. Eccentric position of heart causes apical truncation artifact (arrowheads), illustrated in vertical (A) and horizontal (B) long-axis views; for comparison, same views are given without truncation artifact (C and D).



Obesity may often affect the quality of SPECT MPI scans, mainly because of reduction of test specificity by diaphragm soft-tissue attenuation and extracardiac activity (17–21). CT-based AC has been found to compensate at least in part for inferior soft-tissue attenuation, resulting in improved SPECT MPI diagnostic (22) and prognostic (23) accuracy. The latest generation of  $\gamma$ -cameras with CZT detectors was expected to offer improved image quality in obese patients, as its detector geometry with pinhole collimation should help avoid image degradation by soft-tissue attenuation. Attenuation artifacts can nevertheless occur but can be corrected with x-ray–based CT attenuation maps (12). In the new generation of cardiac CZT cameras the target organ, the heart, has to be centered accurately within the field of view, which is substantially smaller than that on standard SPECT cameras. For most patients in our daily routine, this requirement does not present any limitation. However, in patients with morbid obesity this limitation becomes critical, particularly in a center such as ours, which receives regular referrals for preoperative MPI from an associated busy bariatric surgery program.

Our data show that AC may improve image quality but fails to solve the fundamental problem of imaging obese patients with CZT cameras. Even careful repositioning frequently remains unsuccessful in some very obese patients, in whom the standard SPECT camera remains the first-choice tool. By receiver-operating-curve analysis, we have identified a BMI of 39 kg/m<sup>2</sup> as the cutoff for direct scheduling of scanning on a standard camera. BMI rather than absolute weight is used to categorize obesity, as the absolute weight in tall persons may be high without reflecting obesity. Consequently, BMI rather than absolute weight is most appropriate for identifying patients who should not undergo CZT scanning. Very rarely, however, the patient's circumference exceeds the gantry even of such a camera, as was the case in 2 of our patients, rendering scanning impossible on any of our available devices. The ability of the patient to fit within the scanner should therefore be routinely tested before any tracer activity is injected.

It may be seen as a potential limitation of the present study that we did not assess the accuracy of CZT by comparing it with a reference standard such as invasive coronary angiography with fractional flow reserve. Such an assessment, however, was beyond the scope of the present feasibility study, which was designed to evaluate how severe obesity interacts with diagnostic image quality in the new-generation CZT  $\gamma$ -camera. Furthermore, not all patients were rescanned on a conventional SPECT camera for direct comparison, and therefore the relatively small size of the study subgroups may appear as a limitation. However, all patients with BMI  $\geq 45$  kg/m<sup>2</sup> ( $n = 15$ ) were rescanned, and this rescanning increased the rate of diagnostic image quality to 100%. It may be reasonable to assume that in less obese patients, MPI on a standard SPECT camera would not be less successful. Similarly, only 8 of 15 patients—mainly those with nondiagnostic image quality after AC—were repositioned and rescanned with the heart better centered in the field of view. However, the subjective discomfort induced by repositioning of

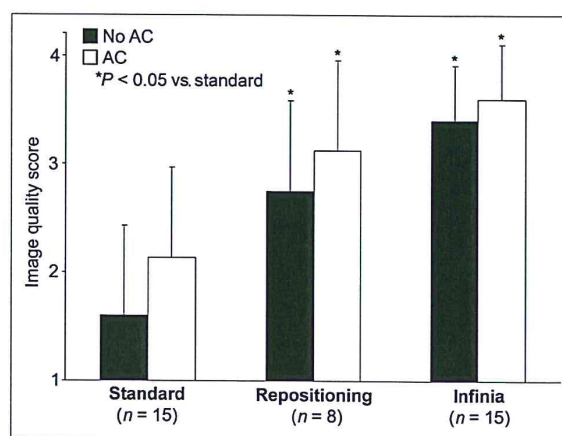


**FIGURE 3.** Image quality in patients with BMI  $\geq 45$  kg/m<sup>2</sup>. Shown is image quality of standard CZT MPI ( $n = 15$ ), CZT MPI after repositioning ( $n = 8$ ), and conventional SPECT ( $n = 15$ ).

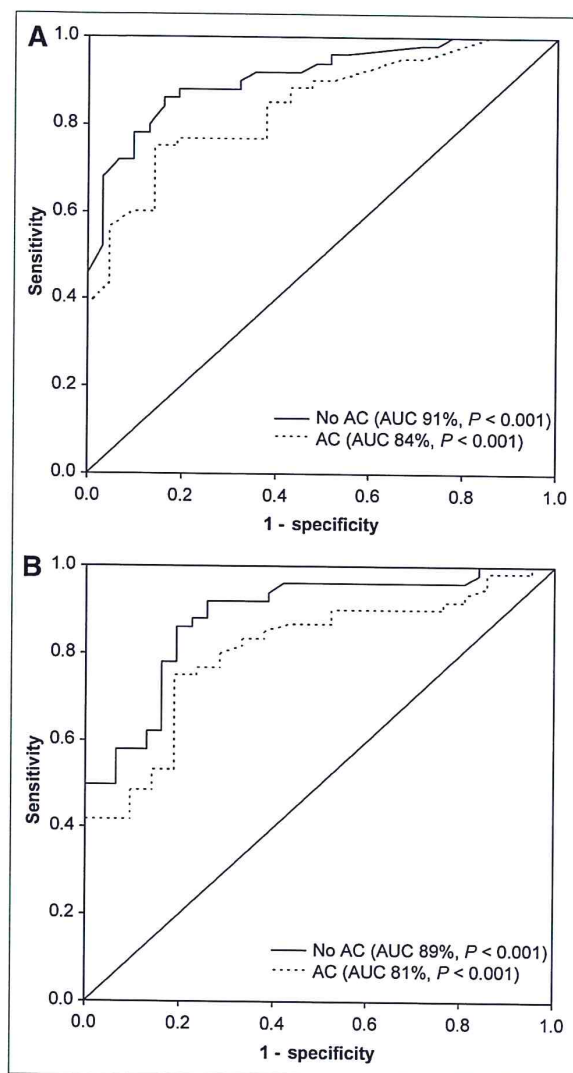


**FIGURE 4.** Receiver-operating-curve analysis for CZT MPI image quality and BMI (A) or chest wall circumference (B).

super obese patients was considered too high to justify such a maneuver in patients with diagnostic image quality. Although image quality was higher in men than women overall, the present study was not designed to provide such comparison data for each BMI group. Further, the present study used vasodilator stress although the use of physical exercise stress might have reduced extracardiac activity and potentially improved image quality. However, severe obesity often hampers the ability to perform adequate physical exercise. Finally, in this non-heart-failure population, heart size was similar in obese and nonobese patients. The role of increased heart size on image quality from CZT cameras with a small field of view remains to be evaluated in patients with an enlarged left ventricle.

## CONCLUSION

The introduction of CZT  $\gamma$ -cameras, with their advantages over conventional SPECT cameras, has not solved the issue of image quality degradation from obesity. On the contrary, it appears that the actual design of CZT cameras, with pinhole collimation geometry and a smaller field of view, is more prone to artifacts in very obese patients. Therefore, patients with a BMI of 40 kg/m<sup>2</sup> and above should be scheduled on a conventional SPECT camera for MPI scanning.

## DISCLOSURE STATEMENT

The costs of publication of this article were defrayed in part by the payment of page charges. Therefore, and solely to indicate this fact, this article is hereby marked "advertisement" in accordance with 18 USC section 1734.

## ACKNOWLEDGMENTS

We thank Ennio Mueller and Patrick von Schulthess for their excellent technical support. This study was supported by a grant from the Swiss National Science Foundation. No other potential conflict of interest relevant to this article was reported.

## REFERENCES

- Valenta I, Treyer V, Husmann L, et al. New reconstruction algorithm allows shortened acquisition time for myocardial perfusion SPECT. *Eur J Nucl Med Mol Imaging*. 2010;37:750–757.
- Giorgetti A, Rossi M, Stanislao M, et al. Feasibility and diagnostic accuracy of a gated SPECT early-imaging protocol: a multicenter study of the Myoview Imaging Optimization Group. *J Nucl Med*. 2007;48:1670–1675.
- Herzog BA, Husmann L, Buechel RR, et al. Rapid cardiac hybrid imaging with minimized radiation dose for accurate non-invasive assessment of ischemic coronary artery disease. *Int J Cardiol*. 2011;153:10–13.
- Esteves FP, Raggi P, Folks RD, et al. Novel solid-state-detector dedicated cardiac camera for fast myocardial perfusion imaging: multicenter comparison with standard dual detector cameras. *J Nucl Cardiol*. 2009;16:927–934.
- Berman DS, Kang X, Tamarappoo B, et al. Stress thallium-201/rest technetium-99m sequential dual isotope high-speed myocardial perfusion imaging. *JACC Cardiovasc Imaging*. 2009;2:273–282.
- Herzog BA, Buechel RR, Katz R, et al. Nuclear myocardial perfusion imaging with a cadmium-zinc-telluride detector technique: optimized protocol for scan time reduction. *J Nucl Med*. 2010;51:46–51.
- Sharir T, Ben-Haim S, Merzon K, Prochorov V, Dickman D, Berman DS. High-speed myocardial perfusion imaging initial clinical comparison with conventional dual detector angio camera imaging. *JACC Cardiovasc Imaging*. 2008;1:156–163.
- Sturm R. Increases in morbid obesity in the USA: 2000–2005. *Public Health*. 2007;121:492–496.
- Buechel RR, Herzog BA, Husmann L, et al. Ultrafast nuclear myocardial perfusion imaging on a new gamma camera with semiconductor detector technique: first clinical validation. *Eur J Nucl Med Mol Imaging*. 2010;37:773–778.
- Fiechter M, Ghadri JR, Kuest SM, et al. Nuclear myocardial perfusion imaging with a novel cadmium-zinc-telluride detector SPECT/CT device: first validation versus invasive coronary angiography. *Eur J Nucl Med Mol Imaging*. 2011;38:2025–2030.
- Herzog BA, Buechel RR, Husmann L, et al. Validation of CT attenuation correction for high-speed myocardial perfusion imaging using a novel cadmium-zinc-telluride detector technique. *J Nucl Med*. 2010;51:1539–1544.



12. Fiechter M, Ghadri JR, Wolfrum M, et al. Downstream resource utilization following hybrid cardiac imaging with an integrated cadmium-zinc-telluride/64-slice CT device. *Eur J Nucl Med Mol Imaging*. 2012;39:430–436.
13. Schepis T, Gaemperli O, Koepfli P, et al. Use of coronary calcium score scans from stand-alone multislice computed tomography for attenuation correction of myocardial perfusion SPECT. *Eur J Nucl Med Mol Imaging*. 2007;34:11–19.
14. Germano G, Kavanagh PB, Waechter P, et al. A new algorithm for the quantitation of myocardial perfusion SPECT. I: technical principles and reproducibility. *J Nucl Med*. 2000;41:712–719.
15. Askew JW, Miller TD, Ruter RL, et al. Early image acquisition using a solid-state cardiac camera for fast myocardial perfusion imaging. *J Nucl Cardiol*. 2011;18:840–846.
16. Wosnitzer B, Gadiraju R, Depuey G. The truncation artifact. *J Nucl Cardiol*. 2011;18:187–191.
17. Berman DS, Kang X, Nishina H, et al. Diagnostic accuracy of gated Tc-99m sestamibi stress myocardial perfusion SPECT with combined supine and prone acquisitions to detect coronary artery disease in obese and nonobese patients. *J Nucl Cardiol*. 2006;13:191–201.
18. Duvall WL, Croft LB, Corriel JS, et al. SPECT myocardial perfusion imaging in morbidly obese patients: image quality, hemodynamic response to pharmacologic stress, and diagnostic and prognostic value. *J Nucl Cardiol*. 2006;13:202–209.
19. Gemignani AS, Muhlebach SG, Abbott BG, Royce GD, Harrington DT, Arrighi JA. Stress-only or stress/rest myocardial perfusion imaging in patients undergoing evaluation for bariatric surgery. *J Nucl Cardiol*. 2011;18:886–892.
20. Elhendy A, Schinkel AF, van Domburg RT, et al. Prognostic stratification of obese patients by stress <sup>99m</sup>Tc-tetrofosmin myocardial perfusion imaging. *J Nucl Med*. 2006;47:1302–1306.
21. Ghanem MA, Kazim NA, Elgazzar AH. Impact of obesity on nuclear medicine imaging. *J Nucl Med Technol*. 2011;39:40–50.
22. Masood Y, Liu YH, Depuey G, et al. Clinical validation of SPECT attenuation correction using x-ray computed tomography-derived attenuation maps: multicenter clinical trial with angiographic correlation. *J Nucl Cardiol*. 2005;12:676–686.
23. Pazhenkottil AP, Ghadri JR, Nkoulou RN, et al. Improved outcome prediction by SPECT myocardial perfusion imaging after CT attenuation correction. *J Nucl Med*. 2011;52:196–200.



The Journal of  
NUCLEAR MEDICINE

## Cadmium-Zinc-Telluride Myocardial Perfusion Imaging in Obese Patients

Michael Fiechter, Cathérine Gebhard, Tobias A. Fuchs, Jelena R. Ghadri, Julia Stehli, Egle Kazakauskaitė, Bernhard A. Herzog, Aju P. Pazhenkottil, Oliver Gaemperli and Philipp A. Kaufmann

*J Nucl Med.* 2012;53:1401-1406.

Published online: June 29, 2012.

Doi: 10.2967/jnumed.111.102434

---

This article and updated information are available at:  
<http://jnm.snmjournals.org/content/53/9/1401>

---

Information about reproducing figures, tables, or other portions of this article can be found online at:  
<http://jnm.snmjournals.org/site/misc/permission.xhtml>

Information about subscriptions to JNM can be found at:  
<http://jnm.snmjournals.org/site/subscriptions/online.xhtml>

*The Journal of Nuclear Medicine* is published monthly.  
SNMMI | Society of Nuclear Medicine and Molecular Imaging  
1850 Samuel Morse Drive, Reston, VA 20190.  
(Print ISSN: 0161-5505, Online ISSN: 2159-662X)

© Copyright 2012 SNMMI; all rights reserved.

The logo for the Society of Nuclear Medicine and Molecular Imaging (SNMMI) consists of the letters 'SNMMI' in a bold, sans-serif font, with the 'S' and 'N' stacked vertically, and the 'M' and 'I' stacked vertically. To the right of the logo, the text 'SOCIETY OF NUCLEAR MEDICINE AND MOLECULAR IMAGING' is written in a smaller, sans-serif font.  
SOCIETY OF  
NUCLEAR MEDICINE  
AND MOLECULAR IMAGING







# NIH Public Access

## Author Manuscript

*Semin Nucl Med.* Author manuscript; available in PMC 2011 March 6.

Published in final edited form as:

*Semin Nucl Med.* 2008 May ; 38(3): 177–198. doi:10.1053/j.semnuclmed.2008.01.001.

## Technological Development and Advances in SPECT/CT

Youngho Seo, PhD, Carina Mari Aparici, MD, and Bruce H Hasegawa, PhD

### Abstract

SPECT/CT has emerged over the past decade as a means of correlating anatomical information from CT with functional information from SPECT. The integration of SPECT and CT in a single imaging device facilitates anatomical localization of the radiopharmaceutical to differentiate physiological uptake from that associated with disease and patient-specific attenuation correction to improve the visual quality and quantitative accuracy of the SPECT image. The first clinically available SPECT/CT systems performed emission-transmission imaging using a dual-headed SPECT camera and a low-power x-ray CT sub-system. Newer SPECT/CT systems are available with high-power CT sub-systems suitable for detailed anatomical diagnosis, including CT coronary angiography and coronary calcification that can be correlated with myocardial perfusion measurements. The high-performance CT capabilities also offer the potential to improve compensation of partial volume errors for more accurate quantitation of radionuclide measurement of myocardial blood flow and other physiological processes and for radiation dosimetry for radionuclide therapy. In addition, new SPECT technologies are being developed that significantly improve the detection efficiency and spatial resolution for radionuclide imaging of small organs including the heart, brain, and breast, and therefore may provide new capabilities for SPECT/CT imaging in these important clinical applications.

### Introduction

Medical diagnosis is a complex process which relies ultimately on the human perception and intellect to gather information from multiple sources, to sort through many possible actions, and to arrive at the course which best dictates care for an individual patient. Whereas we now rely on a full spectrum of technological innovations that span the discipline of medical imaging, for centuries the only medical image was that gathered by human vision. The most fundamental type of medical imaging was established by Roentgen with the discovery of x-rays one century ago which forever changed the means by which information can be gathered from the human body. Additional advances arose in the 1960s and 1970s when modern medical imaging methods were developed, including Nuclear Medicine (SPECT and PET), computed tomography, digital radiography, and diagnostic ultrasound, and when the fundamentals of nuclear magnetic resonance imaging were established and tested. The development of these technologies has been rapid over the past several decades and has led to use of sophisticated instruments that are both cost-effective and yield diagnostic information that cannot be discerned with unaided human vision. Along with these technological advances, both the quantity and the complexity of information used in the medical diagnostic process have reached levels that were unimaginable even a decade ago. For this reason, it is important to seek and refine technology that not only can increase the information available, but also can assist the diagnostician in synthesizing and relating data that are available from all of these multiple sources.

Diagnosis of disease involves a subtle yet challenging process, one which seeks to identify disorders at the earliest stages of development and biological expression. Imaging methods



such as projection radiography, angiography, computed tomography, magnetic resonance imaging, and ultrasound offer the highest levels of spatial resolution for defining anatomical structures. Furthermore, by administration of contrast media, these methods can visualize blood flow and other functional processes in the cardiovascular, pulmonary, gastrointestinal, urinary, and musculoskeletal systems. However, detection of disease with anatomical imaging methods often requires gross structural changes to be apparent before the diagnosis is definitive. The reliance on anatomical information for diagnosis also makes it difficult to monitor the response of diseased and normal tissues in the critical post-therapy period. In comparison, radiotracer imaging methods such as single photon emission tomography (SPECT) and positron emission tomography (PET) are well-suited to provide critical information about the functional, metabolic, and molecular status of tissues and organs. Radionuclide imaging also can extract measurement data at picomolar and nanomolar concentration levels, rather than the millimolar levels needed for imaging contrast agents with anatomical imaging methods. As a result, subtle and often earlier changes can be detected with targeted radionuclide agents using nuclear imaging than is possible with anatomical imaging methods. While radionuclide imaging has important characteristics for disease detection, it also has well-recognized limitations in spatial resolution and statistical quality [1,2]. Furthermore, while Nuclear Medicine relies on imaging radiopharmaceuticals that are targeted at specific biochemical processes, uptake can occur in both diseased and normal sites and it is important to differentiate these sites to correctly evaluate the patient's status. It therefore has been long recognized and practiced in Nuclear Medicine and Radiology that images acquired using multiple modalities can provide complementary diagnostic information.

A fundamental form of dual-modality imaging occurs when the physician acquires functional (eg SPECT, PET) and anatomic (eg CT, MRI) images of a patient using separate systems. The physician then can view the functional and anatomical images side-by-side on a view box or display monitor to identify complementary features in the images, and thereby extract a decision from that correlated information. However, the practical process of acquiring and spatially (and sometimes temporally) correlating data from two or more imaging systems is complicated by several factors. First, the multiple data sets for an individual generally are acquired on separate days, on different systems, and following unrelated protocols at different locations and by different operators. As a result, operational details of each study may be unknown and such information as well as the images themselves may be difficult to access at a common site. Second, it generally is difficult to maintain the patient in a consistent geometry across separate imaging studies with respect to body position in terms of the curvature of the spine and neck, location of the extremities, the shape of the patient table, the patient respiratory state and cardiac cycle, and shape and status of the patient's gastric, intestinal, and urinary contents. Software techniques have been developed that can register and fuse images from multiple sources [3-7], and are best suited for correlating images from rigid structures such as the brain [8] and skeleton [9,10]. Even when multi-modality image data are available from dual-modality systems, structures within the images can be displaced by respiration, cardiac motion, and other voluntary and involuntary motions. This implies that software-based methods will retain important roles in achieving accurate levels of image registration even when patient studies are performed with PET/CT or SPECT/CT devices [11].

Nevertheless, image registration has proved to be difficult when applied alone in the thorax, abdomen, and pelvis where body structures are elastic and deformable, and can change shape over short periods of time due to internal and external patient motion. The problem of image co-registration is complicated when the images represent fundamentally different information (eg PET vs. MRI, SPECT vs. CT) that may offer few commonly-recognizable landmarks and are acquired at different levels of spatial resolution. For these reason, dual-

modality systems [12-19] increasingly are being used to acquire complementary image data with geometrical configurations that are as consistent to one another as possible, and in a way that facilitates the logistics of spatially registering data and then combining or fusing data from multi-modality imaging procedures. These systems have proven beneficial in facilitating attenuation correction of radionuclide data with patient-specific attenuation maps acquired from CT [20-23], and in correlating functional information from the radionuclide image with anatomical studies visualized with CT. Multi-modality image correlation is gaining increased importance in defining treatment planning options for radiation oncology and surgery [7,24-27]. It also promises to have an important role in improving quantitation of radiopharmaceutical uptake [28,29] needed for radiation dosimetry [26,30-32] and to monitor subtle changes such as those needed for assessing therapeutic response and therapeutic monitoring. These recognized capabilities have advanced the use and adoption of dual-modality imaging represented by PET/CT and SPECT/CT.

## Dual-Modality Imaging Systems

Direct methods of combining structural and functional information were conceived and implemented in prototype form during the historical beginning of emission and transmission computed tomography, most notably the work by Kuhl, Hale, and Eaton who obtained the first transaxial transmission CT scan of a patient's thorax using their Mark II brain SPECT scanner in the mid-1960s [33]. Despite this pioneering work, the modern use of transmission imaging with external radionuclide transmission sources was not introduced for attenuation correction in SPECT [34,35] and PET [36,37] until the 1980s. The use of external transmission scanning is still used with SPECT to perform both attenuation correction and anatomical localization at sites of radionuclide accumulations. However, this approach has some fundamental limitations, primarily with regard to relatively poor statistical quality which limits the anatomical detail and contrast resolution produced by the transmission scan. As a result, transmission imaging using external radionuclide sources has not achieved routine widespread use with SPECT.

Over the past decade, dual-modality imaging has evolved as a method to facilitate the process of integrating and correlating medical images. For SPECT/CT and PET/CT, such imaging is performed with a system that acquires data from two image modalities supported on a single integrated gantry. The imaging study is performed with the patient remaining on the patient table, which is translated from the CT scanner to the PET or SPECT system to acquire the correlated x-ray and radionuclide image data. The resulting dual-modality image data then can be transferred electronically to a common computer for data correction, reconstruction, display, integration, and analysis. Both SPECT/CT [12,38] and PET/CT systems [16,18,39] are commercially available for clinical as well as pre-clinical imaging. Furthermore, dual-modality PET/MRI systems are under development for small-animal imaging [40,41] and for human brain imaging; SPECT/MRI systems are being developed for pre-clinical imaging of small animal models [42]. (One manufacturer (Gamma Medica) has marketed a tri-modality (PET, SPECT, and CT) device for small-animal imaging.) In comparison to traditional single-modality imaging approaches, the dual-modality systems offer unique capabilities in combining data from two imaging modalities in way that simplifies, yet facilitates, image correlation with the goal of revealing useful diagnostic information that is not easily extracted when the imaging studies are performed independently.

## Early Development of SPECT/CT

In the late 1980s, researchers began devising methods to combine radionuclide emission imaging directly with x-ray transmission imaging in a single system. Possibly the earliest



such system was proposed by Mirshanov [43], who received a Soviet patent for a combined transmission-emission tomograph in 1987. This system (Figure 1) was designed so that the patient could undergo simultaneous radionuclide and x-ray imaging with separate scintillation and semiconductor detector viewing the same patient volume, with the resulting emission and transmission data then were recorded with a common image buffer. Although apparently not reduced to practice, this system was perhaps the first that envisioned a combined system with which an x-ray rather than a radionuclide source was integrated directly to produce the transmission data as part of a radionuclide imaging study. Another early design for a dual-modality imaging system was disclosed in an international patent application "Transmission/emission and registered imaging (TERI) computed tomography scanners" by Kaplan [44]. This work proposed acquiring the CT transmission and SPECT emission data simultaneously using imaging detectors (Figure 2) to maintain spatial registration between the two image data sets and to obtain maps of attenuation coefficients to compensate the SPECT data for attenuation. A critical challenge in implementing a simultaneous SPECT/CT system lies in the still-unsolved difficulty of designing a common detector with sufficient temporal and energy resolution to discriminate the primary radionuclide photons from both the x-ray signal and from scatter of the radionuclide photons. Designing a detector capable of simultaneous x-ray and radionuclide imaging remains a fundamental technical barrier in developing a system for truly simultaneous emission and transmission imaging with performance levels matching those achieved with currently available CT and SPECT systems.

The development of experimental SPECT/CT systems was undertaken by Hasegawa et al at the University of California, San Francisco (CSF) in the late 1980s and early 1990s [45,46]. These investigators envisioned a radionuclide imaging system that incorporated a low-power x-ray generator and source for transmission imaging [46]. A prototype system (Figure 3a) included a collimated array of high-purity germanium (HPGe) detectors [47,48] to record photons from both the external x-ray source and the internal radionuclide distribution that then were processed with photon-counting electronics to discriminate the x-ray data (eg produced at 120 kV) and the radionuclide data (eg emitted at 140 keV for  $^{99m}\text{Tc}$ ). An image (Figure 3b) of a pig administered a myocardial perfusion agent ( $^{99m}\text{Tc}$ -sestamibi) shows radiopharmaceutical uptake in the myocardium displayed in red superimposed on the grayscale CT image of the animal [49,50]. The development of the UCSF emission-transmission CT system demonstrated the technical feasibility of acquiring the x-ray and radionuclide image data simultaneously using an HPGe detector array with high-performance photon-counting electronics. However, this system also revealed several important limitations. First, the prototype system had a physically small (ie 24-element) detector that required several hours to acquire both the emission and transmission data. Moreover, the expense of HPGe made it difficult to envision how this detector technology could be implemented practically at a realistic size and cost. Second, the x-ray tube in the prototype system was operated at a very low power level (eg approximately 100-120 kV at 1 mA) but still produced x-ray data with sufficiently high count-rates to cause pulse pile-up that contaminated both the emission and transmission data [51]. The UCSF group designed and tested prototype electronics that allowed the HPGe detector array in the SPECT/CT system to be switched between photon-counting mode for radionuclide imaging and current-mode for x-ray imaging [52-54] for near-simultaneous x-ray and radionuclide imaging using a single detector array. However, it was difficult to envision how such an approach could be cost-effective or practical in a clinical setting. Third, a SPECT/CT system operated with an x-ray tube equivalent to that in a modern CT scanner also would have to account for a roughly  $10^7$ -fold difference in photon fluence encountered in x-ray and radionuclide imaging. For example, a Siemens Somatom x-ray source operated at 125 kV with 2.5-mm aluminum plus 0.4-mm of copper filtration and with a  $24^\circ$  tungsten target produces  $3.5 \times 10^6$  photons/mAs/mm<sup>2</sup> at a distance of 75 cm [55], or  $1.18 \times 10^9$  photons/mm<sup>2</sup> at a distance of 1

m when the x-ray tube is operated with a filament current of 600 mA typical of a modern x-ray source. This is equivalent to the photon fluence from a  $1.5 \times 10^{16}$  GBq ( $4.0 \times 10^5$  Ci) radionuclide source assuming a yield of 1 photon per disintegration (although it is unlikely that a radionuclide source having this strength could be configured physically since self-absorption within the source would limit the photon fluence rate). Similarly, the amount of radioactivity injected in the patient typically is limited by dosimetry concerns to  $\sim 20$  mCi (740 MBq), or roughly 20-million-fold lower. Furthermore, the amount of x-ray scatter that occurs within the patient can be estimated roughly as 0.1% of the primary photon fluence, equivalent to a source strength of  $\sim 400$  Ci ( $1.5 \times 10^{13}$  GBq), or a scatter fluence rate  $1.2 \times 10^6$  photons/s/mm<sup>2</sup>. The photon fluence rates of both the primary and scatter fields are beyond the count-rate capabilities of modern radionuclide imaging system. As a result, it is difficult to envision how a simultaneous SPECT/CT system could be developed with performance matching currently available separate SPECT and CT systems. However, the foregoing analysis helps to emphasize the advantages of transmission imaging with an x-ray versus a radionuclide source in that the former offers faster scans, higher statistics, and better spatial resolution. Furthermore, unlike a radionuclide source, an x-ray source can be turned off and discarded when necessary without any radioactive waste-disposal issues.

The “modern” SPECT/CT system was also originally developed by Hasegawa, et al, at USCF in the mid-1990s [21]. The development of the system grew out of prior experience with the prototype dual-modality system described above which used a single detector to acquire the SPECT/CT data either sequentially or simultaneously. However, as previously discussed, these studies demonstrated the difficulty in acquiring the otherwise incompatible SPECT/CT data simultaneously with a single detector. The modern SPECT/CT system utilizes an alternative approach which has proven to be more robust and incorporates separate state-of-the-art SPECT and CT sub-systems. The SPECT and CT sub-systems can be placed in tandem (ie in-line) for imaging and integrated with a common patient (or animal) table and computer system (Figure 4). This group integrated a GE XR/T SPECT and GE 9800 Quick CT systems with an elongated table that could be positioned for either CT or SPECT imaging [21] without removing the patient from the system. The patient table was mechanically supported with an external brace at the far end of the CT system to minimize downward table deflection when it was extended to the SPECT sub-system. This allowed the CT and SPECT data to be acquired sequentially with the CT data reconstructed in the CT scanner with a conventional filtered backprojection algorithm, then transferred to an external host computer via magnetic tape. The CT data were available for anatomical display, or could be converted (as described below) to obtain a CT-derived map of linear attenuation coefficients to correct the radionuclide data for photon attenuation. The radionuclide projection data acquired with the scintillation camera system were transferred via diskette onto the host computer for iterative reconstruction, allowing the SPECT data to be reconstructed with attenuation correction using the CT-derived attenuation map. These reconstruction and post-processing steps produced three different displays: the x-ray CT data reconstructed from the CT scanner; the radionuclide emission data reconstructed with attenuation correction from the x-ray CT data; and a fused image in which the radionuclide data were displayed in color over a co-registered CT image displayed in grayscale.

## Fundamentals of SPECT/CT

### Image Registration

Several aspects of the prototype SPECT/CT system remain as important in current SPECT/CT systems, and many of these are important in PET/CT as well. First, the general experience with both SPECT/CT and PET/CT is that dual-modality imaging can simplify the spatial registration of emission and transmission data in comparison to images obtained on separate systems at separate times. This is especially helpful when uptake of a given



radiopharmaceutical is associated with both disease and normal processes. For example, PET accumulation of  $^{18}\text{F}$ -FDG occurs in normal heart, brain, kidney, and urinary bladder as well as in regions of inflammation and malignant disease [56,57]. Similarly, SPECT visualized uptake of agents such as  $^{111}\text{In}$ -ProstaScint in normal structures such as the prostate, blood pool, and bone marrow, and such uptake can be difficult to differentiate from that associated with prostate carcinoma [58]. By simplifying the process of localizing radiopharmaceutical uptake with CT correlation, dual-modality imaging can help to identify a specific site of radiopharmaceutical accumulation for planning radiation or surgical treatment planning or to differentiate uptake that occurs physiologically from that indicative of disease [14,24,59].

Image registration is improved in dual-modality imaging since the radionuclide and CT data are obtained while the patient maintains the same body position, posture, arm and leg configuration, and table shape during image acquisition. To the extent that the body position remains static throughout image acquisition, this will help to assure accurate image registration even with table translation during the SPECT and CT scanning process. However, the SPECT image acquisition commonly requires 15 to 60 minutes. For myocardial perfusion imaging, the SPECT study requires both rest and stress acquisitions at separate times between which the patient commonly is removed from the table. Similarly, the CT image can be performed within one or a few breath holds with high-performance diagnostic CT, but may require 5 minutes for a low-dose x-ray system. The patient can move, cough, or stretch, or twitch during the scanning process, and internal organs will move due to cardiac or respiratory motion, peristalsis, gas motility, and/or bladder filling [60,61]. Mis-registration errors due to respiratory motion often can be reduced by acquiring the image during quiet tidal respiration which provides fairly consistent acquisitions of the SPECT and CT data. However, the dual-modality acquisitions can exhibit geometrical changes between the SPECT and CT images, making it impossible to simply merge the data without correcting for gross mis-registration errors of several millimeters or more. The primary method of improving image registration relies on image translation following image acquisition and reconstruction, without applying the more subtle transforms of image rotation or regional image warping or shear. Image registration can be applied globally when needed, for example, to compensate for patient table sag, gross patient motion, or mis-calibration between the digital images used to form the CT and SPECT data [62,63]. Current clinical practice continues to rely on the physician's knowledge and experience in interpreting mis-registration errors that remain in the dual-modality image data, generally by comparison of the SPECT data before and following attenuation correction and CT co-registration [64,65]. These studies [64,66] suggest that the combination of SPECT and CT imaging facilitates attenuation correction of myocardial perfusion SPECT with CT co-registration but emphasizes the challenges of translating results from static phantoms to living, breathing patients who move both voluntarily and involuntarily [65,67].

### Attenuation Correction

CT can be used to perform attenuation correction of radionuclide emission data since the CT image inherently represents an anatomical map of linear attenuation coefficients ( $\mu\text{s}$ ) reconstructed at the effective energy of the x-ray beam [20,21,34,35]. This process of generating a map of linear attenuation coefficients in CT is complicated by "beam hardening," the process in which lower-energy photons are preferentially absorbed as they pass through the patient in a thickness-dependent manner that increases the mean energy in the transmitted x-ray beam emerging from the patient [68,69]. If uncorrected, x-ray beam hardening will, for example, produce images in which the CT values in the center of the body (ie that recorded in the thickest part of the object) are reconstructed with lower attenuation coefficient values than in the periphery, where x-ray absorption is lower and

beam hardening less severe. Modern CT scanners largely account for and correct beam hardening so that a CT scan of uniformly soft tissue regions are reconstructed with uniform image intensity. Beyond normal beam-hardening corrections, when the CT scan is used to derive  $\mu$  values to correct SPECT (or PET) data for photon attenuation, it must be calibrated so that it represents the linear attenuation coefficients at the photon energy of the radionuclide used to acquire the emission data rather than the mean energy of the x-ray beam used to form the CT image [20-23]. The necessary calibration data can be obtained by acquiring CT scans of a phantom [21] having chambers filled with various concentrations of biologically equivalent materials, for example, air, 60% ethanol (ie a fat simulant), water, normal saline, and various concentrations (ie 50, 100, 200, 300, 400 mg/cm<sup>3</sup>) of dipotassium hydrogen phosphate (K<sub>2</sub>HPO<sub>4</sub>) as a bone-mineral simulant. Alternatively, it is possible to use solid tissue-equivalent materials for the calibration measurement [70]. The CT value of each calibration material then is extracted by defining a region of interest corresponding to each calibration region in the phantom. The linear attenuation coefficient for each such material also can be calculated from the known chemical contents of each region. The calibration data then are represented by relating the extracted image value (in Hounsfield Units, HU) and the calculated linear attenuation coefficient (in units of cm<sup>-1</sup>) of each calibration material at the photon energy of the  $\gamma$ -rays emitted by the radionuclide source. These data are represented as a piecewise linear calibration curve across the range of image densities seen in clinical CT scans (eg from -1000 to +2000 HU). Typically, the calibration curve is represented as a piecewise bilinear fit in which has different slopes below 0 HU representing regions which are combinations of air and soft tissue and above 0 HU representing regions which are composed of soft-tissue and bone (Figure 5). The resulting curve is used to convert values in the patient's CT scan from Hounsfield units to those representing the linear attenuation coefficient (ie cm<sup>-1</sup>) for each CT image pixel. The resulting tomographic image of linear attenuation coefficients (ie commonly known as an "attenuation (or  $\mu$ ) map") then can be incorporated into an iterative reconstruction algorithm to correct the radionuclide tomogram (ie SPECT or PET image) for errors due to photon attenuation. If only used to correct the radionuclide image for photon attenuation, the CT data can be acquired with a considerably lower statistical quality and coarser spatial resolution than required for diagnostic-quality imaging and therefore can deliver significantly lower dose than that for a diagnostic CT study. However, if improved signal-to-noise performance is needed for direct anatomical diagnosis of the CT scan at higher spatial resolution, including the use of iodine contrast, the anatomical image must be acquired with a diagnostic CT system with a conventional, albeit high, CT radiation dose and spatial resolution.

### Patient Table Design

SPECT/CT systems ideally would be designed with all of the radionuclide and x-ray imaging components placed around a common field of view. However, as noted above, the primary x-ray beam used to form the CT image can produce x-ray scatter fluence rate significantly higher than that emitted by the radiopharmaceutical administered to the patient for the emission image. For this reason, modern SPECT/CT (and PET/CT) systems typically separate the imaging planes of the x-ray source and the radionuclide distance by an axial distance of 50 cm or more. This physical separation prevents the primary x-ray beam from striking the radionuclide detectors and minimizes the magnitude of x-ray cross-scatter and related perturbations in the acquisition of radionuclide data of modern SPECT/CT cameras. This requires a patient table that can support the patient while extended between the CT scanner and SPECT sub-system without sagging under the patient's weight and without otherwise vertically displacing the patient between the SPECT and CT imaging positions. As a result, the patient table must be designed with minimal sag while extended for imaging with the SPECT/CT system. Often, table deflection is minimized by supporting the table on



both ends in a way that allows the acquired SPECT and CT data to be spatially correlated and co-registered in a consistent way.

## Applications and Capabilities of SPECT/CT

### Image Quality in SPECT/CT

Over the past decade, the introduction of SPECT/CT coincided with advances in computing power and iterative reconstruction algorithms and these have led to significant improvements in SPECT image quality obtained. The details of iterative reconstruction in radionuclide imaging have been discussed widely in the scientific literature and will not be repeated here. However, iterative reconstruction methods such as maximum-likelihood expectation-maximization (ML-EM) [71,72] and ordered-subset expectation-maximization (OS-EM) [73-75] offer benefits by allowing incorporation of mathematical models for physical effects [76] that can introduce errors into the SPECT data. These include photon attenuation [50,77], depth-dependent spatial resolution loss (also known as the “geometrical response”) of the radionuclide collimator, and scatter [78-81]. Use of iterative reconstruction for correction of photon attenuation requires an attenuation map derived by transmission imaging with an external radionuclide transmission source or with transmission x-ray imaging with SPECT/CT. X-ray transmission imaging in SPECT/CT also provides a patient-specific map of Compton coefficients that can be used for model-based scatter estimation [78-81] to compensate the radionuclide data for scatter. A final method of improving image quality models the geometrical configuration of the radionuclide collimator (ie including parallel-hole or pinhole collimators) that corrects the SPECT for the geometrical response of the collimator [82-85]. These compensation methods are becoming common for improving the spatial resolution, contrast, and signal-to-noise characteristics of SPECT imaging, including those obtained with SPECT/CT (Figure 6).

### Quantitative Accuracy with SPECT/CT

SPECT increasingly is used to quantify the uptake of the radiopharmaceutical in a tumor, the myocardium, or other target region. Typically, this is done by defining volumes-of-interest (Ovis) around the target region to integrate the number of events (ie or counts), assumed to be proportional to the activity in the volume thus defined. The activity (ie in units of MBq or mCi) then is calculated using a calibration factor obtained by imaging a phantom containing a known concentration of the same radionuclide as the radiopharmaceutical used to image the patient. However, as noted, the quantitative accuracy of radionuclide measurements with SPECT can be compromised by several physical factors, attenuation [20,21,35,76,86] and scatter [87-92]. In addition, the quantitative accuracy of SPECT can be compromised by partial-volume errors [93]. That is, the spatial resolution of the radionuclide imaging system causes “spill-out” of radioactivity (ie counts) from the target region into the background and “spill-in” of counts from the background into the target region. These errors are inherent to radionuclide imaging but can be compensated using patient-specific information derived from CT in a SPECT/CT scanner. For example, radionuclide data can be compensated for errors from photon attenuation and scatter radiation [82,94-96] using patient-specific images or “maps” of linear attenuation coefficients derived from CT. When correlated CT data are available, they also can be used to define the size and shape of target regions, and thereby compensate the image of the apparent distribution of activity for partial volume errors caused by the finite spatial resolution of the radionuclide imaging system [32]. Therefore, while it often is noted in the scientific literature that SPECT is not quantitative [97-100] and suffers both accuracy and precision errors, it increasingly is being recognized that SPECT/CT with appropriate reconstruction algorithms can compensate the radionuclide data for photon attenuation, partial volume errors, and scatter radiation [29,76,82,94-96,101] in a

way that significantly improves the accuracy of radionuclide quantitation in comparison to measurements obtained with SPECT alone.

Koral, et al, [31,102] have used correlated SPECT and CT data to quantify the radionuclide content of individual tumor regions. The study acquired SPECT and CT data from separate imaging systems that then were fused in software from patients with non-Hodgkin's lymphoma who were undergoing radioimmunotherapy with  $^{131}\text{I}$ -labeled monoclonal antibodies. The quantitation process used CT to derive patient-specific attenuation maps for attenuation correction and CT-defined tumor volumes to correct small (<200 g) tumors for partial-volume correction of the radionuclide data. The shape of the time-activity curve was derived from daily conjugate-view images of a tracer administration of the radiolabeled anti- $\text{B}_1$  antibody. This approach allows estimation of the radionuclide content and therefore the radiation dose delivered to individual tumors that could be resolved with CT but were not necessarily visualized on the conjugate-view scintigraphic images.

### Clinical Applications of SPECT/CT

SPECT/CT has been applied and its clinical benefits have been demonstrated across a wide spectrum of applications (Table 1), including both cardiovascular and oncologic imaging. Specifically, correlated CT data facilitate attenuation correction that improves both the contrast [103] and quantitative accuracy of radionuclide imaging performed with SPECT. Furthermore, SPECT/CT provides anatomical data to localize radiotracer uptake and facilitate SPECT diagnoses.

SPECT/CT is important for tumor imaging in terms of improving anatomical localization of disease, helping to define the extent of disease, and improving differentiation of physiological and pathological uptake [14,104-108]. This parallels the clinical experience with  $^{18}\text{F}$ -FDG PET and PET/CT imaging.

A role not commonly shared with PET and PET/CT involves the use of SPECT and SPECT/CT for analyzing radionuclide uptake and radiation dosimetry of tumor-specific SPECT agents in radioimmunotherapy [109-111]. In this setting, SPECT/CT has the potential to improve quantitative accuracy by facilitating the correction for photon attenuation and scatter radiation, as described above. Finally, as also noted above, the size and shape of target regions in the field of view can be quantified and used to correct partial-volume errors in the radionuclide data [30-32]. These methods offer the potential of improving quantitation of radionuclide uptake in and therefore radiation dosimetry of tumor, bone marrow [112], and other normal sites as well as in the targeted tumors in radioimmunotherapy. In addition, the use of the SPECT/CT offers the possibility of calculating patient-specific radiation dose estimates using anatomical information from CT [27,113], rather than relying on generalized anatomic models (such as those used in the Medical Internal Radionuclide Dosimetry (MIRD) formalism).

Myocardial perfusion imaging is a particularly important clinical application of SPECT and therefore is a special focus for SPECT/CT, where a correlated CT-derived map of patient-specific linear attenuation coefficients used to correct the SPECT data for attenuation can potentially introduce false positive defects into the perfusion data. Figure 7 shows an example in which a patient with chest pain was referred for myocardial perfusion SPECT. SPECT data obtained without attenuation correction demonstrated an inferior-wall defect suggestive of right coronary artery disease and the patient was referred to coronary angiography. The SPECT data then were reconstructed with attenuation correction using a CT-derived patient-specific attenuation map obtained from SPECT/CT and were correctly interpreted as normal, as confirmed by the normal coronary angiographic results. A multi-center trial evaluating myocardial perfusion SPECT with  $^{99\text{m}}\text{Tc}$ -sestamibi or  $^{99\text{m}}\text{Tc}$ -



tetrofosmin stress imaging in 118 patients found that x-ray-derived attenuation correction obtained with SPECT/CT improved diagnostic interpretation, particularly in normal subjects using coronary angiography as the “gold standard” [114]. Beyond these capabilities for attenuation correction, SPECT/CT with high-performance CT offers the potential for CT coronary angiography that be fused with myocardial imaging performed with SPECT/CT [115-117] or with CT-derived measurements of ventricular function [118,119] as well as the potential to correlate results of radionuclide myocardial perfusion imaging correlated with CT coronary calcium scoring [120]. The latter has been shown to increase the sensitivity of SPECT for detection of coronary artery disease without any significant decrease in specificity. Eventually, it may be possible to use these capabilities to quantify regional myocardial radionuclide uptake and regional myocardial perfusion noninvasively with SPECT/CT [29].

While SPECT with CT-derived attenuation correction can improve the sensitivity, specificity, and diagnostic accuracy of myocardial perfusion imaging [121,122] versus conventional techniques, the accuracy of the results can be affected by registration errors, which are reduced but not eliminated with dual-modality imaging. Specifically, patient motion, including that from respiration and cardiac contraction, during image acquisition can spatially offset the emission and transmission data (Figure 8) and lead to false-positive perfusion defects and other artifacts in the reconstructed SPECT images [67,123]. For example, Tonge et al [63] reconstructed  $^{99m}\text{Tc}$ -tetrofosmin SPECT data with x-ray derived attenuation correction. They found that the SPECT data reconstructed from attenuation maps taken directly from the SPECT/CT study contained perfusion defects in the apex and anterior wall, which subsequently were reduced when corrected for registration errors. Furthermore, attenuation corrections reduced the presence of defects in the inferior wall, but were not significantly improved by application of registration correction.

Both phantom and patient studies have shown that spatial displacements between the emission and transmission data of more than 1 pixel (measured in the SPECT image) can compromise the quality of the emission data reconstructed with attenuation correction [60,124]. In one study, Fricke et al [62] found that 27 of 140 patients undergoing  $^{99m}\text{Tc}$ -sestamibi SPECT demonstrated pronounced defects in the apical or anterior wall following CT-based attenuation correction. Of the original 27 studies with artifacts, improved co-registration produced normal perfusion patterns in 6 and reduced the presence and severity of defects in 15. No improvement was seen in only 4 of 27 patients; in these studies, the mismatch was less than 1 pixel (7 mm) in the ventro-dorsal direction along which co-registration correction was applied, but had spatial mismatches in the craniocaudal direction which were not corrected [62]. In a separate study with 60 consecutive patients, Goetze et al, found that 42% of the CT attenuation-corrected images had moderate to severe misregistration errors in the SPECT/CT data when evaluated qualitatively [61]. Goetze et al [60] also quantified the spatial mismatch of emission-transmission data from 105 consecutive patients acquired with SPECT/CT and found that 64% of studies exhibited spatial misregistration of 1 pixel or greater. Furthermore, they found significant differences in the segmental distribution of radiotracer distribution between the SPECT images reconstructed prior to and following spatial registration. Software-based methods also have been used to improve anatomical registration of SPECT/CT data and to thereby improve diagnostic evaluation of attenuation-corrected myocardial perfusion SPECT [125] as well as SPECT correlation with CT coronary angiography [116,126]. These techniques have been reported to be feasible and reproducible in demonstrating improved diagnostic evaluation of myocardial perfusion imaging with SPECT/CT and for confirming as well as excluding the functional significance of lesions found with CT coronary angiography [116,126]. While the results to date are preliminary, they point to the need to verify and correct, if possible, the

spatial misregistration of the SPECT image and the CT-based attenuation map and other anatomical information obtained from a SPECT/CT system.

## Current SPECT/CT Technologies

The clinical use of dual-modality imaging began with the commercial introduction of SPECT/CT in 1999 and of PET/CT in 2000, and is continuing to advance rapidly, with approximately 2000 PET/CT systems and almost 1000 SPECT/CT systems currently in use worldwide. An annotated list of clinically approved SPECT/CT systems, as of May 2006, is available on-line<sup>1</sup>. The first commercial SPECT/CT system, the GE Discovery VG Hawkeye, was introduced in 1999 and was based on a GE Discovery VG SPECT system, (designed and introduced originally as the Elscint Varicam), a dual-head variable-geometry SPECT system capable of performing planar scintigraphy, SPECT, and <sup>18</sup>F-fluorodeoxyglucose (FDG) coincidence imaging. The x-ray sub-system originally was planned by Elscint but was not released until integrated with the GE Discovery VG with the "Hawkeye option", an x-ray source operated at 140 kV and 2.5 mA and an x-ray detector operated with a slip ring for continuous-rotation CT acquisition. The Hawkeye sub-system acquires x-ray transmission data with a rotation time of 20 seconds with 2.5 mm in-plane resolution and a slice width of 1-cm or 2.5-mm for one- or four-slice configuration, respectively. The current SPECT/CT system from General Electric Healthcare now has been upgraded as the GE Infinia Hawkeye (Figure 9a). Like the Discovery VG Hawkeye, the Infinia Hawkeye SPECT/CT system incorporates an x-ray source with significantly lower power than a conventional diagnostic CT scanners (which operate at 120-140 kV, 500 mA, and 0.4-s (or faster) rotation speed). Although these first-generation SPECT/CT systems are relatively limited in their spatial resolution, scan speed, and signal-to-noise performance of their CT sub-systems, overall they are well-suited in terms of cost and performance to addressing the needs of attenuation correction and low-resolution anatomical localization and provide useful information that improves diagnostic accuracy compared to SPECT scans alone.

SPECT/CT systems with advanced CT capabilities were introduced in 2004 and now are being adopted in clinical practice. These systems, such as the Siemens Symbia [127] (Figure 9b) and the Philips Precedence (Figure 9c), typically match a dual-head SPECT system with a multi-slice CT scanner having performance similar to that obtained with conventional diagnostic CT (Table 2). The Siemens Symbia is also available with a single-slice low-resolution CT scan for attenuation correction and anatomical mapping or with a diagnostic 2-, 6-, or 16-slice CT. Similarly, the Precedence SPECT/CT system from Philips is available with a 6- or 16 slice CT capability. Both the low- and high-power CT systems available from the commercial vendors can be used to perform attenuation correction and anatomical localization of the radionuclide data suitable for myocardial perfusion measurements, tumor imaging (Figure 10), and other radionuclide studies. However, the improved signal-to-noise characteristics and multi-slice capability of the higher-power CT systems offer detailed anatomical information with improved spatial resolution, excellent soft-tissue contrast enhancement [128]. These characteristics are especially suitable for oncology [14,104-108] where detailed anatomical localization is needed. Other investigators have reported using the higher-performance SPECT/CT systems for applications in orthopedics [129-132], infection and inflammation [133-138], pulmonary function [139,140], and endocrinology[141], where the improved anatomical localization helps identify areas of disease that can be difficult to discriminate with SPECT alone. As previously mentioned, high-resolution CT performance

<sup>1</sup>[http://www.advanceforioa.com/sharedresources/advanceforioa/resources/DownloadableResources/AR50106\\_p58ChartSmart.pdf](http://www.advanceforioa.com/sharedresources/advanceforioa/resources/DownloadableResources/AR50106_p58ChartSmart.pdf)



also can be used to define target anatomy to improve the quantitation of absolute radionuclide uptake in small lesions such as tumors or in the myocardium.

Finally, a SPECT/CT system with cardiac and coronary CT capability is likely to be well-matched to myocardial perfusion radionuclide measurements, which still account for almost 50% of SPECT imaging. SPECT/CT systems are now available with 64-slice CT subsystems, capable of ultra-short scan times which “freeze” cardiac motion as required for CT coronary angiography [115,116,126] and calcium scoring [142] (Figure 11). The high-performance SPECT/CT systems also have the potential for absolute quantitation of radionuclide content [29] with corrections for photon attenuation, scatter radiation, and partial-volume errors in a way that could offer accurate non-invasive assessment of regional myocardial blood flow and coronary flow reserve. These capabilities are just beginning to emerge, but are likely to be developed and tested as the capabilities and performance of SPECT/CT mature.

### Future Developments in SPECT/CT

The scintillation camera technology currently in use for clinical studies still relies on the technology invented by Hal Anger in 1957 [143]. Nevertheless, SPECT and SPECT/CT is continuing to evolve with the introduction of new technologies that have the potential to improve performance beyond that possible with Anger's pioneering approach. Recent advances in detector technology that incorporate silicon photodiode or solid-state materials offer the potential for improved spatial resolution and energy resolution, with greater stability and more compact size [144-148], compared to conventional camera designs based on photomultiplier tube technology. At this early stage in their development, the use of solid-state and semiconductor detectors has focused on imaging of the heart [145,148], breast [149], and other small organs [150]. Nevertheless, it is likely that as these newer detector technologies will mature, they will become more robust in performance and cost-effectiveness and therefore eventually replace the photomultiplier tube in radionuclide imaging detectors.

### Innovative SPECT/CT Designs for Cardiac Imaging

A SPECT protocol for myocardial perfusion imaging can consume 2.5 hours or more in procedure time, including 40-50 minutes of camera time, (longer if soft-tissue attenuation is suspected and the patient is imaged with prone positioning) [151-153]. Recently, myocardial perfusion cameras have been developed with novel detector and collimator geometries that significantly improve detection efficiency while maintaining or improving spatial resolution for myocardial perfusion imaging in comparison to conventional scintillation camera designs. For example, dedicated nuclear cardiology cameras have been developed by Spectrum Dynamics, Ltd.<sup>2</sup> (Caesarea, Israel) and by Cardiac, Inc.<sup>3</sup> (Canton, MI) and are designed to acquire myocardial perfusion images in only 2 to 3 minutes (Figure 12) versus the 10 to 15 minutes needed with conventional dual-head SPECT systems. Similar performance now is being reported as a works-in-progress (as of 2007) with a new myocardial SPECT camera developed by GE Healthcare. These new instruments offer significant advantages over conventional SPECT/CT systems in which an expensive CT scanner remains idle while the slow SPECT scan is completed. The inclusion of a highly efficient SPECT system can decrease the scan time of the SPECT study, and in doing so also increases the utilization of CT and patient throughput compared to conventional SPECT/CT systems. The clinical procedure includes 5-6 minutes needed to acquire the correlated

<sup>2</sup><http://www.spectrum-dynamics.com/>

<sup>3</sup><http://www.cardiac.com/>

radionuclide and x-ray data with an efficient SPECT camera plus a modern multi-slice CT system versus the 20-25 minutes required with conventional SPECT technology. The total procedure will be lengthened for acquiring both rest and stress myocardial perfusion data, between which the patient typically leaves the imaging system for administration of the radiopharmaceutical for the second perfusion scan. However, significant reductions in scan time would be obtained if the rest/stress images were obtained with simultaneous dual-isotope imaging in which, for example, the patient first was administered  $^{201}\text{Tl}$  at rest followed immediately by exercise or pharmacological stress after which the patient would be injected with the  $^{99\text{m}}\text{Tc}$  perfusion agent for the stress perfusion study. If the imaging system included a high-performance CT scanner, the radionuclide imaging studies could be followed immediately by CT coronary angiography [115,116,126] and assessment of coronary calcification [142]. It is conceivable that the volumetric CT data also could quantify myocardial thickness to improve the measurement of radionuclide uptake in the myocardium [29]. Both CT coronary angiography and quantitation of myocardial perfusion are illustrative the potential for a high-performance myocardial SPECT/CT with a fast and cost-effective acquisition protocol.

### Innovative Breast Imaging with SPECT/CT

Tornai et al [154-157] at Duke University are developing a compact dual-modality SPECT/CT system for dedicated tomographic imaging of the pendant, uncompressed female breast. A prototype system is designed to perform SPECT with a 1.620-cm<sup>2</sup> CZT-based compact gamma camera having 2.5-mm pixels that allow flexible angular positioning with a goniometer. This dual-modality breast imager also includes a flat-panel digital detector coupled to a CsI(Tl) phosphor to perform CT with a quasi-monoenergetic x-ray cone-beam produced with a heavily-filtered tungsten anode. The CT system has a stationary polar orientation and is laterally offset from the center of rotation for imaging pendant, uncompressed breasts that are larger than the detector's field of view. Both the x-ray and radionuclide sub-systems are coupled to a common rotation stage and have a common field of view. As independent systems, both dedicated SPECT and CT have yielded visualization of small lesions in the breast, including those located close to the chest wall [154,158-160]. Results from the combined system show that emission projection images can be contaminated by x-ray scatter photons that artifactually increase the apparent signal in reconstructed emission images. Emission contamination also can increase noise in the transmission image resulting in reduced signal-to-noise ratios in reconstructed CT images. Nevertheless, measurements with the combined system components show that optimal placement of the SPECT and CT sub-systems is limited by physical constraints rather than signal cross-contamination that can occur with a SPECT/CT system that shares a common field of view. Overall, integrating both modalities on a single gantry is designed to simplify data acquisition, SPECT-CT image registration, and necessary image corrections with the goals of correlating radionuclide uptake with anatomical structure, improving detection and staging of cancer, monitoring treatment response, and improving selection of surgical biopsy sites.

### Concluding Remarks

As we emerge from the first decade of the clinical use of SPECT/CT, several challenges still remain. First, unlike PET/CT, which has essentially replaced PET-only systems commercially, SPECT/CT has not achieved comparable commercial dominance over conventional SPECT. This likely is due in part to the clinical flexibility of SPECT, which is used for a wide spectrum of clinical applications with different radiopharmaceuticals. This is a decidedly different situation than that with PET and PET/CT, which are used predominantly for tumor imaging with  $^{18}\text{F}$ -fluorodeoxyglucose. Secondly, as noted above, SPECT/CT suffers an imbalance in cost-effectiveness due to the differences in acquisition



time between SPECT and modern CT. However, as also noted above, advances in SPECT instrumentation, CT technology, and radiopharmaceutical development have the potential to advance SPECT/CT beyond its current level of performance. Potential clinical applications of SPECT/CT are numerous and include more efficient studies of myocardial perfusion imaging with the potential for correlation with CT coronary angiography. CT also has the potential to provide anatomically guided partial-volume correction for absolute quantitation of tumor uptake and dosimetry of tumor-specific agents with an accuracy not achievable using SPECT alone. SPECT/CT also has the potential to advance imaging application in infectious diseases, orthopedics, neurology, and breast cancer. Finally, on the horizon, is the potential for SPECT imaging with new tumor-specific agents now entering clinical trials. Given these characteristics and potential applications, it is likely that the clinical use of SPECT/CT will expand, becoming an increasingly important tool in diagnostic imaging for a wide spectrum of disease.

## Acknowledgments

The authors gratefully acknowledge support from Grants 1 R21 HL083073, 5 R21 EB006373, 5 K25 CA114254, 5 R01 EB000288, 2 R44 CA095936, 4 R44 EB001685, 2 R44 H083494, 2 R44 ES012361, and 1 R41 AG030241 from the National Institutes of Health, Grant FG02-07ER84903 from the Department of Energy, Grants dig04-10174 and dig06-10210 from the UC Discovery Grant Program, Grant A107695 from the University of California, Berkeley, Award number 02821-6 from the Thrasher Research Fund, and from General Electric Healthcare, Inc., Philips Medical Systems, Inc., Siemens Medical Solutions, Inc., and Radiation Monitoring Devices.

## References

1. Cherry, SR.; Sorenson, JA.; Phelps, ME. Physics in Nuclear Medicine. Philadelphia: Saunders; 2003.
2. Jaszczyk RJ, Coleman RE, Lim CB. SPECT: Single photon emission computed tomography. IEEE Tran Nucl Sci 1980;NS-27:1137–1153.
3. Loats H. CT and SPECT image registration and fusion for spatial localization of metastatic processes using radiolabeled monoclonals. J Nucl Med 1993;34:562–566. [PubMed: 8441058]
4. Maintz JB, Viergever MA. A survey of medical image registration. Med Image Anal 1998;2:1–36. [PubMed: 10638851]
5. Hill DL, Batchelor PG, Holden M, Hawkes DJ. Medical image registration. Phys Med Biol 2001;46:R1–45. [PubMed: 11277237]
6. Hutton BF, Braun M, Thurfjell L, Lau DYH. Image registration: an essential tool for Nuclear Medicine. Eur J Nucl Med Mol Imaging 2002;29:559–577. [PubMed: 11914898]
7. Kessler ML. Image registration and data fusion in radiation therapy. Br J Radiol 2006;79(Spec No 1):S99–108. [PubMed: 16980689]
8. Gholipour A, Kehtarnavaz N, Briggs R, Devous M, Gopinath K. Brain functional localization: A survey of image registration techniques. IEEE Tran Med Imag 2007;26:427–451.
9. Barratt DC, Penney GP, Chan CS, Slomczykowski M, Carter TJ, Edwards PJ, Hawkes DJ. Self-calibrating 3D-ultrasound-based bone registration for minimally invasive orthopedic surgery. IEEE Trans Med Imaging 2006;25:312–23. [PubMed: 16524087]
10. Ma B, Ellis RE. Robust registration for computer-integrated orthopedic surgery: laboratory validation and clinical experience. Med Image Anal 2003;7:237–50. [PubMed: 12946466]
11. Pietrzyk U. Does PET/CT render software registration obsolete? Nuklearmedizin 2005;44 1:S13–7. [PubMed: 16395973]
12. Hasegawa BH, Wong KH, Iwata K, Barber WC, Hwang AB, Sakdinawat AE, Ramaswamy M, Price DC, Hawkins RA. Dual-modality imaging of cancer with SPECT/CT. Technol Cancer Res Treat 2002;1:449–58. [PubMed: 12625772]
13. Townsend DW, Beyer T. A combined PET/CT scanner: the path to true image fusion. Brit J Radiol 2002;75:S24–S30. [PubMed: 12519732]

14. Keidar Z, Israel O, Krausz Y. SPECT/CT in tumor imaging: technical aspects and clinical applications. *Semin Nucl Med* 2003;33:205–18. [PubMed: 12931322]
15. Schillaci O, Simonetti G. Fusion imaging in Nuclear Medicine--applications of dual-modality systems in oncology. *Cancer Biother Radiopharm* 2004;19:1–10. [PubMed: 15068606]
16. Townsend DW, Yap JT, Carney JP, Hall NC. Developments in PET/CT: From concept to practice. *Med Phys* 2004;31(abst):1694.
17. Schillaci O. Hybrid SPECT/CT: a new era for SPECT imaging? *Eur J Nucl Med Mol Imaging* 2005;32:521–4. [PubMed: 15747153]
18. von Schulthess GK, Steinert HC, Hany TF. Integrated PET/CT: current applications and future directions. *Radiology* 2006;238:405–22. [PubMed: 16436809]
19. Tagliabue L, Schillaci O. SPECT/CT in oncology: the fusion of two imaging modalities is a new standard of care. *Q J Nucl Med Mol Imaging* 2007;51:285–9. [PubMed: 17923823]
20. LaCroix KJ, Tsui BMW, Hasegawa BH, Brown JK. Investigation of the use of x-ray CT images for attenuation correction in SPECT. *IEEE Trans Nucl Sci* 1994;41:2793–2799.
21. Blankespoor SC, Wu X, Kalki K, Brown JK, Tang HR, Cann CE, Hasegawa BH. Attenuation correction of SPECT using x-ray CT on an emission-transmission CT system: Myocardial perfusion assessment. *IEEE Trans Nucl Sci* 1996;43:2263–2274.
22. Kinahan PE, Townsend DW, Beyer T, Sashin D. Attenuation correction for a combined 3D PET/CT scanner. *Med Phys* 1998;25:2046–2053. [PubMed: 9800714]
23. Kinahan PE, Hasegawa BH, Beyer T. X-ray-based attenuation correction for position tomography/computed tomography scanners. *Semin Nucl Med* 2003;33:166–179. [PubMed: 12931319]
24. Munley MT, Marks LB, Scarfone C, Sibley GS, Patz EF Jr, Turkington TG, Jaszczak RJ, Gilland DR, Anscher MS, Coleman RE. Multi-modality Nuclear Medicine imaging in three-dimensional radiation treatment planning for lung cancer: challenges and prospects. *Lung Cancer* 1999;23:105–14. [PubMed: 10217614]
25. Paulino AC, Thorstad WL, Fox T. Role of fusion in radiotherapy treatment planning. *Semin Nucl Med* 2003;33:238–243. [PubMed: 12931325]
26. Ellis RJ, Kaminsky DA. Fused radioimmunoscinigraphy for treatment planning. *Rev Urol* 2006;8 1:S11–9. [PubMed: 17021622]
27. Prideaux AR, Song H, Hobbs RF, He B, Frey EC, Ladenson PW, Wahl RL, Sgouros G. Three-dimensional radiobiologic dosimetry: application of radiobiologic modeling to patient-specific 3-dimensional imaging-based internal dosimetry. *J Nucl Med* 2007;48:1008–16. [PubMed: 17504874]
28. Liu A, Williams LE, Raubitschek AA. A CT assisted method for absolute quantitation of internal radioactivity. *Med Phys* 1996;23:1919–1228. [PubMed: 8947907]
29. Da Silva AJ, Tang HR, Wong KH, Wu MC, Dae MW, Hasegawa BH. Absolute quantitation of regional myocardial uptake of  $^{99m}\text{Tc}$ -sestamibi with SPECT: experimental validation in a porcine model. *J Nucl Med* 2001;42:772–779. [PubMed: 11337575]
30. Koral KF, Zasadny KR, Kessler ML, Luo JQ, Buchbinder SF, Kaminski MS, Francis I, Wahl RL. CT-SPECT fusion plus conjugate views for determining dosimetry in iodine-131-monoclonal antibody therapy of lymphoma patients. *J Nucl Med* 1994;35:1714–1720. [PubMed: 7931676]
31. Koral KF, Dewaraja Y, Li J, Barrett CL, Regan DD, Zasadny KR, Rommelfanger SG, Francis IR, Kaminski MS, Wahl RL. Initial results for Hybrid SPECT--conjugate-view tumor dosimetry in  $^{131}\text{I}$ -anti-B1 antibody therapy of previously untreated patients with lymphoma. *J Nucl Med* 2000;41:1579–86. [PubMed: 10994741]
32. Tang HR, Da Silva AJ, Matthay KK, Price DC, Huberty JP, Hawkins RA, Hasegawa BH. Neuroblastoma imaging using a combined CT scanner-scintillation camera and I-131 MIBG. *J Nucl Med* 2001;42:237–247. [PubMed: 11216522]
33. Kuhl DE, Hale J, Eaton WL. Transmission scanning: A useful adjunct to conventional emission scanning for accurately keying isotope deposition to radiographic anatomy. *Radiology* 1966;87:278–284. [PubMed: 5915433]
34. Bailey DL, Hutton BF, Walker PJ. Improved SPECT using simultaneous emission and transmission tomography. *J Nucl Med* 1987;28:844–851. [PubMed: 3494829]



35. Tsui BMW, Gullberg GT, Edgerton ER, Ballard JG, Perry JR, McCartney WH, Berg J. Correction of nonuniform attenuation in cardiac SPECT imaging. *J Nucl Med* 1989;30:497–507. [PubMed: 2786944]
36. Huang SC, Hoffman EJ, Phelps ME, Kuhl DE. Quantitation in positron emission computed tomography: 2. Effects of inaccurate attenuation correction. *J Comput Assist Tomogr* 1979;3:804–14. [PubMed: 315970]
37. Carson RE, Daube-Witherspoon ME, Green MV. A method for postinjection PET transmission measurements with a rotating source. *J Nucl Med* 1988;29:1558–67. [PubMed: 3261786]
38. Bocher M, Balan A, Krausz Y, Shrem Y, Lonn A, Wilk M, Chisin R. Gamma camera-mounted anatomical x-ray tomography: technology, system characteristics, and first images. *Eur J Nucl Med* 2000;27:619–627. [PubMed: 10901447]
39. Townsend DW, Carney JP, Yap JT, Hall NC. PET/CT today and tomorrow. *J Nucl Med* 2004;45:14S–14S. [PubMed: 14736831]
40. Shao Y, Cherry SR, Farahani K, Meadors K. Simultaneous PET and MR imaging. *Phys Med Biol* 1997;42:1965–1970. [PubMed: 9364592]
41. Pichler BJ, Judenhofer MS, Catana C, Walton JH, Kneilling M, Nutt RE, Siegel SB, Claussen CD, Cherry SR. Performance test of an LSO-APD detector in a 7-T MRI scanner for simultaneous PET/MRI. *J Nucl Med* 2006;47:639–47. [PubMed: 16595498]
42. Wagenaar D, Nalcioğlu O, Muftuler L, Meier D, Parnham K, Szawlowski M, Kapusta M, Azman S, Gjaerum J, Maehlum G, Wang Y, Tsui B, Patt BE. A multi-ring small animal CZT system for simultaneous SPECT/MRI imaging. *J Nucl Med* 2007;48(Suppl 2):89P.
43. Mirshanov, DM. Transmission-Emission Computer Tomograph. Tashkent Branch, All-Union Research Surgery Center, USSR Academy of Medical Science; USSR: 1987.
44. Kaplan, CH. Transmission/emission registered image (TERI) computed tomography scanners. International patent application PCT/US90/03722. 1989.
45. Hasegawa BH, Reilly SM, Gingold EL, Cann CE. Design considerations for a simultaneous emission-transmission CT scanner. *Radiology* 1989;173(P):414.
46. Hasegawa BH, Gingold EL, Reilly SM, Liew SC, Cann CE. Description of a simultaneous emission-transmission CT system. *Proc SPIE* 1990;1231:50–60.
47. Gutknecht D. Photomask technique for fabricating high purity germanium detectors. *Nucl Instr and Meth* 1990;288:13–18.
48. Hasegawa BH, Stebler B, Rutt BK, Martinez A, Gingold EL, Barker CS, Faulkner KG, Cann CE, Boyd DP. A prototype high-purity germanium detector system with fast photon-counting circuitry for medical imaging. *Med Phys* 1991;18:900–9. [PubMed: 1961152]
49. Kalki K, Heanue JA, Blankespoor SC, Wu X, Brown JK, Cann CE, Hasegawa BH, Carver JA, Dae MW, Chin M, Stillson C. A combined SPECT and CT medical imaging system. *Proc SPIE* 1995;2432:367–375.
50. Kalki K, Blankespoor SC, Brown JK, Hasegawa BH, Dae MW, Chin M, Stillson C. Myocardial perfusion imaging with a combined x-ray CT and SPECT system. *J Nucl Med* 1997;38:1535–1540. [PubMed: 9379188]
51. Wu X, Brown JK, Kalki K, Hasegawa BH. Characterization and correction of pulse pile-up in simultaneous emission-transmission computed tomography. *Med Phys* 1996;23:569–575. [PubMed: 9157271]
52. Boles CD, Boser BE, Hasegawa BH, Heanue JA. A multimode digital detector readout for solid-state medical imaging detectors. *IEEE J Solid-State Circuits* 1998;33:733–742.
53. Heanue, JA. Department of Electrical Engineering and Computer Science. University of California; Berkeley, CA: 1996. Detector and electronics design considerations for an emission-transmission medical imaging system.
54. Heanue JA, Boser BE, Hasegawa BH. CMOS detector readout electronics for an emission-transmission imaging system. *IEEE Trans Nucl Sci* 1995;42:1133–1138.
55. Birch, R.; Marshall, M.; Adran, GM. Catalogue of spectral data for diagnostic x-rays. London: Hospital Physicists Association; 1979.
56. Rosenbaum SJ, Lind T, Antoch G, Bockisch A. False-positive FDG PET uptake--the role of PET/CT. *Eur Radiol* 2006;16:1054–65. [PubMed: 16365730]

57. Strauss LG. Fluorine-18 deoxyglucose and false-positive results: a major problem in the diagnostics of oncological patients. *Eur J Nucl Med* 1996;23:1409–15. [PubMed: 8781149]
58. Schettino CJ, Kramer EL, Noz ME, Taneja S, Padmanabhan P, Lepor H. Impact of fusion of indium-111 capromab pendetide volume data sets with those from MRI or CT in patients with recurrent prostate cancer. *AJR Am J Roentgenol* 2004;183:519–24. [PubMed: 15269050]
59. Schillaci O. Functional-anatomical image fusion in neuroendocrine tumors. *Cancer Biother Radiopharm* 2004;19:129–34. [PubMed: 15068621]
60. Goetze S, Brown TL, Lavelly WC, Zhang Z, Bengel FM. Attenuation correction in myocardial perfusion SPECT/CT: effects of misregistration and value of reregistration. *J Nucl Med* 2007;48:1090–5. [PubMed: 17574985]
61. Goetze S, Wahl RL. Prevalence of misregistration between SPECT and CT for attenuation-corrected myocardial perfusion SPECT. *J Nucl Cardiol* 2007;14:200–6. [PubMed: 17386382]
62. Fricke H, Fricke E, Weise R, Kammeier A, Lindner O, Burchert W. A method to remove artifacts in attenuation-corrected myocardial perfusion SPECT introduced by misalignment between emission scan and CT-derived attenuation maps. *J Nucl Med* 2004;45:1619–25. [PubMed: 15471824]
63. Tonge CM, Ellul G, Pandit M, Lawson RS, Shields RA, Arumugam P, Prescott MC. The value of registration correction in the attenuation correction of myocardial SPECT studies using low resolution computed tomography images. *Nucl Med Commun* 2006;27:843–52. [PubMed: 17021423]
64. O'Connor MK, Kemp B, Anstett F, Christian P, Ficaro EP, Frey E, Jacobs M, Kritzman JN, Pooley RA, Wilk M. A multicenter evaluation of commercial attenuation compensation techniques in cardiac SPECT using phantom models. *J Nucl Cardiol* 2002;9:361–76. [PubMed: 12161711]
65. Wackers FJT. Attenuation compensation of cardiac SPECT: a critical look at a confusing world. *J Nucl Cardiol* 2002;9:438–40. [PubMed: 12161721]
66. Romer W, Fiedler E, Pavel M, Pfahlberg A, Hothorn T, Herzog H, Bautz W, Kuwert T. Attenuation correction of SPECT images based on separately performed CT: Effect on the measurement of regional uptake values. *Nuklearmedizin* 2005;44:20–8. [PubMed: 15711725]
67. Takahashi Y, Murase K, Higashino H, Mochizuki T, Motomura N. Attenuation correction of myocardial SPECT images with X-ray CT: effects of registration errors between X-ray CT and SPECT. *Ann Nucl Med* 2002;16:431–435. [PubMed: 12416584]
68. Herman GT. Correction for beam hardening in computed tomography. *Phys Med Biol* 1979;24:81–106. [PubMed: 432276]
69. Kijewski PK, Bjarnagard BE. Correction for beam hardening in computed tomography. *Med Phys* 1978;5:209–14. [PubMed: 672814]
70. Hwang AB, Taylor CC, VanBrocklin HF, Dae MW, Hasegawa BH. Attenuation correction of small animal SPECT images acquired with 125I-iodorotone. *IEEE Tran Nucl Sci* 2006;53:1213–1220.
71. Lange K, Carson R. EM reconstruction algorithms for emission and transmission tomography. *J Comput Assist Tomogr* 1984;8:306–316. [PubMed: 6608535]
72. Shepp LA, Vardi Y. Maximum likelihood reconstruction for emission tomography. *IEEE Trans Med Imag* 1982;MI-1:113–122.
73. Li J, Jaszczak RJ, Greer KL, Coleman RE. Implementation of an accelerated iterative algorithm for cone-beam SPECT. *Phys Med Biol* 1994;39:643–53. [PubMed: 15551605]
74. Hudson HM, Larkin RS. Accelerated image reconstruction using ordered subsets of projection data. *IEEE Trans Med Imag* 1994;13:601–609.
75. Romer W, Reichel N, Vija HA, Nickel I, Hornegger J, Bautz W, Kuwert T. Isotropic reconstruction of SPECT data using OSEM3D: correlation with CT. *Acad Radiol* 2006;13:496–502. [PubMed: 16554230]
76. Zeng GL, Gullberg GT, Tsui BMW, Terry JA. Three-dimensional iterative reconstruction algorithms with attenuation and geometric point response correction. *IEEE Trans Nucl Sci* 1991;38:693–701.



77. Gullberg GT, Huesman RH, Malko JA, Pelc NJ, Budinger TF. An attenuated projector-backprojector for iterative SPECT reconstruction. *Phys Med Biol* 1985;30:799–816. [PubMed: 3840265]
78. Beekman FJ, den Harder JM, Viergever MA, van Rijk PP. SPECT scatter modeling in nonuniform attenuating objects. *Phys Med Biol* 1997;42:1133–1142. [PubMed: 9194133]
79. Frey EC, Tsui BMW. A new method for modeling the spatially-variant, object-dependent scatter response function in SPECT. *IEEE Nucl Sci Symp Med Imag Conf Rec* 1996;2:1082–1086.
80. Larsson A, Johansson L, Sundstrom T, Riklund Ahlstrom K. A method for attenuation and scatter correction of brain SPECT based on computed tomography images. *Nucl Med Comm* 2003;24:411–420.
81. Meikle SR, Hutton BF, Bailey DL. A transmission-dependent method for scatter correction in SPECT. *J Nucl Med* 1994;35:360–7. [PubMed: 8295011]
82. Laurette I, Zeng GL, Welch A, Christian PE, Gullberg GT. A three-dimensional ray-driven attenuation, scatter and geometric response correction technique for SPECT in inhomogeneous media. *Phys Med Biol* 2000;45:3459–80. [PubMed: 11098917]
83. Beekman FJ, Slijpen ET, de Jong HW, Viergever MA. Estimation of the depth-dependent component of the point spread function of SPECT. *Med Phys* 1999;26:2311–22. [PubMed: 10587212]
84. Frey EC, Tsui BM, Gullberg GT. Improved estimation of the detector response function for converging beam collimators. *Phys Med Biol* 1998;43:941–50. [PubMed: 9572517]
85. Formiconi AR, Pupi A, Passeri A. Compensation of spatial system response in SPECT with conjugate gradient reconstruction technique. *Phys Med Biol* 1989;34:69–84. [PubMed: 2784572]
86. Ficaro EP, Fessler JA, Shreve PD, Kritzman JN, Rose PA, Corbett JR. Simultaneous transmission/emission myocardial perfusion tomography: Diagnostic accuracy of attenuation-corrected Tc-99m-sestamibi single-photon emission computed tomography. *Circulation* 1996;93:463–473. [PubMed: 8565163]
87. Jaszcak RJ, Greer KL, Floyd CE. Improved SPECT quantitation using compensation for scattered photons. *J Nucl Med* 1984;25:893–900. [PubMed: 6611390]
88. Koral KF, Wang X, Rogers WL, Clinthorne NH, Wang X. SPECT Compton-scattering correction by analysis of energy spectra. *J Nucl Med* 1988;29:195–202. [PubMed: 3258023]
89. Mukai T, Links JM, Douglass KH, Wagner HN. Scatter correction in SPECT using non-uniform attenuation data. *Phys Med Biol* 1988;33:1129–1140. [PubMed: 3264074]
90. Ljungberg M, Strand SE. Attenuation and scatter correction in SPECT for sources in a nonhomogeneous object: a Monte Carlo study. *J Nucl Med* 1991;32:1278–1284. [PubMed: 2045947]
91. Galt JR, Cullom SJ, Garcia EV. SPECT quantitation: A simplified method of attenuation and scatter correction for cardiac imaging. *J Nucl Med* 1992;33:2232–2237. [PubMed: 1460522]
92. Frey EC, Tsui BMW. Modeling the scatter response function in inhomogeneous scattering media for SPECT. *IEEE Trans Nucl Sci* 1994;41:1585–1593.
93. Kessler RM, Ellis JR, Eden M. Analysis of emission tomographic scan data: Limitations imposed by resolution and background. *J Comput Assist Tomogr* 1984;8:514–522. [PubMed: 6609942]
94. Ljungberg M, Strand S. Scatter and attenuation correction in SPECT using density maps and Monte Carlo simulated scatter functions. *J Nucl Med* 1990;31:1560–1567. [PubMed: 2395025]
95. Liang Z, Turkington TG, Gilland DR, Jaszcak RJ, Coleman RE. Simultaneous compensation for attenuation, scatter, and detector response for SPECT reconstruction in three dimensions. *Phys Med Biol* 1992;37:587–603. [PubMed: 1565692]
96. Seo Y, Wong KH, Sun M, Franc BL, Hawkins RA, Hasegawa BH. Correction of Photon Attenuation and Collimator Response for a Body-Contouring SPECT/CT Imaging System. *J Nucl Med* 2005;46:868–77. [PubMed: 15872362]
97. Germain P, Baruthio J, Roul G, Dumitresco B. First-pass MRI compartmental analysis at the chronic stage of infarction: myocardial flow reserve parametric map. *Computers in Cardiology* 2000;27:675–678.

98. Lewis DH, Bluestone JP, Savina M, Zoller WH, Meshberg EB, Minoshima S. Imaging cerebral activity in recovery from chronic traumatic brain injury: a preliminary report. *J Neuroimaging* 2006;16:272–7. [PubMed: 16808830]
99. Peters AM. Scintigraphic imaging of renal function. *Exp Nephrol* 1998;6:391–7. [PubMed: 9730654]
100. Sidoti C, Agrillo U. Chronic cortical stimulation for amyotrophic lateral sclerosis: a report of four consecutive operated cases after a 2-year follow-up: technical case report. *Neurosurgery* 2006;58:E384. discussion E384. [PubMed: 16462467]
101. Tsui BMW, Hu HB, Gilland DR, Gullberg GT. Implementation of simultaneous attenuation and detector response correction in SPECT. *IEEE Trans Nucl Sci* 1988;NS-35:778–783.
102. Koral KF, Dewaraja Y, Li J, Lin Q, Regan DD, Zasadny KR, Rommelfanger SG, Francis IR, Kaminski MS, Wahl RL. Update on hybrid conjugate-view SPECT tumor dosimetry and response in  $^{131}\text{I}$ -tositumomab therapy of previously untreated lymphoma patients. *J Nucl Med* 2003;44:457–464. [PubMed: 12621015]
103. Ruf J, Steffen I, Mehl S, Rosner C, Denecke T, Pape UF, Plotkin M, Amthauer H. Influence of attenuation correction by integrated low-dose CT on somatostatin receptor SPECT. *Nucl Med Commun* 2007;28:782–8. [PubMed: 17728608]
104. Krausz Y, Keidar Z, Kogan I, Even-Sapir E, Bar-Shalom R, Engel A, Rubinstein R, Sachs J, Bocher M, Agranovitz S, Chisin R, Israel O. SPECT/CT hybrid imaging with  $^{111}\text{In}$ -pentetreotide in assessment of neuroendocrine tumours. *Clin Endocrinol (Oxf)* 2003;59:565–73. [PubMed: 14616879]
105. Hillel PG, van Beek EJ, Taylor C, Lorenz E, Bax ND, Prakash V, Tindale WB. The clinical impact of a combined gamma camera/CT imaging system on somatostatin receptor imaging of neuroendocrine tumours. *Clin Radiol* 2006;61:579–87. [PubMed: 16784943]
106. Schillaci O, Danieli R, Manni C, Simonetti G. Is SPECT/CT with a hybrid camera useful to improve scintigraphic imaging interpretation? *Nucl Med Commun* 2004;25:705–10. [PubMed: 15208498]
107. Ingui CJ, Shah NP, Oates ME. Endocrine neoplasm scintigraphy: added value of fusing SPECT/CT images compared with traditional side-by-side analysis. *Clin Nucl Med* 2006;31:665–72. [PubMed: 17053381]
108. Roach PJ, Schembri GP, Ho Shon IA, Bailey EA, Bailey DL. SPECT/CT imaging using a spiral CT scanner for anatomical localization: Impact on diagnostic accuracy and reporter confidence in clinical practice. *Nucl Med Commun* 2006;27:977–87. [PubMed: 17088684]
109. Larson SM. Radioimmunology. Imaging and therapy. *Cancer* 1991;67:1253–1260. [PubMed: 1991286]
110. DeNardo DA, DeNardo GL, Yuan A, Shen S, DeNardo SJ, Macey DJ, Lamborn KR, Mahe M, Groch MW, Erwin WD. Prediction of radiation doses from therapy using tracer studies with iodine-131-labeled antibodies. *J Nucl Med* 1996;37:1970–1975. [PubMed: 8970516]
111. O'Donoghue JA. Optimal therapeutic strategies for radioimmunotherapy. *Recent Results in Cancer Research* 1996;141:77–99. [PubMed: 8722421]
112. Boucek JA, Turner JH. Validation of prospective whole-body bone marrow dosimetry by SPECT/CT multi-modality imaging in ( $^{131}\text{I}$ )-anti-CD20 rituximab radioimmunotherapy of non-Hodgkin's lymphoma. *Eur J Nucl Med Mol Imaging* 2005;32:458–69. [PubMed: 15821965]
113. Song H, Du Y, Sgouros G, Prideaux A, Frey E, Wahl RL. Therapeutic potential of  $^{90}\text{Y}$ - and  $^{131}\text{I}$ -labeled anti-CD20 monoclonal antibody in treating non-Hodgkin's lymphoma with pulmonary involvement: a Monte Carlo-based dosimetric analysis. *J Nucl Med* 2007;48:150–7. [PubMed: 17204712]
114. Masood Y, Liu YH, Depuey G, Taillefer R, Araujo LI, Allen S, Delbeke D, Anstett F, Peretz A, Zito MJ, Tsatkin V, Wackers FJ. Clinical validation of SPECT attenuation correction using x-ray computed tomography-derived attenuation maps: multicenter clinical trial with angiographic correlation. *J Nucl Cardiol* 2005;12:676–86. [PubMed: 16344230]
115. Ghersin E, Keidar Z, Rispler S, Litmanovich D, Bar-Shalom R, Roguin A, Soil A, Israel O, Engel A. Images in cardiovascular medicine. Hybrid cardiac single photon emission computed tomography/computed tomography imaging with myocardial perfusion single photon emission



- computed tomography and multidetector computed tomography coronary angiography for the assessment of unstable angina pectoris after coronary artery bypass grafting. *Circulation* 2006;114:e237–9. [PubMed: 16894043]
116. Gaemperli O, Schepis T, Valenta I, Husmann L, Scheffel H, Duerst V, Eberli FR, Luscher TF, Alkadhi H, Kaufmann PA. Cardiac image fusion from stand-alone SPECT and CT: clinical experience. *J Nucl Med* 2007;48:696–703. [PubMed: 17475956]
  117. Rispler S, Keidar Z, Ghersin E, Roguin A, Soil A, Dragu R, Litmanovich D, Frenkel A, Aronson D, Engel A, Beyar R, Israel O. Integrated single-photon emission computed tomography and computed tomography coronary angiography for the assessment of hemodynamically significant coronary artery lesions. *J Am Coll Cardiol* 2007;49:1059–67. [PubMed: 17349885]
  118. Schepis T, Gaemperli O, Koepfli P, Valenta I, Strobel K, Brunner A, Leschka S, Desbiolles L, Husmann L, Alkadhi H, Kaufmann PA. Comparison of 64-slice CT with gated SPECT for evaluation of left ventricular function. *J Nucl Med* 2006;47:1288–94. [PubMed: 16883007]
  119. Utsunomiya D, Tomiguchi S, Awai K, Shiraishi S, Nakaura T, Yamashita Y. Multidetector-row CT and quantitative gated SPECT for the assessment of left ventricular function in small hearts: the cardiac physical phantom study using a combined SPECT/CT system. *Eur Radiol* 2006;16:1818–25. [PubMed: 16456651]
  120. Schepis T, Gaemperli O, Koepfli P, Namdar M, Valenta I, Scheffel H, Leschka S, Husmann L, Eberli FR, Luscher TF, Alkadhi H, Kaufmann PA. Added value of coronary artery calcium score as an adjunct to gated SPECT for the evaluation of coronary artery disease in an intermediate-risk population. *J Nucl Med* 2007;48:1424–30. [PubMed: 17785727]
  121. Utsunomiya D, Tomiguchi S, Shiraishi S, Yamada K, Honda T, Kawanaka K, Kojima A, Awai K, Yamashita Y. Initial experience with X-ray CT based attenuation correction in myocardial perfusion SPECT imaging using a combined SPECT/CT system. *Ann Nucl Med* 2005;19:485–9. [PubMed: 16248385]
  122. Fricke E, Fricke H, Weise R, Kammeier A, Hagedorn R, Lotz N, Lindner O, Tschoepe D, Burchert W. Attenuation Correction of Myocardial SPECT Perfusion Images with Low-Dose CT: Evaluation of the Method by Comparison with Perfusion PET. *J Nucl Med* 2005;46:736–44. [PubMed: 15872344]
  123. Tonge CM, Manoharan M, Lawson RS, Shields RA, Prescott MC. Attenuation correction of myocardial SPECT studies using low resolution computed tomography images. *Nucl Med Commun* 2005;26:231–7. [PubMed: 15722903]
  124. Chen J, Caputlu-Wilson SF, Shi H, Galt JR, Faber TL, Garcia EV. Automated quality control of emission-transmission misalignment for attenuation correction in myocardial perfusion imaging with SPECT-CT systems. *J Nucl Cardiol* 2006;13:43–9. [PubMed: 16464716]
  125. Guetter C, Wacker M, Xu C, Hornegger J. Registration of cardiac SPECT/CT data through weighted intensity co-occurrence priors. *Med Image Comput Comput Assist Interv Int Conf Med Image Comput Comput Assist Interv* 2007;10:725–33.
  126. Gaemperli O, Schepis T, Kalff V, Namdar M, Valenta I, Stefani L, Desbiolles L, Leschka S, Husmann L, Alkadhi H, Kaufmann PA. Validation of a new cardiac image fusion software for three-dimensional integration of myocardial perfusion SPECT and stand-alone 64-slice CT angiography. *Eur J Nucl Med Mol Imaging* 2007;34:1097–106. [PubMed: 17245532]
  127. Kappadath SC, Erwin WD, Wendt RE 3rd. Observed inter-camera variability of clinically relevant performance characteristics for Siemens Symbia gamma cameras. *J Appl Clin Med Phys* 2006;7:74–80. [PubMed: 17533558]
  128. Boone JM. Multidetector CT: opportunities, challenges, and concerns associated with scanners with 64 or more detector rows. *Radiology* 2006;241:334–7. [PubMed: 17057062]
  129. Horger M, Eschmann SM, Pfannenberger C, Storek D, Dammann F, Vonthein R, Claussen CD, Bares R. The value of SPET/CT in chronic osteomyelitis. *Eur J Nucl Med Mol Imaging* 2003;30:1665–73. [PubMed: 14523585]
  130. Filippi L, Schillaci O. Usefulness of hybrid SPECT/CT in <sup>99m</sup>Tc-HMPAO-labeled leukocyte scintigraphy for bone and joint infections. *J Nucl Med* 2006;47:1908–13. [PubMed: 17138732]

131. Horger M, Eschmann SM, Pfannenberger C, Storek D, Vonthein R, Claussen CD, Bares R. Added value of SPECT/CT in patients suspected of having bone infection: preliminary results. *Arch Orthop Trauma Surg* 2007;127:211–21. [PubMed: 17146681]
132. Coutinho A, Fenyo-Pereira M, Dib LL, Lima EN. The role of SPECT/CT with  $^{99m}\text{Tc}$ -MDP image fusion to diagnose temporomandibular dysfunction. *Oral Surg Oral Med Oral Pathol Oral Radiol Endod* 2006;101:224–30. [PubMed: 16448926]
133. Bar-Shalom R, Yefremov N, Guralnik L, Keidar Z, Engel A, Nitecki S, Israel O. SPECT/CT using  $^{67}\text{Ga}$  and  $^{111}\text{In}$ -labeled leukocyte scintigraphy for diagnosis of infection. *J Nucl Med* 2006;47:587–94. [PubMed: 16595491]
134. Filippi L, Schillaci O. SPECT/CT with a hybrid camera: a new imaging modality for the functional anatomical mapping of infections. *Expert Rev Med Devices* 2006;3:699–703. [PubMed: 17280534]
135. Nathan J, Crawford JA, Sodee DB, Bakale G. Fused SPECT/CT imaging of Peri-iliopsoas infection using Indium-111-labeled leukocytes. *Clin Nucl Med* 2006;31:801–2. [PubMed: 17117077]
136. Ingui CJ, Shah NP, Oates ME. Infection scintigraphy: added value of single-photon emission computed tomography/computed tomography fusion compared with traditional analysis. *J Comput Assist Tomogr* 2007;31:375–80. [PubMed: 17538282]
137. Filippi L, Biancone L, Petruzzello C, Schillaci O. Tc-99m HMPAO-labeled leukocyte scintigraphy with hybrid SPECT/CT detects perianal fistulas in Crohn disease. *Clin Nucl Med* 2006;31:541–2. [PubMed: 16921278]
138. Hendrix CW, Fuchs EJ, Macura KJ, Lee LA, Parsons TL, Bakshi RP, Khan WA, Guidos A, Leal JP, Wahl R. Quantitative Imaging and Sigmoidoscopy to Assess Distribution of Rectal Microbicide Surrogates. *Clin Pharmacol Ther.* 2007
139. Suga K, Kawakami Y, Zaki M, Yamashita T, Shimizu K, Matsunaga N. Clinical utility of co-registered respiratory-gated ( $^{99m}\text{Tc}$ -Technegas/MAA SPECT-CT images in the assessment of regional lung functional impairment in patients with lung cancer. *Eur J Nucl Med Mol Imaging* 2004;31:1280–90. [PubMed: 15197501]
140. Suga K, Kawakami Y, Iwanaga H, Tokuda O, Matsunaga N. Automated breath-hold perfusion SPECT/CT fusion images of the lungs. *AJR Am J Roentgenol* 2007;189:455–63. [PubMed: 17646474]
141. Tan KG, Bartholomeusz FD, Chatterton BE. Detection and follow up of biliary leak on Tc-99m DIDA SPECT-CT scans. *Clin Nucl Med* 2004;29:642–3. [PubMed: 15365441]
142. Schepis T, Gaemperli O, Koepfli P, Ruegg C, Burger C, Leschka S, Desbiolles L, Husmann L, Alkadhi H, Kaufmann PA. Use of coronary calcium score scans from stand-alone multislice computed tomography for attenuation correction of myocardial perfusion SPECT. *Eur J Nucl Med Mol Imaging* 2007;34:11–9. [PubMed: 16896667]
143. Anger HO. Scintillation camera. *Rev Sci Instru* 1957;29:27–33.
144. Despres P, Funk T, Shah KS, Hasegawa BH. Monte Carlo simulations of compact gamma cameras based on avalanche photodiodes. *Phys Med Biol* 2007;52:3057–74. [PubMed: 17505089]
145. Kubo N, Mabuchi M, Katoh C, Arai H, Morita K, Tsukamoto E, Morita Y, Tamaki N. Validation of left ventricular function from gated single photon computed emission tomography by using a scintillator-photodiode camera: a dynamic myocardial phantom study. *Nucl Med Commun* 2002;23:639–43. [PubMed: 12089486]
146. Mori I, Takayama T, Motomura N. The CdTe detector module and its imaging performance. *Ann Nucl Med* 2001;15:487–94. [PubMed: 11831395]
147. Zeng GL, Gagnon D. Image reconstruction algorithm for a spinning strip CZT SPECT camera with a parallel slat collimator and small pixels. *Med Phys* 2004;31:3461–73. [PubMed: 15651629]
148. Kumita S, Tanaka K, Cho K, Sato N, Nakajo H, Toba M, Fukushima Y, Mizumura S, Takano T, Kumazaki T. Assessment of left ventricular function using solid-state gamma camera equipped with a highly-sensitive collimator. *Ann Nucl Med* 2003;17:517–20. [PubMed: 14575391]



149. Hruska CB, O'Connor MK, Collins DA. Comparison of small field of view gamma camera systems for scintimammography. *Nucl Med Commun* 2005;26:441–5. [PubMed: 15838427]
150. Fukumitsu N, Tsuchida D, Ogi S, Uchiyama M, Mori Y, Ooshita T, Narrita H, Yamamoto H, Takeyama H. Use of Digirad 2020tc Imager, a multi-crystal scintillation camera with solid-state detectors in one case for the imaging of autografts of parathyroid glands. *Ann Nucl Med* 2001;15:533–6. [PubMed: 11831402]
151. Hayes SW, De Lorenzo A, Hachamovitch R, Dhar SC, Hsu P, Cohen I, Friedman JD, Kang X, Berman DS. Prognostic implications of combined prone and supine acquisitions in patients with equivocal or abnormal supine myocardial perfusion SPECT. *J Nucl Med* 2003;44:1633–40. [PubMed: 14530478]
152. Stowers SA, Umfrid R. Supine-prone SPECT myocardial perfusion imaging: the poor man's attenuation compensation. *J Nucl Cardiol* 2003;10:338. [PubMed: 12812195]
153. Malkernek D, Brenner R, Martin WH, Sampson UK, Feurer ID, Kronenberg MW, Delbeke D. CT-based attenuation correction versus prone imaging to decrease equivocal interpretations of rest/stress Tc-99m tetrofosmin SPECT MPI. *J Nucl Cardiol* 2007;14:314–23. [PubMed: 17556165]
154. Brzymialkiewicz CN, Tornai MP, McKinley RL, Bowsher JE. Evaluation of fully 3-D emission mammotomography with a compact cadmium zinc telluride detector. *IEEE Trans Med Imaging* 2005;24:868–77. [PubMed: 16011316]
155. Tornai MP, Bowsher JE, Jaszczak RJ, Pieper BC, Greer KL, Hardenbergh PH, Coleman RE. Mammothography with pinhole incomplete circular orbit SPECT. *J Nucl Med* 2003;44:583–93. [PubMed: 12679403]
156. Brzymialkiewicz CN, Tornai MP, McKinley RL, Cutler SJ, Bowsher JE. Performance of dedicated emission mammothography for various breast shapes and sizes. *Phys Med Biol* 2006;51:5051–64. [PubMed: 16985287]
157. McKinley RL, Tornai MP, Samei E, Bradshaw ML. Simulation study of a quasi-monochromatic beam for x-ray computed mammothography. *Med Phys* 2004;31:800–13. [PubMed: 15124997]
158. Tornai MP, McKinley RL, Brzymialkiewicz CN, Madhav P, Cutler SJ, Crotty DJ, Bowsher JE, Samei E, Floyd CE. Design and development of a fully-3D dedicated x-ray computed mammothography system. *Proc SPIE* 2005;5745:189–197.
159. McKinley RL, Brzymialkiewicz CN, Madhav P, Tornai MP. Investigation of cone-beam acquisitions implemented using a novel dedicated mammothography system with unique arbitrary orbit capability. *Proc SPIE* 2005;5745:609–617.
160. Brzymialkiewicz CN, McKinley RL, Tornai MP. Towards patient imaging with dedicated emission mammothography. *IEEE Nucl Sci Symp Med Imag Conf Rec* 2005;3:1519–1523.
161. Even-Sapir E, Keidar Z, Sachs J, Engel A, Bettman L, Gaitini D, Guralnik L, Werbin N, Iosilevsky G, Israel O. The new technology of combined transmission and emission tomography in evaluation of endocrine neoplasms. *J Nucl Med* 2001;42:998–1004. [PubMed: 11438618]
162. Horger M, Eschmann SM, Pfannenberger C, Vonthein R, Besenfelder H, Claussen CD, Bares R. Evaluation of combined transmission and emission tomography for classification of skeletal lesions. *AJR Am J Roentgenol* 2004;183:655–61. [PubMed: 1533352]
163. Even-Sapir E. Imaging of malignant bone involvement by morphologic, scintigraphic, and hybrid modalities. *J Nucl Med* 2005;46:1356–67. [PubMed: 16085595]
164. Goerres GW, Schmid DT, Schuknecht B, Eyrich GK. Bone invasion in patients with oral cavity cancer: comparison of conventional CT with PET/CT and SPECT/CT. *Radiology* 2005;237:281–7. [PubMed: 16118155]
165. Utsunomiya D, Shiraishi S, Imuta M, Tomiguchi S, Kawanaka K, Morishita S, Awai K, Yamashita Y. Added value of SPECT/CT fusion in assessing suspected bone metastasis: comparison with scintigraphy alone and nonfused scintigraphy and CT. *Radiology* 2006;238:264–71. [PubMed: 16304081]
166. Even-Sapir E, Metser U, Mishani E, Lievshitz G, Lerman H, Leibovitch I. The detection of bone metastases in patients with high-risk prostate cancer: <sup>99m</sup>Tc-MDP Planar bone scintigraphy, single- and multi-field-of-view SPECT, <sup>18</sup>F-fluoride PET, and <sup>18</sup>F-fluoride PET/CT. *J Nucl Med* 2006;47:287–97. [PubMed: 16455635]

167. Romer W, Nomayr A, Uder M, Bautz W, Kuwert T. SPECT-guided CT for evaluating foci of increased bone metabolism classified as indeterminate on SPECT in cancer patients. *J Nucl Med* 2006;47:1102–6. [PubMed: 16818944]
168. Even-Sapir E, Flusser G, Lerman H, Lievshitz G, Metser U. SPECT/multislice low-dose CT: a clinically relevant constituent in the imaging algorithm of nononcologic patients referred for bone scintigraphy. *J Nucl Med* 2007;48:319–24. [PubMed: 17268031]
169. Schulz V, Nickel I, Nomayr A, Vija AH, Hocke C, Hornegger J, Bautz W, Romer W, Kuwert T. Effect of CT-based attenuation correction on uptake ratios in skeletal SPECT. *Nuklearmedizin* 2007;46:36–42. [PubMed: 17299653]
170. Filippi L, Schillaci O, Santoni R, Manni C, Danieli R, Simonetti G. Usefulness of SPECT/CT with a hybrid camera for the functional anatomical mapping of primary brain tumors by [ $^{99m}\text{Tc}$ ] tetrafosmin. *Cancer Biother Radiopharm* 2006;21:41–8. [PubMed: 16480330]
171. Schillaci O, Danieli R, Filippi L, Romano P, Cossu E, Manni C, Simonetti G. Scintimammography with a hybrid SPECT/CT imaging system. *Anticancer Res* 2007;27:557–62. [PubMed: 17348441]
172. Denecke T, Hildebrandt B, Lehmkuhl L, Peters N, Nicolaou A, Pech M, Riess H, Rieke J, Felix R, Amthauer H. Fusion imaging using a hybrid SPECT-CT camera improves port perfusion scintigraphy for control of hepatic arterial infusion of chemotherapy in colorectal cancer patients. *Eur J Nucl Med Mol Imaging*. 2005
173. Gruning T, Brogssitter C, Khonsari M, Jones IW, Ormsby PL, Burchert W. X-ray-based attenuation correction of myocardial perfusion scans: practical feasibility and diagnostic impact. *Nucl Med Commun* 2006;27:853–8. [PubMed: 17021424]
174. Cense HA, Sloof GW, Klaase JM, Bergman JJ, van Hemert FJ, Fockens P, van Lanschot JJ. Lymphatic drainage routes of the gastric cardia visualized by lymphoscintigraphy. *J Nucl Med* 2004;45:247–52. [PubMed: 14960643]
175. Plotkin M, Wurm R, Eisenacher J, Szerewicz K, Michel R, Schlenger L, Pech M, Denecke T, Kuczer D, Bischoff A, Felix R, Amthauer H. Combined SPECT/CT imaging using  $^{123}\text{I}$ -IMT in the detection of recurrent or persistent head and neck cancer. *Eur Radiol* 2006;16:503–11. [PubMed: 15983775]
176. Plotkin M, Wurm R, Kuczer D, Wust P, Michel R, Denecke T, Ruf J, Schlenger L, Bischoff A, Felix R, Amthauer H. Diagnostic value of  $^{123}\text{I}$ -IMT SPECT in the follow-up of head and neck cancer. *Onkologie* 2006;29:147–52. [PubMed: 16601370]
177. Birchler MT, Thuerl C, Schmid D, Neri D, Waibel R, Schubiger A, Stoeckli SJ, Schmid S, Goerres GW. Immunoscintigraphy of patients with head and neck carcinomas, with an anti-angiogenic antibody fragment. *Otolaryngol Head Neck Surg* 2007;136:543–8. [PubMed: 17418248]
178. Schillaci O, Danieli R, Manni C, Capocchetti F, Simonetti G. Technetium-99m-labelled red blood cell imaging in the diagnosis of hepatic haemangiomas: the role of SPECT/CT with a hybrid camera. *Eur J Nucl Med Mol Imaging* 2004;31:1011–5. [PubMed: 15057491]
179. Zheng JG, Yao ZM, Shu CY, Zhang Y, Zhang X. Role of SPECT/CT in diagnosis of hepatic hemangiomas. *World J Gastroenterol* 2005;11:5336–41. [PubMed: 16149142]
180. Ikeda O, Kusunoki S, Nakaura T, Shiraishi S, Kawanaka K, Tomiguchi S, Yamashita Y, Takamori H, Chikamoto A, Kanemitsu K. Comparison of fusion imaging using a combined SPECT/CT system and intra-arterial CT: assessment of drug distribution by an implantable port system in patients undergoing hepatic arterial infusion chemotherapy. *Cardiovasc Intervent Radiol* 2006;29:371–9. [PubMed: 16502168]
181. Sergiacomi G, Schillaci O, Leporace M, Laviani F, Cariani M, Manni C, Danieli R, Simonetti G. Integrated multislice CT and Tc-99m Sestamibi SPECT-CT evaluation of solitary pulmonary nodules. *Radiol Med (Torino)* 2006;111:213–24. [PubMed: 16671379]
182. Ferran N, Ricart Y, Lopez M, Martinez-Ballarín I, Roca M, Gamez C, Carrerea D, Guirao S, Leon AF, Martín-Comin J. Characterization of radiologically indeterminate lung lesions:  $^{99m}\text{Tc}$ -depreotide SPECT versus  $^{18}\text{F}$ -FDG PET. *Nucl Med Commun* 2006;27:507–14. [PubMed: 16710105]



183. Yang A, Xue J, Li X, Yu Y, Deng H, Hu G, Meng X, Li J. Experimental and clinical observations of  $^{99m}\text{Tc}$ -MIBI uptake correlate with P-glycoprotein expression in lung cancer. *Nucl Med Commun* 2007;28:696–703. [PubMed: 17667748]
184. Bar-Shalom R, Yefremov N, Haim N, Dann EJ, Epelbaum R, Keidar Z, Gaitini D, Frenkel A, Israel O. Camera-based FDG PET and  $^{67}\text{Ga}$  SPECT in evaluation of lymphoma: comparative study. *Radiology* 2003;227:353–60. [PubMed: 12637679]
185. Even-Sapir E, Israel O. Gallium-67 scintigraphy: A cornerstone in functional imaging of lymphoma. *Eur J Nuc Med Mol Imaging* 2003;30:S65–81.
186. Palumbo B, Sivoletta S, Palumbo I, Liberati AM, Palumbo R.  $^{67}\text{Ga}$ -SPECT/CT with a hybrid system in the clinical management of lymphoma. *Eur J Nucl Med Mol Imaging* 2005;32:1011–7. [PubMed: 15895228]
187. Kraitchman DL, Tatsumi M, Gilson WD, Ishimori T, Kedziorek D, Walczak P, Segars WP, Chen HH, Fritzges D, Izbudak I, Young RG, Marcelino M, Pittenger MF, Solaiyappan M, Boston RC, Tsui BM, Wahl RL, Bulte JW. Dynamic imaging of allogeneic mesenchymal stem cells trafficking to myocardial infarction. *Circulation* 2005;112:1451–61. [PubMed: 16129797]
188. Pfannenberger AC, Eschmann SM, Horger M, Lamberts R, Vonthein R, Claussen CD, Bares R. Benefit of anatomical-functional image fusion in the diagnostic work-up of neuroendocrine neoplasms. *Eur J Nucl Med Mol Imaging* 2003;30:835–43. [PubMed: 12682789]
189. Ozer S, Dobrozemsky G, Kienast O, Beheshti M, Becherer A, Niederle B, Kainberger F, Dudczak R, Kurtaran A. Value of combined XCT/SPECT technology for avoiding false positive planar ( $^{123}\text{I}$ )-MIBG scintigraphy. *Nuklearmedizin* 2004;43:164–70. [PubMed: 15480505]
190. Amthauer H, Denecke T, Rohlfing T, Ruf J, Bohmig M, Gutberlet M, Plockinger U, Felix R, Lemke AJ. Value of image fusion using single photon emission computed tomography with integrated low dose computed tomography in comparison with a retrospective voxel-based method in neuroendocrine tumours. *Eur Radiol* 2005;15:1456–62. [PubMed: 15627182]
191. Ikeda O, Tamura Y, Nakasone Y, Shiraishi S, Kawanaka K, Tomiguchi S, Morishita S, Takamori H, Chikamoto A, Kanemitsu K, Yamashita Y. Evaluation of extrahepatic perfusion of anticancer drugs in the right gastric arterial region on fused images using combined CT/SPECT: is extrahepatic perfusion predictive of gastric toxicity? *Cardiovasc Intervent Radiol* 2007;30:392–7. [PubMed: 17225975]
192. Ikeda O, Tamura Y, Nakasone Y, Shiraishi S, Kawanaka K, Tomiguchi S, Takamori H, Chikamoto A, Kanemitsu K, Yamashita Y. Evaluation of intrahepatic perfusion on fusion imaging using a combined CT/SPECT system: influence of anatomic variations on hemodynamic modification before installation of implantable port systems for hepatic arterial infusion chemotherapy. *Cardiovasc Intervent Radiol* 2007;30:383–91. [PubMed: 17225972]
193. Ikeda O, Tamura Y, Nakasone Y, Shiraishi S, Kawanaka K, Tomiguchi S, Yamashita Y, Takamori H, Kanemitsu K, Baba H. Comparison of intrahepatic and pancreatic perfusion on fusion images using a combined SPECT/CT system and assessment of efficacy of combined continuous arterial infusion and systemic chemotherapy in advanced pancreatic carcinoma. *Cardiovasc Intervent Radiol* 2007;30:912–21. [PubMed: 17710478]
194. Kaczirek K, Prager G, Kienast O, Dobrozemsky G, Dudczak R, Niederle B, Kurtaran A. Combined transmission and ( $^{99m}\text{Tc}$ )-sestamibi emission tomography for localization of mediastinal parathyroid glands. *Nuklearmedizin* 2003;42:220–3. [PubMed: 14571319]
195. Gayed IW, Kim EE, Broussard WF, Evans D, Lee J, Broemeling LD, Ochoa BB, Moxley DM, Erwin WD, Podoloff DA. The value of  $^{99m}\text{Tc}$ -sestamibi SPECT/CT over conventional SPECT in the evaluation of parathyroid adenomas or hyperplasia. *J Nucl Med* 2005;46:248–52. [PubMed: 15695783]
196. Krausz Y, Bettman L, Guralnik L, Yosilevsky G, Keidar Z, Bar-Shalom R, Even-Sapir E, Chisin R, Israel O. Technetium-99m-MIBI SPECT/CT in primary hyperparathyroidism. *World J Surg* 2006;30:76–83. [PubMed: 16369710]
197. Ruf J, Seehofer D, Denecke T, Stelter L, Rayes N, Felix R, Amthauer H. Impact of image fusion and attenuation correction by SPECT-CT on the scintigraphic detection of parathyroid adenomas. *Nuklearmedizin* 2007;46:15–21. [PubMed: 17299650]
198. Lavery WC, Goetze S, Friedman KP, Leal JP, Zhang Z, Garret-Mayer E, Dackiw AP, Tufano RP, Zeiger MA, Ziessman HA. Comparison of SPECT/CT, SPECT, and planar imaging with single-

- and dual-phase ( $^{99m}\text{Tc}$ -sestamibi parathyroid scintigraphy. *J Nucl Med* 2007;48:1084–9. [PubMed: 17574983]
199. Wong TZ, Turkington TG, Polascik TJ, Coleman RE. ProstaScint (capromab pendetide) imaging using hybrid gamma camera-CT technology. *AJR Am J Roentgenol* 2005;184:676–80. [PubMed: 15671397]
  200. Seo Y, Wong KH, Hasegawa BH. Calculation and validation of the use of effective attenuation coefficient for attenuation correction in In-111 SPECT. *Med Phys* 2005;32:3628–35. [PubMed: 16475761]
  201. Seo Y, Franc BL, Hawkins RA, Wong KH, Hasegawa BH. Progress in SPECT/CT imaging of prostate cancer. *Technol Cancer Res Treat* 2006;5:329–36. [PubMed: 16866563]
  202. Ellis RJ, Zhou H, Kim EY, Fu P, Kaminsky DA, Sodee B, Colussi V, Vance WZ, Spirnak JP, Kim C, Resnick MI. Biochemical disease-free survival rates following definitive low-dose-rate prostate brachytherapy with dose escalation to biologic target volumes identified with SPECT/CT capromab pendetide. *Brachytherapy* 2007;6:16–25. [PubMed: 17284381]
  203. Ellis RJ, Zhou H, Kaminsky DA, Fu P, Kim EY, Sodee DB, Colussi V, Spirnak JP, Whalen CC, Resnick MI. Rectal morbidity after permanent prostate brachytherapy with dose escalation to biologic target volumes identified by SPECT/CT fusion. *Brachytherapy* 2007;6:149–56. [PubMed: 17434109]
  204. Sodee DB, Sodee AE, Bakale G. Synergistic value of single-photon emission computed tomography/computed tomography fusion to radioimmunoscintigraphic imaging of prostate cancer. *Semin Nucl Med* 2007;37:17–28. [PubMed: 17161036]
  205. Even-Sapir E, Lerman H, Lievshitz G, Khafif A, Fliss DM, Schwartz A, Gur E, Skornick Y, Schneebaum S. Lymphoscintigraphy for sentinel node mapping using a hybrid SPECT/CT system. *J Nucl Med* 2003;44:1413–20. [PubMed: 12960185]
  206. Belhocine TZ, Scott AM, Even-Sapir E, Urbain JL, Essner R. Role of Nuclear Medicine in the management of cutaneous malignant melanoma. *J Nucl Med* 2006;47:957–67. [PubMed: 16741305]
  207. De Cicco C, Trifiro G, Calabrese L, Bruschini R, Ferrari ME, Travaini LL, Fiorenza M, Viale G, Chiesa F, Paganelli G. Lymphatic mapping to tailor selective lymphadenectomy in cN0 tongue carcinoma: beyond the sentinel node concept. *Eur J Nucl Med Mol Imaging* 2006;33:900–5. [PubMed: 16604345]
  208. Shiraishi S, Tomiguchi S, Utsunomiya D, Kawanaka K, Awai K, Morishita S, Okuda T, Yokotsuka K, Yamashita Y. Quantitative analysis and effect of attenuation correction on lymph node staging of non-small cell lung cancer on SPECT and CT. *AJR Am J Roentgenol* 2006;186:1450–7. [PubMed: 16632744]
  209. Ishihara T, Kaguchi A, Matsushita S, Shiraishi S, Tomiguchi S, Yamashita Y, Kageshita T, Ono T. Management of sentinel lymph nodes in malignant skin tumors using dynamic lymphoscintigraphy and the single-photon-emission computed tomography/computed tomography combined system. *Int J Clin Oncol* 2006;11:214–20. [PubMed: 16850128]
  210. Khafif A, Schneebaum S, Fliss DM, Lerman H, Metser U, Ben-Yosef R, Gil Z, Reider-Trejo L, Genadi L, Even-Sapir E. Lymphoscintigraphy for sentinel node mapping using a hybrid single photon emission CT (SPECT)/CT system in oral cavity squamous cell carcinoma. *Head Neck* 2006;28:874–9. [PubMed: 16933311]
  211. Sherif A, Garske U, de la Torre M, Thorn M. Hybrid SPECT-CT: an additional technique for sentinel node detection of patients with invasive bladder cancer. *Eur Urol* 2006;50:83–91. [PubMed: 16632191]
  212. Keski-Santti H, Matzke S, Kauppinen T, Tornwall J, Atula T. Sentinel lymph node mapping using SPECT-CT fusion imaging in patients with oral cavity squamous cell carcinoma. *Eur Arch Otorhinolaryngol* 2006;263:1008–12. [PubMed: 16830118]
  213. Mar MV, Miller SA, Kim EE, Macapinlac HA. Evaluation and localization of lymphatic drainage and sentinel lymph nodes in patients with head and neck melanomas by hybrid SPECT/CT lymphoscintigraphic imaging. *J Nucl Med Technol* 2007;35:10–6. quiz 17–20. [PubMed: 17337652]



214. Roarke MC, Ram P, Nguyen BD. Utility of SPECT/CT in preoperative planning for sentinel lymph node biopsy in melanoma and head/neck carcinoma: three illustrative cases. *Clin Nucl Med* 2007;32:464–5. [PubMed: 17515756]
215. Warncke SH, Mattei A, Fuechsel FG, Z'Brun S, Krause T, Studer UE. Detection rate and operating time required for gamma probe-guided sentinel lymph node resection after injection of technetium-99m nanocolloid into the prostate with and without preoperative imaging. *Eur Urol* 2007;52:126–32. [PubMed: 17258385]
216. Mattei A, Fuechsel FG, Bhatta Dhar N, Warncke SH, Thalmann GN, Krause T, Studer UE. The template of the primary lymphatic landing sites of the prostate should be revisited: results of a multi-modality mapping study. *Eur Urol* 2008;53:118–25. [PubMed: 17709171]
217. Nomori H, Ikeda K, Mori T, Shiraishi S, Kobayashi H, Iwatani K, Kawanaka K, Kobayashi T. Sentinel node identification in clinical stage Ia non-small cell lung cancer by a combined single photon emission computed tomography/computed tomography system. *J Thorac Cardiovasc Surg* 2007;134:182–7. [PubMed: 17599506]
218. Lerman H, Metser U, Lievshitz G, Sperber F, Shneebaum S, Even-Sapir E. Lymphoscintigraphic sentinel node identification in patients with breast cancer: the role of SPECT-CT. *Eur J Nucl Med Mol Imaging* 2006;33:329–37. [PubMed: 16220303]
219. Lerman H, Lievshitz G, Zak O, Metser U, Schneebaum S, Even-Sapir E. Improved sentinel node identification by SPECT/CT in overweight patients with breast cancer. *J Nucl Med* 2007;48:201–6. [PubMed: 17268015]
220. Horger M, Eschmann SM, Lengerke C, Claussen CD, Pfannenberger C, Bares R. Improved detection of splenosis in patients with haematological disorders: the role of combined transmission-emission tomography. *Eur J Nucl Med Mol Imaging* 2003;30:316–9. [PubMed: 12552353]
221. Alvarez R, Diehl KM, Avram A, Brown R, Piert M. Localization of splenosis using <sup>99m</sup>Tc-damaged red blood cell SPECT/CT and intraoperative gamma probe measurements. *Eur J Nucl Med Mol Imaging* 2007;34:969. [PubMed: 17457584]
222. Franzius C, Hermann K, Weckesser M, Kopka K, Juergens KU, Vormoor J, Schober O. Whole-body PET/CT with <sup>11</sup>C-meta-hydroxyephedrine in tumors of the sympathetic nervous system: feasibility study and comparison with <sup>123</sup>I-MIBG SPECT/CT. *J Nucl Med* 2006;47:1635–42. [PubMed: 17015899]
223. Yamamoto Y, Nishiyama Y, Monden T, Matsumura Y, Satoh K, Ohkawa M. Clinical usefulness of fusion of <sup>131</sup>I SPECT and CT images in patients with differentiated thyroid carcinoma. *J Nucl Med* 2003;44:1905–10. [PubMed: 14660715]
224. Tharp K, Israel O, Hausmann J, Bettman L, Martin WH, Daitzchman M, Sandler MP, Delbeke D. Impact of <sup>131</sup>I-SPECT/CT images obtained with an integrated system in the follow-up of patients with thyroid carcinoma. *Eur J Nucl Med Mol Imaging* 2004;31:1435–42. [PubMed: 15221294]
225. Ruf J, Lehmkuhl L, Bertram H, Sandrock D, Amthauer H, Humplik B, Ludwig Munz D, Felix R. Impact of SPECT and integrated low-dose CT after radioiodine therapy on the management of patients with thyroid carcinoma. *Nucl Med Commun* 2004;25:1177–82. [PubMed: 15640775]
226. Minarik D, Sjogreen K, Ljungberg M. A new method to obtain transmission images for planar whole-body activity quantitation. *Cancer Biother Radiopharm* 2005;20:72–6. [PubMed: 15778584]
227. Mirshanov, DM. USSR Academy of Medical Science. Tashkent Branch, All-Union Research Surgery Center; USSR: 1987. Transmission-emission computer tomograph.
228. Hasegawa BH, Iwata K, Wong KH, Wu MC, Da Silva J, Tang HR, Barber WC, Hwang AH, Sakdinawat AE. Dual-modality imaging of cancer with SPECT/CT. *Acad Radiol* 2002;9:1305–1321. [PubMed: 12449363]
229. Hasegawa BH, Tang HR, Da Silva AJ, Iwata K, Wu AM, Wong KH. Implementation and applications of a combined CT/SPECT system. *IEEE Nucl Sci Symp Med Imag Conf Rec* 1999;3:1373–1377.

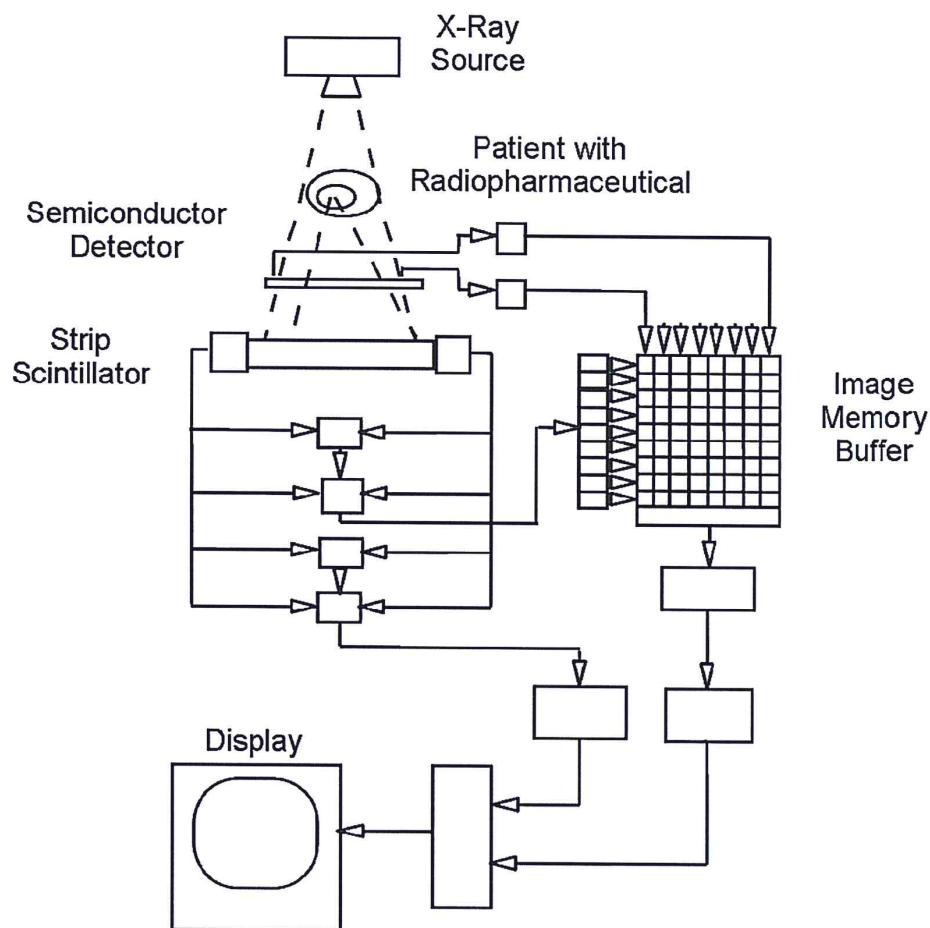


**Figure 1.** Schematic of transmission-emission computer tomography system proposed by Mirshanov for simultaneous SPECT/CT with tandem semiconductor and scintillation strip detectors. (Figure from reference [227]).



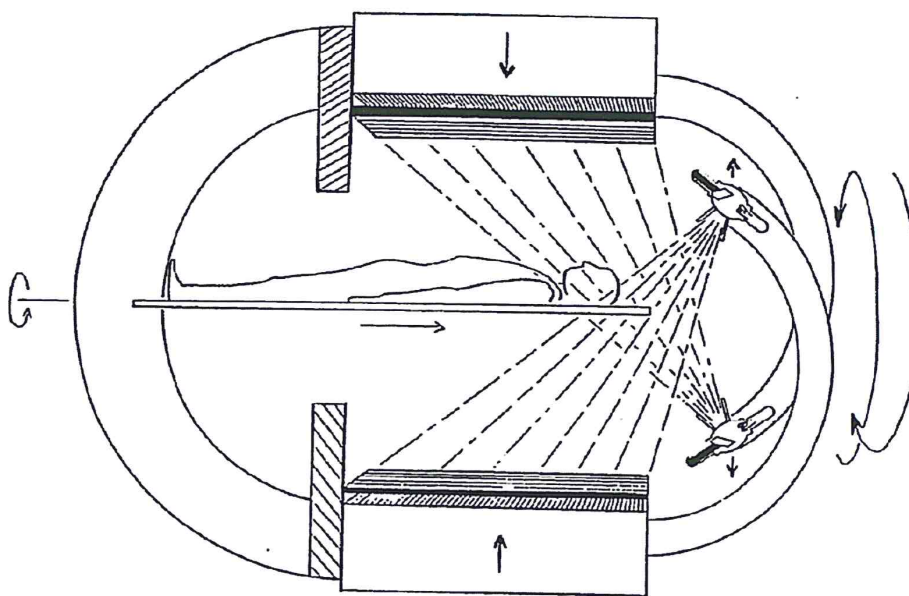


**Figure 2.** Schematic of “Transmission/Emission Registered Imaging (TERI) Computed Tomography Scanner” proposed by Kaplan for simultaneous SPECT/CT imaging. (Figure from reference [44]).

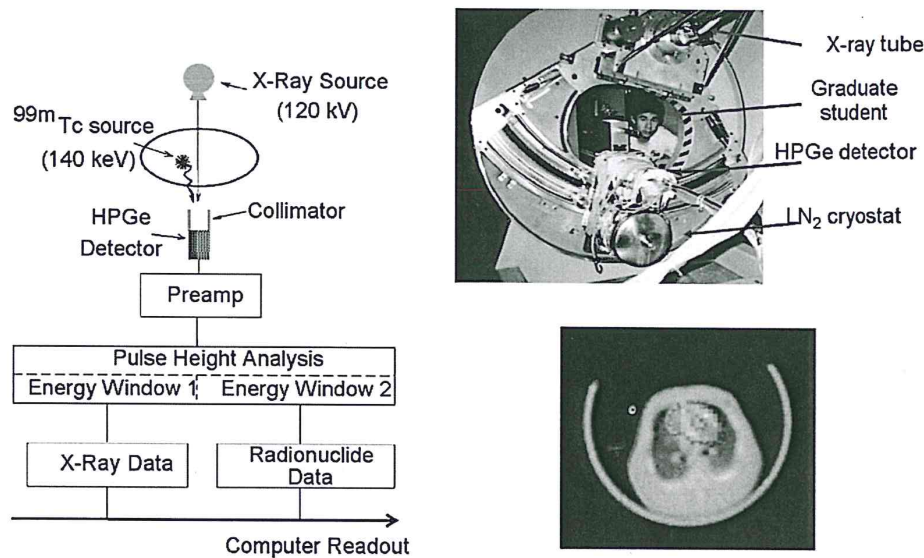


**Figure 3.** (left) Schematic of data acquisition system for UCSF Emission-Transmission CT (ETCT) System. (Top right) Photograph of prototype ETCT system. (Bottom right) Transaxial image showing myocardial uptake of  $^{99m}\text{Tc}$ -sestamibi SPECT image (red) superimposed on a gray-scale CT image of a porcine model of myocardial perfusion. (Figure on left, upper right, and bottom right reproduced with permission from references [46], [228], and [50], respectively.)



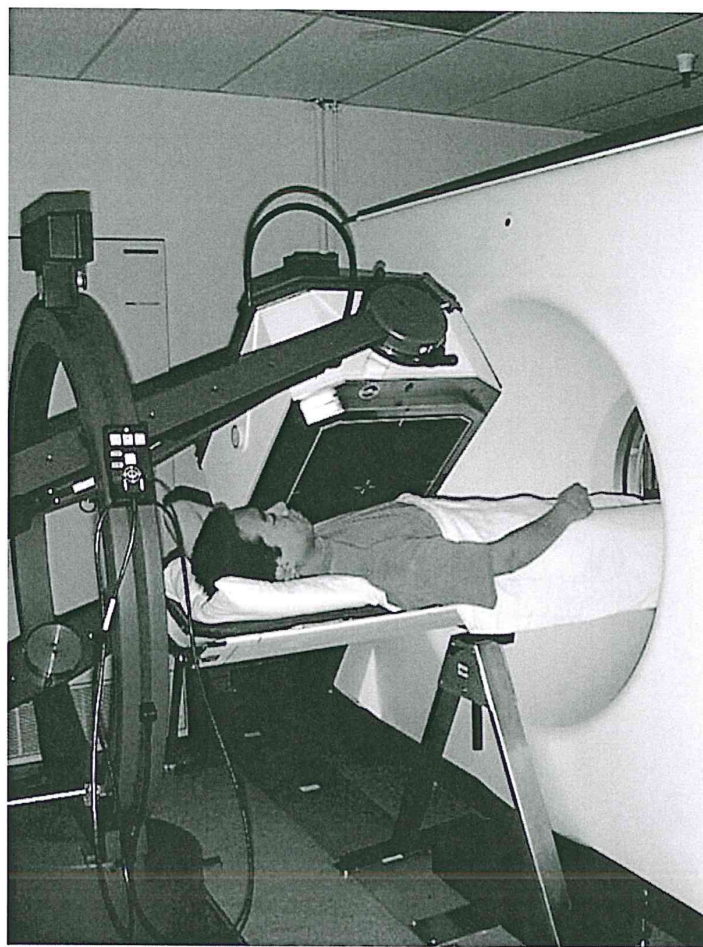


**Figure 4.** Prototype SPECT/CT system configured at UCSF from GE 9800 Quick CT system and single-detector GE XR/T SPECT system. Extended table and external table support allows both SPECT and CT imaging without removing patient from system. (Reproduced with permission from reference [229]).

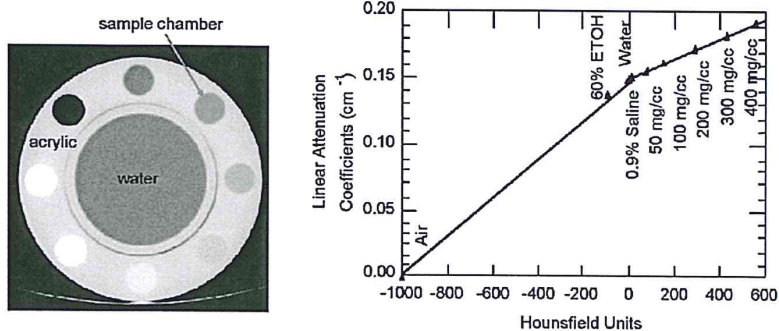


**Figure 5.**

Calibration of CT for x-ray derived attenuation coefficients performed with cylindrical phantom (left) containing different tissue equivalent materials. CT values (ie Hounsfield units) are correlated with values of linear attenuation coefficients (ie  $\text{cm}^{-1}$ ) calculated from known composition of tissue equivalent materials calculated at energy of radionuclide used for emission imaging. Calibration curve (right) used to convert values in CT image to form patient-specific map of attenuation coefficients for attenuation correction of emission image (Reproduced with permission from reference [21]).



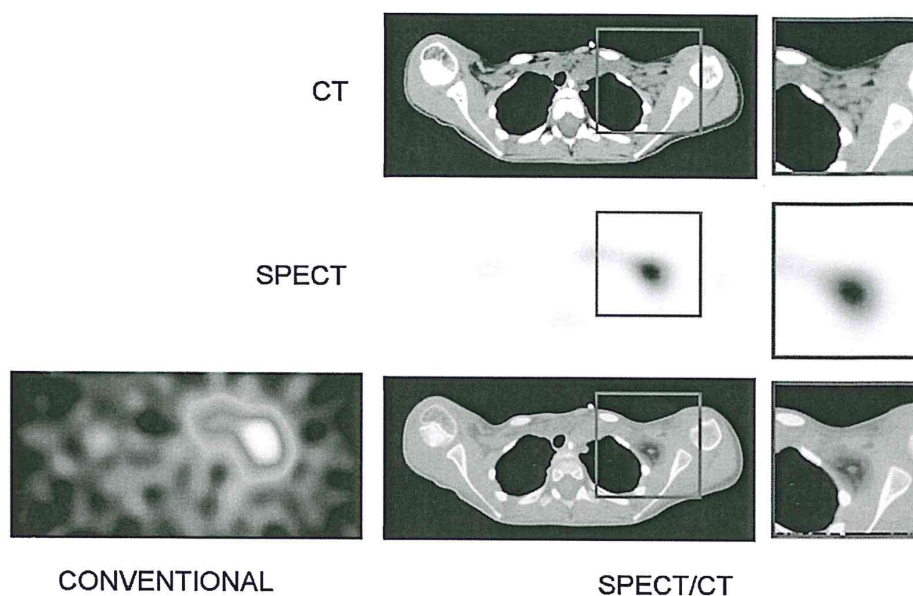


**Figure 6.** Images of  $^{131}\text{I}$ -metaiodobenzylguanidine (MIBG) of 7 year-old female with neuroblastoma with conventional SPECT (left) and CT (top right). SPECT image (middle right) and fused SPECT/CT image (bottom right) following compensation for photon attenuation and the geometrical response of the collimator (middle right). (Adapted and reproduced with permission from reference [32]).

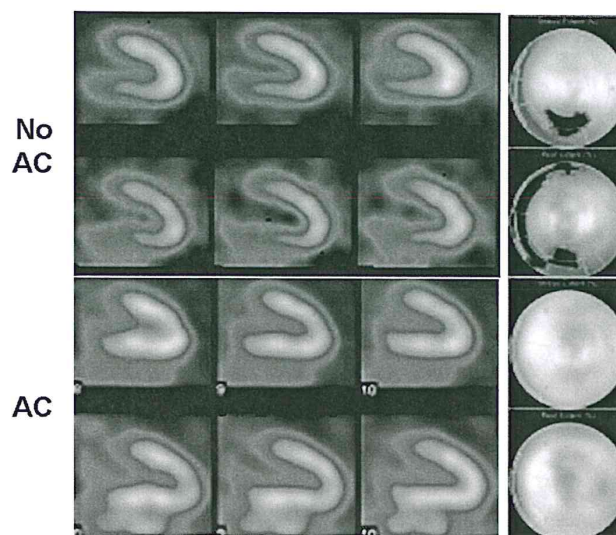


**Figure 7.**  $^{99m}\text{Tc}$ -sestamibi SPECT scan of 66 year old male with atypical chest pain reconstructed using conventional filtered backprojection without attenuation correction (top) and using iterative reconstruction with x-ray based attenuation correction (bottom). Conventional perfusion SPECT showed defect in the inferior wall. Iterative reconstruction with attenuation correction produced a perfusion image which was read as being normal as was confirmed with coronary angiography. (Courtesy of General Electric Healthcare, Inc.)



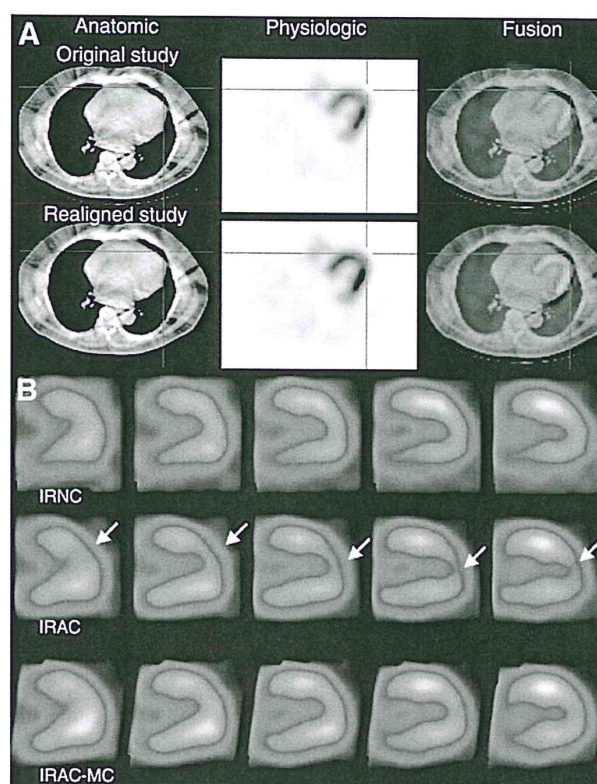
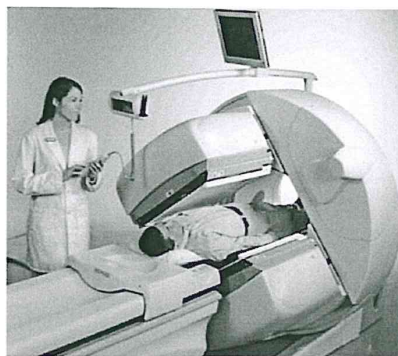
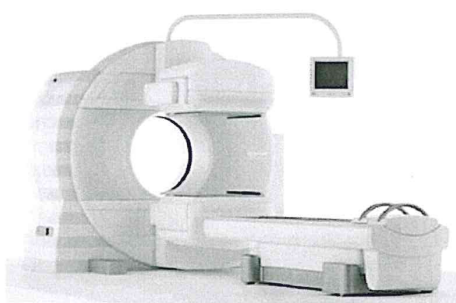


**Figure 8.**

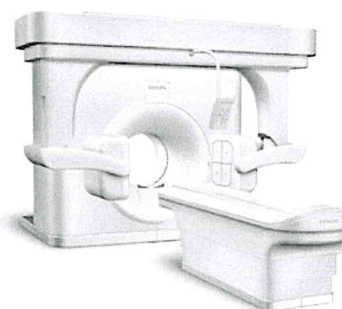
(A) Co-registered CT (top), SPECT (middle), and fused SPECT/CT (bottom) myocardial perfusion images with  $^{99m}\text{Tc}$ -sestamibi. Top row shows images with misalignment of SPECT/CT images. Bottom row show SPECT/CT images following registration using vendor-supplied software. (b) Vertical long-axis slices of  $^{99m}\text{Tc}$ -sestamibi images without attenuation correction (IRNC), with attenuation correction of original data (IRAC), and with attenuation correction following correction for spatial misalignment (IRAC-MC). Defects in apical anterior wall of original attenuation-corrected SPECT images are not apparent in uncorrected SPECT images and in attenuation corrected SPECT images following correction for misalignment. (Reproduced with permission from reference [62]).



GE Infinia Hawkeye



Siemens Symbia



Philips Precedence

**Figure 9.** Clinical SPECT/CT systems in 2007. (Top) GE Infinia Hawkeye; (Bottom left) Siemens Symbia; (Bottom right) Philips Precedence (Courtesy of GE Healthcare, Inc., Siemens Medical Solutions, Inc., Philips Medical Systems, Inc.)



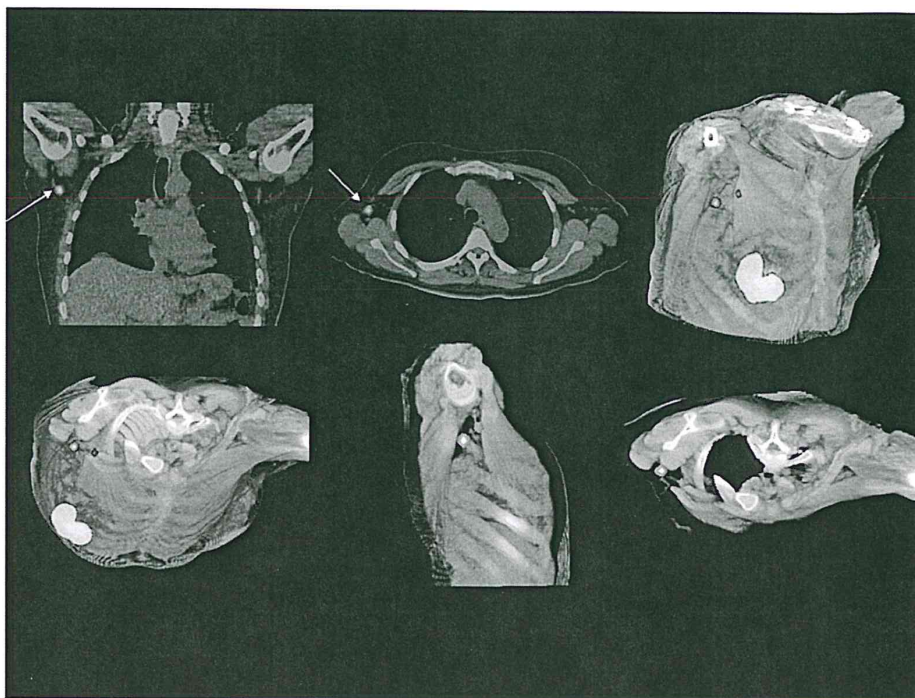


**Figure 10.**

Lymphoscintigraphy for sentinel node detection of patient with primary breast carcinoma. SPECT/CT study demonstrates two sentinel lymph nodes in the axilla adjacent to the trapezius and pectoralis major muscles. Volume rendering of fused datasets from thin slice spiral CT and SPECT demonstrate positions of the sentinel nodes in preparation of surgical planning for node removal. (Courtesy of Siemens Medical Solutions, Inc.)

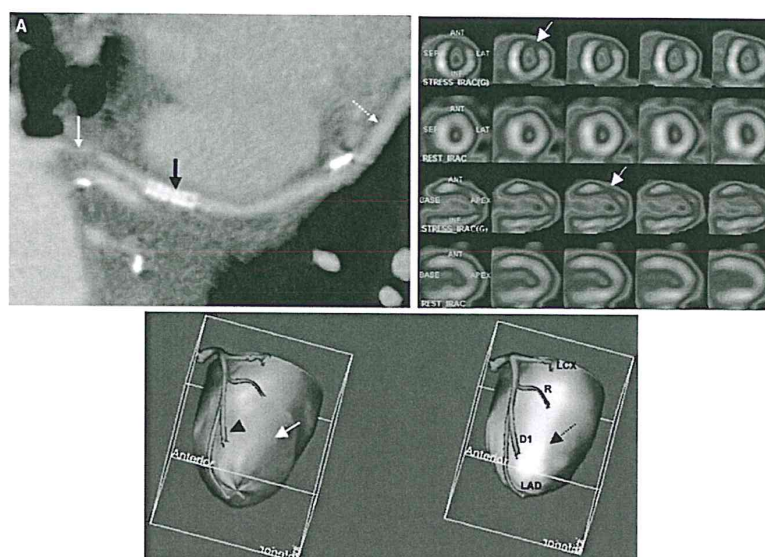


**Figure 11.**

CT coronary angiography (CTCA) and  $^{99m}\text{Tc}$ -sestamibi stress/ $^{201}\text{Tl}$  rest SPECT images with x-ray based attenuation correction. Study performed with 16-slice CT scanner and dual-head variable-angle SPECT system with shared patient table to spatially register images from patient with coronary artery bypass graft. (Top left) Curved multiplanar re-formats of CTCA data shows severe irregular stenosis (solid white arrow), patient stent (black arrow), and patent diagonal artery distal to anastomosis with saphenous vein graft (dotted white arrow). (Top right) Cardiac perfusion SPECT study at stress (first and third rows) and rest (second and forth rows) shows reversible perfusion defect in the anterolateral wall (arrows) consistent with myocardial ischemia. (Bottom) Surface rendered image showing myocardial perfusion from SPECT study fused on left ventricular surface with native left coronary tree. At bottom left, decreased perfusion in the anterolateral wall (blue region, arrow) corresponds to region of first diagonal artery (arrow head). Fused data (bottom right) shows normal perfusion at rest in the same area (dotted arrow). The fused SPECT/CTCA image is consistent with myocardial ischemia related to a tight, irregular stenosis of the proximal saphenous vein graft to the first diagonal artery. LAD indicates left anterior descending coronary; D1, first diagonal branch; R, ramus intermedius coronary; and LCX, left circumflex coronary. (Adapted and reproduced permission of reference [115].)



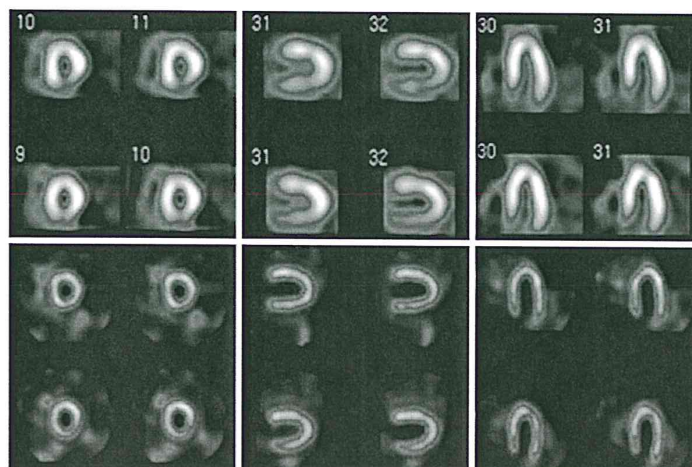


**Figure 12.**

$^{99m}\text{Tc}$ -sestamibi myocardial perfusion images obtained with conventional SPECT (top) and with novel high-efficiency “D-SPECT” system (bottom) using  $^{99m}\text{Tc}$ -sestamibi stress/rest gated protocol. High-dose (first row) and low-dose (second row) images acquired with 28 mCi and 10 mCi respectively of  $^{99m}\text{Tc}$ -sestamibi, and required 16 min and 20 min with conventional SPECT versus 4 min and 2 min with D-SPECT. Conventional SPECT interpreted as having reversible inferior wall defect. D-SPECT interpreted as normal and was confirmed by coronary angiography. (Courtesy of Spectrum Dynamics, Ltd.)

Table 1

Clinical Applications of SPECT/CT Cited

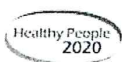
Anatomical/Disease Site	Radiopharmaceutical	SPECT/CT Application
Adrenal masses	$^{123}\text{I}$ -metaiodobenzylguanidine, $^{75}\text{Se}$ -cholesterol	Anatomical localization [161]
Biliary leak	$^{99\text{m}}\text{Tc}$ -diisopropyl iminodiacetic acid	Anatomical localization [141]
Bone scintigraphy	$^{99\text{m}}\text{Tc}$ -methylene diphosphonate, $^{99\text{m}}\text{Tc}$ -dicarboxypropane diphosphonate	Anatomical localization, attenuation correction [162-169]
Brain cancer	$^{99\text{m}}\text{Tc}$ -tetrofosmin	Anatomical localization [170]
Breast cancer	$^{99\text{m}}\text{Tc}$ -sestamibi	Anatomical localization [171]
Colorectal cancer	$^{99\text{m}}\text{Tc}$ -labelled macroaggregated albumin	Hepatic artery infusion of chemotherapy [172]
Coronary artery calcification	$^{99\text{m}}\text{Tc}$ -tetrofosmin	Coronary artery calcification correlated with myocardial perfusion imaging [120,142]
Coronary artery disease	Thallium-201, $^{99\text{m}}\text{Tc}$ -sestamibi, $^{99\text{m}}\text{Tc}$ -tetrofosmin	CT coronary artery calcification correlated with myocardial perfusion imaging [116,117,126]
Coronary artery disease, myocardial perfusion imaging	Thallium-201, $^{99\text{m}}\text{Tc}$ -sestamibi, $^{99\text{m}}\text{Tc}$ -tetrofosmin	Attenuation correction [29,60-64,114,121-124,153,173]
Coronary bypass graft	Thallium-201, $^{99\text{m}}\text{Tc}$ -sestamibi	Bypass graft definition and localization [115]
Crohn's disease	$^{99\text{m}}\text{Tc}$ -HMPAO-labeled leukocytes	Anatomical localization [137]
Esophageal cancer, adenocarcinoma of gastric cardia	$^{99\text{m}}\text{Tc}$ -nanocolloid or $^{99\text{m}}\text{Tc}$ -sulfur colloid	Anatomical localization, surgical planning [174]
Head/neck cancer	L-3- $^{123}\text{I}$ -iodine-alpha-methyl-tyrosine, $^{123}\text{I}$ -labeled L19(scFv)2 antibody	Anatomical localization [175-177]
Hepatic haemangioma	$^{99\text{m}}\text{Tc}$ -labelled red blood cells	Anatomical localization [178,179]
Hepatic carcinoma	$^{99\text{m}}\text{Tc}$ -macroaggregated albumin	Anatomical localization [180]
Human immunodeficiency virus (HIV)	$^{99\text{m}}\text{Tc}$ -sulfur colloid	Anatomical localization of microbicide surrogate [138]
Infection	Gallium-67, $^{111}\text{In}$ -labeled leukocytes	Anatomical localization [133-136]
Left ventricular function	$^{99\text{m}}\text{Tc}$ -tetrofosmin	Regional wall motion evaluation, myocardial muscle mass, ejection fraction, cardiac volumes [118]
Lung (ventilation/perfusion)	$^{99\text{m}}\text{Tc}$ -Technegas, $^{99\text{m}}\text{Tc}$ -macroaggregated albumin	Anatomical localization and registration of ventilation-perfusion patterns [139,140]
Lung cancer	$^{99\text{m}}\text{Tc}$ -sestamibi, $^{99\text{m}}\text{Tc}$ -depreotide	Anatomical localization [181-183]
Lymphoma	Gallium-67	Anatomical localization [184-186]
Myocardium	$^{111}\text{In}$ -oxime-labeled mesenchymal stem cells	Stem cell imaging [187]
Neuroendocrine tumor	$^{111}\text{In}$ -octreotide, $^{123}\text{I}$ -metaiodobenzylguanidine, $^{99\text{m}}\text{Tc}$ -depreotide	Attenuation correction, depth-dependent compensation for collimator response [32,59,75,103-105,161,188-190]
Non-Hodgkin's lymphoma	$^{131}\text{I}$ -anti-CD20 rituximab	Radioimmunotherapy dosimetry [112]
Osteomyelitis	$^{99\text{m}}\text{Tc}$ -labelled antigranulocyte antibodies, $^{99\text{m}}\text{Tc}$ -dicarboxypropane diphosphonate, $^{99\text{m}}\text{Tc}$ -hexamethylpropylene amine oxime (HMPAO)	Anatomical localization [129-131]



Anatomical/Disease Site	Radiopharmaceutical	SPECT/CT Application
Pancreatic carcinoma	$^{99m}\text{Tc}$ -macroaggregated albumin	Anatomic localization, evaluation of therapeutic efficacy for pancreatic chemotherapy [180,191-193]
Parathyroid gland	$^{99m}\text{Tc}$ -sestamibi	Anatomical localization [161,194-198]
Pheochromocytoma	$^{123}\text{I}$ -metaiodobenzylguanidine	Anatomical localization [189]
Prostate cancer	$^{111}\text{In}$ -capromab pendetide	Attenuation correction, anatomical localization, monitoring brachytherapy [12,26,199-204]
Sentinel lymph node biopsy (bladder cancer, head/neck carcinoma, lung cancer, melanoma, oral cavity prostate cancer, squamous cell carcinoma)	Thallium-201, $^{99m}\text{Tc}$ -albumin colloid (albures), $^{99m}\text{Tc}$ -sulfur colloid, $^{99m}\text{Tc}$ -tin colloid, $^{99m}\text{Tc}$ -colloidal human serum albumin, $^{99m}\text{Tc}$ -antimony sulphide colloid	Anatomical localization, attenuation correction, surgical planning [183,205-217]
Sentinel lymph node biopsy (breast cancer)	$^{99m}\text{Tc}$ -rhenium colloid	Attenuation correction, anatomical localization [218,219]
Splenosis	$^{99m}\text{Tc}$ -labelled colloids, $^{99m}\text{Tc}$ -labelled heat-damaged red blood cells	Anatomical localization [220,221]
Sympathetic nervous system tumors	$^{123}\text{I}$ -labeled metaiodobenzylguanidine	Anatomical localization, attenuation correction [222]
Temporomandibular joint (TMJ)	$^{99m}\text{Tc}$ -methylene diphosphonate	Anatomical localization, TMJ dysfunction [132]
Thyroid carcinoma	Iodine-131	Anatomical localization, therapeutic monitoring [161,223-225]
Whole body (phantom study)	Technetium-99m	Attenuation correction, radioimmunotherapy dosimetry [226]







Search HealthyPeople.gov

Log in

Go

[Topics & Objectives](#)[Leading Health Indicators](#)[Data Search](#)[Healthy People in Action](#)[Tools & Resources](#)[Webinars & Events](#)[About](#)[Home](#) » [2020 Topics & Objectives](#) » Heart Disease and Stroke [Print](#) [Share](#)

## Heart Disease and Stroke

[Overview](#)[Objectives](#)[Interventions & Resources](#)[National Snapshots](#)

### Goal

Improve cardiovascular health and quality of life through prevention, detection, and treatment of risk factors for heart attack and stroke; early identification and treatment of heart attacks and strokes; and prevention of repeat cardiovascular events.<sup>2</sup>

### Overview

Heart disease is the leading cause of death in the United States.<sup>1</sup> Stroke is the third leading cause of death in the United States. Together, heart disease and stroke are among the most widespread and costly health problems facing the Nation today, accounting for more than \$500 billion in health care expenditures and related expenses in 2010 alone.<sup>2</sup> Fortunately, they are also among the most preventable.



View HP2020 Data for:  
[Heart Disease and Stroke](#)

The leading modifiable (controllable) risk factors for heart disease and stroke are:

- High blood pressure
- High cholesterol
- Cigarette smoking
- Diabetes
- Poor diet and physical inactivity
- Overweight and obesity

Over time, these risk factors cause changes in the heart and blood vessels that can lead to heart attacks, heart failure, and strokes. It is critical to address risk factors early in life to prevent the potentially devastating complications of chronic cardiovascular disease.

Controlling risk factors for heart disease and stroke remains a challenge. High blood pressure and cholesterol are still major contributors to the national epidemic of cardiovascular disease. High blood pressure affects approximately 1 in 3 adults in the United States,<sup>3</sup> and more than half of Americans with high blood pressure do not have it under control.<sup>3</sup> High sodium intake is a known risk factor for high blood pressure and heart disease,<sup>4</sup> yet about 90 percent of American adults exceed their recommendation for sodium intake.<sup>5</sup>

The risk of Americans developing and dying from cardiovascular disease would be substantially reduced if major improvements were made across the U.S. population in diet and physical activity, control of high blood pressure and cholesterol, smoking cessation, and appropriate aspirin use.<sup>6</sup>

### Why Are Heart Disease and Stroke Important?

Currently more than 1 in 3 adults (81.1 million) live with 1 or more types of cardiovascular disease.<sup>2</sup> In addition to being the first and third leading causes of death, heart disease and stroke result in serious illness and disability, decreased quality of life, and hundreds of billions of dollars in economic loss every year.

### Related Topic Areas

[Chronic Kidney Disease](#)[Diabetes](#)[Nutrition and Weight Status](#)[Physical Activity](#)[Tobacco Use](#)

The burden of cardiovascular disease is disproportionately distributed across the population. There are significant disparities in the following based on gender, age, race/ethnicity, geographic area, and socioeconomic status:<sup>2</sup>

- Prevalence of risk factors
- Access to treatment
- Appropriate and timely treatment
- Treatment outcomes
- Mortality

#### [Back to Top](#)

### Understanding Heart Disease and Stroke

Disease does not occur in isolation, and cardiovascular disease is no exception. Cardiovascular health is significantly influenced by the physical, social, and political environment, including:

- Maternal and child health
- Access to educational opportunities
- Availability of healthy foods, physical education, and extracurricular activities in schools
- Opportunities for physical activity, including access to safe and walkable communities
- Access to healthy foods
- Quality of working conditions and worksite health
- Availability of community support and resources
- Access to affordable, quality health care

### Emerging Issues in Heart Disease and Stroke

No national system exists to collect data on how often cardiovascular events occur or recur, or how often they result in death. Similarly, there is inadequate tracking of quality indicators across the continuum of care, from risk factor prevention through treatment of acute events to posthospitalization and rehabilitation. New measures and tools are needed to monitor improvement in cardiovascular health over the next decade.

Other emerging issues in cardiovascular health include:

- Defining and measuring overall cardiovascular health.
- Assessing and communicating lifetime risk for cardiovascular disease.
- Addressing depression as a risk factor for and associated condition of heart disease and stroke.
- Examining cognitive impairment due to vascular disease.
- Dealing with substantial gaps in the cardiovascular surveillance system.

#### Learn More

[CDC Heart Disease and Stroke Prevention](#)  
[NIH National Heart, Lung, and Blood Institute](#)  
[NIH National Institute of Neurological Disorders and Stroke \(NINDS\)](#)  
[Interactive Atlas of Heart Disease and Stroke](#)

### References

<sup>1</sup>Xu J, Kochanek KD, Murphy SL, et al. Deaths: Final data for 2007. Natl Vital Stat Rep. 2010;58(19).

<sup>2</sup>Lloyd-Jones D, Adams RJ, Brown TM, et al. Heart disease and stroke statistics—2010 update: A report from the American Heart Association statistics committee and stroke statistics subcommittee. Circulation. 2010;121:e1-e170.

<sup>3</sup>Ostchega Y, Yoon SS, Hughes J, et al. Hypertension awareness, treatment, and control—continued disparities in adults: United States, 2005–2006. [NCHS Data Brief] Centers for Disease Control and Prevention, National Center for Health Statistics, Division of Health and Nutrition Examination Surveys; 2008. Available from: <http://www.cdc.gov/nchs/data/databriefs/db03.pdf> [PDF - 1.16 MB]


<sup>4</sup>Institute of Medicine. Dietary reference intakes for water, potassium, sodium, chloride, and sulfate, 1st ed. Washington, DC: National Academies Press; 2004.

<sup>5</sup>Centers for Disease Control and Prevention. Sodium intake among adults—United States, 2005–2006. MMWR. 2010;59:746–9.



8/10/2015

Heart Disease and Stroke | Healthy People 2020

<sup>6</sup>Agency for Healthcare Research and Quality (AHRQ), U.S. Preventive Services Task Force. Aspirin for the prevention of cardiovascular disease [Internet]. AHRQ; 2009. Available from: <http://www.uspreventiveservicestaskforce.org/uspstf/uspasm.htm> 

<sup>7</sup>Agency for Healthcare Research and Quality (AHRQ). 2008 National Healthcare Quality & Disparities Reports [Internet]. AHRQ; 2009. Available from: <http://www.ahrq.gov/research/findings/nhqdr/index.html>

#### Footnote

\*Cardiovascular events are defined for this purpose as heart attacks, hospitalizations for heart failure, and strokes.

[Back to Top](#)

Find us on:



Enter your email for updates:

[Sign Up](#)

[About](#)

[Contact Us](#)

[Site Map](#)

[Accessibility](#)

[Privacy Policy](#)

[Disclaimers](#)

[Freedom of Information Act](#)

[Healthy People 2010 Archive](#)

[Web Badges](#)

[Viewers and Players](#)



A Federal Government Web site managed by the U.S. Department of Health and Human Services • 200 Independence Avenue, S.W., Washington, DC 20201 • © 2014

Site last updated 08/10/15

# **EXHIBIT D**



## SARAH BULL

## EXPERIENCE

2008-Present     Stamford Hospital, Stamford, CT

*Chief Physicist, RSO*

- Developed Cyberknife center from installation, Linac, robot and TPS commissioned, daily treatment protocols.
- Developed and implemented QA program.
- In process of commissioning Monte Carlo for Multiplan
- Coverage for therapy department at main hospital. Two accelerators, orthovoltage, IMRT/IGRT, brachytherapy. Implemented Enhanced Dynamic Wedge, Field-in-Field treatment.

2005- 2008     New Milford Hospital, New Milford, CT

*Chief Physicist – Faculty Appointment Columbia University*

- All the Senior Physicist duties plus work with biomedical engineers and IT staff to effectively support the Department's needs; ensured that safe, accurate and efficient treatment planning and treatment delivery carried out in the Department; promoted teaching, research and development activities throughout the hospital.
- Developed and oversaw all quality assurance at Regional Cancer Center as AMP. Managed onsite Physics Staff and support Radiation Safety needs in the hospital.

1999-2005     Columbia University, New York Presbyterian Regional Cancer Center at New Milford Hospital, New Milford, CT

*Physicist/Senior Physicist*

- Commissioned/accepted Varian 2100 C/D, Ximatron, CAD Plan, Eclipse, MMS, Varisource, Advantage workstation and Brachyvision systems.
- Implemented external beam, LDR, HDR and therapy radionuclide programs and associate QA programs. Implemented Helios IMRT and therapeutic Radiopharmaceutical program.
- Wrote and implemented all NRC licenses. Maintain federal and state regulatory standards for Radiation Oncology. Radiation in-services for hospital staff.
- Developed and oversaw all quality assurance at Regional Cancer Center as AMP. Managed onsite Physics Staff. Participated in research and developing technologies at CPMC.

1997-1999     Memorial Sloan-Kettering Cancer Center Sleepy Hollow, NY

*Junior Physicist*

- Assisted chief physicist in all areas of clinical duties, and with treatment measurements and maintaining federal and state regulatory standards and weekly quality assurance.
- Utilized three-dimensional planning techniques along with MLC, IMRT, and portal vision imaging.
- Monthly and annual calibration of Ximatron Simulator and 2100 C/D Varian accelerator. Prepared staff education and personnel training
- Devised measuring techniques for measuring radiation doses in unusual clinical situations. Experience with most dosimetry measuring systems.

1993-1997     Memorial Sloan-Kettering Cancer Center     NY, NY

*Dosimetrist*

- External beam treatment planning using both traditional and three-dimensional conformal radiation planning and weekly quality assurance
- Development of planning techniques utilizing dynamic MLC (DMLC) and participated in research and protocol implementation.
- Monthly and annual calibration of Ximatron Simulator and 600 C Varian accelerator

## EDUCATION

---

- ABR Certification - Therapy (Current MOC)
- |           |                        |              |
|-----------|------------------------|--------------|
| 1995-1998 | Columbia University    | NY, NY       |
| o         | MS., Medical Physics   |              |
| 1988-1992 | University of Redlands | Redlands, CA |
| o         | BA, Physics/Philosophy |              |

## RESEARCH& PUBLICATIONS

---

- o "Effects of Lung Inhomogeneity for Intensity Modulated Fields" Poster presentation AAPM 2005
- o State of Connecticut DEP board to review new regulations for submission to legislator and to become agreement state. Presented to state congress fall 2005.
- o "Evaluation of Simplified Electron Beam Setup for CadPlan" Poster presentation AAPM 2003
- o State of Connecticut board to develop and implement Radiological Dispersion Disaster plan.
- o "Dosimetry Study of Re-188 liquid balloon for intravascular brachytherapy using optical laser CT scanner for polymer gel dosimeters". Radiotherapy & Oncology Journal of the European Society for Therapeutic Radiology and Oncology. #439 Poster 2001
- o "A Study of the effects of internal organ motion and setup error on dose escalation in conformal prostate treatments". Presented at the 40<sup>th</sup> Annual Meeting of the American Society for Therapeutic Radiology and Oncology, Phoenix Civic Center, October 27, 1998
- o Prone versus supine treatment position for patients with prostatic cancer treated with three-dimensional conformal external beam radiation therapy. 1996





**CURRICULUM VITAE**

Harvey Leon Hecht, MD, D.A.B.R., F.A.C.R., D.A.B.N.M.  
 50 Brewster Road  
 Scarsdale, NY 10583

**EMPLOYMENT**

1970 – Present	Attending Radiologist The Stamford Hospital, Stamford, CT
2006 – 2009	Chief of Radiology Stamford Hospital, Stamford, CT
1967 –now	Clinical Associate Professor of Radiology College of Physicians and Surgeons Columbia University, New York, New York Chief of Service: Larry Schwartz, MD
1968 – 1970	Head of G.I. Section Columbia Presbyterian Radiology Department
1967 – 1968	Head of Bone Room Columbia Presbyterian Radiology Department
1970 – 1998 and Continuing currently	Columbia Presbyterian Hospital, New York, NY Teaching Radiology elective students 2 hours, once a month Teaching Residents 1 hour per month Noon conference twice per year

**EDUCATION**

**RESIDENCIES:** Columbia-Presbyterian Hospital, New York, NY  
 Radiology: 3<sup>rd</sup> Year (July 1966 – June 1967)  
 Radiology: 2<sup>nd</sup> Year (July 1965 – June 1966)  
~~Radiology 1<sup>st</sup> Year (July 1964 – June 1966)~~

Montefiore Hospital, Bronx, NY  
 Medicine: One year (July 1963 – June 1964)

**INTERNSHIP:** Montefiore Hospital, Bronx, NY  
 Mixed Internship in medicine and surgery 7/1/62 – 6/30/63

**MEDICAL SCHOOL:**

Albert Einstein College of Medicine, Bronx, New York  
 MD degree – 1962



**CURRICULUM VITAE**  
**HARVEY LEON HECHT, MD**  
 (Continued)

**UNDERGRADUATE:** Amherst College, Amherst, Massachusetts  
 A.B. degree, cum laude – 1958

**PROFESSIONAL LICENSES  
 AND ASSOCIATIONS:** Certified by:  
 American Board of Radiology – 1968  
 American Board of Nuclear Medicine – 1972

Current license in New York - #90654  
 Current license in Connecticut - #14685  
 Current License in California - #G12841

**MEDICAL SOCIETY  
 MEMBERSHIPS:** American Roentgen Ray Society – 1992 to present  
 Radiological Society of North America – 1975 to present  
 New York Roentgen Ray Society – 1967 to present  
 Stamford Medical Society – 1972 to present  
 Radiological Society of Connecticut – 1972 to present  
 Fairfield County Medical Society – 1972 to present  
 American College of Radiology – 1970 to present  
 American Medical Association – 1967 to present  
 NY State Chapter of American College of Radiology 1976

International Society of Lymphology – 1968 – 1970  
 New York County Medical Society – 1967 – 1972

**AWARDS:** American College of Radiology  
 Fellowship: September 1983  
Physicians Recognition Award from Stamford Hospital  
 2010 – Integrity, Compassion, Respect, Teamwork,  
 Accountability  
Stamford Hospital Medical Staff, Administration and  
Employees

**LECTURES GIVEN:**

**1970:** Organized and moderated course on Radiology of the  
 Gastrointestinal Tract Under the Auspices of the Department  
 Of Radiology. Columbia University College of Physicians  
 And Surgeons, May 6-8, 1970.

**1974:** Post Graduate Course at Columbia-Presbyterian Hospital,  
 Marcy 1974. Gave lecture on Arthrography in course  
 "Radiology of Bones and Joints"

**REFERENCES FOR DR. HARVEY L. HECHT****At Stamford Hospital:**

Noel Robin, MD, Chief of Medicine and Endocrinology (203) 276-7485  
Charles Littlejohn, MD, Chief of Colorectal Surgery (203) 323-8989  
Frank Masino, MD, Chief of Radiation Therapy (203) 276-7886  
Neil Dreyer, MD, Nephrology (203) 327-1187  
Michael Parry, MD, Chief of Infectious Disease (203) 353-1427  
Jason Podber, MD, Chief of ER (203) 276-7054  
Peter Tenicki, MD, Chief Hospitalist (203) 276-7298  
Antonio Pantaleo, MD, Endocrinologist (203) 359-2009  
Mary Arden Cardone, MD, Endocrinologist (203) 359-2009  
Paul Weinstein, MD, Head of Hematology Oncology (203) 325-2695  
Steve Lo, MD  
Neil Cohen, MD

**At Columbia Presbyterian:**

Dr. Frieda Feldman, MD, Chief of Musculo-Skeletal (212) 305-9869 (office)  
(212) 305-9023 (reading room)  
Dr. Rashad Fawwaz, MD, Chief of Nuclear Medicine (212) 305-7138 or 2721

**At Montefiore Hospital:**

Dr. Leonard Freeman, MD, Chief of Nuclear Medicine (718) 920-6060

**At New York Presbyterian:**

Ravi Thakur, MD - (917) 359-3727

**At Stamford Hospital:**

Steve Horowitz, MD, Chief of Cardiology (203) 325-7480  
Stuart Waldstreicher, MD, GI (203) 967-2100  
Peter Gardiner, MD, GI (203) 967-2100  
Peter Hughes, MD, Orthopedic (203) 325-4087

---



**CURRICULUM VITAE**  
**HARVEY LEON HECHT, M.D.**  
**(Continued)**

**LECTURES GIVEN (continued)**

- 1975** Post Graduate Course at Columbia-Presbyterian Hospital; March 1975  
Gave lecture on Arthrography at course "Radiology of Bones and Joints."
- 1978** Radiology of Bones and Joints. Post graduate course sponsored by  
Columbia Medical School. October 17-20, 1978.  
Gave lecture on Arthrography of Ankle, Wrist and Elbow - October 20.
- Gave lecture on Arthrography at Orthopedic section of New Jersey  
College of Medicine and Dentistry - November 30.
- 1980** Gave lecture on Arthrography of Knee, Shoulder and Elbow.  
Symposium on Arthrography at Albert Einstein College of Medicine  
September, 1980.
- 1982** Gave lecture on Arthrography of Ankle and Elbow at course "Radiology  
Of Bones & Joints" sponsored by Columbia Medical School  
May 30 - April 2.

**MILITARY SERVICE:**

United States Army Reserve Medical Corps  
Captain - 6 years (1962-1969)  
Honorable discharge

**PERSONAL:**

Date and place of birth: February 10, 1937; Brooklyn, New York  
Married to Gail E. Solomon, M.D.  
Three children





**EILISH C. HOURIHAN MS, RN, NEA-BC**  
 2970 Farmwalk Road Yorktown Heights, New York 10598  
[eilishcmc@msn.com](mailto:eilishcmc@msn.com) (914) 962-1604

---

### EXECUTIVE MANAGEMENT

Dynamic Healthcare Executive with extensive accomplishments in operations, change management, driving quality initiatives, developing proactive teams accountable for their actions and initiating programs that foster best practices and patient satisfaction in acute care, long term care and psychiatric organizations. Decisive leader who excels in progressive and demanding environments while remaining pragmatic and focused. Effective strategic planner with the vision and fortitude to achieve and exceed operational goals. Proven track record of establishing collaborative relationships with medical staff. Established champion for patient care, quality and nursing professionalism.

### CORE COMPETENCIES

- |                           |                           |
|---------------------------|---------------------------|
| • Organizational redesign | • Regulatory compliance   |
| • Leadership development  | • Contract management     |
| • Business skills         | • Performance improvement |
| • Effective communication | • Relationship management |
- 

### PROFESSIONAL EXPERIENCE

#### **Stamford Hospital System, Stamford, CT**

##### **Director of the Heart and Vascular Institute and Cardiovascular Services** **2015-Present**

Provide direct responsibility for the operations and management of the Heart and Vascular Institute services and programs to include Cardiovascular Services, Outpatient Cardiology Diagnostic services, Open Heart services exclusive of the operating room. Responsible for 100 FTEs with a \$10 million budget.

Key Achievement:

- Successfully lead the Cardiovascular and Open Heart teams to their first two Transaortic Valve replacement (TAVR) procedures

##### **Director of Clinical Operations** **2012-2015**

##### **Emergency Department, Immediate Care Center, Cardiac Catheterization Suite, Infusion Center, Stroke Program**

Provide overall administrative, operational and clinical management of the Nursing department units for this Level 2 Trauma Center. Responsible for 120 FTEs with an \$8 million budget. Currently developing the ANCC Journey to Excellence Magnet document. Member of the Master Facility Planning strategic team for the new Stamford Hospital currently under construction.

Key Achievements:

- Achieved Joint Commission Disease Specific Stroke re-certification
- Developed unit specific Quality Improvement dashboards for clinical areas
- Improved first case on time start by 66% over six months in Cardiac Catheterization Lab
- Assisted in the coordination of the construction for the new Electrophysiology Lab
- Restructured the Cath Lab Operations Group meeting to improve operational outcomes, supplies cost savings and physician satisfaction

**VillageCare of New York, New York, N Y****2012****Vice President Residential Services****Village Care Rehabilitation and Nursing Center, Rivington House and 46<sup>th</sup> and Ten**

Provided organization specific leadership and operational goals for three distinct facilities. Village Care Rehabilitation and Nursing Center is a 105 bed Subacute facility. Rivington House is a 206 bed AIDS designated Long Term Care facility. 46<sup>th</sup> and Ten is an 85 bed Assisted Living facility. Responsible for three budgets for a total of \$61 million with approximately 430 employees. Provided organizational oversight for Quality Program for both residential and community based services. Co-Chair of Executive Credentialing Committee.

**Key Achievements:**

- Developed structure for providing monthly operational updates to the Board of Directors
- Assisted with the recruitment of key physician leadership positions
- Guided all three facilities through successful NYS Department of Health annual surveys

**Westchester County Healthcare Corporation, Valhalla, NY****1987-2012****Vice President Patient Care Services****2008-2012****Neuroscience Units, Trauma ICU, Emergency Department,****Burn Unit, Critical Care Transport Team and Nursing Operations**

Provided overall administrative, operational and clinical management of the Nursing department units for this Level 1 Trauma and Tertiary/Quaternary care facility. Managed a \$20 million budget with 120 employees and 66 inpatient beds. Developed Quality Assurance and Performance Improvement initiatives for all nursing units. Chair/member of multiple hospital and nursing committees including the development of the Electronic Medical Record and Joint Commission (Provision of Care) Chapter Leader. Provided nursing oversight to the Nurse Practitioners in the Neuroscience Service. Participated in Nursing union negotiations.

**Key Achievements:**

- Improved patient satisfaction scores from 76% to 86% over two quarters in 2010
- Expanded services of Critical Care Transport Team
- Implemented Critical Care services in the Burn Unit
- Increased the capacity and capability of the Neuroscience Step-down unit from four to eight beds
- Maintained 0% Wound Prevalence rate for three consecutive quarters (2010-2011) in the Neuroscience units

**Vice President Patient Care Services, Behavioral Health Hospital****Children's Unit, Adolescent Unit, Adult Units, Medically Complex Geriatric Unit, Comprehensive Psychiatric Program, ECT Program**

Provided overall administrative, operational and clinical management of all nursing department units in the 105 bed hospital. Managed a \$10 million budget with 180 employees. Developed Quality Assurance and Performance Improvement initiatives of all units/programs

**Key Achievements:**

Implemented new staffing standards to improve patient outcomes



- Developed Patient Teaching folders as a result of a Performance Improvement Project
- Successfully participated in Office of Mental Health (OMH) as well as Joint Commission Surveys

### **Taylor Care Center at Westchester, Long Term Care Facility**

**2005-2009**

#### **Executive Director**

Provided overall administrative responsibility for planning, implementing and evaluating delivery of quality care for a 229 bed hospital-based long term care facility. Responsible for a \$30 million budget with a staff of 260 employees. Direct reports included Director of Nursing, Director of Finance, Medical Director and Director of Pastoral Care. Responsibilities also extended to Westchester Medical Center (WMC), a Level 1 tertiary/quaternary care facility to include the Physical Medicine and Rehabilitation Nursing unit and the Physical and Occupational Therapy Departments. Assisted WMC with Joint Commission survey readiness via operational improvement initiatives.

#### **Key Achievements:**

- Increased census of sub-acute services by 33% over three years (2005 to 2008)
- Expanded ventilator weaning program to maximum census of 20 residents from census of 10-12 pts
- Decreased average number of annual New York State Department of Health survey deficiencies from six to one over 4 years
- Improved accounts receivables of Taylor Care Center by \$5 million
- Developed Resource Manual for Hospital Administrator On-Call group
- Ensured that standards for certification for Association for Clinical Pastoral Education (ACPE) program for WMC were maintained
- Selected and implemented a web-based policy management software application for all hospital policies to streamline processes and minimize risk
- Developed and implemented a facility Closure Plan and provided a seamless transition for residents/families and employees

### **Taylor Care Center at Westchester, Long Term Care Facility**

**1999-2004**

#### **Director of Nursing**

Provided overall responsibility for administrative and clinical management of Nursing Department. Responsible for a \$10 million budget with a staff of 200 employees. Ensured regulatory compliance with New York State Department of Health, Joint Commission and OSHA standards. Developed Nursing staff to meet increasing acuity needs of hospital patients by expanding competencies. Responsibilities also extended to WMC for the Wound Care Program and the Respiratory Therapy Department.

#### **Key Achievements:**

- Implemented cost savings initiative in both hospital and long term care facility in supply chain management
- Developed new programs to maximize Case Mix Index and improve revenue
- Decreased cost of Wound Program by \$50,000 over one year

### **Case Manager Sub-Acute Services**

**1997-1998**

### **Westchester Medical Center**

#### **Nursing Care Coordinator**

**1996-1996**

**1991- 1992**

Associate Nursing Care Coordinator	1997- 1997 1992- 1996
General Staff Nurse Coronary Care Unit	1987- 1991
St. Joseph's Medical Center Yonkers, New York Nurse Recruiter, Head Nurse Medical-Surgical Unit, Staff Nurse Medical Intensive Care Unit, Staff Nurse Medical-Surgical Unit	1982- 1987

### EDUCATION AND LICENSES

- **Master of Science** Case Management Pace University, Pleasantville, New York
- **Bachelor of Science Nursing** Dominican College, Orangeburg, New York
- **Nursing Diploma** Cochran School of Nursing, Yonkers, New York
- **Nurse Executive Advanced NEA-BC**
- **Licensed Nursing Home Administrator** State of New York (Inactive Status)
- **Registered Nurse** States of New York and Connecticut

### PROFESSIONAL ASSOCIATIONS

- **American Organization of Nurse Executives** (current)
- **New York Organization of Nurse Executives** (past)
- **New York Association of Homes and Services for the Aging**  
**Chair and Co-Chair of Downstate Nursing Council** (past)





**David H. Hsi, MD***Curriculum Vitae*CV Date: July 1, 2015PERSONAL INFORMATION

Name David H. Hsi

Work: 30 Shelburne Road, Stamford, CT 06902

Telephone

Work 203-276-7474

Cell 203-274-3746

E-Mail Address: [dhsi@stamhealth.org](mailto:dhsi@stamhealth.org) [davidhsi.md@gmail.com](mailto:davidhsi.md@gmail.com)

Citizenship: United States of America

EDUCATION

Shanghai Medical University, Shanghai, China. 1978-1986

(Shanghai First Medical College: Medicine, Bachelor Degree 1978-1983)

(Shanghai Medical University: Vascular Medicine, Master Degree, 1983-1986)

Massachusetts College of Pharmacy

Specialty program in radiopharmacy. Boston, MA.

1994-1995

POSTDOCTORAL TRAINING

Research in Neuro-Vascular Surgery, Boston Children's Hospital, MA. 1986-1988

Mentor: Dr. Anthony Lorenzo &amp; Dr. E. Gary Fisher

Echocardiography Lab. Brigham &amp; Women's Hospital, Boston, MA. 1988-1989

Mentor: Dr. Martin St. John Sutton

Internship and Residencies in Internal Medicine: Newton-Wellesley Hospital, Tufts School of Medicine, Boston, MA. 1989-1992 Intern, Resident, and Chief Resident.

Cardiology Fellowship: Brigham &amp; Women's Hospital &amp; West Roxbury VA Medical Center, Harvard Medical School, Boston, MA. 1992-1995

LICENSURE INFORMATION

Massachusetts 09-11-1990, #74941

New York 02-28-1995, #198769-1

California 10-01-2002, #C-50978

New Jersey 10-28-2010, #25MA08855900

Educational Commission for Foreign Medical Graduates

1989-Lifetime

American Board of Internal Medicine

1992, 2002 &amp; 2012

American Board of Internal Medicine, Cardiovascular Disease.

1995 &amp; 2005



Certification Board of Nuclear Cardiology	1998 & 2008
National Board of Echocardiography (Adult Comprehensive Level)	1999 & 2009
American Board of Vascular Medicine	2010
Certification Board of Cardiovascular Computer Tomography	2011

#### Postdoctoral Fellowship Award(s)

Excel Award for best medical resident, Newton-Wellesley Hospital, Tufts School of Medicine, Boston 1992. Chief: Dr. Henry Yager

ACC Travel Award for Cardiology Fellows, West Roxbury VA Medical Center, Harvard Medical School 1986. Chief: Dr. Richard Shannon (currently Chief of Medicine at University of Pennsylvania Hospital, Philadelphia, PA)

#### FACULTY APPOINTMENTS

Professor of Clinical Medicine, Robert Wood Johnson School of Medicine, NJ,	2013-Now
Clinical Professor of Medicine, Philadelphia College of Osteopathic Medicine, Philadelphia, PA	Aug. 2011- June 2015
Clinical Associate Professor of Medicine, University of Rochester School of Medicine and Dentistry, Rochester, NY	April 2007-March 2011
Clinical Assistant Professor of Medicine, University of Rochester School of Medicine and Dentistry, Rochester, NY	April 2005-March 2007
Senior Clinical Instructor of Medicine, University of Rochester School of Medicine and Dentistry, Rochester, NY	July 2003-March 2005

#### PROFESSIONAL HOSPITAL AND ADMINISTRATIVE APPOINTMENTS

Attending cardiologist, Newark-Wayne Hospital, Newark, NY and Park Ridge Hospital, Rochester, NY	July 1995-Jan1997
Director of Nuclear Cardiology, St. Francis Hospital Heart Center, Roslyn, NY	Jan 1997-Oct. 1997
Director of Nuclear Cardiology, Director of Echocardiography and Chief of Cardiology, (Park Ridge Hospital) Unity Hospital, Rochester, NY.	1997-2011
Partner at University Cardiovascular Associates, Rochester, NY	2009-2011
Chair of Cardiology, Deborah Heart, Lung & Vascular Center, Brown Mills, New Jersey	March 2011- October 2104
Chief of Cardiology, Co-Director of the Heart & Vascular Institute, Stamford Hospital, Stamford, CT	October 1, 2014-Now

#### MEMBERSHIPS IN LOCAL AND STATE ACADEMIC AND PROFESSIONAL ORGANIZATIONS

New York State ACC	1995-2011
New Jersey State ACC	2011-Now
Fellow, American College of Cardiology	1992-Present
American Society of Nuclear Cardiology	1998-Present
Fellow, American Society of Echocardiography	1999-Present
One of the Founding Members, Society of Cardiovascular Computed Tomography	2005-Present

#### LECTURESHIPS AND VISITING PROFESSORSHIPS

Case presentations and Expert Panel at the Annual Noninvasive Cardiology Conference, University of Rochester Medical Center 1998, 1999, 2001, 2002, 2004, 2005, 2006, 2007, 2008, 2009, and 2010.

Grand rounds at Unity Hospital 2008: Food, Wine, & Heart Disease  
 Lecture at the First UCVA Cardiovascular Conference, Rochester, NY, 2009: Unusual Presentation of Hypertension  
 Grand rounds at Unity Hospital 2012; Review of Aortic Diseases  
 Grand rounds at Robert Wood Johnson University Hospital, NJ, 2012: Aortic & Vascular Diseases.  
 Grand rounds at Deborah Heart & Vascular Center, NJ 2013: Pregnancy & Heart Disease  
 Grand rounds at Deborah Heart & Vascular Center, NJ 2014: Review of TAVR clinical trials and hospital experience  
 Grand rounds at St. Christopher Children's Hospital, Drexel University, Philadelphia 2014: Syncope and Sudden Cardiac Death in Young Athletes

Expert Lectures: Mitral Valve Prolapse and Imaging in Mitral Valve Disease at the Great Wall International Congress of Cardiology, China 2013 (equivalent of ACC in the USA)

#### HONORS AND AWARDS

Outstanding Service in Cardiology, Department of Medicine, Unity Hospital, Rochester, NY, February 17, 2011  
 Mentor Award for Teaching of Fellows, Deborah Heart & Lung Hospital 2011-2012, and 2012-2013  
 Best Physician (Cardiology) in Southern New Jersey, 2011, 2013, and 2014  
 Top Doctors (Cardiology): Philadelphia Magazine 2014

#### EDUCATIONAL CONTRIBUTIONS

Daily teaching rounds, weekly and monthly lectures, mentoring residents for clinical research with multiple publications. Unity Hospital 1995-2010.  
 Dr. Vinodh Jeevanantham, currently at Wake Forrest University Hospital;  
 Dr. Ashim Aggarwal, currently at Heart Transplant Service, Advocate Christ Medical Center, Oak Lawn, Illinois,  
 Clinical cardiology fellows: daily teaching rounds, outpatient clinic, didactic and hands-on teaching for clinical cardiology, trans-thoracic and trans-



esophageal echocardiography, nuclear cardiology, and cardiovascular CT.  
Mentoring fellows for clinical research and publications, 2010-Now.

### PROFESSIONAL SERVICE ASSIGNMENTS AND RESPONSIBILITIES

Overseeing clinical cardiologists, physician assistants and cardiology fellows for their clinical rotation and patient care responsibilities. Receiving reports from the director of fellowship program. Providing cardiology, adult congenital heart disease, and vascular service in the outpatient clinic, executive cardiovascular evaluation, and intensive care unit, comprehensive echo service, interpretation of nuclear cardiology studies and cardiac CT images.

### PROFESSIONAL ADMINISTRATIVE ASSIGNMENTS AND RESPONSIBILITIES

At Deborah Heart and Lung Hospital, NJ 2011-Now  
Chair of the Graduate Medical Education Committee  
Member of the Medical Executive Committee  
Member of the Utilization Review Committee  
Member of the Clinical Information Systems Oversight Committee

Principle Investigator: Assessment of myocardial perfusion using PET imaging of Flurpiridaz F 18 injection in patients with suspected or known CAD, 2011. (Approved by the Sponsor: Lantheus Medical Imaging BMS747158-301.)

Sub-investigator: PROspective Multicenter Imaging Study for Evaluation of Chest Pain (PROMISE) 2011, Deborah Heart Center, NJ 2012-Now. Sponsor: NIH

Co-Principle Investigator: Percutaneous renal denervation in patients with resistant hypertension-SIMPLICITY-HTN-3 Deborah Heart Center, NJ 2011-now. Sponsor: Medtronic

Sub-Investigator: Echo-CRT for Patients with Heart Failure and Narrow QRS Complexes, Deborah Heart Center, NJ, 2011-now. Sponsor: Biotronics

Co-Principle Investigator: Parachute IV trial: for severe ischemic cardiomyopathy 2014

### PUBLICATIONS

#### **1. Original (scientific) articles**

Hsi DH, Bhagwath G, Coto M. Radionuclide and angiographic evidence of right coronary artery spasm. Journal of Nuclear Cardiology 8 (1), 2001

David H. Hsi, MD, Gerald F. Ryan, MD, Steven O. Helmets, MD, David C. Cheeron, MD. Large Aneurysms of the Ascending Aorta and Major Coronary Arteries in a Patient with Osler-Weber-Rendu Disease.

Mayo Clinic Proceedings 78:774-776, June, 2003

David Hsi, Gerald Ryan, Janice Taft, Thomas Arnone A 29-Year-Old Harken Disk Mitral Valve ---- Long-Term Follow-up by Echocardiographic and Cineradiographic Imaging. Texas Heart Inst J 2003;30:319-21

Vinodh Jeevanantham, Natasha Singh, Kenneth Izuora, John P. D'Souza, David H. Hsi  
Correlation of High Sensitivity C Reactive Protein and Calcific Aortic Valvular Disease Mayo  
Clinic Proceedings February 2007;82(2):171-174

Sankri-Tarbichi, P. Mathew, M. Matos, D. Hsi. Stress Related Cardiomyopathy  
Heart & Lung: The Journal of Acute and Critical Care, 2007 Jan; 36 (1): 43-46.

DH Hsi, A Roshandel, N Singh, T Szombathy, Z S Meszaros  
Headache response to (nitroglycerin) glyceryl trinitrate in patients with and without obstructive  
coronary artery disease.  
Heart (BMJ) 2005;91 (9): p. 1164-66

David H. Hsi, MD; Thomas N. Thompson; MD; Alexander Fructer, MD; Michael S. Collins, MD;  
Olaf U. Lieberg, MD; Hartwig Boepple  
Simultaneous Coronary and Cerebral Air Embolism after CT-guided Core Needle Biopsy of the  
Lung. Tex Heart Inst J 2008;35(3):555-7

Osuorji, Ikenna; Williams, Christina; Hessney, Joanne; Patel, Tejan; Hsi, David  
Acute Stress Cardiomyopathy Following Treatment of Status Asthmaticus  
Southern Medical Journal. 102(3):301-303, March 2009.

Garg, Praveen MD; Gupta, Ruchi MD; Hsi, David H. MD; Sheils, Lucy A. MD; DiSalle, Michael  
R. MD; Woodlock, Timothy J. MD  
Hypertrophic Cardiomyopathy and Symptomatic Conduction System Disease in Cardiac  
Amyloidosis. Southern Medical Journal: December 2006 - Volume 99 - Issue 12 - pp 1390-  
1392

Vinodh Jeevanantham,MD, Kavitha Manne,MDB, Mohan Sengodan,MD,  
James M Haley, MD, David H Hsi, MD: Predictors of Coronary Artery Disease in Patients with  
Left Bundle Branch Block who undergo Myocardial Perfusion Imaging Cardiology Journal  
2009;16(4):321-6.

David H. Hsi, Mahesh Krishnamurthy, Gerald F. Ryan, Pifu Luo, Timothy J. Woodlock,  
Successful Management of Hemopericardium and Cardiac Tamponade Secondary to Occult  
Malignancy and Anticoagulation  
Exp Clin Cardiol 2010;(2)e33-35

Umashankar Lakshmanadoss, Bryana M Levitan, David H Hsi  
Right Ventricular Failure in Sepsis. Cardiology Research 2011;2(1):48-49

Umashankar Lakshmanadoss, f, Saadia Sherazi, Ashim Aggarwal, David Hsi  
Mehmet K. Aktas, James P. Daubert, Abrar H Shah  
Underutilization of Implantable Cardioverter Defibrillator in Primary Prevention of Sudden  
Cardiac Arrest. Cardiology Research • 2011;2(1):1-6

Ashim Aggarwal, Saadia Sherazi, Bryana Levitan, Umashankar Lakshmanadoss,  
Naila Choudhary, Abrar Shah, David Hsi  
Corrected QT interval as a predictor of mortality in elderly patients with syncope  
Cardiology Journal 2011;18 ( 4): 395-400



Aggarwal A, Ritter N, Reddy L, Lingutla D, Nasar F, El-Daher N, Hsi D.  
Recurrent Pseudomonas aortic root abscess complicating mitral valve endocarditis.  
Heart & Lung Journal 2012 Mar-Apr;41(2):181-3

His DH, Patel B, George JC (Comments) Intraaortic Balloon Support for Myocardial Infarction  
with Cardiogenic Shock. N Engl J Med 2012; 367:1287-1296

David H. Hsi, Rajeev Marreddy, Mark Moshiyakhov, Ulrich Luft  
Regadenoson Induced Acute ST-Segment Elevation Myocardial Infarction and Multivessel  
Coronary Thrombosis J of Nuclear Cardiology March 5, 2013

Jennifer Ayers, DO, Ryan Mandell, DO, Kintur Sanghvi, MD, Rania Aboujaoude\*, MD, David H.  
Hsi, MD: Acute Coronary Thrombosis and Multiple Coronary Aneurysms in a 22 Year-old HIV  
Positive Patient. Texas Heart Institute Journal, April 2014 208-211.

David H. Hsi, Lynn B. McGrath, Judd Salamat, Mitchell Simon, and Jon C. George  
Epicardial Coronary Artery Compression Secondary to Pericardial Adhesions Demonstrated by  
Multi-modality Imaging, and Treated by Coronary Stenting  
Circulation: Images in Cardiovascular Medicine, 2014 (in revision)

#### Reviews:

David Hsi & G.V.R.K. Sharma: Treatment Options for Acute Myocardial Infarction in the  
Elderly. Federal Practitioner 13 (3) 15-24, 1996

Kintur Sanghvi, MD, David Hsi, MD: Transradial Renal Artery Stenting  
Cath Lab Digest Nov 14, 2012  
<http://www.cathlabdigest.com/Transradial-Renal-Artery-Stenting>

Omer Aziem, DO, David H. Hsi, MD, and Jon C. George, MD: Incremental Cardiac Output in  
Cardiogenic Shock with Percutaneous Hemodynamic Support Device. Cath Lab Digest  
Volume 21 - Issue 3 - March 2013  
<http://www.cathlabdigest.com/articles/Incremental-Cardiac-Output-Cardiogenic-Shock-Percutaneous-Hemodynamic-Support-Device>

Harit Desai, DO, David Hsi, MD, and Jon C. George, MD: Treatment of Fibromuscular  
Dysplasia of the Renal Artery With Cryoplasty. VASCULAR DISEASE MANAGEMENT  
2013;10(5):E86-E88 <http://www.vascular-disease-management.com/content/treatment-fibromuscular-dysplasia-renal-artery-cryoplasty>

## 2. Letters, editorials, short articles and other contributions

Hsi DH, Mock DJ, Rocco TA. Toxic Erythroderma due to Ticlopidine.  
New England Journal of Medicine 340 (15), 1999

Hsi DH, Alaimo DJ: Comparison of warfarin and aspirin for the prevention of recurrent ischemic  
stroke.  
New England Journal of Medicine 346 (15) 1170, April 2002

Hsi DH, Ryan GF: Prosthetic Heart Valves  
Cleveland Clinical Journal of Medicine 69 (6) 448, June 2002

Hsi DH, Patel B, George JC (Comments) Intraaortic Balloon Support for Myocardial Infarction with Cardiogenic Shock. N Engl J Med 2012; 367:1287-1296

David H. Hsi, Rajeev Marreddy, Mark Moshikhov, Ulrich Luft  
Regadenoson Induced Acute ST-Segment Elevation Myocardial Infarction and Multivessel Coronary Thrombosis J of Nuclear Cardiology, 2013 Jun;20(3):481-4

Jennifer Ayers, Ryan Mandell, Kintur Sanghvi, Rania Aboujaoude, David H. Hsi\*: Acute Coronary Thrombosis and Multiple Coronary Aneurysms in a 22 Year-old HIV Positive Patient. Texas Heart Institute Journal, April 2014 208-211.

Hsi DH, McGrath LB, Salamat J, Simon M, George JC.  
Epicardial coronary artery compression secondary to pericardial adhesions demonstrated by multi-modality imaging, and treated by coronary stenting.  
Circulation. 2014 Oct 7;130(15):e129-30

Manuscript reviewer (Cardiology) for Mayo Clinic Proceedings 2010-Now.

Manuscript reviewer (Cardiology) for Journal of Applied Physiology 2012-Now.

### 3. Abstracts

Farhat T, Zankoul FE, Hsi DH, Kirdar J, Rocco T, Khait I, Healey N, Birjiniuk, Khuri S.  
Myocardial tissue acidosis during aortic clamping predicts post-operative regional contractile dysfunction in patients undergoing cardiac surgery. Circulation 92 (8), 1995

Hsi DH, Manders WT, Shannon RP. SIV in non-human primates causes myocardial injury and cardiomyopathy following chronic but not acute infection. Circulation 92 (8), 1995

D.H. Hsi, N. Singh, Z. Meszaros, J.L. Thomas Clinical significance of hypotensive response in patients undergoing dipyridamole stress myocardial perfusion studies.  
Journal of Nuclear Cardiology July-August 2004 Vol.11 Number 4 • pS5

V Jeevanantham, K Manne, JM Haley, J Thomas, PK Mathew, DH Hsi  
PREVALENCE AND PREDICTORS OF CORONARY ARTERY DISEASE IN 307 PATIENTS WITH LEFT BUNDLE BRANCH BLOCK. American Society of Nuclear Cardiology Annual Scientific Session, 2006

K. Manne, V Jeevanantham, M Sengodan, JM Haley, DH Hsi:  
GENDER DIFFERENCES OF TREADMILL STRESS TEST WITH MYOCARDIAL PERFUSION IMAGING IN EVALUATION OF MYOCARDIAL ISCHEMIA in 538 PATIENTS  
American Society of Nuclear Cardiology Annual Scientific Session, 2006



Vinodh Jeevanantham, M.D., Rakesh Shrivastava MD, Aameera Khan MD, Srikant Nanapanneni MD, Mohan Sengodan MD, David Hsi MD  
Correlation of Body Mass Index and B type Natriuretic Peptide in Patients Presenting with Shortness of Breath  
European Society of Cardiology Heart Failure 2006

Vinodh Jeevanantham, Michael DiSalle, David H. Hsi  
RESPONSE TO NITROGLYCERIN PREDICT CORONARY ARTERY DISEASE IN PATIENTS PRESENTING WITH CHEST PAIN, 13th World Congress on Heart Disease, Vancouver, Canada, June 13, 2007

David H Hsi, Bryana Levitan, Kristin Peters, Ashim Aggarwal, Joan Thomas: Identification of Abdominal Aortic Aneurysm during Routine Echocardiography in 15,482 Patients  
Annual Scientific Meeting of the American Society of Echocardiography, Toronto, Canada, 2008 and Journal of American Society of Echocardiography, June 2008

David. H. Hsi, A. Aggarwal, R. Kepple, D. Barz, C. Becker, S. Frisone, C. Quaranto, K. Ross, J. Thomas, P. Mathew  
Adenosine Induced High-grade Heart Block During Stress Test -Incidence and Risk Profile in 1376 Patients, Annual Scientific Meeting of the American Society of Nuclear Cardiology, Boston, MA, Sep. 2008

Umashankar Lakshmanadoss, MD, Ashim Aggarwal MD, Kavitha Manne, MD, Vinodh Jeevanantham, MD, David H Hsi, MD, Saadia Sherazi, MD, Abrar H Shah, MD. Disparities in the Use of ICD For Primary Prevention Of Sudden Cardiac Death American College of Cardiology 58th Annual Scientific Session, March 2009

David H. Hsi, Ashim Aggarwal, Bryana Levitan, Peggy Manzer, Umashankar L Doss, Naila Choudhry, Nathan Ritter, Abrar H. Shah, Nayef T. El-Daher: Utilization of Transesophageal Echocardiography in 394 Patients with Suspected Bacterial Endocarditis—Clinical Profile and Appropriateness Criteria. The American Society of Echocardiography (ASE), 20th Annual Scientific Sessions, Washington DC, June 2009

Ashim Aggarwal, Naila Choudhary, Bryanna Levitan, Nayef T. El-Daher, David H. Hsi: Emerging Trends of Drug-Resistant Bacteria Causing Infective Endocarditis  
The 48th Annual Meeting of the Infectious Diseases Society of America (IDSA), October 21 - 24, 2010, Vancouver, British Columbia, Canada

D. H. Hsi, J. Ilonze, L. Reddy, R. Kepple, D. Nguyen, N. Ritter, J. L. Thomas, P. Mathew, A. H. Shah, S. Sheraz. Myocardial Perfusion Imaging with Treadmill Stress Test in 979 Patients: Evaluation of Clinical Parameters and Mortality Risk  
The 16th Annual Scientific Meeting of the American Society of Nuclear Cardiology, September 9-11, 2011, Denver, Colorado

A. Aggarwal, N. Ritter, L. Reddy, C. Burke, J. Haley, D. Hsi: Neurovascular imaging in evaluation of syncope: a study of 408 patients. European Society of Cardiology Congress 2011, Paris

#### 4. Book Chapters

Nova Science Publishers, Inc.

Myocardial Infarctions: Risk Factors, Emergency Management and Long-Term Health Outcomes (Published in July 2014)

Chapter: Myocardial Infarction and Cardiogenic Shock

Denise M. Zingrone, D.O., FACC, David H. Hsi, MD, FACC, FASE





**MICHAEL H. KING, M.D.**

Cell: (203) 252-8725

[mking@stamhealth.org](mailto:mking@stamhealth.org)**CURRENT:**

11/2011- Present

**Interim Chairman, Department of Radiology, Stamford Hospital, Stamford, CT.**

- Overall leadership of administrative and clinical activities within the Department
- Provide oversight and guidance to radiologists, nurses, technologists and support staff
- Formulate in conjunction with the administration, a clear vision and strategic plan for the short and long term goals and objectives for the Department of Radiology
- Demonstrate leadership, management ability and administrative experience to take the department to the next level of achievement
- Display financial stewardship and oversight of the budget for the department
- Articulate spokesman and advocate for the department and the hospital within the community
- Implemented Peer Review Oversight Committee and implemented hospital policies and procedures within the department
- Oversee clinical operations and quality assurance to optimize effectiveness and efficiency
- Successfully with a team approach launched Stamford Hospital's Lung Screening Program

2000-2011

**Radiologist, Stamford Hospital, Stamford, CT.**

Body CT, MRI, US and Musculoskeletal MRI specialist involving all MRI and CT and US diagnostic interpretations.

**AWARDS:****New York Magazine Best Doctors Award 2013****Connecticut Magazine Best Doctors Award 2010 through 2014****Best Doctors in America Award 2007 through 2014****Castle Connolly Top Doctors Award January 2013, 2014****MEDICAL****LICENSES:**

7 States

Arizona	38137	Massachusetts'	2227444
California	C53308	New Jersey	25MA08063500
Connecticut	038618	New York	213662-1
Florida	ME96537		

**EDUCATION:**

1999 - 2000

**Fellowship: Columbia University, Presbyterian Hospital, New York, NY.**

Body Imaging Fellowship (MRI, CT and Ultrasound)

995-1999

**Residency: Yale University, Norwalk Hospital and New Haven Hospital, CT.***Chief Radiology Resident* and Diagnostic Radiology Resident

1991-1995

**Medical School: University of Health Sciences Chicago Medical School, Chicago, IL**

1988-1991

**Undergraduate: Clark University, Worcester, MA.****SCHOLASTIC****TESTING:**

Board Certified Radiologist

Diplomate of the National Board of Medical Examiners

**HONORS:**

Chief Radiology Resident, 1998-1999

*Magna cum Laude*, Clark University, 1991

Viola D. Fuller Research Fellowship American Cancer Society, 1990

**PUBLICATIONS:**

Thoracic splenosis: non invasive diagnosis using Technetium – 99 sulfur colloid.

Viraj, Bhalani, Hecht, Harvey, Sachs, Paul, King, Michael. Connecticut Magazine 76(10)585-7

Management of afferent loop obstruction from recurrent metastatic pancreatic cancer using a vented gastrojejunostomy. Bakes, Debbie, Cain, Christian, King, Michael, Xiang Da Dong. World Journal of Gastrointestinal Oncology, July 15, 2013/volume 5/Issue 7

**COMMITTEES AND CONFERENCES:**

GU Tumor Board

General Tumor Board

Surgical M&amp;M

Medical Executive Committee

Cancer Coordinating Committee

GI Service Line Steering Committee

Patient Safety and Quality Committee

GYN Tumor Board

Lung Tumor Board

Oncology Grand Rounds

Credentialing Committee

Lung Cancer Committee

Technology Committee

Clinical Leadership Conferences

GI Tumor Board

Hematology Tumor Board

IRB Alternate

Medicine Critical Care

Champion Lung Cancer Screening

Trauma Performance Improvement

Chair Nominating Committee





## Marci D. Paulk, RT(R), CRA, MHA

### CONTACT INFORMATION

Marci D. Paulk  
193 Dogwood Lane  
Stamford, CT 06903

Cell: (203) 517-8390  
Work: (203) 276-4770  
Email: mpaulk@stamhealth.org

### SUMMARY

Results and productivity-driven administrator with ten years of diversified leadership experience in both the academic and investor-owned sides of health-delivery with increasing responsibilities in regulatory compliance, multi-facility leadership, project management, patient satisfaction and physician recruitment. Professional activities include having served on the Board of Directors for the AHRA, which is the professional organization for imaging managers, three terms as a United Way Loan Executive, an Air Force Honorary Commander for Eglin Air Force Base, and always a healthcare advocate. I recently completed the ACHE COO Boot Camp and I am actively pursuing my FACHE.

### EDUCATIONAL BACKGROUND

Masters of Health Administration Pfeiffer University, Charlotte, NC	2007
--	------

Bachelor of Arts in Kinesiology University of Colorado at Boulder, CO	2000
--	------

Associate of Science - Radiography Middlesex County College, NJ	1994
--	------

Associate of Business - Accounting Tidewater Community College, VA	1992
---	------

### WORK EXPERIENCE

<b>Executive Director of Radiology</b> Stamford Hospital, Stamford, CT	<b>August 2013 - Present</b>
---	------------------------------

Responsible for the growth and strategic planning for all of Radiology Services across the Stamford Health System. In collaboration with physician leadership, is accountable for development, implementation and oversight of quality improvements plans with a focus on operational and service excellence. Provides executive oversight to those managing the routine day to day operations of the respective Radiology Imaging Departments, including knowledge of key operations. <http://www.Stamfordhospital.org>

#### *Key Roles and Responsibilities*

- Promotes a professional environment with which patient care is delivered
- Program improvements to meet the needs of patients, physicians, staff and the community.
- Forecast, prepare and monitor operating and capital budgets for system for Radiology Imaging Services
- Increasing outpatient services revenue growth.
- Fiscal management for multi-facility imaging centers.

**Director of Radiology**

**Oct 2009 - Present**



Fort Walton Beach Medical Center, Fort Walton Beach, FL

Provides leadership for both Fort Walton Beach Medical Center and Destin Emergency Care Center imaging departments. Responsible for Physician relations and growing revenues for outpatient services. Provides the necessary administration, guidance and mentorship of all imaging departments ensuring appropriate staffing levels and policy adherence. Initiates strategic plans through direct involvement with the Fort Walton Beach executive leadership team. Continually evaluates all departments for regulatory, non-regulatory and accreditation programs such as JCAHO, HIPAA, Press Ganey and various other acts and initiatives. <http://www.fwbmc.com/>

*Key Roles and Responsibilities*

- Responsible for adhering to Joint Commission standards.
- Program improvements to meet the needs of patients, physicians, staff and the community.
- Responsible for adhering to the UOS for appropriate staffing models.
- Increasing outpatient services revenue growth.
- Fiscal management for multi-facility imaging centers.

**Director of Radiology and Cardiology Service Lines**

**May 2008 – Oct 2009**

Dosher Memorial Hospital, Southport, NC

Direct responsibilities include growing revenues for all Radiology and Cardiology services. Major recent projects include facilitating a permanent MRI solution within our brand new outpatient facility resulting in increased access for our MRI service line. Successfully migrated Dosher Memorial to a second generation PACS system as well as upgraded the organization to a complete digital mammography service line. Another area of emphasis is working towards completing departmental ACR accreditation. <http://www.dosher.org/>

*Key Roles and Responsibilities*

- Radiology and Cardiology physician relations.
- Fiscal accountability for Radiology and Cardiology Service Lines.
- Development and oversight of service line operating and strategic plans.
- ACR accreditation to comply with 2010 Medicare guidelines.

**Assistant Director of Radiology, Registration and Scheduling**

**Nov 2005 – May 2008**

Hunterdon Healthcare System, Flemington, NJ

Assists the Director of Radiology in managing, planning and organizing activities in Diagnostic and Supportive sections of Radiology Services including budget development and review as well as policy development and implementation to support organizational goals such as HIPAA and Press Ganey initiatives. Direct supervision responsibility of all imaging modalities within Radiology and support staff to include registration, scheduling, transcription and archivists. Major recent projects include PACS/RIS implementation and new Pre-Registration/Verification program. <http://www.hunterdonhealthcare.org/>

*Key Roles and Responsibilities*

- Responsible for planning, coordinating, and facilitating the use of personnel, financial, and technical resources in the daily operations of imaging services.
- Prepare work schedules, assign personnel, evaluate work performance and make recommendations for personnel actions.
- Accountable for adherence to state and federal rules and regulations on safety and quality assurance programs; ensures compliance with JCAHO, MQSA, federal, state and local agencies.

**Director of Radiology**

Coordinated Health (Six Campus Orthopedic Practice), Bethlehem, PA

Oct 2004 – Nov 2005

Assists the CFO in the development of programs for increasing new business revenues for five large outpatient orthopedic facilities and one imaging and surgery center located in the Lehigh Valley. Responsible for management over all modalities within Radiology spanning six facilities including the management of support staff.  
<http://www.coordinatedhealth.com/>

*Key Roles and Responsibilities*

- Monitors operations of assigned functions through supervision of key staff.
- Ensures the maintenance of quality standards, and compliance with all accreditation standards and licensure regulations.
- Direct the maintenance of department facilities, equipment, supplies and materials in a condition to promote efficiency, health, comfort, and safety of patients and staff.



**Assistant Director of Radiology, Coding and Transcription**  
Bassett Healthcare, Cooperstown, NY

Dec 2002 – Oct 2004

Primary responsibilities included direct supervision over all modalities within Radiology and support staff. Managed major PACS integration project from vendor selection and equipment acquisition till “go-live.” Acted as Interim Director of Radiology for 5 months while department operated without a Director. <http://www.bassett.org/>

*Key Roles and Responsibilities*

- Prepare work schedules, assign personnel, evaluate work performance and make recommendations for personal actions. Hire, train, and direct the work of outpatient radiology staff.
- Generate and discuss on a regular basis management reports from the system for analysis and consultation with the Director to ensure timely course corrections to operations as needed.
- Manages the strategic planning of major facilities construction/renovation projects to ensure the safe and effective placement of imaging equipment and efficiency of operations.

**Various Positions**

Nov 1994 – Dec 2002

UNC, Chapel Hill, NC, Radiographer  
University Hospital, Denver, CO, Radiographer  
Boulder Community Hospital, Boulder, CO, Radiographer  
Cambridge College, Aurora, CO, Radiology Program Manager  
Memorial Hospital, Colorado Springs, CO, Radiographer  
St. Joseph’s Hospital, Savannah, GA, Radiographer  
Hilton Head Hospital, Hilton Head Island, SC, Radiographer  
Orthopedic Reconstruction, Hilton Head Island, SC, Chief Radiographer  
Associated Radiology, Plainfield, NJ, Intern Radiographer

**PROFESSIONAL ACTIVITIES/CERTIFICATIONS**

**Professional Activities**

- |  |                       |
|--|-----------------------|
| • <b>Board of Directors, AHRA</b> – The Association for Medical Imaging Management | <b>2009 - 2011</b>    |
| • <b>Honorary Commanders Program</b> – Eglin Air Force Base                        | <b>2010 - Present</b> |
| • <b>United Way Loan Executive</b> – Okaloosa United Way                           | <b>2010 - Present</b> |
| • <b>Good Government Group</b> – Volunteer to increase membership                  | <b>2011 - Present</b> |
| • <b>AHRA</b> – Annual Conference Design Team Member                               | <b>2008 - 2009</b>    |
| • <b>AHRA</b> – Spring/Fall Conference Design Team Member                          | <b>2007 - 2009</b>    |
| • <b>Partners in Learning Recipient</b> – Florida Hospital                         | <b>2007</b>           |

**Licenses, Affiliations and Publications**

- |   |                       |
|---|-----------------------|
| • <b>RT® (ARRT)</b> – The American Registry of Radiologic Technologists                         | <b>1997 - Present</b> |
| • <b>Certified Radiology Administrator</b> – Professional Radiology Administrator Certification | <b>2009 - Present</b> |
| • <b>AHRA</b> – The Association for Medical Imaging Management                                  | <b>2005 - Present</b> |
| • <b>ACHE</b> – American College of Healthcare Executives                                       | <b>2010 - Present</b> |
| • <b>LINK Magazine Author</b> – Partners in Learning Article                                    | <b>2007</b>           |
| • <b>LINK Magazine Author</b> – Employee Satisfaction Article                                   | <b>2006</b>           |

**REFERENCES**

Available upon request.





Kathleen A. Silard, RN, BSN, MS, FACHE  
 6 Intrieri Lane  
 Greenwich, CT 06830  
 E-mail: [ksilard@stamhealth.org](mailto:ksilard@stamhealth.org)

(Home) 203-861-4068

(Business) 203-276-7505

### **PROFESSIONAL PROFILE:**

Senior Healthcare Executive with extensive experience in health care system operations, strategic planning and ambulatory care system development. A knowledgeable leader with strong financial, analytical and problem solving skills. Excellent communication skills with diverse constituencies including trustees, physicians, patients, employees and the community.

### **PROFESSIONAL EXPERIENCE:**

1/6/03 - Present

**Executive Vice President/Chief Operating Officer**  
**Stamford Health System**  
**30 Shelburne Road**  
**Stamford, CT**

- Responsible for operations and patient care executive leadership of 305 bed Stamford Hospital with an operating budget of \$600 million dollars.
- Senior executive leading the Facility Master Plan development and plans for the replacement hospital – a \$450 million dollar project.
- From 2010-2012 served as the CNO for Stamford Hospital in addition to COO.
- Achieved three successful JCAHO surveys with Distinction. Achieved JCAHO certification in Stroke, Joint Replacement and Spine. First hospital in Fairfield County to achieve all three certifications.
- Lead Womens Breast Center to receive the Gold Prize in the Connecticut Quality Improvement Award. A first step towards the Malcolm Baldrige National Quality Award.
- Implemented emergency and Elective Angioplasty and Electrophysiology Programs. Redesigned patient care delivery to reduce door to balloon time to under 90 minutes.
- Led the team to implement a full service Open Heart Surgery program with superior quality outcomes and volume tracking to budget.
- Improved inpatient satisfaction from the 20<sup>th</sup> to 90<sup>th</sup> percentile.
- Improved patient satisfaction in ED from 40<sup>th</sup> to 87<sup>th</sup> percentile.
- Improved patient experience in Hospital and Tully Surgical Centers to 91<sup>st</sup> and 93<sup>rd</sup> percentile rankings.
- Led Lean Six Sigma Management team that improved throughput in Emergency Services to reduce wait times and overall LOS.
- Led the team that performed a financial turnaround of \$30 million dollars through revenue enhancements and cost reductions.
- With Board of Trustees, transferred VNHC losing \$1 million per year, to independent status and later merged with Greenwich VNA.
- Orchestrated the sale of Edgehill to Benchmark Senior Living for \$71.5M.
- Implemented Lab Outreach Program that aligned physician practices with the hospital. Grew volume from 70,000 to 1.5 million tests and had a net positive operating margin of \$20 million dollars.

- With physician leadership developed service line growth in Heart & Vascular Institute Surgery, Orthopedics, GI, Women's Service and Cancer.
- Implemented PACS film-less all digital imaging, voice recognition technology and multiple new technologies in the Imaging areas (IMRT, IGRT, CyberKnife, 64 Slice CT/CTA).
- Opened Darien Imaging Center with Planetree model of care that exceeded business plan in first year of operations. Grew Imaging procedures from 150,000 to 180,000 procedures in three years.
- With Foundation, secured \$5 million dollar gift for new Pediatric Inpatient unit and \$10 million dollar gift for new Emergency Department and \$6M gift for Bennett Cancer Center.

1/1/99 - 12/02

**Executive Vice President and Chief Operating Officer**  
**St. Joseph's Health Care System**  
**703 Main Street**  
**Paterson, NJ**

- Responsible for the executive leadership of: 651 bed St. Joseph's Regional Medical Center; 151 bed St. Vincent's Nursing Home, 600,000 visit Ambulatory Care System; 200 bed St. Joseph's Wayne Hospital; 200,000 visit Visiting Health Services of New Jersey.
- Under executive leadership, Patient Care Services became one of 14 hospitals nationwide to achieve Magnet Award Status from the ANCC.
- Responsible for an operating budget of over \$500 million dollars.
- Developed and implemented strategic plan to assume sponsorship of Wayne General Hospital as part of St. Joseph's Health Care System.
- Reduced operating expenses by \$45 million over two years.
- Built and occupied a new nursing home facility increasing from 141 to 151 beds.
- Developed program growth in Cardiovascular, Surgical, Renal, Geriatrics, Women's & Children's Services that achieved 1,600 increased admissions over two years.
- Built and occupied a new state of the art dialysis facility increasing from 50 to 60 stations.
- Achieved a successful JCAHO Survey.
- Built and opened a new Pediatric Emergency Room.
- Implemented several new Information Technology projects including PACS Radiology System (Picture Archiving System), Cerner Laboratory Information System, Cineless Cath Lab, SMS Pharmacy System and SMS Lifetime Clinical Record.
- Developed plans for a new Ambulatory Imaging and Women's Center.

9/94 - 1/99

**Executive Director**  
**Montefiore Medical Group**  
**Montefiore Medical Center**  
**Bronx, NY**

- Provided executive leadership for the Montefiore Medical Group which merged and reorganized the original Medical Group and the former Ambulatory Care Network into a primary care and multi-specialty group practice of 150 physicians that provided 500,000 visits to 170,000 patients in 31 offices throughout the Bronx and Westchester. Operated the School Health and Homeless programs with 50,000 visits. The total operating budget for the Montefiore Medical Group was \$72 million dollars.



- Project leader for the architectural plans and construction of over 16 new health centers and satellite offices.
- Developed a comprehensive 3 tiered physician compensation plan that rewarded physicians for meeting quality of care, patient satisfaction and income objectives.
- Developed and implemented a business plan to bring 1,000 obstetrical deliveries to Montefiore.
- Managed and negotiated full risk and primary care contracts with Oxford, US Healthcare, Aetna, Blue Cross (Healthnet & Healthease), Prucare, MetraHealth and Local 1199.
- Installed IDX Billing and Managed Care System applications to automate billing and medical management of 30,000 managed care patients, half of which were insured through full risk capitation agreements.

5/90 - 9/94

**Associate Director****Montefiore Medical Center****The Jack D. Weiler Hospital of the Albert Einstein****College of Medicine, Bronx, NY**

- Managed the Departments of Anesthesia, Anatomical and Clinical Pathology, Ambulatory and Same Day Surgery, Operating Room, Post-Anesthesia Care, Emergency Department, Patient Relations, Nutrition/Cafeteria, Chaplaincy, Endoscopy, Perfusion, Vascular Laboratory and Volunteers with total annual operating budgets of \$27 million.
- Administratively responsible for the Clinical Departments of Surgery, Urology, Dentistry, Otolaryngology, Obstetrics/Gynecology, Pediatrics, Orthopedics, Psychiatry, Plastic, Vascular, and Cardiothoracic Surgery.
- Developed and implemented plans to expand the Ambulatory Surgery Unit from 4 to 14 beds and increased volume of Ambulatory Surgery procedures by 6,100 in two years.
- Project leader in the development of Montefiore Medical Park, a 60,000 square foot multi-specialty Medical Practice for the Departments of Medicine, Dentistry, Radiology, Surgery, Otolaryngology, Neurology, Vascular, Cardiothoracic and Plastic Surgery.

5/84 - 5/90

**Assistant to Vice President of Operations****Montefiore Medical Center****The Jack D. Weiler Hospital of the Albert****Einstein College of Medicine****Bronx, NY**

- Responsible for the management of the Pharmacy, Respiratory Care, Pre-Admission Testing, Anatomical and Clinical Pathology, Admitting, Radiation Oncology, Volunteers, Adult and Pediatric Dialysis Departments with total annual operating budgets of \$12.5 million.

9/82 - 4/84

**Assistant Director, Health Service****Iona College****New Rochelle, NY**

- Cooperative operation of college health service which provided health screening, maintenance and teaching as well as community referral services to students, faculty and administration.

7/79 - 8/82

**Staff Nurse - Pediatric and Neonatal Intensive Care Units****Montefiore Medical Center****The Jack D. Weiler Hospital of the Albert Einstein****College of Medicine****Bronx, NY**

- Direct nursing management for neonates and pediatric patients requiring hospitalization

**EDUCATION:**

June 1984

**Iona College - Master of Science - Honors**

Major in Health Care Systems Management

June 1979

**Herbert H. Lehman College - Bachelor of Science**

Major in Nursing

**HONORS:**

Sigma Theta Tau

1985 Brother Richard Power Award for Academic Excellence in Health Care Systems Management

2008 Greenwich YWCA BRAVA Award recipient for Leadership and Community Service

Chairperson of 2008 Fairfield County Heart Walk

Chairperson of 2002-2008 Greenwich Scholarship Committee, Greenwich PTA Council

**LICENSE:**

Registered Nurse New York and Connecticut

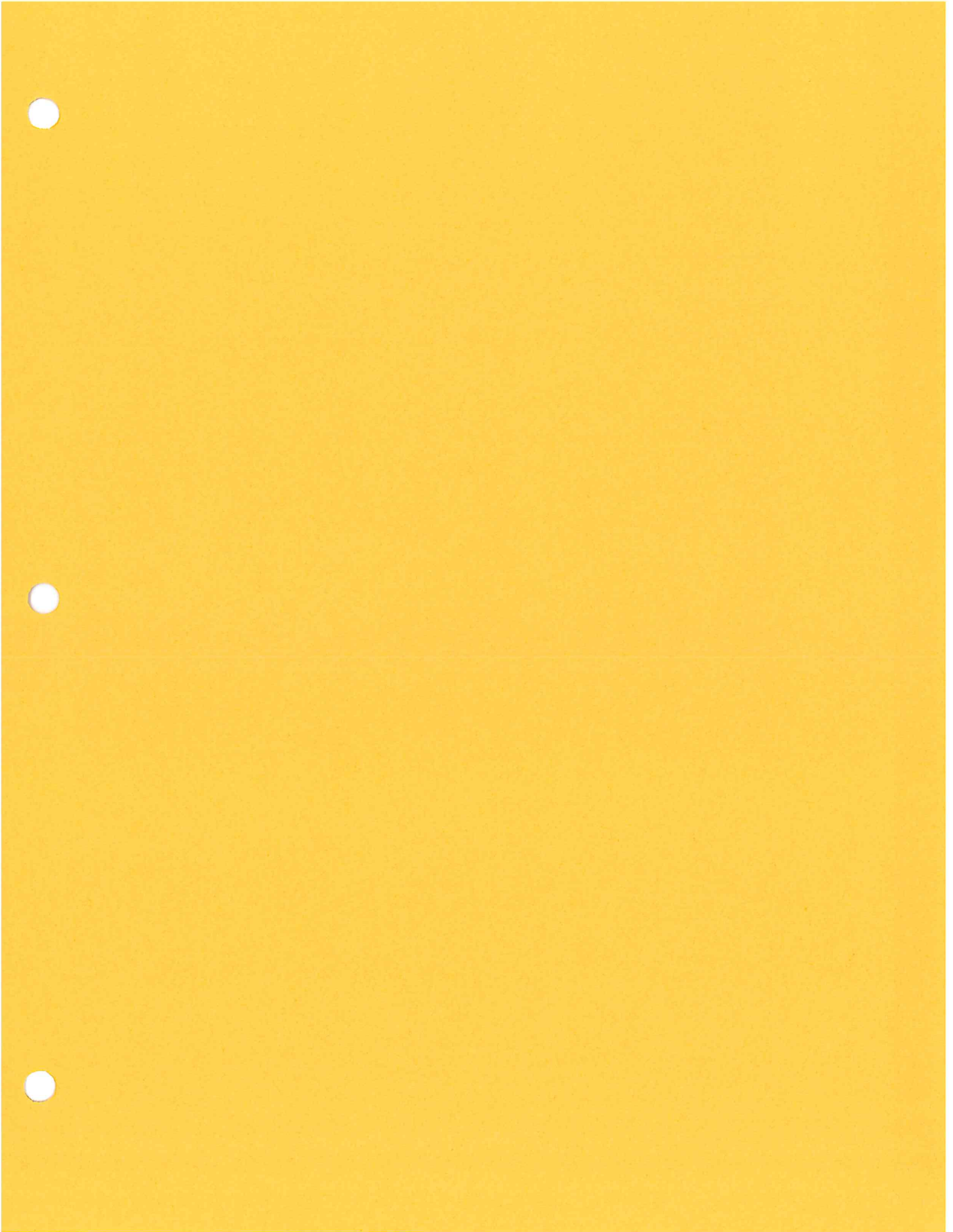
**MEMBERSHIPS:**

Fellow American College of Healthcare Executives

American Hospital Association

Medical Group Management Association





BETH ANN VARA  
 8 New Street #C  
 Ridgefield, CT  
 203.482.8849  
 bvara@stamhealth.org

#### DEGREES/ACCREDITATIONS/CERTIFICATIONS

**Radiologic Technologist, School of Radiology** 1992 - 1994

**United Hospital Medical Center, Port Chester, NY**

Registered Radiologic Technologist (ARRT)

Registered Mammography Technologist (ARRT)

State of Connecticut RT Licensee

**Ithaca College, Ithaca, NY**

1981 - 1985

Bachelor of Arts/Economics; Minor: Physics & Art History

**Western Connecticut State University, Danbury, CT**

2011 - Present

Master Degree Health Administration

Expected graduation date: May 2014

#### WORK EXPERIENCE

**Stamford Hospital, Stamford, CT**

Dec. 2013 – Present

**Director of Radiology**

- Direct, coordinate, and oversee the daily activities of all operations of the Department of Radiology, including all modalities and sites of service
- Assist with the development of capital and expense budget for imaging sites and administrative cost centers
- Manage expenses associated with staff, supply inventory, and equipment maintenance focusing on maximizing efficiencies and cost saving measure
- Regularly examines alternative methods of providing department services in order to reduce operational costs
- Investigates trends and development in Radiologic practices and techniques
- Establish and maintain strong/positive relationships with referring physicians and their office staff, vendors, and other department staff throughout the
- Determines measurable check points for various department projects, programs and services
- Maintain authority for recruitment, hiring, and progressive discipline processes for clinical and administrative staff associated with imaging and support services
- Demonstrate understanding of staff needs and mentor/train staff in order to achieve highest level of productivity and performance while developing/implementing opportunities for staff growth
- Perform annual and mid-year reviews, mentoring, and idea sharing with direct reports.
- Establish, review, and oversight of updating policies and procedures on an annual basis
- Ensure compliance with regulatory agencies such as, JCAHO, ACR, MQSA, and other regulatory agencies as required
- Manage customer service and service recovery efforts as necessary; train and oversee staff to handle situations directly and appropriately.
- Continually seek opportunities to further refine leadership skills and expertise in all areas related to healthcare administration
- Maintain active membership in related industry, professional associations

**Stamford Hospital, Stamford, CT****Assistant Director of Radiology****Sept. 2011 – Dec. 2013**

- Directly responsible for managing operations of all ambulatory imaging services, radiology central scheduling office, radiology coding/insurance preauthorization team and support services at Stamford Hospital
- Budget preparation for radiology ambulatory imaging services
- Monitor revenue, expenses, exam volume and FTE utilization
- Promote positive relationship with referring physicians through strong communication skills and outreach
- Perform mid-year and annual reviews for managers of ambulatory imaging services, radiology central scheduling office, radiology coding/insurance preauthorization team and support services at Stamford Hospital
- Closely involved with growth and design of future ambulatory imaging serves (i.e.: Chelsea Piers)
- Manage customer service and service recovery efforts as necessary

**Stamford Hospital/Tully Center, Stamford, CT****Chief Administrator of Ambulatory Imaging and Stamford Hospital's Women's Breast Center****Aug. 2005 – Aug. 2011**

- Manage outpatient modalities, including:
  - Mammography
  - Radiography
  - Ultrasound
  - CT Scan
  - MRI
  - Nuclear Medicine
  - Bone Densitometry
  - Immediate Care Center
- Manage a staff of 50+ employees. Responsibilities include:
  - Conduct new employee interviewing and hiring
  - Shift and vacation scheduling
  - Staff mentoring and daily task management
  - Development and execution of disciplinary action plans
  - 90 day initial, ongoing and annual competency reviews
  - Oversee new employee training
- Time card and payroll processing
- Bill and invoice processing for department
- Departmental budgeting
- Conduct all departmental related meetings
- Responsible for all aspects of departmental Customer Service
- Oversee equipment maintenance
- Clinical imaging as patient load dictates
- Active involvement in planning and implementation of new satellite office in Darien, CT. Scheduled to open May 2006.

**Stamford Hospital/Tully Center, Stamford, CT****Staff Radiology and Mammography Technologist****Oct. 2004 – July 2005**

- Radiography
- Mammography
  - Stereotactic Biopsy
  - Needle Localization
  - Quality Assurance
- Bone Densitometry

**Radiology Associates, Wallingford, CT****Staff Radiology and Mammography Technologist****June 2000 – Sept. 2004**



Diagnostic Radiology, Mammography and Ultrasound, Mt. Kisco, NY  
Chief Radiology and Mammography Technologist

May 1997 – Sept. 2004

New Rochelle Radiology, New Rochelle, NY  
Mammography Technologist – Per Diem

Jan. 1997 – Mar. 1997

United Hospital Medical Center, Port Chester, NY  
Mammography Technologist – Per Diem

Oct. 1996 – Aug. 1997

United Hospital Medical Center, Port Chester, NY  
Coordinator of Mammography Department

July 1995 – May 1996

United Hospital Medical Center, Port Chester, NY  
Staff Radiology Technologist

Aug. 1994 – June 1995

#### **PUBLICATION**

"The Quest for a Winning Breast Center"  
Radiology Management November/December 2010

2010

#### **PRESENTATION**

"The Quest for a Winning Breast Center"  
AHRA Annual Meeting 2010, August 2009 – Las Vegas, Nevada

2009



Jane Vigilante, RT,R,N  
26 Knox Road  
Stamford, Connecticut, 06907

### Curriculum Vitae

**Employment:**

2005 to present: Chief Nuclear Medicine Technologist  
Stamford Hospital, Tully Health Center,  
Mill River Cardiology

1998 – 2005: Chief Nuclear Medicine Technologist  
Tully Health Center, Stamford Hospital

1991- 1998: Chief Nuclear Medicine Technologist  
St. Joseph Medical Center, Stamford, Ct

1988 – 1991: Nuclear Medicine Technologist  
St. Joseph Hospital, Stamford, Ct.

1964 – 1970: X-ray Technologist & Nuclear Medicine  
Technologist.

**Licensure:**

American Registry of Radiologic Technologist  
American Registry of Nuclear Medicine  
ARRT, R,N.

**Responsibilities:** Oversees daily operations at:

Stamford Hospital: General Nuclear Medicine  
Cardiac Nuclear Medicine  
Tully Health Center: General Nuclear Medicine,  
Cardiac Nuclear Medicine  
Mill River Cardiology: Cardiac Nuclear Medicine  
PET Services at Tully Health Center

Directs, coordinates and controls the quality control of all sites.  
Knowledge of Nuclear Medicine Policies  
Responsible for radiation safety



Oversees equipment maintenance, supply inventory, focusing on inventory resolution and cost savings.  
Serves as liaison between physicians, management and staff and other service departments.  
Participates directly in departmental productivity as necessitated by staffing, volume and departmental needs.  
Assist in budget preparation.

**INSPECTIONS PASSED:**

Nuclear Regulatory Commission  
JACHO  
State of Connecticut

**Professional Membership:** Society of Nuclear Medicine

**EXHIBIT E**

**Internal Revenue Service****Date:** June 29, 2006

STAMFORD HEALTH SYSTEM INC  
% STAMFORD HOSPITAL  
P O BOX 9317  
STAMFORD CT 06904-9317

Department of the Treasury  
P. O. Box 2508  
Cincinnati, OH 45201

**Person to Contact:**

Cheryl Skaggs 31-04010  
Correspondence Specialist/Screening

**Toll Free Telephone Number:**  
877-829-5500

**Federal Identification Number:**  
22-2476636

Dear Sir or Madam:

This is in response to your request of June 29, 2006, regarding your organization's tax-exempt status.

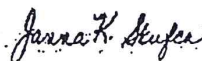
In November 1983 we issued a determination letter that recognized your organization as exempt from federal income tax. Our records indicate that your organization is currently exempt under section 501(c)(3) of the Internal Revenue Code.

Our records indicate that your organization is also classified as a public charity under sections 509(a)(1) and 170(b)(1)(A)(vi) of the Internal Revenue Code.

Our records indicate that contributions to your organization are deductible under section 170 of the Code, and that you are qualified to receive tax deductible bequests, devises, transfers or gifts under section 2055, 2106 or 2522 of the Internal Revenue Code.

If you have any questions, please call us at the telephone number shown in the heading of this letter.

Sincerely,



Janna K. Skufca, Director, TE/GE  
Customer Account Services



**EXHIBIT F**

## STATE OF CONNECTICUT

## Department of Public Health

## LICENSE

License No. 0059

## General Hospital

In accordance with the provisions of the General Statutes of Connecticut Section 19a-493:

The Stamford Hospital of Stamford, CT d/b/a The Stamford Hospital is hereby licensed to maintain and operate a General Hospital.

**The Stamford Hospital** is located at 30 Shelburne Road, Stamford, CT 06904.

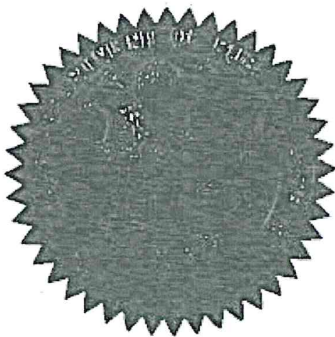
The maximum number of beds shall not exceed at any time:

25 Bassinets  
305 General Hospital Beds

This license expires **June 30, 2017** and may be revoked for cause at any time.  
Dated at Hartford, Connecticut, July 1, 2015. RENEWAL.

## Satellites:

Tully Health Center, 32 Strawberry Hill Court, Stamford, CT  
1351 Washington Boulevard, Stamford, CT

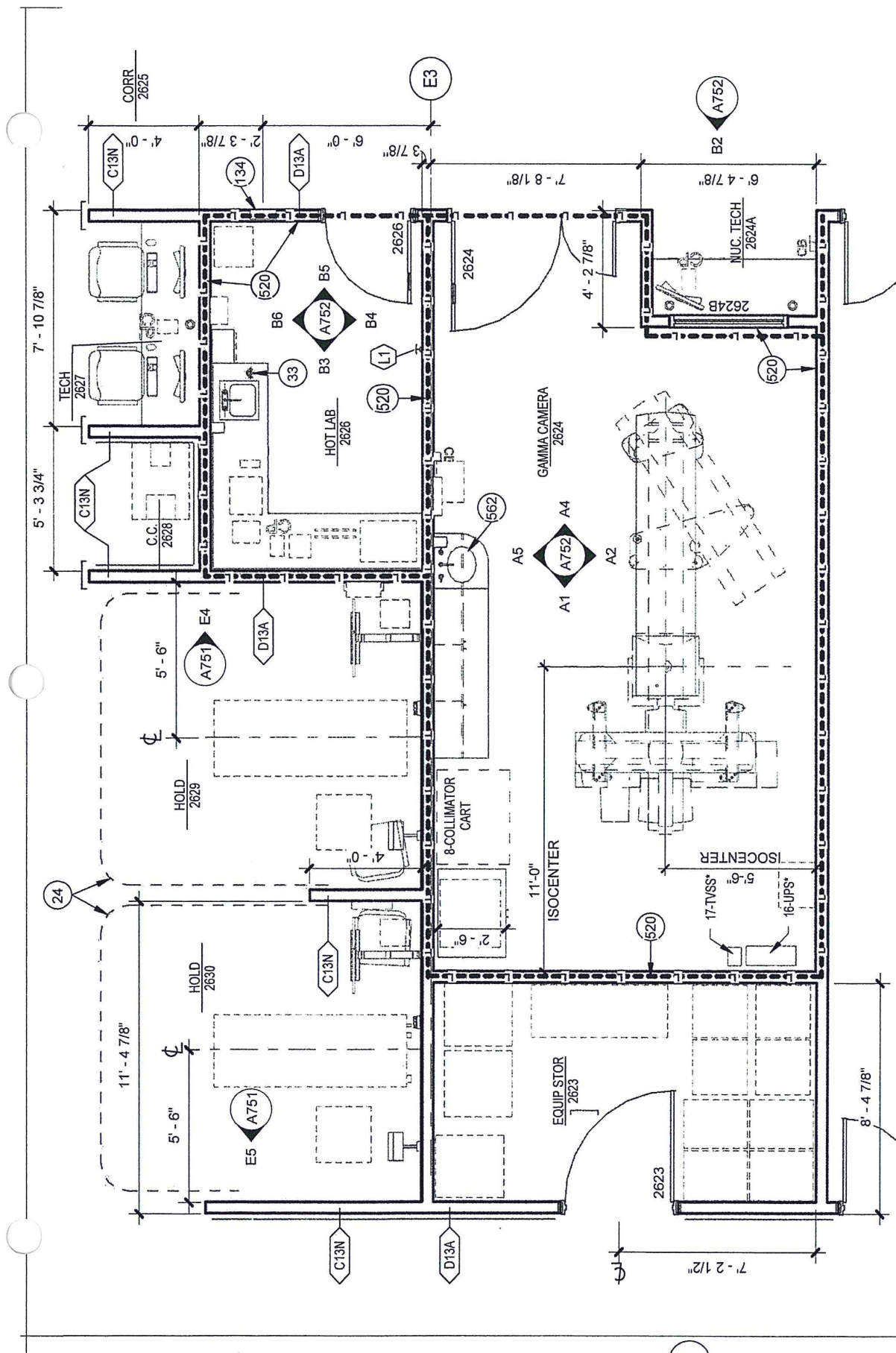


A handwritten signature in cursive script that reads "Jewel Mullen".

Jewel Mullen, MD, MPH, MPA  
Commissioner

**EXHIBIT G**



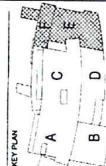


WHR ARCHITECTS

2000 Main Street, Suite 200  
Stamford, CT 06907  
Tel: 203.359.3333  
Fax: 203.359.3334  
www.whrarchitects.com

PROJECT: STAMFORD HOSPITAL SYSTEM  
FLOOR PLAN LEVEL 2  
AREA E AND F

No.	Date	Revised/Description
1	01/15/11	ISSUED FOR PERMIT
2	01/15/11	REVISIONS TO CONSTRUCTION
3	01/15/11	REVISIONS TO CONSTRUCTION
4	01/15/11	REVISIONS TO CONSTRUCTION
5	01/15/11	REVISIONS TO CONSTRUCTION



EXPANSION & RENOVATION



STAMFORD HOSPITAL SYSTEM  
The Regional Center for Health  
300 Main Street, Suite 200  
Stamford, CT 06907



FLOOR PLAN LEVEL 2  
AREA E AND F

DATE: 01/15/11  
CD ISSUE  
PROJECT: STAMFORD HOSPITAL SYSTEM  
FLOOR PLAN LEVEL 2  
AREA E AND F  
A1102.E  
Copyright © 2011 by WHR Architects, Inc.

General Notes

1. REFER TO PROJECT MANUAL, SUPPLEMENT SPECIFICATIONS FOR PART 1 - MECHANICAL, ELECTRICAL, AND PLUMBING.
2. ALL WORK SHALL BE IN ACCORDANCE WITH THE 2009 INTERNATIONAL MECHANICAL, ELECTRICAL, AND PLUMBING CODE (IMC), 2009 INTERNATIONAL ELECTRICAL CODE (IEC), 2009 INTERNATIONAL PLUMBING CODE (IPC), AND 2009 INTERNATIONAL FIRE CODE (IFC).
3. ALL WORK SHALL BE IN ACCORDANCE WITH THE 2009 INTERNATIONAL MECHANICAL, ELECTRICAL, AND PLUMBING CODE (IMC), 2009 INTERNATIONAL ELECTRICAL CODE (IEC), 2009 INTERNATIONAL PLUMBING CODE (IPC), AND 2009 INTERNATIONAL FIRE CODE (IFC).
4. ALL WORK SHALL BE IN ACCORDANCE WITH THE 2009 INTERNATIONAL MECHANICAL, ELECTRICAL, AND PLUMBING CODE (IMC), 2009 INTERNATIONAL ELECTRICAL CODE (IEC), 2009 INTERNATIONAL PLUMBING CODE (IPC), AND 2009 INTERNATIONAL FIRE CODE (IFC).
5. ALL WORK SHALL BE IN ACCORDANCE WITH THE 2009 INTERNATIONAL MECHANICAL, ELECTRICAL, AND PLUMBING CODE (IMC), 2009 INTERNATIONAL ELECTRICAL CODE (IEC), 2009 INTERNATIONAL PLUMBING CODE (IPC), AND 2009 INTERNATIONAL FIRE CODE (IFC).

FIRE RATING LEGEND

SYMBOL	DESCRIPTION	LOCATION
1	1 HOUR FIRE RATED PARTITION	ALL CORRIDORS
2	2 HOUR FIRE RATED PARTITION	ALL ELEVATORS
3	3 HOUR FIRE RATED PARTITION	ALL STAIRS
4	4 HOUR FIRE RATED PARTITION	ALL MECHANICAL ROOMS
5	5 HOUR FIRE RATED PARTITION	ALL STORAGE AREAS
6	6 HOUR FIRE RATED PARTITION	ALL LABORATORIES
7	7 HOUR FIRE RATED PARTITION	ALL OPERATING ROOMS
8	8 HOUR FIRE RATED PARTITION	ALL INTENSIVE CARE UNITS
9	9 HOUR FIRE RATED PARTITION	ALL TRANSFUSION SERVICES
10	10 HOUR FIRE RATED PARTITION	ALL RADIOLOGY DEPARTMENTS
11	11 HOUR FIRE RATED PARTITION	ALL SURGICAL SUITES
12	12 HOUR FIRE RATED PARTITION	ALL ORTHOPEDIC SURGICAL CENTERS
13	13 HOUR FIRE RATED PARTITION	ALL OBSTETRIC AND GYN DEPARTMENTS
14	14 HOUR FIRE RATED PARTITION	ALL PEDIATRIC DEPARTMENTS
15	15 HOUR FIRE RATED PARTITION	ALL PSYCHIATRIC DEPARTMENTS
16	16 HOUR FIRE RATED PARTITION	ALL SKIN SURGERY CENTERS
17	17 HOUR FIRE RATED PARTITION	ALL DERMATOLOGY DEPARTMENTS
18	18 HOUR FIRE RATED PARTITION	ALL OPHTHALMOLOGY DEPARTMENTS
19	19 HOUR FIRE RATED PARTITION	ALL ENT DEPARTMENTS
20	20 HOUR FIRE RATED PARTITION	ALL NEUROLOGY DEPARTMENTS
21	21 HOUR FIRE RATED PARTITION	ALL NEUROSURGERY DEPARTMENTS
22	22 HOUR FIRE RATED PARTITION	ALL RADIOLOGY DEPARTMENTS
23	23 HOUR FIRE RATED PARTITION	ALL RADIOLOGY DEPARTMENTS
24	24 HOUR FIRE RATED PARTITION	ALL RADIOLOGY DEPARTMENTS
25	25 HOUR FIRE RATED PARTITION	ALL RADIOLOGY DEPARTMENTS
26	26 HOUR FIRE RATED PARTITION	ALL RADIOLOGY DEPARTMENTS
27	27 HOUR FIRE RATED PARTITION	ALL RADIOLOGY DEPARTMENTS
28	28 HOUR FIRE RATED PARTITION	ALL RADIOLOGY DEPARTMENTS
29	29 HOUR FIRE RATED PARTITION	ALL RADIOLOGY DEPARTMENTS
30	30 HOUR FIRE RATED PARTITION	ALL RADIOLOGY DEPARTMENTS

NOTES TO SHEET

1. WALL MOUNTED CHARTING STATION.
2. CARD READER.
3. LINEN CHUTE.
4. WALL MOUNTED SINK.
5. MOP SINK.
6. FIRE VALVE CABINET AND FIRE EXTINGUISHER.
7. FIRE EXTINGUISHER CABINET - RECESSED.
8. EYE WASH.
9. SHOWER CONTAINER.
10. WALL MOUNTED TV.
11. WINDOW DETAILS (SEE S.D.).
12. ANTI-MICROBIAL DEFENSE (M.D.).
13. SLOPED HOPPER.
14. ALUMINUM DOOR AND FRAME, 55-S.
15. ALUMINUM DOOR AND FRAME, 55-S.
16. ALUMINUM DOOR AND FRAME, 55-S.
17. ALUMINUM DOOR AND FRAME, 55-S.
18. ALUMINUM DOOR AND FRAME, 55-S.
19. ALUMINUM DOOR AND FRAME, 55-S.
20. ALUMINUM DOOR AND FRAME, 55-S.
21. ALUMINUM DOOR AND FRAME, 55-S.
22. ALUMINUM DOOR AND FRAME, 55-S.
23. ALUMINUM DOOR AND FRAME, 55-S.
24. ALUMINUM DOOR AND FRAME, 55-S.
25. ALUMINUM DOOR AND FRAME, 55-S.
26. ALUMINUM DOOR AND FRAME, 55-S.
27. ALUMINUM DOOR AND FRAME, 55-S.
28. ALUMINUM DOOR AND FRAME, 55-S.
29. ALUMINUM DOOR AND FRAME, 55-S.
30. ALUMINUM DOOR AND FRAME, 55-S.



A1 LEVEL 2 AREA E AND F  
SCALE: 1/8" = 1'-0"

# **EXHIBIT H**



12. C (I). Please provide one year of actual results and three years of projections of Total Facility revenue, expense and volume statistics without, incremental to and with the CON proposal in the following reporting format:

Total Facility:	FY 2012	FY 2013	FY 2014	FY 2015	FY 2016	FY 2016	FY 2017	FY 2017	FY 2018	FY 2018	FY 2019	FY 2019
Description	Actual	Actual	Actual	Projected	Projected	Projected	Projected	Projected	Projected	Projected	Projected	Projected
	Results	Results	Results	Without CON	Incremental	With CON	Without CON	Incremental	With CON	Incremental	Without CON	With CON
<b>NET PATIENT REVENUE</b>												
Non-Government	\$309,105	\$312,977	\$302,070	\$315,268	\$332,844	\$332,844	\$349,979	\$349,979	\$367,842	\$367,842	\$386,462	\$386,462
Medicare	\$112,070	\$114,539	\$117,132	\$122,249	\$126,559	\$126,559	\$130,490	\$130,490	\$134,487	\$134,487	\$138,551	\$138,551
Medicaid and Other Medical Assistance	\$36,820	\$38,167	\$38,402	\$40,079	\$41,492	\$41,492	\$42,781	\$42,781	\$44,092	\$44,092	\$45,424	\$45,424
Other Government	\$599	\$202	\$204	\$212	\$220	\$220	\$227	\$227	\$234	\$234	\$241	\$241
Total Net Patient Revenue	\$458,354	\$463,884	\$457,807	\$477,859	\$501,114	\$501,114	\$523,476	\$523,476	\$546,654	\$546,654	\$570,678	\$570,678
Other Operating Revenue	\$18,946	\$19,192	\$22,613	\$16,895	\$17,064	\$17,064	\$17,235	\$17,235	\$17,407	\$17,407	\$17,581	\$17,581
Revenue from Operations	\$477,300	\$485,076	\$480,420	\$494,754	\$518,178	\$518,178	\$540,710	\$540,710	\$564,061	\$564,061	\$588,259	\$588,259
<b>OPERATING EXPENSES</b>												
Salaries and Benefits	\$236,770	\$244,302	\$229,708	\$232,172	\$242,137	\$242,137	\$251,920	\$251,920	\$262,054	\$262,054	\$272,552	\$272,552
Professional / Contracted Services	\$51,110	\$54,972	\$52,046	\$48,749	\$50,841	\$50,841	\$52,895	\$52,895	\$55,023	\$55,023	\$57,228	\$57,228
Supplies and Drugs	\$68,453	\$66,721	\$72,145	\$70,511	\$73,537	\$73,537	\$76,508	\$76,508	\$79,586	\$79,586	\$82,774	\$82,774
Bad Debts	\$0	\$0	\$0	\$0	\$0	\$0	\$0	\$0	\$0	\$0	\$0	\$0
Other Operating Expense	\$47,500	\$51,465	\$54,221	\$54,445	\$56,782	\$56,782	\$59,039	\$59,039	\$61,415	\$61,415	\$63,878	\$63,878
Subtotal	\$393,833	\$417,460	\$408,120	\$416,957	\$433,297	\$433,297	\$449,782	\$449,782	\$468,078	\$468,078	\$487,168	\$487,168
Depreciation/Amortization	\$24,839	\$24,839	\$24,089	\$24,919	\$25,883	\$25,883	\$26,084	\$26,084	\$26,718	\$26,718	\$27,404	\$27,404
Interest Expense	\$5,641	\$6,274	\$6,007	\$5,544	\$6,323	\$6,323	\$6,581	\$6,581	\$6,815	\$6,815	\$7,091	\$7,091
Lease Expense	\$5,673	\$5,093	\$5,278	\$5,102	\$5,239	\$5,239	\$5,381	\$5,381	\$5,526	\$5,526	\$5,675	\$5,675
Total Operating Expense	\$430,186	\$453,666	\$443,491	\$440,442	\$468,842	\$468,842	\$482,925	\$482,925	\$501,165	\$501,165	\$520,443	\$520,443
Gain/(Loss) from Operations	\$47,114	\$31,410	\$36,929	\$54,312	\$49,336	\$49,336	\$57,785	\$57,785	\$62,896	\$62,896	\$67,815	\$67,815
Plus: Non-Operating Revenue	(\$10,089)	\$1,089	\$2,718	\$0	\$0	\$0	\$0	\$0	\$0	\$0	\$0	\$0
Revenue Over/(Under) Expense	\$37,025	\$32,499	\$39,647	\$54,312	\$49,336	\$49,336	\$57,785	\$57,785	\$62,896	\$62,896	\$67,815	\$67,815
FTEs	2,034.60	2,064.40	2,087.12	2,124.60	2,178.60	2,178.60	2,223.60	2,223.60	2,268.60	2,268.60	2,313.60	2,313.60

\*Volume Statistics:  
Provide projected inpatient and/or outpatient statistics for any new services and provide actual and projected inpatient and/or outpatient statistics for any existing services which will change due to the proposal.

# EXHIBIT I

12.C(ii). Please provide **three** years of projections of incremental revenue, expense and volume statistics **attributable to the proposal** in the following reporting format:

Type of Service Description		SPECT / CT Nuclear Camera System								
Type of Unit Description:		Scans								
# of Months in Operation		12								
FY 2017	(1)	(2)	(3)	(4)	(5)	(6)	(7)	(8)	(9)	(10)
FY Projected Incremental		Rate	Units	Gross	Allowances/	Charity	Bad	Net	Operating	Gain/(Loss)
Total Incremental Expenses:	\$125,364			Revenue	Deductions	Care	Debt	Revenue	Expenses	from Operations
				Col. 2 * Col. 3				Col. 4 - Col. 5	Col. 1 Total *	Col. 8 - Col. 9
								-Col. 6 - Col. 7	Col. 4 / Col. 4 Total	
<b>Total Facility by Payer Category:</b>										
Medicare		\$0		\$0				\$0	\$0	\$0
Medicaid		\$0		\$0				\$0	\$0	\$0
CHAMPUS/TriCare		\$0		\$0				\$0	\$0	\$0
<b>Total Governmental</b>			0	\$0	\$0	\$0	\$0	\$0	\$0	\$0
<b>Commercial Insurers</b>										
Uninsured		\$0		\$0				\$0	\$0	\$0
<b>Total NonGovernment</b>		\$0	0	\$0	\$0	\$0	\$0	\$0	\$0	\$0
<b>Total All Payers</b>		\$0	0	\$0	\$0	\$0	\$0	\$0	\$125,364	(\$125,364)



12.C(ii). Please provide **three** years of projections of incremental revenue, expense and volume statistics **attributable to the proposal** in the following reporting format:

Type of Service Description	SPECT / CT Nuclear Camera System		(1)	(2)	(3)	(4)	(5)	(6)	(7)	(8)	(9)	(10)
Type of Unit Description:	Scans			Rate	Units	Gross Revenue Col. 2 * Col. 3	Allowances/ Deductions	Charity Care	Bad Debt	Net Revenue Col. 4 - Col. 5 -Col. 6 - Col. 7	Operating Expenses Col. 1 Total *	Gain/(Loss) from Operations Col. 8 - Col. 9
# of Months in Operation	12											
FY 2018												
FY Projected Incremental												
Total Incremental Expenses:				\$125,364								
Total Facility by												
Payer Category:												
Medicare						\$0				\$0		\$0
Medicaid				\$0		\$0				\$0		\$0
CHAMPUS/TriCare				\$0		\$0				\$0		\$0
Total Governmental					0	\$0	\$0	\$0	\$0	\$0	\$0	\$0
Commercial Insurers				\$0		\$0				\$0		\$0
Uninsured				\$0		\$0				\$0		\$0
Total NonGovernment					0	\$0	\$0	\$0	\$0	\$0	\$0	\$0
Total All Payers				\$0	0	\$0	\$0	\$0	\$0	\$0	\$125,364	(\$125,364)



**Greer, Leslie**

---

**From:** Schaeffer-Helmecki, Jessica  
**Sent:** Thursday, September 10, 2015 4:10 PM  
**To:** Greer, Leslie  
**Subject:** FW: Completeness Questions: CON Application 15-32020

Hi Leslie, please add this e-mail delivery receipt to The Stamford Hospital docket. Email to come shortly.

---

**From:** Microsoft Outlook  
**Sent:** Thursday, September 10, 2015 4:09 PM  
**To:** Schaeffer-Helmecki, Jessica  
**Subject:** Relayed: Completeness Questions: CON Application 15-32020

Your message

To: 'DSmith@stamhealth.org'  
Cc: Riggott, Kaila  
Subject: Completeness Questions: CON Application 15-32020  
Sent: 9/10/2015 4:09 PM

was delivered to the following recipient(s):

'DSmith@stamhealth.org' on 9/10/2015 4:09 PM



## Greer, Leslie

---

**From:** Schaeffer-Helmecki, Jessica  
**Sent:** Thursday, September 10, 2015 4:11 PM  
**To:** Greer, Leslie  
**Subject:** FW: Completeness Questions: CON Application 15-32020

Leslie, please add the below email to The Stamford Hospital docket. Thank you!

---

**From:** Schaeffer-Helmecki, Jessica  
**Sent:** Thursday, September 10, 2015 4:09 PM  
**To:** 'DSmith@stamhealth.org'  
**Cc:** Riggott, Kaila  
**Subject:** Completeness Questions: CON Application 15-32020

Dear Mr. Smith,

On August 17, 2015, OHCA received The Stamford Hospital's application (docket number 15-32020) to acquire a SPECT-CT. We have reviewed your application and need a bit more information. Specifically, please update the payer mix table on **page 28** to include:

- The payer mix by *number of patients* (as well as the overall percentages) for 2014 through 2017
- Updated year-to-date figures through at least August 2015 by *number of patients*

If you respond via e-mail, please attach your response as both a word document and pdf. Please paginate your response, beginning your submission using "Page 205" and reference "Docket Number: 15-32020-CON."

Pursuant to Section 19a-639a(c) of the Connecticut General Statutes, you must submit your response to this request for additional information not later than sixty days after the date that this request was transmitted. Therefore, please provide your written responses to OHCA no later than **November 9, 2015**, otherwise your application will be automatically considered withdrawn.

If you have any questions concerning this letter, please feel free to contact me by email or phone.

Sincerely,

**Jessica Schaeffer-Helmecki**  
Office of Health Care Access  
Connecticut Department of Public Health  
410 Capitol Avenue, MS #13 HCA, Hartford, Connecticut 06134  
P: (860) 509-8075 | F: (860) 418-7053 | E: [jessica.schaeffer-helmecki@ct.gov](mailto:jessica.schaeffer-helmecki@ct.gov)



## Greer, Leslie

---

**From:** Schaeffer-Helmecki, Jessica  
**Sent:** Wednesday, October 14, 2015 4:19 PM  
**To:** Greer, Leslie  
**Subject:** FW: Completeness Questions: CON Application 15-32020  
**Attachments:** Updated Table 4 of SPECT-CT Camera System (00057193xAE9B0).docx; 15-32020-CON Updated Table 4 (00057194xAE9B0).pdf

Leslie, Please add this to docket 15-32020. Thank you.

---

**From:** Smith, David L (SVP, Administration) [<mailto:DSmith@stamhealth.org>]  
**Sent:** Wednesday, October 14, 2015 4:17 PM  
**To:** Schaeffer-Helmecki, Jessica  
**Cc:** Riggott, Kaila; Kearns, Gregory; Cowherd Stephen ([SCowherd@jeffire.com](mailto:SCowherd@jeffire.com))  
**Subject:** Completeness Questions: CON Application 15-32020

Dear Ms. Schaeffer-Helmecki:

Attached please find the requested updated Table 4 that now includes:

- The payer mix *by number of patients* (as well as the overall percentages) for 2014 through 2019.
- Updated year-to-date figures through SEPTEMBER 2015 by *number of patients (and percentage)*

At your request, I've attached both .pdf and .doc versions of the updated table.

Please do not hesitate to contact me at 203-276-7510, Greg Kearns, Director of Planning at 203-276-2224, or our outside counsel, Stephen Cowherd at 203-259-7900 if you have any further questions regarding this application. Thank you for your assistance with this application.

David L. Smith  
Senior Vice President, Strategy  
Chief Strategy and Network Development Officer  
Stamford Health System  
30 Shelburne Road  
Stamford, CT 06904-9317  
(203) 276-7510

**The Stamford Hospital**

**Docket Number 15-32020-CON; Certificate of Need Application for Acquisition of SPECT/CT Camera System**

**Responses to September 10, 2015 Completeness Questions**

As requested, please find an updated Table 4 which now includes the payer mix by *number of patients* (as well as the overall percentages) for 2014 through 2017 and updated year-to-date figures through at least August 2015 by *number of patients*.

**Table 4: Patient Population Mix**

	Actual	Actual	Actual	Actual	<i>interim - pre proposed equipment</i>	<i>interim - pre proposed equipmen t</i>	Year 1	Year 1	Year 2	Year 2	Year 3	Year 3
	<b>FY14 (# pts.)</b>	<b>FY14 (%)</b>	<b>FY15 (September - # pts.)</b>	<b>FY15 (September - %)</b>	<b>FY16 (# pts.)</b>	<b>FY16 (%)</b>	<b>FY17 (# pts.)</b>	<b>FY17 (%)</b>	<b>FY18 (# pts.)</b>	<b>FY18 (%)</b>	<b>FY19 (# pts.)</b>	<b>FY 19 (%)</b>
Medicare*	1065	54%	1073	54%	1,091	54%	1,091	54%	1,091	54%	1,091	54%
Medicaid*	259	13%	242	12%	232	12%	232	12%	232	12%	232	12%
CHAMPUS & TriCare	1	0%	0	0%	0	0%	0	0%	0	0%	0	0%
<b>Total Government</b>	1325	67%	1315	66%	1,323	66%	1,323	66%	1,323	66%	1,323	66%
Commercial Insurers*	595	30%	640	32%	654	33%	654	33%	654	33%	654	33%
Uninsured	52	3%	29	1%	30	1%	30	1%	30	1%	30	1%
Workers Compensation	1	0%	0	0%	4	0%	4	0%	4	0%	4	0%
<b>Total Non- Government</b>	648	33%	674	34%	689	34%	689	34%	689	34%	689	34%
<b>Total Payer Mix</b>	1973	100%	1989	100%	2,012	100%	2,012	100%	2,012	100%	2,012	100%

\* Includes managed care activity.

\*\* New programs may leave the “current” column blank.

\*\*\* Fill in years. Ensure the period covered by this table corresponds to the period covered in the projections provided.



## Greer, Leslie

---

**From:** Schaeffer-Helmecki, Jessica  
**Sent:** Wednesday, November 04, 2015 3:02 PM  
**To:** 'Smith, David L (SVP, Administration)'  
**Cc:** Greer, Leslie; Fernandes, David  
**Subject:** Deemed Complete: 15-32020  
**Attachments:** 15-32020-Stamford CON Notification of Application Deemed Complete.pdf

Dear Dr. Smith

This letter is to inform you that, pursuant to Section 19a-639a (d) of the Connecticut General Statutes, the Office of Health Care Access has deemed the above-referenced application complete as of November 4, 2015.

If you have any questions regarding this matter, please feel free to contact me at (860) 509-8075 or David Fernandes at (860) 509-8162.

**Jessica Schaeffer-Helmecki**

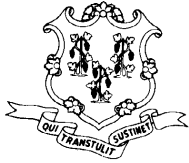
Office of Health Care Access

Connecticut Department of Public Health

410 Capitol Avenue, MS #13 HCA, Hartford, Connecticut 06134

P: (860) 509-8075 | F: (860) 418-7053 | E: [jessica.schaeffer-helmecki@ct.gov](mailto:jessica.schaeffer-helmecki@ct.gov)





# STATE OF CONNECTICUT

DEPARTMENT OF PUBLIC HEALTH

*Office of Health Care Access*

November 4, 2015

VIA EMAIL ONLY

David Smith  
Senior Vice President  
The Stamford Hospital  
30 Shelburne Road  
Stamford, CT 06907

RE: Certificate of Need Application Docket Number: 15-32020-CON  
The Stamford Hospital  
Acquisition of a SPECT-CT  
Notification Deeming the CON Application Complete

Dear Mr. Smith:

This letter is to inform you that, pursuant to Section 19a-639a (d) of the Connecticut General Statutes, the Office of Health Care Access has deemed the above-referenced application complete as of November 4, 2015.

If you have any questions regarding this matter, please feel free to contact me at (860) 509-8075 or David Fernandes at (860) 509-8162.

Sincerely,

A handwritten signature in black ink, reading "J Schaeffer Helmecki".

Jessica Schaeffer-Helmecki  
Planning Analyst (CCT)

*An Equal Opportunity Provider*

*(If you require aid/accommodation to participate fully and fairly, contact us either by phone, fax or email)*

410 Capitol Ave., MS#13HCA, P.O.Box 340308, Hartford, CT 06134-0308  
Telephone: (860) 418-7001 Fax: (860) 418-7053 Email: OHCA@ct.gov

## Greer, Leslie

---

**From:** Smith, David L (SVP, Administration) <DSmith@stamhealth.org>  
**Sent:** Wednesday, November 04, 2015 4:41 PM  
**To:** Schaeffer-Helmecki, Jessica  
**Cc:** Greer, Leslie; Fernandes, David  
**Subject:** Re: Deemed Complete: 15-32020  
**Attachments:** image001.jpg

Thank you.

Sent from my iPhone

On Nov 4, 2015, at 3:01 PM, Schaeffer-Helmecki, Jessica <[Jessica.Schaeffer-Helmecki@ct.gov](mailto:Jessica.Schaeffer-Helmecki@ct.gov)> wrote:

Dear Dr. Smith

This letter is to inform you that, pursuant to Section 19a-639a (d) of the Connecticut General Statutes, the Office of Health Care Access has deemed the above-referenced application complete as of November 4, 2015.

If you have any questions regarding this matter, please feel free to contact me at (860) 509-8075 or David Fernandes at (860) 509-8162.

**Jessica Schaeffer-Helmecki**

Office of Health Care Access

Connecticut Department of Public Health

410 Capitol Avenue, MS #13 HCA, Hartford, Connecticut 06134

P: (860) 509-8075 | F: (860) 418-7053 | E: [jessica.schaeffer-helmecki@ct.gov](mailto:jessica.schaeffer-helmecki@ct.gov)



<15-32020-Stamford CON Notification of Application Deemed Complete.pdf>



## Greer, Leslie

---

**From:** Olejarz, Barbara  
**Sent:** Tuesday, December 15, 2015 11:19 AM  
**To:** daniels@chime.org; Bruno, Anthony M.; Fletcher, Barbara F.; McLellan, Rose; Johnson, Colleen M  
**Cc:** Greer, Leslie  
**Subject:** Final Decision  
**Attachments:** 32020.pdf

12/15/15

Please see attached Final Decision for The Stamford Hospital.

Barbara K. Olejarz  
Administrative Assistant for Kimberly Martone  
Office of Health Care Access  
Department of Public Health  
Phone: (86) 418-7005  
Email: [Barbara.Olejarz@ct.gov](mailto:Barbara.Olejarz@ct.gov)





**Department of Public Health  
Office of Health Care Access  
Certificate of Need Application**

**Final Decision**

**Applicant:** The Stamford Hospital

**Docket Number:** 15-32020-CON

**Project Title:** Acquisition of a Single Photon Emission Computed Tomography/Computed Tomography Camera

**Project Description:** The Stamford Hospital ("Hospital" or "Applicant") is seeking approval for the acquisition of a Single Photon Emission Computed Tomography-Computed Tomography ("SPECT-CT") camera to replace a nuclear camera.

**Procedural History:** On August 17, 2015, the Office of Health Care Access ("OHCA") received the initial Certificate of Need ("CON") application from the Hospital for the above-referenced project. The Hospital published notice of its intent to file the CON Application in *The Advocate* (Stamford) on June 19, 20 and 21, 2015. The application was deemed complete on November 4, 2015. OHCA received no responses from the public concerning the Hospital's proposal and no hearing requests were received from the public per Connecticut General Statutes § 19a-639a(e). In rendering her decision, Deputy Commissioner Brancifort considered the entire record in this matter.

## Findings of Fact and Conclusions of Law

1. The Hospital is a 305<sup>1</sup> bed not-for-profit general hospital located at 30 Shelburne Road, Stamford, Connecticut. Exhibit A, pp. 12, 195.
2. The Hospital currently operates five nuclear cameras, two at its main campus hospital, two at its Tully Health Center, located at 32 Strawberry Hill Court in Stamford, and one at Mill River Cardiology Imaging Center ("Mill River"), located at 80 Mill River Street in Stamford.

Provider and Location	Equipment	Hours of Operation	Utilization FY14
Stamford Hospital 30 Shelburne Road Stamford, CT 06902	Unit 1: GE Infinia Unit 2: GE Infinia Hawkeye – CT Slice 2	M-F 7 AM to 4 PM Emergency calls 7 days	1,308
Tully Health Center 32 Strawberry Hill Court Stamford, CT 06902	Unit 1: Philips Forte Unit 2: Philips Axis	M-F 7 AM to 4 PM	1,220
Mill River Cardiology Imaging Center 80 Mill River Street Stamford, CT 06902	Unit 1: GE Ventri (to be retired)	M-F 7 AM to 3:30 PM	704

Exhibit. A, p. 18.

3. The GE Ventri located at Mill River has been in operation since 2006 and is at the end of its useful life. The Applicant proposes disposing of the unit through the vendor and replacing it with a 4-slice GE Optima NM/CT 640 SPECT-CT. Exhibit A, pp. 13, 20.
4. The new SPECT-CT will be located in the Hospital's new Heart and Vascular Institute (HVI) suite and will be dedicated solely to cardiac services. Exhibit A, p. 14.
5. The Hospital's Community Health Needs Assessment identified cardiovascular disease to be among the leading causes of hospitalization and death in the Hospital's service area. Exhibit A, p. 15, Stamford, *2013 Community Health Needs Assessment*, pp 35-38.
6. The Hospital's goal is to create a "one-stop" environment that provides patients with integrated interventional and diagnostic cardiac services. The HVI will provide elective and emergency angioplasty procedures, pacemaker/defibrillator implantation, electrophysiology, as well as vascular and peripheral stenting. Exhibit A, pp. 13, 18.
7. Nuclear cardiology imaging has inherent limitations due to the variation and density of tissue within the body, which may result in shadows and attenuation artifacts in the resulting images. The GE Optima SPECT-CT will allow the hospital to provide patients with higher quality myocardial perfusion studies in the comprehensive diagnostic and

---

<sup>1</sup> Excludes 25 bassinets.



interventional HVI. To mitigate attenuation artifacts, the CT component of the proposed GE Optima camera will remove these artifacts, decreasing false positive results and eliminating unnecessary follow-up testing. Exhibit A, p. 16.

8. Currently, patients undergoing myocardial perfusion testing without attenuation correction are required to be scanned twice—initially in a supine position, then in a prone state, the latter of which can be uncomfortable and unstable for some patients. The proposed camera will provide superior image quality with shorter image acquisition times and thus, less radiation exposure to patients. Exhibit A, p. 17.
9. The new SPECT-CT will serve the same patient population as the existing camera. Exhibit A, p. 20.
10. Based on its actual historical utilization, the Hospital has conservatively projected stable utilization volume.

**TABLE 1**  
**THE STAMFORD HOSPITAL'S HISTORICAL AND PROJECTED UTILIZATION**  
**OF CARDIAC SPECT-CT CAMERAS\*\***

	Actual				Projected		
	FY2012	FY2013	FY2014	FY2015*	FY2016	FY2017	FY2018
<b>Proposed GE Optima</b>	n/a	n/a	n/a	n/a	722	722	722
<b>Existing GE Ventra</b>	643	626	685	704	n/a	n/a	n/a
<b>Total</b>	649	626	685	704	722	722	722

\*Annualized based on Sept. 2014 through May 2015 data

\*\* Excludes two cameras in use in the Applicant's radiology department

Exhibit A, p. 21.

11. Studies have shown the benefits of a SPECT-CT over a SPECT camera in the evaluation of coronary artery disease. The enhanced attenuation correction of the SPECT-CT reduces the number of false-positive results, allowing for improved diagnostic accuracy as well as improved risk stratification of patients. Aju P. Pazhenkottil et. al, *Improved Outcome Prediction by SPECT Myocardial Perfusion Imaging After CT Attenuation Correction*, 52 J OF NUCL MED 196, 196-198 (2011). Exhibit C, p. 50.
12. The advancement of SPECT-CT cameras offers the opportunity to shorten acquisition time and provide accurate attenuation correction and fusion imaging. Additional advantages are represented by increased specificity and accurate depiction of localization of disease and of possible involvement of adjacent tissues. Moreover, SPECT-CT imaging is especially suited to support minimally invasive surgery, as well as to precisely define the diagnostic and prognostic profile of cardiovascular patients. Giuliano Mariani et. al., *A review on the clinical uses of SPECT/CT*, 37 J NUCL MED MOL IMAGING 1960 (2010). Exhibit C, p. 57.

13. A primary benefit of SPECT-CT cardiac imaging is the increased efficiency it provides. Recently developed myocardial perfusion cameras have come equipped with novel detector and collimator geometries that improve detection efficiency as well as improve spatial resolution for myocardial perfusion imaging. Youngho Seo et. al., *Technological Development and Advances in SPECT/CT*, 38 SEMIN NUCL MED 177, 12. Exhibit C, p. 106.
14. The costs related to the proposed project are associated with and included in \$450 million funding from the Hospital's previously approved Master Facility Plan CON (Docket #08-31284) and will be financed through a combination of debt, philanthropy and cash from operations.

**TABLE 2**  
**THE STAMFORD HOSPITAL'S TOTAL CAPITAL EXPENDITURE**

Medical Equipment Purchase	\$539,308
Construction/Renovation	\$225,000
<b>Total Capital Expenditure (TCE)</b>	<b>\$764,308</b>

Exhibit A, pp. 26, 27.

15. Incremental losses are projected in each of the next three fiscal years (FY) due to other operating expenses and depreciation.

**TABLE 3**  
**THE STAMFORD HOSPITAL'S PROJECTED INCREMENTAL REVENUES AND EXPENSES**

	<b>FY 2016</b>	<b>FY 2017</b>	<b>FY 2018</b>
Revenue from Operations	-	-	-
Total Operating Expenses*	\$44,000	\$125,000	\$125,000
<b>Gain/(Loss) from Operations</b>	<b>(\$44,000)</b>	<b>(\$125,000)</b>	<b>(\$125,000)</b>

\*Operating expenses represent the change in depreciation amount, which is a non-cash expense.

Exhibit A, pp. 29, 200.

16. Despite incremental losses, the Hospital projects overall operational gains from FY2016 through FY2018 following implementation of the proposal.

**TABLE 4**  
**THE STAMFORD HOSPITAL'S PROJECTED REVENUES & EXPENDITURES WITH CON**

	<b>FY 2016</b>	<b>FY 2017</b>	<b>FY 2018</b>
Revenue from Operations	\$518,178	\$540,710	\$564,061
Total Operating Expenses*	\$468,886	\$503,051	\$521,290
<b>Gain/(Loss) from Operations**</b>	<b>\$49,292</b>	<b>\$37,660</b>	<b>\$42,771</b>

Note: figures are in thousands.

\*Operating expenses include salaries/fringe benefits, professional/contracted services, supplies/drugs, bad debts, other operating expenses, depreciation/amortization, interest expense and lease expense.

\*\* Decreases in operational gains from FY16 to FY18 are due to depreciation and the cost of renovating the space.

Exhibit A, pp. 29, 200.

17. No change in the patient population mix is projected by the Hospital.

**TABLE 5**  
**THE STAMFORD HOSPITAL'S CURRENT & PROJECTED PAYER MIX**

Payer	Most Recently Completed FY 2014**		Projected							
			FY 2015**		FY 2016**		FY 2017**		FY 2018**	
	Volume	%	Volume	%	Volume	%	Volume	%	Volume	%
Medicare*	1,065	54%	1,073	54%	1,091	54%	1,091	54%	1,091	54%
Medicaid*	259	13%	242	12%	232	12%	232	12%	232	12%
CHAMPUS & TriCare	1	0%	0	0%	0	0%	0	0%	0	0%
<b>Total Government</b>	<b>1,325</b>	<b>67%</b>	<b>1,315</b>	<b>66%</b>	<b>1,323</b>	<b>66%</b>	<b>1,323</b>	<b>66%</b>	<b>1,323</b>	<b>66%</b>
Commercial Insurers	595	30%	640	32%	654	33%	654	33%	654	33%
Uninsured	52	3%	29	1%	30	1%	30	1%	30	1%
Workers Compensation	1	0%	0	0%	4	0%	4	0%	4	0%
<b>Total Non-Government</b>	<b>648</b>	<b>33%</b>	<b>674</b>	<b>34%</b>	<b>689</b>	<b>34%</b>	<b>689</b>	<b>34%</b>	<b>689</b>	<b>34%</b>
<b>Total Payer Mix</b>	<b>1,973</b>	<b>100%</b>	<b>1,989</b>	<b>100%</b>	<b>2,012</b>	<b>100%</b>	<b>2,012</b>	<b>100%</b>	<b>2,012</b>	<b>100%</b>

Exhibit. A, p. 28.

17. OHCA is currently in the process of establishing its policies and standards as regulations. Therefore, OHCA has not made any findings as to this proposal's relationship to any regulations adopted by OHCA. (Conn. Gen. Stat. § 19a-639(a)(1))
18. This CON application is consistent with the Statewide Health Care Facilities and Services Plan. (Conn. Gen. Stat. § 19a-639(a)(2))
19. The Applicant has established that there is a clear public need for its proposal. (Conn. Gen. Stat. § 19a-639(a)(3))
20. The Applicant has satisfactorily demonstrated that its proposal is financially feasible. (Conn. Gen. Stat. § 19a-639(a)(4))
21. The Applicant has satisfactorily demonstrated that access to services will be maintained and quality of health care delivery in the region as well as cost effectiveness will be improved. (Conn. Gen. Stat. § 19a-639(a)(5))
22. The Applicant has shown that there will be no change in access to the provision of health care services to the relevant populations and payer mix. (Conn. Gen. Stat. § 19a-639(a)(6))
23. The Applicant has satisfactorily identified the population to be served and has satisfactorily demonstrated that this population has a need as proposed. (Conn. Gen. Stat. § 19a-639(a)(7))



24. The Applicant's historical utilization in the service area supports this proposal. (Conn. Gen. Stat. § 19a-639(a)(8))
25. The Applicant has satisfactorily demonstrated that the proposal will not result in an unnecessary duplication of existing services in the area. (Conn. Gen. Stat. § 19a-639(a)(9))
26. The Applicant has satisfactorily demonstrated that the proposal will not result in a reduction or change in access to services for Medicaid recipients or indigent persons. (Conn. Gen. Stat. § 19a-639(a)(10))
27. The Applicant has satisfactorily demonstrated that the proposal will not result in a negative impact on the diversity of health care providers in the area. (Conn. Gen. Stat. § 19a-639(a)(11))
28. The Applicant has satisfactorily demonstrated that its proposal will not result in any consolidation that would affect health care costs or access to care. (Conn. Gen. Stat. § 19a-639(a)(12))

## Discussion

CON applications are decided on a case by case basis and do not lend themselves to general applicability due to the uniqueness of the facts in each case. In rendering its decision, OHCA considers the factors set forth in General Statutes § 19a-639(a). The Applicant bears the burden of proof in this matter by a preponderance of the evidence. *Jones v. Connecticut Medical Examining Board*, 309 Conn. 727 (2013).

The Stamford Hospital (“Hospital” or “Applicant”), a 305-bed not-for-profit general hospital in Stamford, is seeking authorization for the acquisition of a 4-slice GE Optima NM/CT 640 SPECT-CT camera to replace its 2006 GE Ventri nuclear camera that is at the end of its useful life. *FF1,3*. The Hospital currently operates five nuclear cameras at its main campus and off-site locations. *FF2*.

Acquiring the SPECT-CT and locating it within the new Heart and Vascular Institute (HVI) suite will facilitate the Hospital’s goal of creating a “one-stop” environment with integrated interventional and diagnostic cardiac services. *FF4,6*. A one-stop model will help increase speed of diagnosis and treatment, facilitate the development of clinical pathways and foster collaboration between interventional cardiologists and their non-interventional colleagues. The HVI will provide elective and emergency angioplasty procedures, pacemaker/defibrillator implantation, electrophysiology, as well as vascular and peripheral stenting. *FF6*.

The CT component of the proposed GE Optima Camera delivers attenuation correction for myocardial perfusion imaging studies, which improves diagnostic accuracy. Nuclear cardiology imaging has inherent limitation due to the variation and density of tissue within the body. Variations in tissue can create shadows and attenuation artifacts in the resulting images. *FF7*. The CT component of the proposed GE Optima camera will remove such artifacts, decreasing false positive results and eliminating unnecessary follow-up testing. *FF7*. Additionally, patients who undergo myocardial perfusion testing without attenuation correction are required to be scanned twice—initially in a supine position and then in the prone state, which may be uncomfortable and unsteady for some patients and produce unclear images that necessitate additional scans. *FF8*. The proposed camera will provide superior image quality in less time and reduce the number of required scans and, in turn, reduce patients’ radiation exposure. *FF8*. Based on the foregoing, the proposal will result in improved quality of care.

The Applicant provided numerous scholarly articles that support the benefits of a SPECT-CT camera over a SPECT camera in the evaluation of coronary artery disease. The quality of scans produced by the SPECT-CT cameras is significantly superior to the SPECT camera. The SPECT-CT’s enhanced attenuation correction allows for improved diagnostic accuracy and risk stratification. *FF11*. Moreover, SPECT-CT imaging is suited to precisely define the diagnostic and prognostic profile of cardiovascular patients. *FF12*. With increased accuracy comes increased efficiency that the SPECT-CT provides. Recent advances in SPECT-CT have allowed perfusion cameras to come equipped with novel detector and collimator geometries that improve detection efficiency as well as improve spatial resolution for myocardial perfusion imaging. *FF13*. The SPECT-CT camera will enable the most at-risk patients to be identified more quickly.

Based on historical utilization, the Applicant has conservatively projected stable utilization from FY2016 to FY2018. *FF10*. There is no expected change in the patient population as the Applicant is upgrading old existing imaging equipment and there will be no change in the patient population mix. The Applicant will continue to provide the same access to care to Medicaid patients. *FF9,17*.

The SPECT-CT acquisition cost was included in \$450 million funding from the Hospital's previously approved 2008 Master Facility Plan CON and will be financed through a combination of debt, philanthropy and cash from operations. *FF14*. Despite incremental losses, the Applicant projects overall operational gains of \$49,292,000, \$37,660,000 and \$42,771,000 in FY16, FY17 and FY18, respectively, with the declining gains attributable to depreciation and other operating costs. *FF15,16*. Therefore, OHCA finds the proposal is financially feasible.

The Applicant has satisfactorily demonstrated clear public need for this proposal as access to care will be maintained and quality of care will be improved. These two benefits are consistent with the Statewide Health Care Facilities and Services Plan.



## Order

Based upon the foregoing Findings of Fact and Discussion, the Certificate of Need application of The Stamford Hospital for the acquisition of a SPECT-CT camera is hereby **APPROVED**.

All of the foregoing constitutes the final order of the Office of Health Care Access in this matter.

By Order of the  
Department of Public Health  
Office of Health Care Access

December 15, 2015  
Date

Janet M. Brancifort  
Janet M. Brancifort, RRT, MPH  
Deputy Commissioner

**Olejarz, Barbara**

---

**From:** Microsoft Outlook  
**To:** DSmith@stamhealth.org  
**Sent:** Tuesday, December 15, 2015 10:49 AM  
**Subject:** Relayed: Final Decision

**Delivery to these recipients or groups is complete, but no delivery notification was sent by the destination server:**

DSmith@stamhealth.org (DSmith@stamhealth.org)

Subject: Final Decision

## Olejarz, Barbara

---

**From:** Smith, David L (SVP, Administration) <DSmith@stamhealth.org>  
**Sent:** Wednesday, December 16, 2015 10:15 AM  
**To:** Olejarz, Barbara  
**Subject:** RE: Final Decision

Barbara, yes I did receive the final decision. Thank you. Sorry I keep forgetting to acknowledge.

David

David L. Smith  
Senior Vice President, Strategy  
Chief Strategy and Network Development Officer  
Stamford Health System  
30 Shelburne Road  
Stamford, CT 06904-9317  
(203) 276-7510

---

**From:** Olejarz, Barbara [mailto:Barbara.Olejarz@ct.gov]  
**Sent:** Wednesday, December 16, 2015 9:23 AM  
**To:** Smith, David L (SVP, Administration)  
**Subject:** FW: Final Decision

12/16/15

Good morning,

Can you please let me know if you received the final decision for Docket Number 15-32020 as mentioned below.

Thank you

Barbara K. Olejarz  
Administrative Assistant to Kimberly Martone  
Office of Health Care Access  
Department of Public Health  
Phone: (86) 418-7005  
Email: [Barbara.Olejarz@ct.gov](mailto:Barbara.Olejarz@ct.gov)



---

**From:** Olejarz, Barbara  
**Sent:** Tuesday, December 15, 2015 10:49 AM  
**To:** 'DSmith@stamhealth.org' <DSmith@stamhealth.org>  
**Cc:** Schaeffer-Helmecki, Jessica <[Jessica.Schaeffer-Helmecki@ct.gov](mailto:Jessica.Schaeffer-Helmecki@ct.gov)>; Riggott, Kaila <[Kaila.Riggott@ct.gov](mailto:Kaila.Riggott@ct.gov)>; Martone, Kim <[Kimberly.Martone@ct.gov](mailto:Kimberly.Martone@ct.gov)>  
**Subject:** Final Decision



**Huber, Jack**

---

**From:** Huber, Jack  
**Sent:** Tuesday, December 29, 2015 7:55 AM  
**To:** 'DSmith@stamhealth.org'  
**Cc:** Roberts, Karen  
**Subject:** Notice of CON Expiration Date for the Final Decision Rendered under Docket Number: 15-32020-CON

---

Dear Mr. Smith:

On December 15, 2015, in a final decision under Docket Number: 15-32020-CON, the Office of Health Care Access authorized a Certificate of Need ("CON") to Stamford Hospital for the acquisition of a single photon emission computed tomography-computed tomography ("SPECT-CT") camera, replacing an existing camera, that will be dedicated for use in the Hospital's new Heart and Vascular Institute suite. Pursuant to Section 19a-639b of the Connecticut General Statutes ("C.G.S."), *"a certificate of need shall be valid for two years from the date of issuance by this office."*

With this letter, please be advised that pursuant to Section 19a-639b, C.G.S., the current CON authorization issued under Docket Number: 15-32020-CON will expire on December 15, 2017. Please contact me at (860) 418-7069 or Karen Roberts, Principal Health Care Analyst at (860) 418-7041, if you have any questions regarding this notification. Best wishes for a Happy New Year!

Sincerely,

*Jack A. Huber*

Jack A. Huber

Health Care Analyst

Department of Public Health | Office of Health Care Access | 410 Capitol Avenue

P.O. Box 340308 MS #13HCA | Hartford, CT 06134 | Ph: 860-418-7069 | Fax: 860-418-7053 | email: [Jack.Huber@ct.gov](mailto:Jack.Huber@ct.gov)